UNIVERSITY
OF TASMANIA

Synthesis of New Derivatives Targeting Mitochondrial Dysfunction

Krystel Woolley

BSc (Hons) GradCertRes

School of Physical Sciences – Chemistry

A thesis submitted in fulfilment of the requirements for the degree of Doctor of Philosophy

University of Tasmania September 2017

Table of contents

Declaration:

This thesis contains no material which has been accepted for a degree or diploma by the University or any other institution, except by way of background information and duly acknowledged in the thesis, and to the best of my knowledge and belief no material previously published or written by another person except where due acknowledgement is made in the text of the thesis, nor does the thesis contain any material that infringes copyright.

Krystel Woolley,

September 2017

Authority of Access:

This thesis is not to be made available for loan or copying for two years following the date this statement was signed. Following that time the thesis may be made available for loan and limited copying and communication in accordance with the *Copyright Act 1968.*

Abstract:

Mitochondrial dysfunction is implicated in many diverse diseases, including cancer, diabetes, neurodegeneration (i.e. Glaucoma, Alzheimer's and Parkison's disease) and autoimmune diseases. Although a lot of common diseases are associated with mitochondrial dysfunction, only a very limited number of approved therapeutics are currently available on the market that directly target and normalize mitochondrial function.

One of the most frequent inherited mitochondrial diseases is Leber's Heriditary Optic Neuropahthy (LHON) that is characterized by acute vision loss. As first-in-class, the short chain benzoquinone idebenone was approved only recently by the European Medicine Agency (EMA) to treat LHON patients. Despite its clinical activity, this molecule has several drawbacks. First and foremost, idebenone displays a very short half-life *in vivo*, due to a rapid first-pass metabolism. Furthermore, idebenone depends on a single enzyme for its bioactivation called NQO1 (NAD(P)H:quinone oxidoreductase 1) that reduces the quinioid core by a two-electron mechanism. However, a large section of the general population carry a polymorphic form of the NQO1 gene (C609T) that inactivates the resulting protein. Failure to reduce idebenone to the benzoquinol form not only results in a loss of therapeutic activity but could also increase levels of reactive oxygen species (ROS) and may lead to toxicity and cell death.

Using idebenone as a lead compound, a suite of analogues were synthesized with the aim to establish a structure activity relationship (SAR). A large library of analogues containing a 3-methyl-naphthoquinone core was prepared. The functionality and physical properties of the side chain were investigated and optimisation based on polarity was employed to identify the highest level of cytoprotection against mitochondrial dysfunction. Under these conditions, the ability to restore adenosine triphosphate (ATP) levels and provide cytoprotection was achieved by attaching an amino alcohol or equivalent amine to the quinone core *via* a four-carbon linker that utilised amide coupling. Restoring ATP levels is essential, as insufficient ATP levels may result in cell death.

After significant optimisation of the side chain, core optimisation was undertaken. The importance of the methyl substituent at the C3-position of the naphthoquinone core was identified. Removal of this substituent resulted in a drop in cytoprotection and the ability to restore ATP levels. This effect is proposed to be due to conjugation with glutathione that prevents the analogues to shuttle in and out of the mitochondria. Also a comparative analysis of naphthoquinone, plastoquinone and benzoquinone cores was completed, when tested with a common side chain. The superiority of the naphthoquinone core over both plastoquinone and benzoquinone analogues was identified as these were unable to rescue ATP levels and provide cytoprotection under identical conditions. Using these optimised structural features, a redox active dye capable of sensing a reductive stimulus such as NQO1 was also developed.

Therefore, the identified analogues that are superior to idebenone require a naphthoquinone core with a methyl substituent in the C3 position, a side-chain containing a four-carbon linker and an amino alcohol or equivalent amine attached through an amide linkage. Biological analysis *in vitro* identified 34 analogues significantly superior to idebenone out of a total of 131 synthesised compounds. This is a significant result, as currently idebenone is the only therapeutic approved to treat LHON. Two of those analogues (**70** and **80**) have advanced to *in vivo* studies in two different disease models. Both new idebenone analogues were highly efficient and were shown to restore mitochondrial-dysfunction-induced vision loss in a mouse model of LHON and a rat model of diabetic retinopathy. Therefore, this research significantly advances the development of new therapeutics to treat mitochondrial dysfunction.

As a result of the research presented in this thesis, a provisional patent was filed in 2017.

Acknowledgements:

I wish to express my sincere gratitude to the following people and institutions, without whom, completing this PhD would not have been possible.

Firstly my supervisors, A/Prof Jason Smith, A/Prof Nuri Gueven and Dr Alex Bissember, your guidance and support during the course of my studies has been invaluable. Thank you for making this journey enjoyable, challenging yet rewarding at the same time.

To Monila Nadikudi, thank you for the continuous biological testing of my compounds, without the quick turn around our SAR would never have developed and neither of our PhDs would have been successful.

I would like to thank my friends and colleagues in the Smith and Bissember research group, both past and present. With particular mention to the groups senior members James Howard, Jeremy Just and Kieran Rihak, your help, assistance and friendship has made this journey enjoyable.

To Dr Luke Hunter from the University of New South Whales (UNSW), thank you for the guidance in relation to the solid phase peptide synthesis and your patience in teaching me while we were in different states.

Thanks also to Abraham Daniels for his biological data from the *in vivo* studies investigating diabetic retinopathy, James Horne, for his continual assistance with NMR experiments and Graham Meredith for his assistance with absorption and fluorescence spectrometry.

I would like to acknowledge the University of Tasmania for awarding me the Tasmania Graduate Research Scholarship to undertake my studies.

Finally to my family and friends, for your unconditional love and support throughout the past four years. Particularly my parents, your support and encouragement to begin this journey has made me the person I am today.

Abbreviations:

Boc	*t*-Butyloxycarbonyl
Fmoc	9-Fluorenylmethyl carbonyl
DMAP	Dimethyaminopyridine
DMF	Dimethylformamide
DMT	Dimethyltyrosine
HRMS	High resolution mass spectrometry
h	Hours
IR	Infrared
min	Minutes
r.t.	Room temperature
NMR	Nuclear Magnetic Resonance
ppm	Parts per million
SAR	Structural Activity Relationship
TFA	Trifluoroacetic acid
Tic	1,2,3,4-Tetrahydroisoquinoline-3-carboxylic acid
TLC	Thin Layer Chromatography
o/n	Overnight
AA	Amino Acid
DNA	Deoxyribonucleic Acid
ATP	Adenosine Triphosphate
ROS	Reactive Oxygen Species
CoQ_{10}	Coenzyme Q_{10}

NADPH	Nicotinamide adenine dinucleotide phosphate
Lys	Lysine
Arg	Arginine
Trp	Tryptophan
His	Histidine
Tyr	Tyrosine
Phe	Phenylalanine

List of Publications:

N. Gueven, K. Woolley, J. A. Smith, *Redox Biology*, **2015**, *4*, 289 – 295

List of Patents:

Australian Provisional Patent **Application No. 2017901457** "Therapeutic compounds and methods" – 2017

Chapter 1: Introduction

1.1 Quinones in nature and their role in mitochondria

Quinones represent an important class of molecules, which are ubiquitous in nature. Quinones are compounds that contain a 1,4-quinioid ring structure (**1**) but differ in the substitution on the quinone core and the length and functionalization of the carbon side chain substituent. Biologically active quinones have two key features which are referred to as the 'head' and 'tail', the polar quinone core is the head and the long aliphatic chain is referred to as the tail.[1] Due to their reversible redox-characteristics, quinones are widely found in nature as co-factors, antioxidants, signalling molecules and vitamins, including vitamin K (**2**) and Coenzyme Q_{10} (CoQ_{10}) (**3**) (Figure 1).[2-5] Quinones can be broken down into three subclasses; benzoquinones, plastoquinones and naphthoquinones.

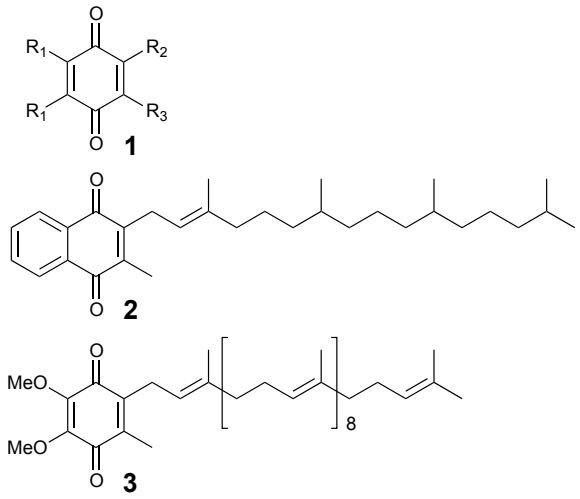

Figure 1: An example of the quinioid ring structure (**1**) and two naturally occurring quinones, Vitamin K (**2**) and CoQ_{10} (**3**).

Vitamin K (**2**) is identified as a naphthoquinone (**4**) as it contains a bicyclic ring structure derived from naphthalene (Figure 2). Plastoquinones (**5**) feature three methyl substituents and are a subclass of benzoquinones, which are all remaining quinones (Figure 2). In comparison, CoQ_{10} (**3**) is classed as a benzoquinone as it contains two methoxy and one methyl substituent on the quinone core (**6**) (Figure 2). Unless otherwise stated, in

this thesis, benzoquinone will refer to a quinone moiety containing two methoxy and one methyl substituent. These particular classes of compound are responsible for the transfer of electrons in many biological processes, particularly within the mitochondria and a disruption to these processes is associated with many diseases.[6]

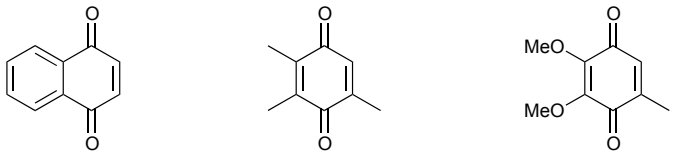

Figure 2: Structures of the naphthoquinone (**4**), plastiquinone (**5**) and benzoquinone (**6**) moieties.

Mitochondria play an essential role in the production of energy within cells; 90 % of cellular energy is provided by the mitochondria through the electron transport chain.[7] The electron transport chain consists of four multimeric protein complexes located in the inner mitochondrial membrane. Electrons are transported along the complexes to molecular oxygen to ultimately produce water. Simultaneously, protons are pumped out of the mitochondrial matrix across the mitochondrial inner membrane by complexes I, III and IV (Figure 3).[8] This forms an electrochemical gradient (also called mitochondrial membrane potential) across the inner mitochondrial membrane, which is utilized by complex V (also called adenosine triphosphate (ATP) synthase) (Figure 3). This multimeric protein complex allows the protons to re-enter the mitochondrial matrix and in this process ADP is phosphorylated to ATP.[8-10]

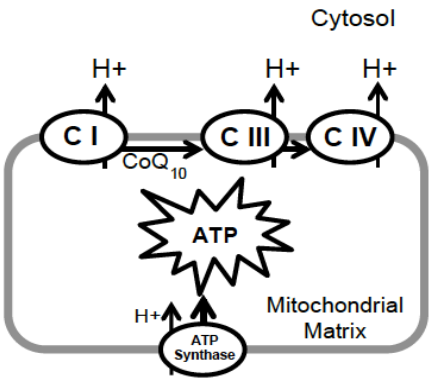

Figure 3: Schematic diagram of the mitochondria, illustrating the shuttle of electrons to Complex I, III and IV and the resulting proton gradient.

One of the best-known physiological quinones is CoQ_{10} (**3**), which belongs to the class of benzoquinones and features a hydrocarbon side-chain of ten isoprenyl units (Figure 1). CoQ_{10} (**3**) acts as a potent, physiological antioxidant in its reduced form and is essential for cellular energy production due to its role as an electron carrier. Because of its ability to undergo reversible redox reactions with enzyme complexes of the mitochondrial respiratory chain,[11,12] CoQ_{10} (**3**), is responsible for the electron transport between mitochondrial complexes I, II and III (Figure 3).

1.2 Mitochondrial Dysfunction

Electron transport through mitochondria, which is aided by quinone compounds such as CoQ_{10} (**3**)(Figure 1), is responsible for supplying all higher organisms with carbohydrate-derived chemical energy in the form of ATP through oxidative phosphorylation.[13] However, inadequate electron transfer within the respiratory chain can lead to the formation of reactive oxygen species (ROS), which results in oxidative damage to cellular macromolecules such as lipids, proteins and DNA that can potentially lead to cell death.[14]

ROS can be generated within the mitochondria at several sites of the electron transport chain, particularly in complexes I and III. Here, electrons can be lost due to ineffective electron transfer within the respiratory complexes as a result of inherited mutations in complex subunits. This process can, in turn, lead to inadequate reduction of CoQ_{10} (**3**) to the semiquinone by a single electron transfer (Figure 4).[11] This forms a phenolic radical, which is the most reactive form of cellular oxygen radicals and under physiological conditions is immediately detoxified to less reactive compounds such as hydrogen peroxide by mitochondrial enzymes. In addition, other enzymatic processes within the mitochondria also have the ability to produce smaller levels of ROS.[13] Under ideal conditions, quinones are reduced by a two-electron transfer to prevent the formation of the semiquinone radical, which results in a ROS (Figure 4).

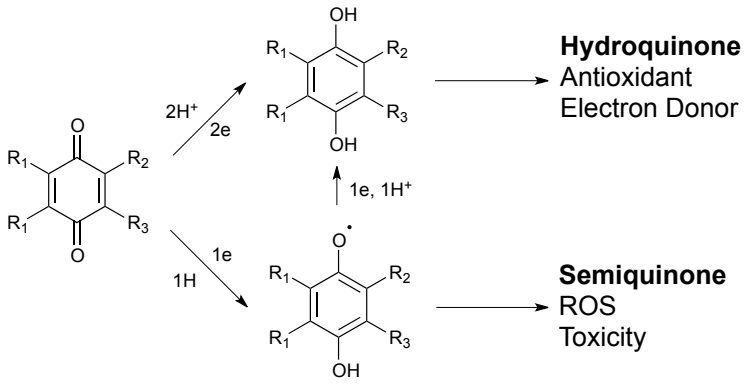

Figure 4: Schematic representation of quinone bioactivation by a two-electron transfer to produce the stable hydroquinone (top) compared to a single electron transfer that generates the unstable semiquinone (bottom).

A break down in this mitochondrial electron transport process and a reduction in these high energy molecules can result in mitochondrial dysfunction and can be classified into primary and secondary dysfunction.[15] Primary dysfunction results from a mutation in a gene encoded by mitochondrial DNA (mtDNA) or a nuclear-encoded gene for a mitochondrial protein that is maternally inherited as the mother is the sole contributor of mitochondria to their offspring.[16] In contrast, secondary dysfunction is an acquired dysfunction and arises from pathological events, environmental factors or lifestyle, that occur outside the mitochondria such as in the case of cancer, diabetes, neurodegeneration (i.e. Alzheimer's, Huntington's and Parkison's disease) and autoimmune diseases.[6,15,16] Despite the large variation in disease types, they all share the common feature of defective cellular energy metabolism with diminished ATP levels, abnormal oxidation metabolism and a surplus production of free radicals.[17]

Although a lot of common diseases are associated with mitochondrial dysfunction, there are very few approved therapeutics available on the market that intentionally target and treat mitochondrial dysfunction.[18] Due to the need for therapeutics to transfer electrons through the respiratory transport chain, quinone analogues, which have the ability to undergo oxidation and reduction, are an obvious choice as potential therapeutics. Currently there are various quinone analogues under investigation as potential therapeutics, which share varied structural features with CoQ_{10} (**3**).

However, the highly lipophilic tail of CoQ_{10} significantly limits its effectiveness as a potential therapeutic. Indeed, the use of naturally occurring quinones is limited by their pharmaco-chemical characteristics such as poor solubility, limited bioavailability and their broad effects on a multitude of physiological processes.[2] Furthermore, variation of their chemical and physiochemical properties can lead to significant differences in pharmacological effects often without clear structure-activity relationships (SAR).[2]

1.3 Potential Therapeutics

Over the past decade significant progress in the development of mitochondrial quinone therapeutics have been made. These all contain similar core motifs but possess different lengths and functionality of their side-chain to reduce hydrophobicity and ultimately produce better pharmacokinetic profiles.[13,19] Typically, CoQ_{10} is administered orally and because it displays poor solubility in aqueous environments, intestinal adsorption of dietary CoQ_{10} is extremely limited.[2,11,14,19] Only chronic ingestion of large doses increase CoQ_{10} concentrations within the body.[11] Thus, synthetic analogues of CoQ_{10} with enhanced pharmaco-chemical characteristics are required. A variety of currently developed quinone analogues will be discussed in detail below.

EPI-743

EPI-743 (α-tocotrienol quinone, **7**) is a vitamin E analogue (Figure 5) and belongs to the class of plastoquinones that are characterised by three methyl substituents on the quinoid core (Figure 1). In addition, EPI-743 also contains a hydrocarbon side chain that is similar to CoQ_{10} but only contains four isoprenyl units with hydroxylation of the isoprenyl unit alpha to the quinone core. α-Tocotrienol quinone (EPI-743, **7**) is described as a natural metabolite of α-tocotrienol, which is a naturally occurring compound that can be isolated from *Elaeis guineensis*, which is commonly referred to as the African oil palm. Like CoQ_{10} (**3**), EPI-743 (**7**) is an electron-acceptor, possesses antioxidant activity and was developed by *Edison Pharmaceuticals* to treat hereditary respiratory chain diseases.[20]

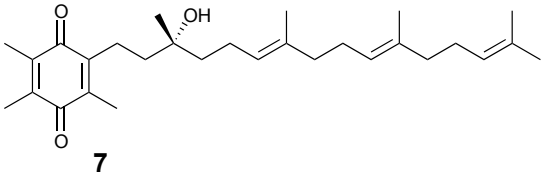

7

Figure 5: Structure of EPI-743 (**7**) featuring the plastoquinone moiety with one of the four isoprenyl hydroxylated.

EPI-743 (**7**) is in clinical trials for a variety of mitochondrial diseases, including Friedreich ataxia, Leigh syndrome (LS), and Lebers hereditary optic neuropathy (LHON).[21-23] EPI-743 (**7**) has been shown to restore mitochondrial redox balance in the mitochondria of patients genetically diagnosed with Leigh syndrome, which is characterised by impaired energy synthesis and increased oxidative stress. LS arises from defects in the mitochondrial, nuclear or X-linked genes.[23] Although the results of this trial were promising, only a small sample size of ten children was treated. Patients received EPI-743 (**7**) three times daily for six weeks and levels of reduced, oxidised and protein-bound glutathione were analysed from blood samples.[23] At the end of the study the children showed an apparent reversal of disease progression. However, due to the small number of patients in this trial these results have to be interpreted with caution.[21]

In an open label study involving a small cohort of patients approaching end-of-life care, EPI-743 (**7**) was reported to improve the quality of life of patients with various inherited mitochondrial diseases. Notably, no serious adverse effects (SAE) were observed. This indicated that although the patients were not cured, EPI-743 (**7**) might have had an effect on the progression of the various mitochondrial diseases.[24] Similarly, some LHON patients showed a recovery of vision when receiving EPI-743 (100 – 400 mg per dose) orally, three times daily.[22] The halt of disease progression and some reversal of vision loss were seen in four of the five patients within three months.[22] Although EPI-743 (**7**) showed promise as a potential therapeutic for a variety of inherited mitochondrial diseases, it should be noted that clinical trials and studies at present have only been performed on small sample sizes, in a relatively uncontrolled manner and therefore further investigation is required.

Mitoquinone (MitoQ)

Mitoquinone (MitoQ, **8**) is a benzoquinone analogue containing a lipophilic cation, which directly targets the molecule into the mitochondria by a mitochondrial membrane potential dependent mechanism. MitoQ features the same benzoquinone moiety of CoQ_{10} but has a triphenylphosphonium (TPP) cation attached to the quinone through a 10-carbon linker with a mesylate counter anion (Figure 6).

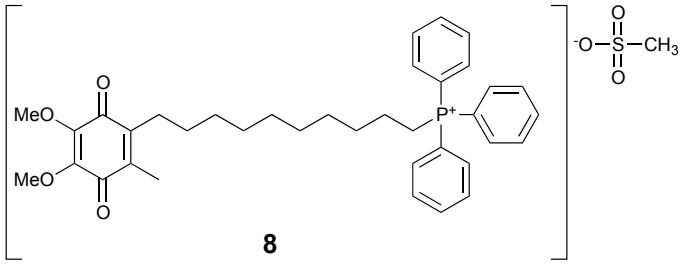

8

Figure 6: MitoQ (**8**) features benzoquinone moiety attached *via* a 10-carbon linker to the TPP cation.

MitoQ (**8**) is a positively-charged molecule that is orally available and is an antioxidant that can easily pass through biological membranes including the blood-brain barrier and muscle cells.[19] Due to its positive charge MitoQ (**8**) accumulates several hundred-fold in the mitochondria as it requires no specific uptake mechanism to pass through the phospholipid bilayers.[25] This is in contrast to other quinone analogues, which distribute into extracellular and intracellular compartments in addition to the mitochondria. This means MitoQ (**8**) provides exceptional protection against oxidative damage.[19,26]

MitoQ (**8**) has been investigated for multiple hereditary mitochondrial diseases *in vivo*, including Alzheimer's disease, multiple sclerosis (MS) and retinopathy.[27-29] MitoQ (**8**) was found to reduce neurological disabilities associated with MS as well as the suppression of inflammatory markers and the reduction of neuronal cell loss, which is a key underlying factor of most motor disabilities.[27] These protective effects, as well as the reduction of oxidative stress levels indicate that MitoQ could be a potential new candidate for MS.

However, further experiments with MitoQ (**8**) in other mitochondrial diseases did not have the same successful outcomes. In a mouse model designed to investigate inherited photoreceptor degeneration (IPD) with a major characteristic being increased oxidative stress, MitoQ (**8**) was unable to reduce oxidative stress, restore complex I activity and glutathione (GSH) levels or provide any protection against IPD.[28] Similarly, a placebo-controlled study into Parkinson's disease showed no effect on the progression of the disease over the treatment period of one year.[30] These unsuccessful outcomes indicate the need to further analyse MitoQ (**8**) as a potential therapeutic for mitochondrial dysfunction before any further conclusions can be made.

SkQ1

SkQ1 (**9**) is an analogue of MitoQ (**8**) where the benzoquinone moiety has been replaced with a plastoquinone moiety, which contains two methyl substituents (Figure 7). SkQ1 (**9**) also features a ten-carbon linker and a triphenylphosphonium (TTP) cation with a bromine counteranion. SkQ1 (**9**) can readily accumulate within the mitochondria in a similar manner to MitoQ (**8**) at a several hundred-fold concentration gradient. This is because it also requires no specific uptake mechanism to pass through the phospholipid bilayer due to its positive charge.[31]

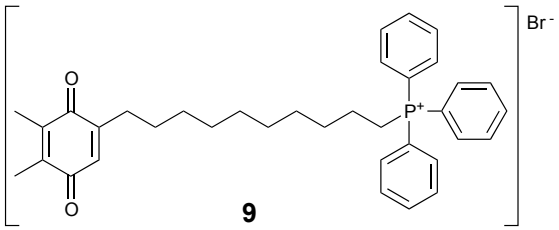

9

Figure 7: Structure of SkQ1 (**9**) featuring a plastiquinone moiety attached *via* a 10-carbon linker to the TPP cation.

Although SkQ1 (**9**) was shown to be a prooxidant at micromolar concentrations, at sub-micromolar concentrations it displays antioxidant activity.[31] SkQ1 has been studied in relation to treatment of senescence, retinopathy, dry eye syndrome and for prolonging life.[31-34] In an animal study investigating retinopathy in rats, SkQ1 (**9**) prevented the onset of retinopathy

as well as reducing the severity of pre-existing pathological changes in the retina at nanomolar concentrations.[32] SkQ1 (**9**) has also been shown to prolong the lifespan of crustaceans, fungus and mice and was particularly effective in the early to middle stages of ageing. In mammals, the effects of SkQ1 (**9**) on ageing were also accompanied by its ability to inhibit the onset of age related diseases and traits.[31] TPP analogues have great potential as therapeutics but also face issues with concentration, as high accumulation of the lipophilic cations in the mitochondrial matrix can result in a disruption to the mitochondrial membrane potential and inhibit mitochondrial respiration and ATP production.[35]

Szeto – Schiller Peptide (SS-31)

SS-31 (**10**) differs from the above analogues in that it does not feature a quinone moiety. SS-31 (**10**) is a small water soluble tetra–peptide, featuring an aromatic-cationic sequence with alternating aromatic and basic residues (Figure 8). This enables it to enter cells without requiring an active form of uptake (i.e. peptide transporters).[36,37] SS-31 (**10**) uptake is thought to be independent of the mitochondrial membrane potential but is reliant on selective binding to the inner membrane.[6] SS-31 (**10**) is an antioxidant due to the presence of the dimethyl tyrosine moiety as it can readily scavenge a variety of ROS and inhibit lipid peroxidation.[36] By analogy to the triphenylphosphonium analogues, SS-31 (**10**) can concentrate approximately 1000 – 5000-fold in the inner mitochondrial membrane.[38,39]

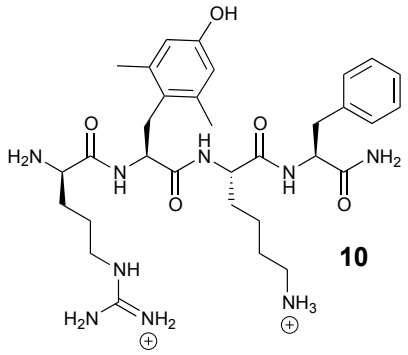

10

Figure 8: SS-31 (**10**) structure featuring the aromatic-cationic structure with Arg-DMT-Lys-Phen-NH_2 fragments.

The effectiveness of SS-31 (**10**) against varying diseases associated with elevated ROS production has been studied in animal models. The results of these studies indicate that SS-31 (**10**) reduced the symptoms associated with the elevated ROS levels, and appeared to have no toxic side-effects.[36] In an animal model investigating diabetic retinopathy, SS-31 (**10**) was found to reverse visual decline without improving glycemic control or body weight.[40] In comparison, progressive visual decline in the untreated animals occurred before obvious symptoms of metabolic and ophthalmic abnormalities were apparent, which was accompanied by compromised glucose clearance and elevated blood glucose and bodyweight.[40] This indicates that treating with SS-31 (**10**) in the early stages of visual dysfunction in the course of diabetes could possibly prevent permanent vision loss.

Similarly, in an animal model investigating Alzheimer's disease, SS-31 restored altered protein expression in mice and rescued memory and learning deficiencies.[41] This indicates that SS-31 (**10**) could be a potential therapeutic to slow down cognitive decline.[41] Similar positive results were obtained from ischemia-reperfusion injury, Parkinson's disease, muscle atrophy and weakness and metabolic syndrome indicating the potential of SS-31 (**10**) as a therapeutic.[39] However, further investigation is required.

1.4 Leber's Hereditary Optic Neuropathy and Idebenone

Leber's Hereditary Optic Neuropathy (LHON's)

A primary dysfunction of interest is Lebers hereditary optic neuropathy (LHON), which is caused by single point mutations within the mitochondrial DNA (mtDNA).[22] LHON is a disease commonly found in young males of all ethnic groups, between 15 – 30 years of age resulting in acute loss of vision leading to permanent blindness with an incidence of approximately 1:45,000.[3,42] Vision loss is observed in 50 % of male carriers but only seen in 10 % of female carriers.[26] Disease onset is painless, rapid and after affecting the first eye, loss of vision in the second eye occurs typically within a few weeks to a couple of months.[3,43] Vision loss is severe and LHON presents with severe unilateral, followed by bilateral, loss of central and colour vision, which finally leads to blindness.[22]

LHON is defined as an inherited respiratory chain disorder but differs from other respiratory chain diseases by its restriction to the retina, whereas most other mitochondrial diseases affect multiple tissues, i.e. the brain, heart, muscles. In contrast, the pathology of LHON is highly specific and only affects the retinal ganglion cells.[22,44] One of three mtDNA mutations are responsible for the majority of LHON's cases (90-95%),[45] which affect the nicotinamide adenine dinucleotide (NADH) dehydrogenase (ND) subunit genes at positions ND4 (11778G > A), ND1 (3460G > A) or ND6 (14484T > C). These mutations result in the dysfunction of complex I of the mitochondrial respiratory chain, which prevents the transport of electrons.[22,26,46] Vision loss is in most cases permanent with the ND4 (11778 G>A) mutation being the most abundant.[42] However, in the case of ND6 (14484T > C), some patients have been described with partial or full spontaneously recovered vision 1–5 years after the onset of the disease without any treatment.[22,47]

The three classical LHON mutations impair oxidative phosphorylation, reduce ATP production and increase oxidative stress.[26] These features can be explained; as a mutation of a complex I subunit results in the failure to transfer electrons from NADH to CoQ10 (**3**), which subsequently prevents proton pumping and the formation of the proton gradient. This failure ultimately stops ATP production, increases oxidative stress and results in cell death.[4] It should be noted that no particular mutation influences the timing or severity of the initial vision loss and although LHON's is hereditary and maternal, up to 40 % of patients have no traceable family history.[48]

It is proposed that environmental factors may increase visual failure and explain the incomplete penetrance observed in LHON, however, there is only limited data to support this hypothesis. A study in 2009 showed a strong and consistent association between vision loss and smoking, irrespective of gender and alcohol intake.[49] However, there was also a slight correlation between vision failure and alcohol consumption but only with heavy alcohol intake.[49] Further studies are required to support these findings before any definitive conclusions can be made.

Due to the fundamental activity of CoQ_{10} (**3**) in cellular energy production, short-chain quinone analogues have been proposed as a therapeutic option for LHON. Since 2015, a synthetic benzoquinone called idebenone (**11**) has been approved by the European Medicine Agency (EMA) for treatment of LHON.[50] However, approval was granted under the category of exceptional circumstances requiring further investigation and analysis. Idebenone (**11**), like CoQ_{10}, contains a benzoquinone moiety but differs in that it features a short ten-carbon side chain containing a terminal hydroxy group (Figure 9).

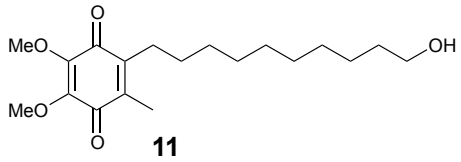

11

Figure 9: Structure of Idebenone (**11**).

Similar to other quinone analogues, idebenone (**11**) acts as an electron carrier in the electron transport chain and is also a potent antioxidant.[2,4,26] Idebenone (**11**) has been investigated for a variety of disorders associated with mitochondrial dysfunction such as Duchene muscular dystrophy (DMD),[51-54] multiple sclerosis (MS),[55] Parkinson's and Huntington's disease,[56] Friedreich's ataxia (FDRA).[57-59] In addition, in depth studies have evaluated the potential of idebenone (**11**) in LHON patients.[60-62] Idebenone (**11**) was found to have consistent tendencies towards visual recovery, with the therapeutic benefit of idebenone (**11**) shown in the acute phase of the disease.[26] In an Expanded Access Program (EAP), higher rates of clinical recovery were observed than expected naturally in patients, which was consistent with other clinical trials.[62]

Despite their structural similarities, CoQ_{10} (**3**) and idebenone (**11**) differ significantly in their physiochemical properties. Due to its highly lipophilic tail containing the 10 isoprenyl units (50 carbon atoms), CoQ_{10} (**3**) with a logD value of 19.12 is sparingly soluble in aqueous environments (LogD is the distribution coefficient between octanol and water at physiological pH (pH = 7.4) and is a measurement of solubility).[11] This results in very limited oral absorption.[11] In contrast, idebenone (**11**) contains a 10-carbon chain with a

terminal hydroxyl unit and a LogD value of 3.91. This provides greater polarity and increases its solubility in aqueous solutions, meaning it is much more readily available when administered as an oral formulation.[11]

In contrast to CoQ_{10}, idebenone (**11**) has been reported to undergo redox reactions outside the mitochondria. In the cytosol, idebenone (**11**) is reduced by NQO1 (recombinant NAD(P)H:quinone oxidoreductase) in a two-electron dependent reduction before re-entering the mitochondria and being oxidised by complex III. This process regenerates the mitochondrial respiratory chain, regenerates the proton gradient and restores ATP synthesis.[4] By this mechanism, idebenone (**11**) can effectively bypass the Complex I inhibition inherent to LHON. Notably, this ability has not been observed for CoQ_{10} (**3**), which is a direct result of its poor solubility.[2,4]

Although idebenone (**11**) was identified as the lead compound, 70 idebenone (**11**) analogues[2] were also tested for their capacity to normalise ATP levels under conditions of complex I dysfunction. The ability to rescue ATP levels was correlated to the solubility of the compounds, expressed as LogD. Unless analogues had a solubility in the range of 2<LogD<7 they were unable to restore ATP levels, which is explained by their inability to shuttle in and out of the mitochondria.[2] A high logD value will see a compound effectively restricted to the lipid bilayer (i.e. membrane) and are therefore unable to enter either the cytoplasm or the mitochondrial matrix. In an extension of this study, idebenone (**11**) was found to increase cell viability *in vitro* and normalise ATP levels.[3] In a subsequent *in vivo* study, idebenone (**11**) was reported to protect against RGC cell loss, retinal pathology and restore visual acuity in a LHON mouse model.[3]

It is known that the electron transport ability of idebenone (**11**) is solely due to the quinone motif,[18] but its ability to pass through the membrane and its association with the membrane is due to the lipophilic portion of the molecule.[4] Idebenone (**11**) has two significant issues due to its structure. The long side-chain of idebenone (**11**) is readily degraded by oxidation processes due to its analogous structure to lipids. In addition to this, idebenone (**11**) is activated solely by NQO1.[4,63]

However, a number of inactivating NQO1 polymorphisms are described in the general population such as 609C>T resulting in decreased or even absent enzymatic activity of NQO1.[14,64,65] This implies that in these individuals bio-activation of quinones is reduced or even absent.[14,64,65] Prevention of the inactivation of the quinone moiety is of high importance as failure to reduce the quinone can lead to cytotoxicity.[2] The prevention of quinone-mediated toxicity can be achieved through the development of molecules that are also bio-activated even in the absence of NQO1.

If the quinone portion is not reduced by a two-electron transfer, these compounds will be metabolized by the cytochrome (CytP450) enzymes as an attempt to detoxify the compounds in the liver. This reaction results in a single electron transfer, which gives rise to the unstable semiquinone and generates superoxide, which leads to cellular damage and can ultimately kill the cells.[2] It should be noted that only the reduced hydroquinone form of the molecule is active as an antioxidant and electron carrier.[14] This indicates that this benzoquinone moiety is not ideal as a therapeutic and as a result requires optimisation due to the possibility that for some individuals these compounds could be ineffective or even toxic. Consequently, the efficient two-electron reduction of quinones has to be targeted to avoid cellular toxicity as well as for the compounds to be of therapeutic potential.

Naphthoquinones, such as vitamin K (**2**), are a related group of quinones, which have a common 1,4-naphthoquinone core (**4**) containing an aromatic ring fused to the quinone moiety (Figure 10). Vitamin K plays well known roles in post transitional modifications of proteins required for blood coagulation and bone metabolism.[66] There is evidence that vitamin K is involved in maintaining brain function,[67] particularly in Alzheimer's[68] and Parkinson's disease.[69,70] A range of naphthoquinone derivatives with differing lengths of the aliphatic side chains in the C2 position and a methyl group at the C3-position have been reported to be highly neuroprotective agents.[66] In an animal model for epilepsy, naphthoquinone derivatives were able to successfully supress seizures.[71] The proposed mechanism for this naphthoquinone-dependent protection was based on their ability to maintain or restore energy (ATP) production.[71]

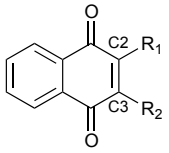

4

Figure 10: Structure of the naphthoquinone core (**4**) with C2 and C3 positions denoted.

Similar to benzoquinones, naphthoquinones are thought to be protective in pre-clinical disease models by modulating mitochondrial function and reducing oxidative stress.[66,69,70] However, in contrast to benzoquinones that are exclusively reduced by NQO1, naphthoquinones can be reduced to the hydroquinone by two different enzymes, vitamin K oxidoreductase 1 (VKORC1)[72,73] and vitamin K oxidoreductase 1 like 1 (VKORC1L1)[74] in addition to NQO1. This suggests that in individuals carrying the inactivating NQO1 polymorphism, naphthoquinones can still be efficiently reduced by two enzymes (Figure 11). Thus, the risk of generating reactive semiquinones as well as the associated elevated ROS production and toxicity should therefore be minimized.

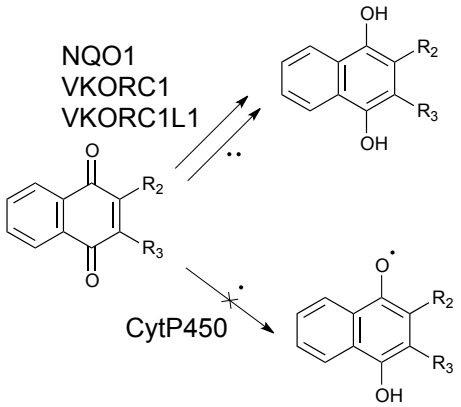

Figure 11: When naphthoquinones are reduced to hydroquinones by VKORC1, VKORC1L1 and NQO1, only minimal amounts of the unstable semiquinones should be formed.

In 2013, derivatives of menadione (3-methyl-1,4-naphthoquinone) (**12**) were synthesised in a preliminary study by the Smith/Gueven group at the University of Tasmania (UTAS) to investigate whether naphthoquinone analogues could provide greater protection against mitochondrial dysfunction

in the wider population.[75] Biological testing for potential therapeutics that could alleviate the molecular problems associated with LHON was performed using a synthetic Complex I inhibitor called rotenone, which replicates the molecular defect associated with LHON. Combining rotenone and retinal ganglion or HepG2 (liver) cell lines it was possible for Woolley *et al.*[75] to investigate the therapeutic potential of the naphthoquinone analogues.[3,4]

1.5 Preliminary Information

In 2013, a range of analogues by Woolley *et al.*[75] were synthesised by two established synthetic methods exploiting the addition of an alkyl radical by decarboxylation of readily available carboxylic acids. In this way, 26 naphthoquinone analogues containing different alkyl chains at the C2-position of menadione (**12**) were synthesised (Table 1).

Table 1: Naphthoquinone analogues **13** – **38** synthesised by Woolley *et al.*[75] in the 2013 preliminary study.

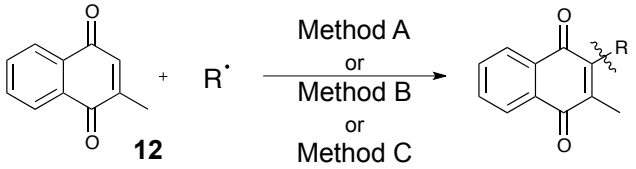

Entry	R =	Entry	R =	Entry	R=
1 [a]	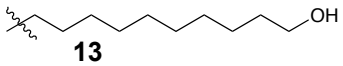 **13**	10 [a]	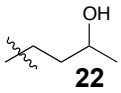 **22**	19 [b]	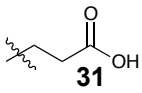 **31**
2 [a]	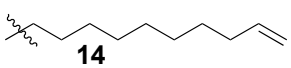 **14**	11 [a]	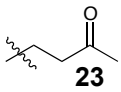 **23**	20 [b]	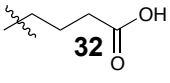 **32**
3 [a]	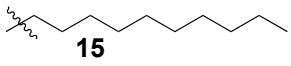 **15**	12 [a]	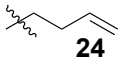 **24**	21 [c]	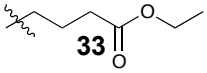 **33**
4 [a]	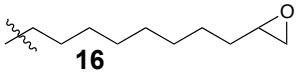 **16**	13 [a]	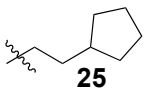 **25**	22 [a]	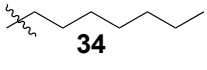 **34**
5 [a]	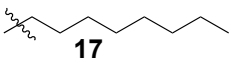 **17**	14 [a]	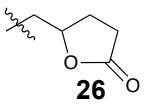 **26**	23 [a]	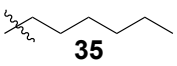 **35**

6 [a]	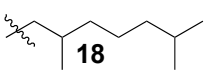	15 [a]	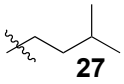	24 [c]	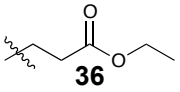
7 [c]	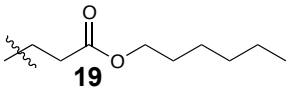	16 [a]	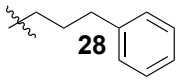	25 [c]	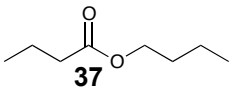
8 [c]	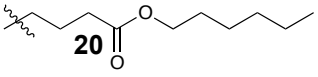	17 [a]	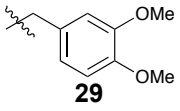	26 [c]	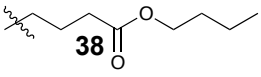
9 [a]	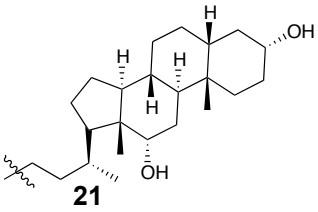	18 [a]	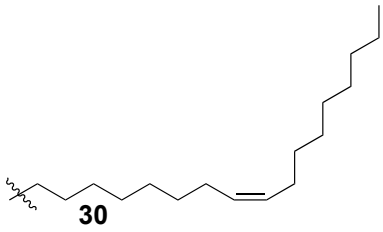		

[a] Synthesised *via* silver mediated radical decarboxylation[76]
[b] Synthesised *via* peroxide generated radical addition to the naphthoquinone[77]
[c] Synthesised *via* fischer esterification of analogues **29** or **30**

Biological evaluation of preliminary analogues from 2013[75]

Initially, analogues were tested for toxicity, as incomplete reduction to the semiquinone is associated with ROS production and oxidative damage. Endogenous toxicity was assessed in two cell lines with either high (HepG2) or low (RGC5) reducing capacity (Figure 12). The significantly higher IC_{50} in the HepG2 cells compared to the low reducing cell line (RGC5), indicated lower toxicity as well as supporting the hypothesis that the cellular reducing capacity of the cell line determines cellular toxicity of the quinones.

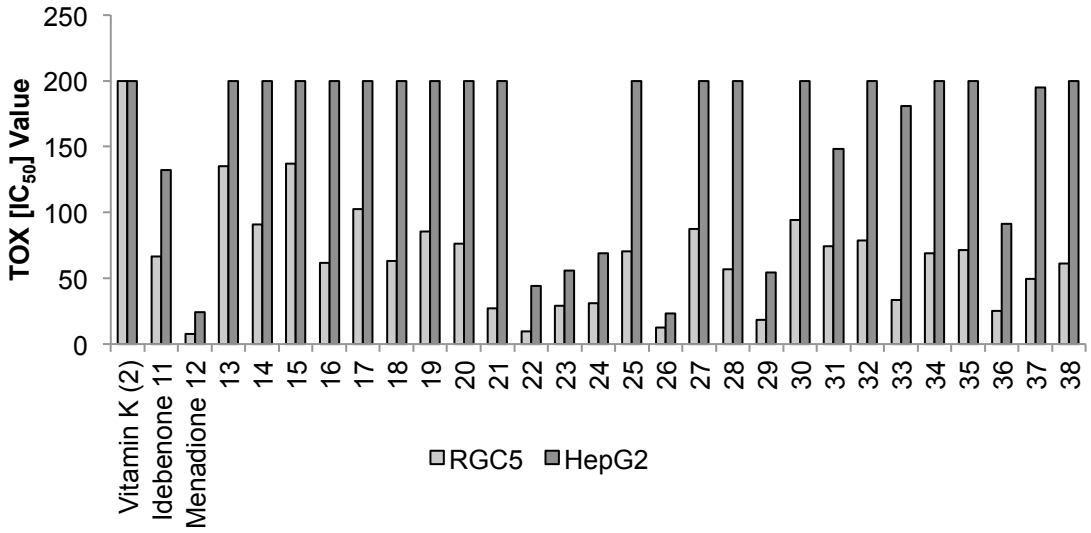

Figure 12: Toxicity of individual naphthoquinones measured in RGC5 and HepG2 cell lines. Concentrations are given as [µM]. IC_{50}: defined as reduction of cellular survival by 50%. Note: maximal concentration tested: 200 µM. *** IC_{50} analysis performed by Nuri Gueven at the University of Tasmania, unpublished results.

However, the most significant information obtained from the toxicity data is the direct comparison between idebenone (**11**) and the idebenone-like naphthoquinone derivative **13**. Besides the change from the benzoquinone core in **11** to the naphthoquinone core in **13**, both compounds are structurally identical (Figure 13). In both cell lines the change in the quinone core doubled the IC_{50} value, which illustrated that in otherwise identical compounds, a naphthoquinone moiety reduces cytotoxicity when compared to a benzoquinone moiety. This effect can likely be attributed to the more efficient reduction of the naphthoquinone core by VKORC1, VKORC1L1 and NQO1. It is known that HepG2 cells express high levels of NQO1,[4] while the level of expression of VKORC1 is currently unknown.

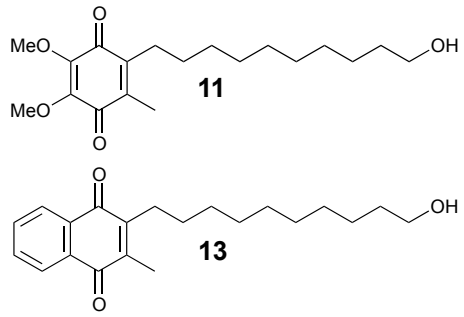

	TOX [IC_{50}] Values	
	RGC5	HepG2
Idebenone (**11**)	66.44	132.4
Analogue **13**	135.2	>200

Figure 13: Direct comparison of structure and toxicity levels of idebenone (**11**) and idebenone-like analogue **13**.

The naphthoquinone analogues were then evaluated for cytoprotection against rotenone-induced mitochondrial dysfunction in the two different cell lines, HepG2 and RGC5. Evaluation of cytoprotection is a five day process. On day one, the cells are seeded and, on day two, the cells receive a two-day pre-treatment with the desired analogue before being subjected to a six-hour rotenone challenge on day four. One day later (day five), ATP levels are measured as a percentage of the control. In both cell lines several novel quinones provided increased protection compared to idebenone (**11**) (Figure 14). However, no clear structure activity relationship (SAR) was detected within this suite of analogues. Nevertheless, it was noted that idebenone-like analogue **13** induced a high level of cytoprotection.

Furthermore, there were two noticeable trends, with removal of the terminal hydroxyl substituent of the idebenone-like naphthoquinone derivative **13** as seen in 10-C alkene derivative **14** and 10-C alkane derivative **15**, all protection was lost indicating the polarity of the hydroxyl substituent is important. Similarly, decreasing the aliphatic chain length to between four and eight carbons resulted in an increase in protection. Combining these two features and synthesising short chain- and oxygen-containing analogues provided a number of compounds exhibiting cytoprotection (**22**, **23**, **33**, **35**) at levels equivalent to idebenone (**11**) (Figure 14a,b).

In addition, cytoprotection was observed to be cell line specific, which is surprising given the previous data reported in the literature for benzoquinones which demonstrated no species or tissue dependency for biological activity.[2] The highest level of protection against rotenone-induced

mitochondrial dysfunction for the RGC5 cells was the ethyl ester analogue **36** (Figure 14b). In contrast, the HepG2 cell line exhibited very little protection by this analogue, with idebenone-like naphthoquinone derivative **13** and hydroxyl-butyl derivative **22** achieving the highest protection (Figure 14a).

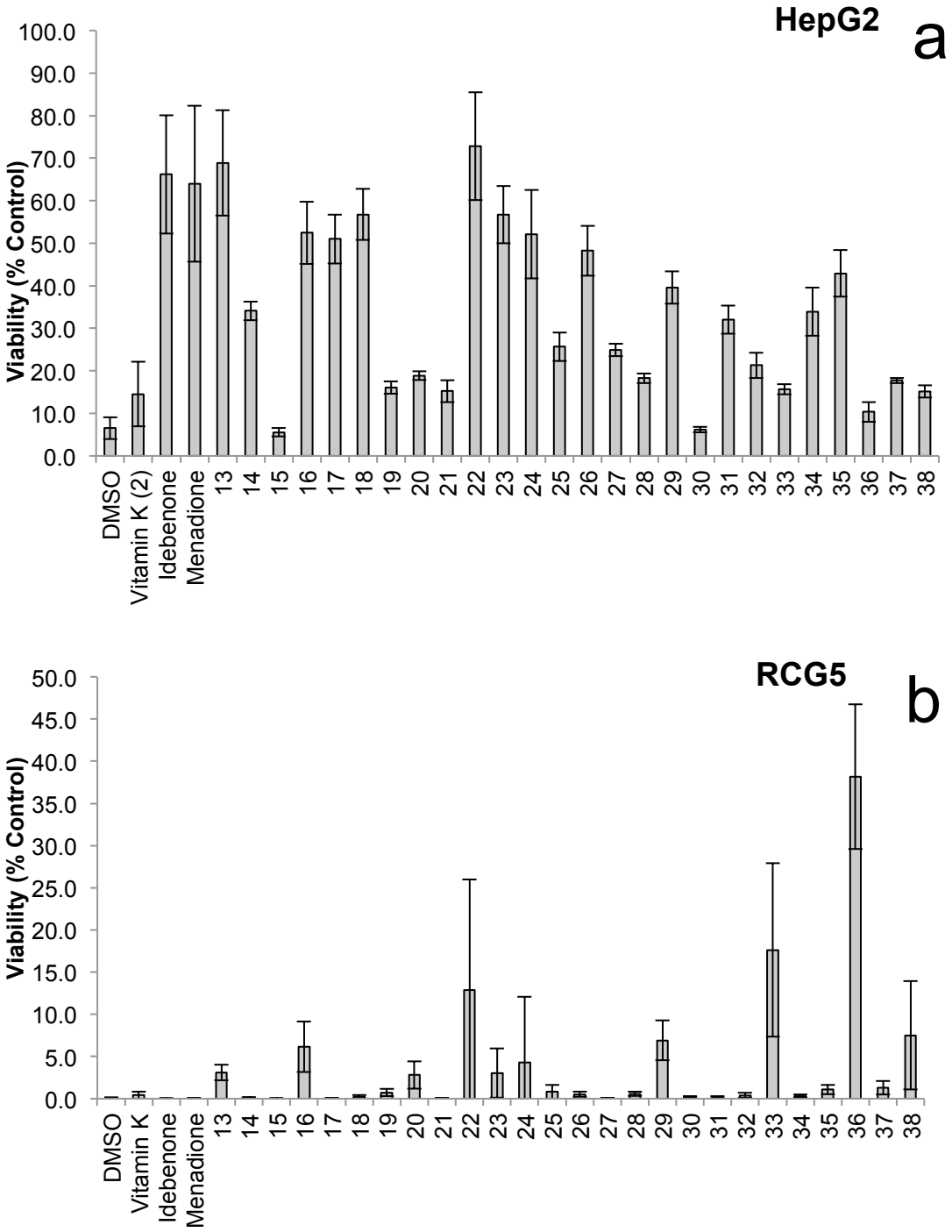

Figure 14: Cytoprotection against rotenone induced complex I dysfunction by quinones (**13** – **38**) at 10μM given as a relative percentage of cell survival compared to untreated HepG2 (a) and RGC5 (b) cell lines. Data represents the mean of n=3 independent experiments with 6 replicates each.

In line with work performed on idebenone (**11**) by Erb *et al.*,[2] analogues were investigated for their ability to restore ATP levels in HepG2 cells only. This was due to the lack of activity seen in the RGC5 cell line as a consequence of their low reducing ability. Evaluation of ATP requires a rapid two-hour assay; the cells are seeded and subjected to desired derivative for one hour before the addition of rotenone. One hour later, ATP levels are measured as a percentage of the control. Due to the proposed mode of action for idebenone (**11**) as a Complex I bypass agent that restores the electron transport chain and ultimately cellular ATP levels, the ability for an analogue to provide cytoprotection was thought to correlate to its ability to restore ATP. For idebenone (**11**) (Figure 15), ATP levels were restored from 15 % to 81 %. However, the remaining novel naphthoquinone derivatives failed to do so. In particular the idebenone-like naphthoquinone derivative **13,** showed no ability to restore ATP levels at all, whereas analogue **22** (3-hydroxybutyl side-chain) showed a slight improvement to 47 % in ATP levels, although nowhere near as substantial as idebenone (**11**). However, both idebenone-like naphthoquinone derivative **13** and hydroxylbutyl derivative **22** provided cytoprotection equal to that of idebenone (**11**). This result was surprising, as it suggested that an alternative ATP-independent pathway was mediating the cytoprotective activities of short-chained quinones.

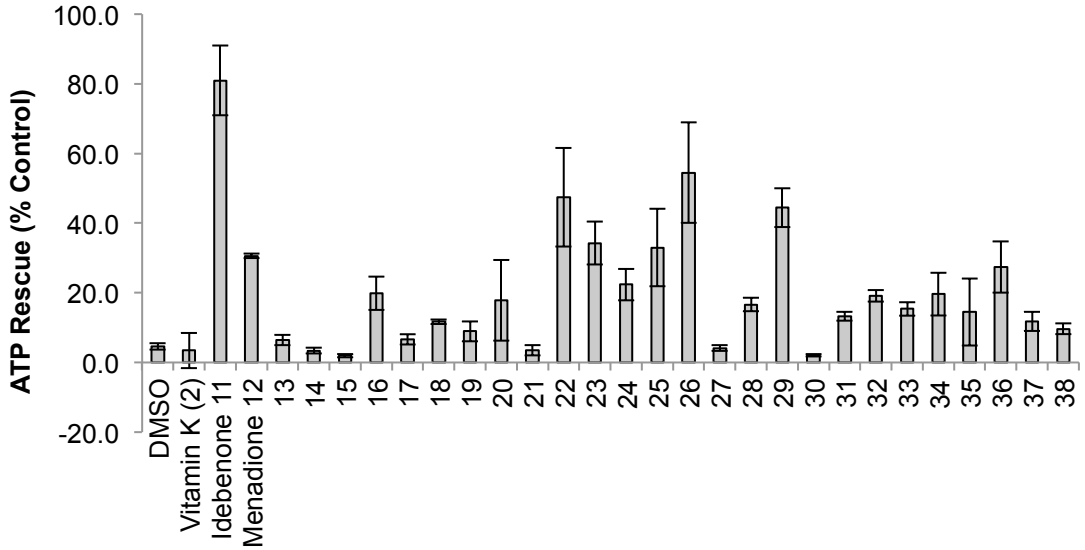

Figure 15: ATP rescue by quinones (**13** – **38**) at 10μM in the presence of rotenone-induced complex I dysfunction as percentage of untreated HepG2 cells. Data represents the mean of n=3 independent experiments with 6 replicates each.

Given the absence of any obvious SAR in either ATP rescue or cytoprotection assays, cytoprotection levels were plotted against cLogP (partition coefficient) to determine if the same correlation with compound solubility was observed as previously reported.[2] Previously, it was reported that for benzoquinones a Log P/D value of 2<LogP/D<7 was required for activity. However, neither cell line provided any support for this hypothesis. For example, hydroxylbutyl derivative **22** exhibited the highest level of cytoprotection in the HepG2 cell line with a cLogP value of 1.57, which is slightly outside of the 2<LogP<7 area, while the majority of the remaining analogues fell between a clogP of 2 – 7 but provided varying levels of cytoprotection (Figure 16).

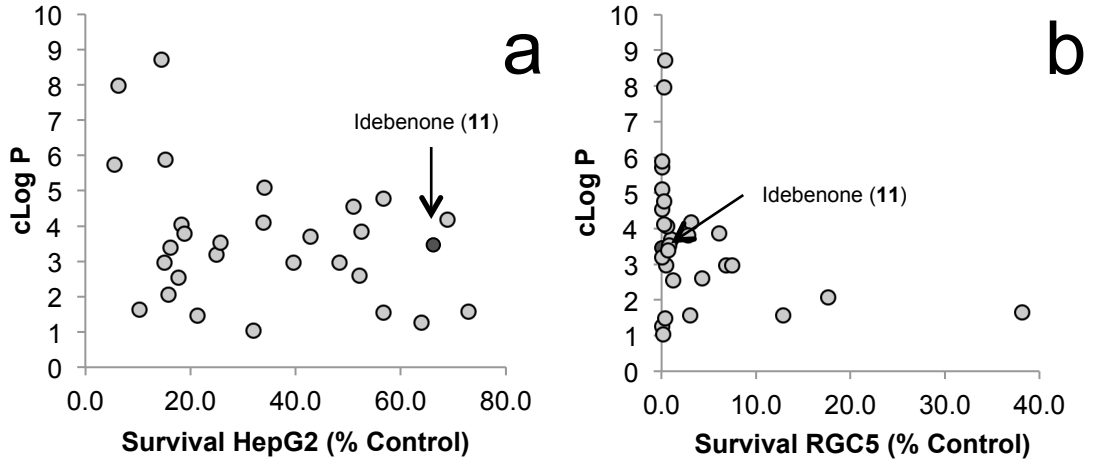

Figure 16: Viability correlation to clogP in both HepG2 (a) and RGC5 (b) cell lines with idebenone (**11**) identified by darker colouring.

Given the success of SS-31 (**10**) with the unique delivery mode to the mitochondria and desired solubility, it was proposed a peptide functionality attached to the quinone moiety might show significant activity. L-Phenylalanine methyl ester (**39**) was coupled to carboxylic acid analogue **32** (Scheme 1) to provide L-phenylalanine methyl ester derivative **40** as a model. This process was carried out using an amide coupling technique, which can readily be used to generate a large library of compounds if required.

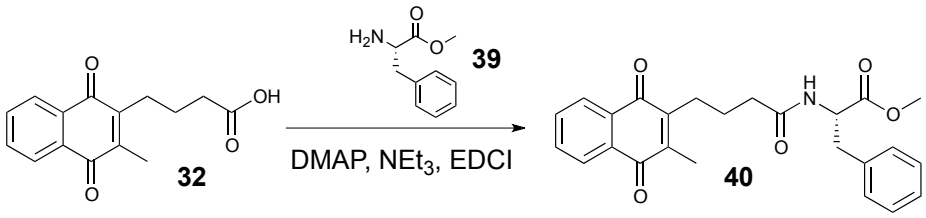

Scheme 1: Synthesis of analogue **40** *via* amide coupling.

Initial testing of L-phenylalanine methyl ester derivative **40** showed the most promising result from the entire initial suite of analogues. In addition to idebenone (**11**) this represented the new lead compound. L-phenylalanine methyl ester derivative **40** rescued ATP levels and provided cytoprotection in a similar manner to idebenone (**11**) (Figure 17). Although L-phenylalanine methyl ester derivative **40** is not a simple hydrocarbon and now contains an amide and ester functionality, the side-chain is somewhat similar in size to the structure of idebenone (**11**) and possesses similar activity.

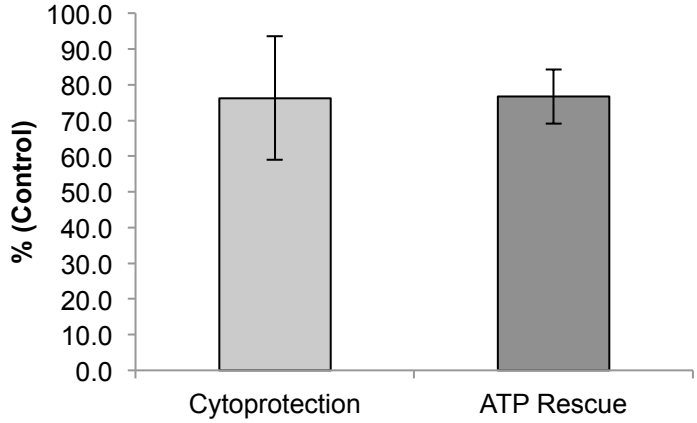

Figure 17: ATP rescue and cytoprotection against rotenone-induced complex I dysfunction by analogue **40** at 10μM given as a relative percentage of cell survival compared to untreated HepG2. Data represents the mean of n=3 independent experiments with 6 replicates each.

In addition to a similar size of the structure, if the solubility requirement is 2<LogP<7, L-phenylalanine methyl ester derivative **40** is in that target range with a cLogP value of 2.74. The correlation between ATP rescue and cytoprotection as well as the correct cLogP value implies that L-phenylalanine methyl ester derivative **40** as well as idebenone (**11**) are the new lead structures for further analogue development. However, with limited

SAR and only one successful structure, it is the basis for further investigation. The outcome of the preliminary study was essential to improve the specific cytoprotective characteristics of this class of compounds and to work towards the development of future therapeutics that can protect against mitochondrial dysfunction and oxidative stress.

1.6 Project Aims

Based upon the previous study by Woolley and co-workers[75] a number of aims were proposed for future analogue development, these being:

1. Investigate the redox properties of the previously synthesised quinone analogues. This will identify if there is a correlation between activity and the ability of an analogue to undergo oxidation and reduction.
2. Synthesise and fully characterize multiple small libraries of naphthoquinone analogues based on L-phenylalanine methyl ester derivative **40** and idebenone (**11**) as lead compounds with continuous biological testing for rapid next generation development.
3. Develop a structure activity relationship (SAR), to identify analogues that have both the ability to provide cytoprotection as well as restore ATP levels. These will then progress to animal models.
4. Optimize the quinone core moiety for further SAR development, to allow for the comparison of activity between quinone moieties.
5. Development of peptide targeting molecules based on Szeto–Schiller Peptide (SS-31) (**7**). The conjugation of these peptides with the quinone moiety would potentially enable the compound to be directly delivered to the mitochondria.
6. Development of a redox active dye capable of sensing a reductive stimulus such as NQO1 .

Chapter 2: Development of Structure-Activity Relationship (SAR) of the side chain

2.1 Investigation into Redox characteristics of preliminary compounds

Prior to synthesising new compounds, the redox properties of the naphthoquinone derivatives from the preliminary study were investigated. The current hypothesis for quinone compounds as therapeutics for electron shuttling in mitochondrial dysfunction has resulted in a general conclusion. This being, that as long as the compound can adequately pass through the mitochondrial membrane, then the quinone moiety should be able to restore the electron transport chain.[2] With no obvious structure activity correlations in the initial suite of 26 analogues by Woolley *et al.*[75] in the preliminary study, it was proposed that the cytoprotective activity observed could be explained through the oxidation and reduction ability of the quinone. If particular analogues were more easily oxidised or reduced than others, then in theory, their ability to provide cytoprotection would be enhanced and this could potentially explain the differences seen within the preliminary study. Therefore the redox properties of all analogues (**13** – **38**) and idebenone (**11**) were analysed by performing cyclic voltammetry. Idebenone (**11**) had an oxidation potential of –0.637 V and a reduction potential of –0.714 V. Similarly the idebenone-like naphthoquinone derivative **13** had an oxidation potential of –0.768 V and a reduction potential of –0.845 V (Figure 18).

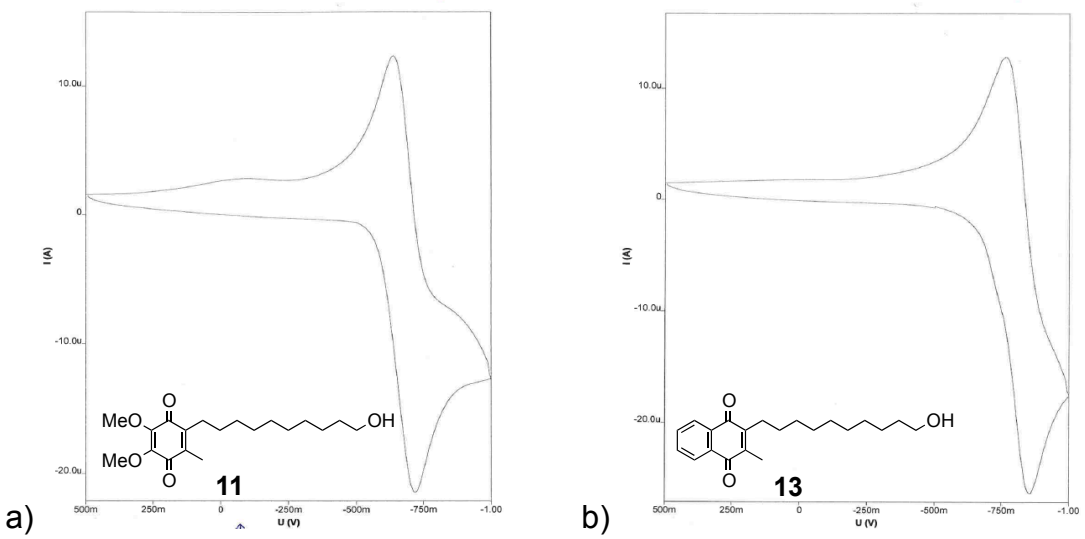

Figure 18: Cyclic voltammograms of a) Idebenone (**11**) and b) the idebenone-like derivative **13**.

Although there was a slight difference, there was no significant information obtained from this analysis, nor from the naphthoquinone derivatives (**14** – **40**). However, one exception to the redox characteristics was if a carboxylic acid or a functionality that could undergo oxidation separately to the quinone core was present. Specifically, carboxylic acid derivatives **31** and **32** underwent irreversible oxidation, *via* Kolbe oxidation. Kolbe oxidation leads to oxidative decarboxylation of a carbonate anion to generate radical intermediates.[78,79] Although this occurs during cyclic voltammetry, it is not possible in the assays and therefore is not of relevance to the comparison.

Therefore, the cytoprotective ability of the current suite of analogues (**13** – **38**), which were assayed in both the HepG2 and RGC5 cell lines, were plotted against both their oxidation and reduction potential. Intriguingly, despite substantial differences with regards to the cytoprotective abilities of these compounds, no correlation between the reduction or oxidation potentials of each analogue to its cytoprotective capacity was observed in both cell lines (Figure 19a – d).

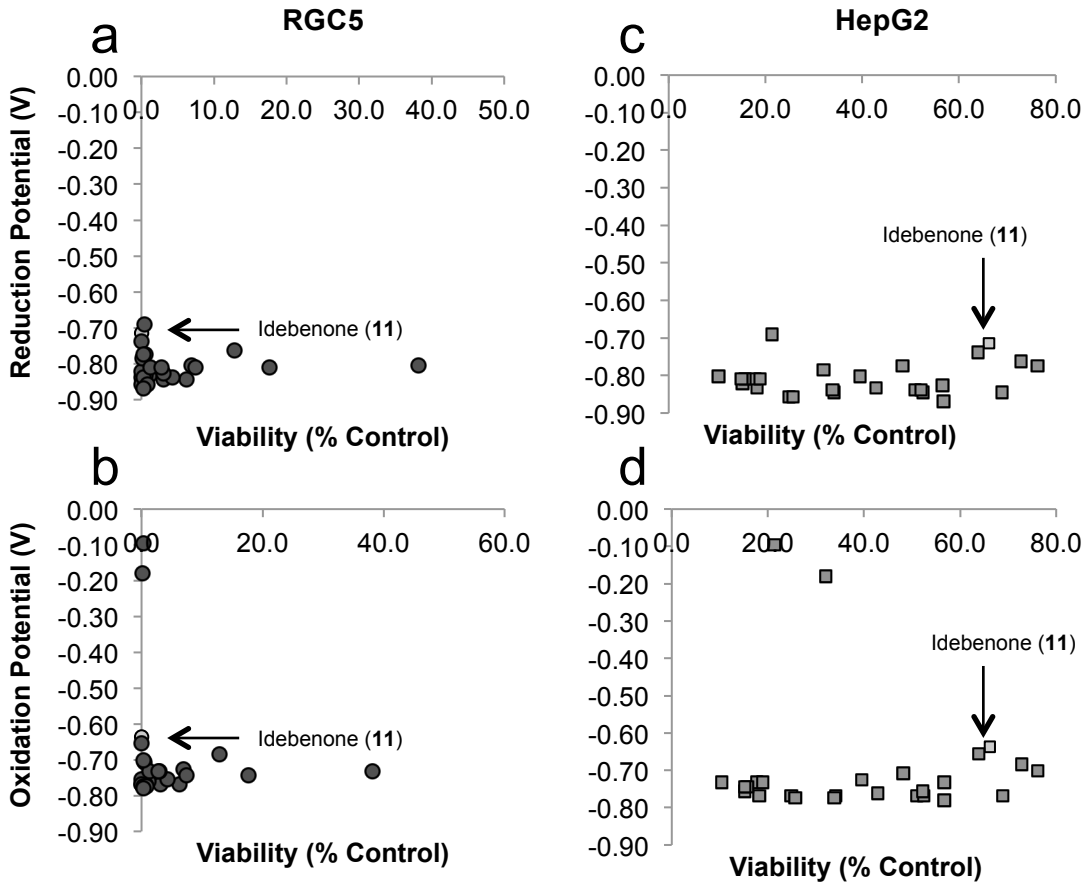

Figure 19: Protection of viability by naphthoquinones (10 mM) versus their redox characteristics as determined by cyclic voltammetry in two cell lines RGC5 (a,b) and HepG2 (c,d). Each data point is the average of 3 independent experiments with 6 replicates within each experiment for viability and 1 experiment for cyclic voltammetry. Error bars were omitted for clarity.

This strongly suggests that the redox characteristics *per se* do not influence cytoprotective function in the naphthoquinone series. Similarly, when comparing the benzoquinone core to naphthoquinone core, no significant difference in the oxidation or reduction potentials were observed, which indicates that the cytoprotective activity is likely associated with the specific functionality of the alkyl side chain rather than the specific redox-characteristics of the quinone. This conclusion is in agreement with earlier studies using a range of benzoquinones.[2]

2.2 Development of Structure Activity Relationships

2.2.1 Synthesis of analogues *via* silver-mediated radical decarboxylation

While initially waiting on further biological data to be obtained on the L-phenylalanine methyl ester derivative **40**, an investigation into the effects of analogues containing perfluorinated side chain was performed. Fluorinated analogues were desired to prevent metabolism of the alkyl side chain, as it was reported in the literature that the alkyl chain present in idebenone (**11**) undergoes rapid metabolism.[4,63] Formation of these analogues utilises radical chemistry, which enables the introduction of the alkyl chains with relative ease on to the naphthoquinone (Scheme 2). The alkyl radical can be generated by a variety of methods depending on the reaction conditions. Examples include Barton esters (*N*-hydroxypyridin-2-thione),[80] peroxy acids to generate the radical through thermal cleavage of the weak O–O bond[77], as well as the formation of metal salts using Mn^{III} acetate or Ce^{IV} ammonium nitrate[81,82].

However, in the case of naphthoquinones the most widely utilised method employs silver nitrate and ammonium persulfate to generate the carbon-centred radical. Silver nitrate forms a Ag^{I} carboxylate salt that is oxidised by persulfate to produce Ag^{II} which decomposes with the release of carbon dioxide. This provides a carbon-centred nucleophilic radical, which attacks the electron-deficient naphthoquinone. Oxidation of the ensuing intermediate delivers the substituted quinone (Scheme 2).[76]

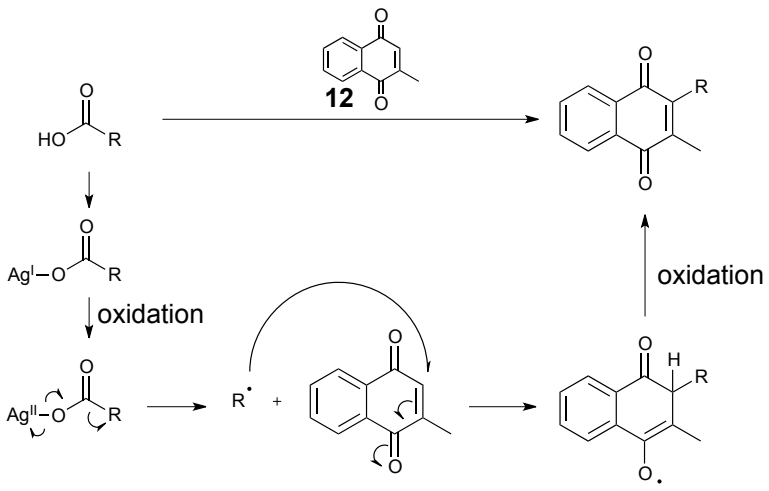

Scheme 2: Mechanism for the introduction of the alkyl chain *via* the silver-mediated radical decarboxylation.

Trifluorobutyric acid and 3-(trifluoro)-3-hydroxybutyric acid were utilised to make the initial fluorinated derivatives due to their ready availability (Table 2). These two acids are also functionally similar to the desired characteristics identified in the previous data, which indicated oxygen containing short alkyl chains provided the high level of cytoprotection. These analogues were synthesised by the silver-mediated radical decarboxylation protocol and isolated using flash chromatography in low to moderate yields. It is worth noting, the low yields are a result of un-optimised reaction conditions.

Table 2: Synthesis of fluorinated analogues **41** and **42**.

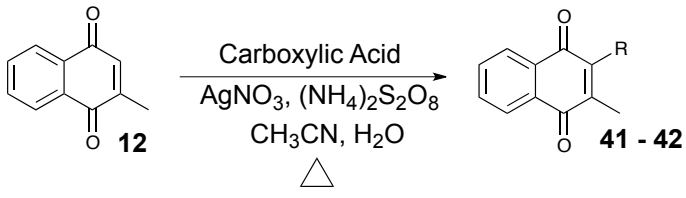

Entry	Carboxylic Acid	Product	Yield %
1	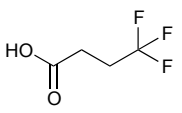	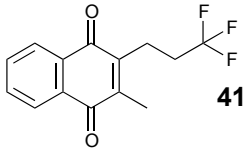 **41**	35
2	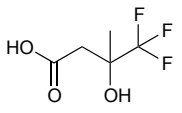	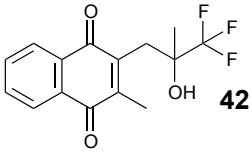 **42**	14

The formation of the fluorinated naphthoquinone analogues were supported by ^{1}H NMR spectroscopy with the absence of a singlet peak at 6.84 ppm indicating the loss of the proton attached to the C3-position of the 2-methylnaphthoquinone (menadione, **12**) along with the additional peaks in the aliphatic region. Both ^{1}H NMR and ^{13}C NMR analysis showed complex splitting patterns due to the presence of fluorine substituents (fluorine is a half spin nucleus). Very clear splitting of the three carbon resonances for the propyl side chain by the three fluorine atoms was observed in the ^{13}C NMR spectra for both analogues (see, for example, Figure 20).

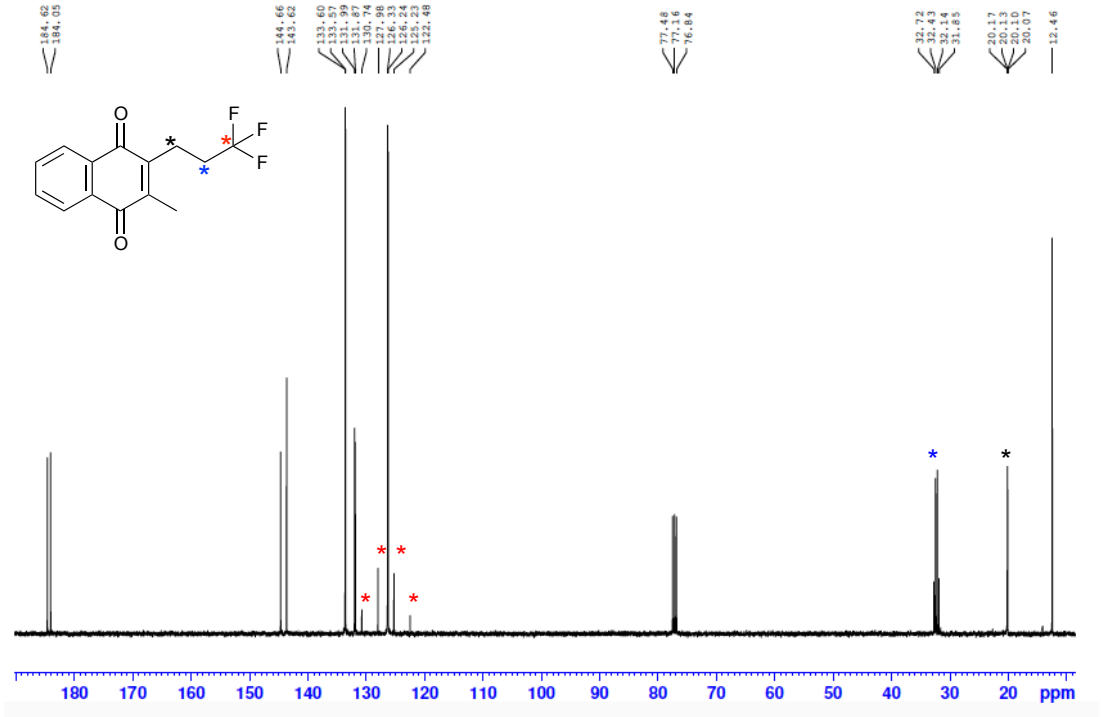

Figure 20: ^{13}C NMR spectrum for analogue **41** illustrating the fluorine splitting pattern.

In addition to fluorinated derivatives, analogues containing two alkyl chains were desired. Di–alkylated analogues were synthesised following the same method described earlier. However, naphthoquinone (**4**) was reacted with excess carboxylic acid to allow for the addition of both alkyl chains. Formation of the di–alkylated species proceeded in exceptionally low yields (Table 3). It appears the first alkylation proceeds with yields comparable to what was previously observed with menadione (**12**). However, formation to

the di–alkylated species proceeds in very low yields and, only from 4-methylpentanoic acid was a di–alkylated product in 10 % yield obtained.

Table 3: Synthesis of mono– and di–alkylated analogues of naphthoquinone (**4**).

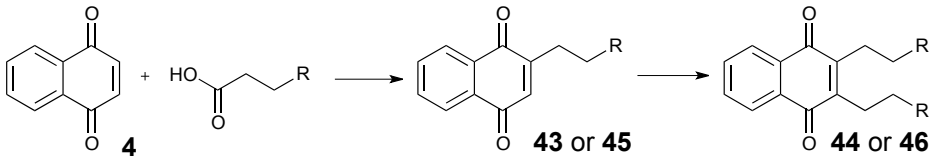

Entry	Carboxylic acid	Product	Yield %	Product	Yield %
1	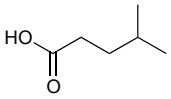	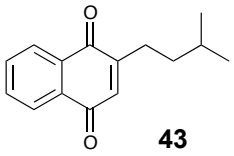 **43**	35	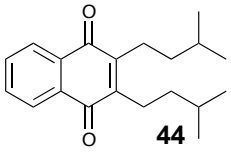 **44**	10
2	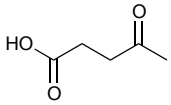	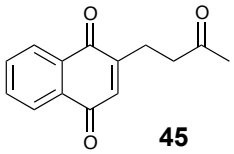 **45**	0	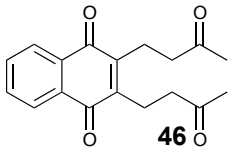 **46**	0

Formation of analogue **43** was supported by NMR spectroscopic analysis. A signal shifted upfield in the ^{1}H NMR spectra from 6.98 ppm to 6.78 ppm, for a singlet integrating for two to a triplet integrating for one with allylic coupling of J = 1.4 Hz indicating the loss of the proton in the C2 position of the naphthoquinone core (**4**) and the new attachment of a single alkyl chain. Comparison of the ^{1}H NMR spectra of the mono-alkylation product to di–alkylated analogue supported the introduction of the second alkyl chain. The highly characteristic triplet at 6.79 ppm for the proton attached to the C3 position of the quinone core was absent and all signals in the aliphatic region responsible for the alkyl chain had doubled in integration values relative to the quinone core.

Analogues **45** and **46** could not be synthesised, which it strongly indicates that there was an issue with the formation of the radical. This method proved to be insufficient for introducing di–alkyl chains on to the naphthoquinone (**4**). Particularly when to develop SAR, a large library of analogues is required.

Biological evaluation of molecules **42** and **43** was investigated before this group of analogues were investigated further.

The capacity of the two new fluorinated analogues (**41** and **42**) and the mono- and di–alkylated analogues of 4-methylpentanoic acid (**43** and **44**) to promote cell viability (cytoprotection) and rescue ATP levels was investigated by colleagues in the School of Medicine. Biological evaluation in both assays illustrated that fluorination or mono– or di–alkylation has no positive impact on the biological activity (Figure 21).

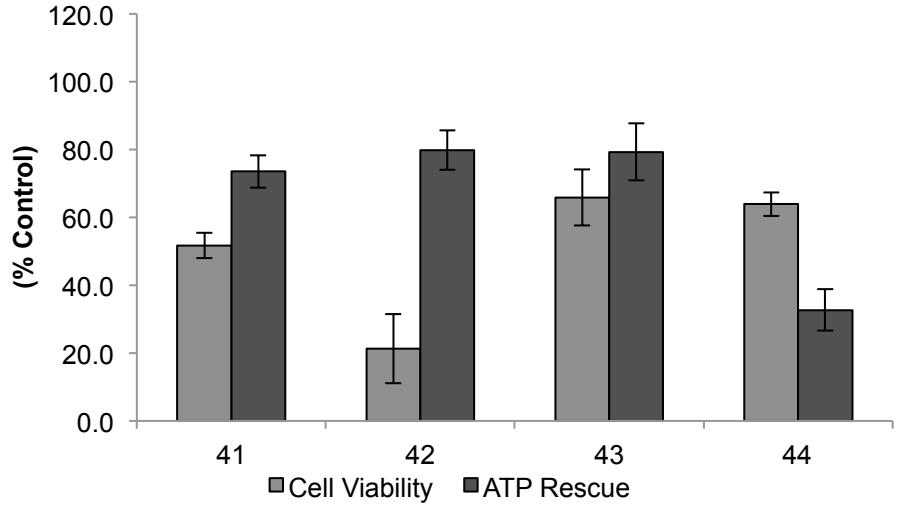

Figure 21: Protection of viability and acute rescue of ATP levels against rotenone induced complex I dysfunction by naphthoquinones. Both cytoprotection and ATP rescue in HepG2 cells by naphthoquinones (10mM) are displayed as percentage of untreated control (no rotenone).

Analogues (**41** – **44**) performed poorly in one (ATP rescue) of the two assays. As previously discussed with the preliminary analogues, if the proposed mechanism for idebenone (**11**) is correct, there should be a correlation between ATP rescue and cytotoxicity. Optimisation of the analogues should result in therapeutics that exhibits high levels of both. Therefore the four new analogues were combined with the initial suite of preliminary analogues and were plotted against each other to identify correlations. Including the four new analogues, the compounds were divided into characteristic groups based on the structure of the side chain (aliphatic, slight polarity (with reference to the straight aliphatic chains, i.e. containing

oxygen), acids and aliphatic esters) in an attempt to identify structure activity relationships (SAR). As seen in Figure 22, neither the new fluorinated analogues, nor the di-alkylated analogues show any significant activity when compared to the initial suite of compounds.

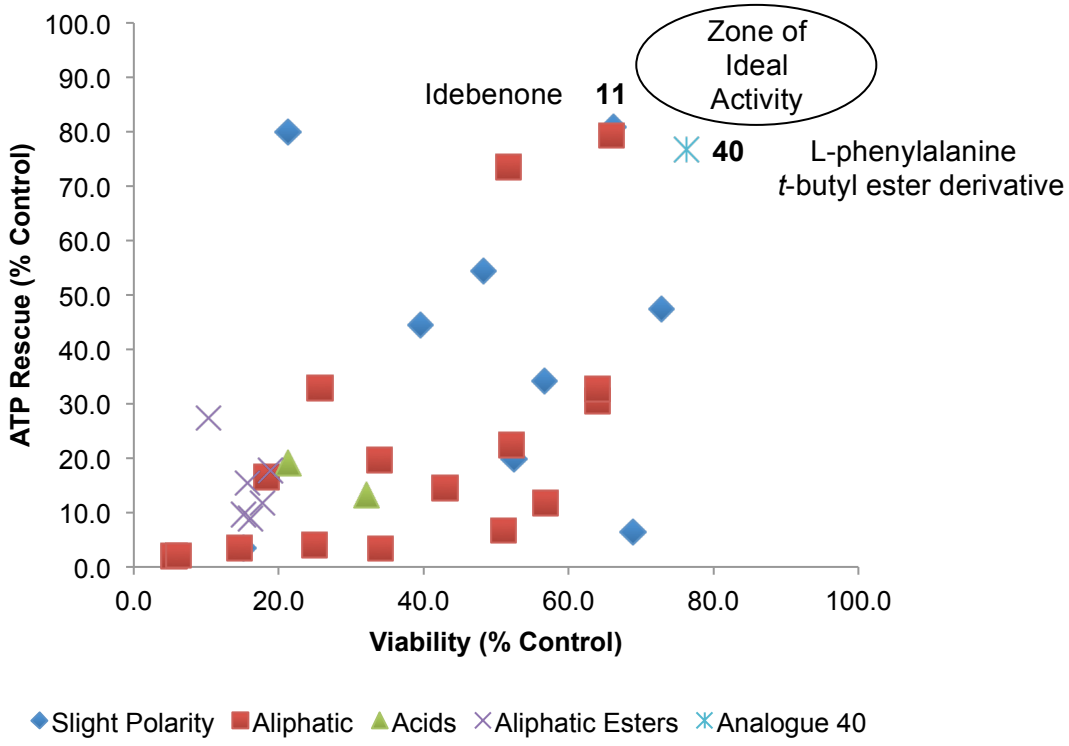

Figure 22: Protection of viability versus acute rescue of ATP levels against rotenone-induced complex I dysfunction by naphthoquinones. Both cytoprotection and ATP rescue in HepG2 cells by naphthoquinones (10mM) are displayed as percentage of untreated control (no rotenone) with error bars omitted for clarity. Data represents the mean of n=3 independent experiments with 6 replicates each.

A general grouping was observed in aliphatic and aliphatic esters, whereas acids and the slightly polar analogues showed varied response in both assays (Figure 22). The aliphatic compounds were unable to rescue ATP levels in the presence of the mitochondrial inhibitor rotenone, whilst having a varied ability to provide cytoprotection. On the other hand, aliphatic esters are grouped tightly but did not protect viability or rescue ATP levels. With no significant data obtained from the recently synthesised analogues (**41** – **44**) as seen in Figure 21 or Figure 22, L-phenylalanine methyl ester derivative **40** still remained the lead compound. L-phenylalanine methyl ester derivative **40**

provided the highest level of cytoprotection and is within error of idebenone (**11**) with respect to the ability to rescue ATP levels, which has not been exceeded by the novel naphthoquinone analogues. With analogues of L-phenylalanine methyl ester derivative **40** containing an amino fragment high priority, optimisation of the synthetic approach to the carboxylic acid precursor **32** was required. In the preliminary study, this analogue was synthesised following a literature procedure[77] *via* thermal decarboxylation of a peroxyacid intermediate to generate the carbon-centred radical which underwent thermal cleavage before addition to the quinone as shown in Scheme 3.

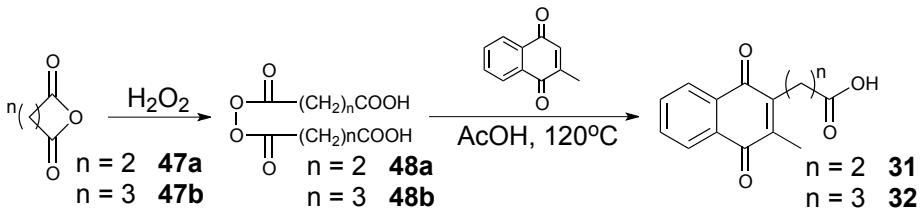

Scheme 3: Synthesis of analogues **31** and **32** *via* a peroxyacid intermediate to generate the carbon centred radical.[75]

However, this method is not viable for a larger scale synthesis for a number of reasons. Firstly, this method is extremely low yielding particularly the first step involving the generation of the peroxyacid intermediate (**48a/b**) and, secondly, due to safety reasons the peroxyacid intermediate was not dried and was used immediately upon formation.[75] With this in mind, a new method needed to be identified, and returning to the silver-mediated method seemed the most viable option as it typically proceeds efficiently with naphthoquinones.

Unfortunately, synthesising an acid-containing naphthoquinone derivative *via* the silver-mediated method provides products (**31** or **32**) that are also susceptible to further decarboxylation. This results in a second radical intermediate causing a dimer formation (**52**) as seen in Scheme 4. As the protocol utilises carboxylic acids to generate the carbon-centred radical, once the carboxylic acid (**32**) is formed, it can undergo oxidative decarboxylation and dimerise with a second molecule of menadione (**12**), resulting in

undesired by-products. Bisquinone (**52**) was subjected to biological evaluation and showed no ability to provide cytoprotection.

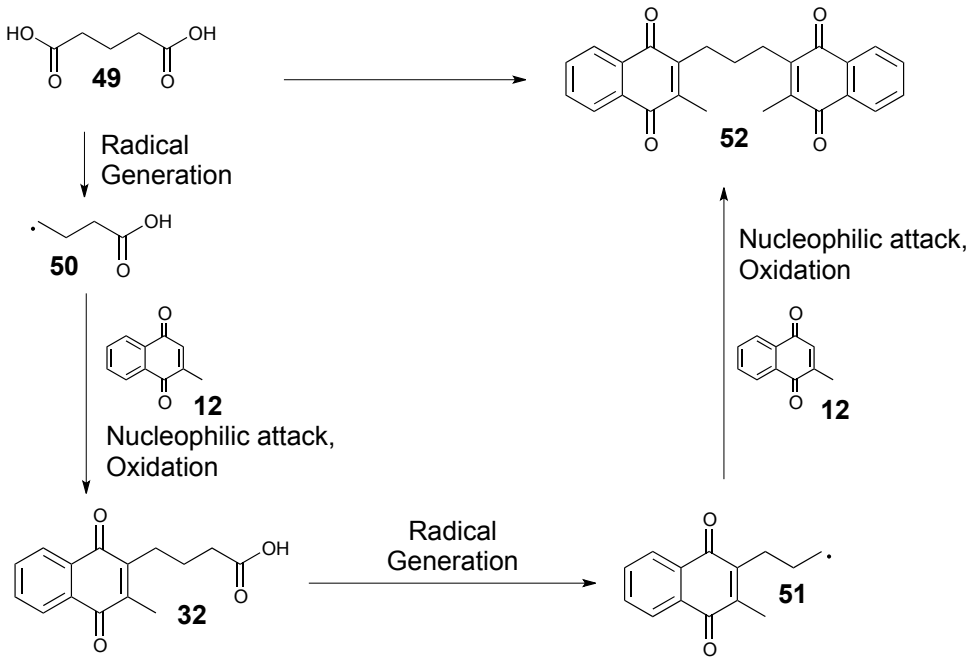

Scheme 4: Potential formation of by-product **52** during the synthesis of carboxylic acid derivative **32** from menadione (**12**).

Formation of the dimer is not ideal and could easily be prevented by protecting the acid as its methyl ester, which would be hydrolysed in a subsequent step. However, hydrolysis in the presence of a quinone normally results in decomposition.[75] Therefore, the simplest option to synthesise analogue **32** *via* this method, was to optimise conditions and prevent formation of bisquinone **52**. The literature method[76] indicates that the addition of a ammonium persulfate solution in water occurs over a 2 h period. However, for the initial suite of analogues in the preliminary study it was found that the slow addition of ammonium persulfate over a 2 h period was not required, with comparative yields obtained over a 15 min addition time frame followed by a 2 h reaction. These conditions were used for all analogues in the initial suite.

When attempting to synthesise carboxylic acid **32**, optimisation of the reaction conditions was undertaken, with investigation into the addition time of the ammonium persulfate as well as the reaction time (Table 4). The very

slow addition over a 2 h period gave rise to carboxylic acid (**32**) and bisquinone (**52**) in very low yields with high levels of impurities. However, with the 15 min addition of ammonium persulfate only carboxylic acid **32** was obtained in reasonable yields.

Table 4: Yield comparison of the two different methods for the synthesis of **32** from menadione **12**.

Entry	Addition of Ammonium Persulfate (h)	Reaction time (h)	Yield % **32**	Yield % **52**	Impurity Present
1	1.0	1.0	18	<1	Yes
2[#]	0.25	0.5	10	0	No
3[#]	0.25	1.0	15	0	No
4[#]	0.25	1.5	15	0	Yes
5[#]	0.25	2.0	15	0	Yes
6*	0.25	1.0	62	0	No

[#] Synthesis performed with what was identified post reaction as a decomposed bottle of ammonium persulfate, * is a repeat with new batch of ammonium persulfate.

However, reaction time proved to be crucial. If the reaction time exceeded 1 h the formation of an unidentified by-product occurred. Purification of the product from this intractable by-product was not possible by flash column chromatography. The impurity, a yellow oil, displayed a broad signal from 1.00 – 4.50 ppm in the ^{1}H NMR spectrum. Unfortunately, this meant that the reaction was quenched before complete consumption of menadione (**12**), as the reaction needed to be quenched prior the formation of the impurity.

However, the starting material can easily be recovered after purification by column chromatography. The starting material menadione (**12**) was eluted with 100 % dichloromethane, while elution with 100 % ethyl acetate afforded the carboxylic acid product (**32**). Similarly, reaction scale was important to obtain high yields. When the scale exceeded one gram of menadione (**12**), formation of the product (**32**) dramatically decreased. Therefore, multiple

one-gram reactions were performed in parallel to provide multi-gram quantities of material. In this way, carboxylic acid **32** was synthesised rapidly and used in subsequent amide coupling reactions to generate a library of amide/peptide analogues.

2.2.2 Synthesis of analogues *via* amide coupling

Synthesis of the analogues *via* amide coupling represents a straightforward method to obtain a wide variety of analogues with diverse functionality. Analogues were synthesised *via* known methods for amide coupling. Formation of an amide bond, with an example being the peptide bond, is the formation of a bond between the carbon terminus of a carboxylic acid fragment and the nitrogen terminus of amine fragment with the use of a coupling agent (Scheme 5).

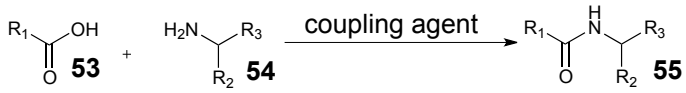

Scheme 5: Formation of a peptide bond.

Due to the nature of amide coupling, when coupling amino acids, protecting groups are selectively introduced and removed on the carboxylic acid group that is not required for coupling to ensure self-coupling does not occur. The carboxylic acid group of the amino acid is commonly protected as its methyl or ethyl ester. However, as demonstrated with carboxylic acid **32** in the preliminary study in 2013 by Woolley *et al.*,[75] base hydrolysis, which is the common removal technique for these type of esters results in decomposition of the compound and therefore alternative protecting group was required. *t*-Butyl esters are also common carboxylic acid protecting groups, due to their ease of deprotection under mild acidic conditions. For this reason, *t*-butyl groups were utilised to generate a library of amino acid derivatives.

A large variety of amide coupling agents are now widely used in synthetic organic chemistry. Originally, dicyclohexylcarbodiimide (DCC) (**56**) (Figure 23) was the first reagent used as a coupling agent due to its insensitivity to moisture and excellent yields. Its use was first reported by Sheehan and Hess in 1955.[83] However, issues with racemisation of stereogenic centres

resulted in the use of additional additives such as 1-hydroxybenzatriazole (HOBt) (**57**) being added to supress these undesired processes and increase the reaction rate.[84]

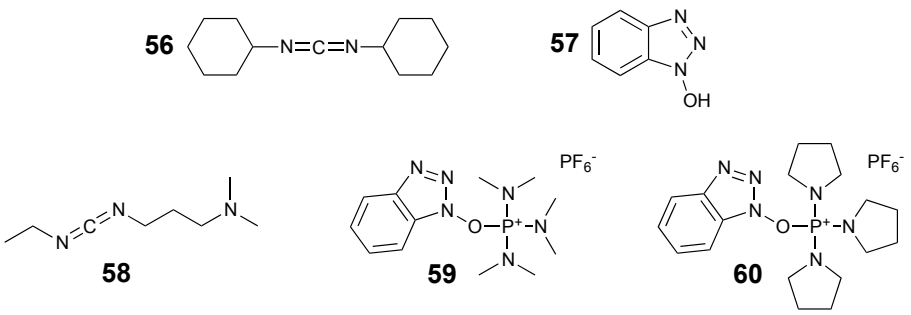

Figure 23: Structures of coupling agents DCC (**56**), EDCI (**58**), BOP (**59**), PyBOP (**60**) and additive HOBt (**57**).

Over recent decades, many new coupling agents have been developed which are superior to DCC (**56**) meaning additives are no longer required and their use is aligned with substrate complexity. For this research, coupling agents EDCI (1-ethyl-3-3(3-dimethylaminopropyl-carbodiimide) (**58**), BOP, (benzotriazol-1-yloxy) tris(dimethylamino)phosphonium hexafluorophosphate, (**59**) and PyBOP (benzotriazol-1-yloxy)-tripyrrolidinophosphonium hexafluorophosphate (**60**) (Figure 23) were used depending on the substrate being synthesised. The reactions proceeded with EDCI (**58**) as the coupling agent unless otherwise stated; while reactions that contained hindered, precious or difficult to make substrates utilised the stronger coupling agents, BOP (**59**) or PyBOP (**60**) as a precaution.

The polarity of idebenone (**11**) appears to be an important factor. This was also demonstrated by the naphthoquinone derivatives in the preliminary study, where the absence of the alcohol functionality in the 10-carbon alkene derivative **14** and the 10-carbon alkane derivative **15** showed a significant decrease in the cytoprotective capacity when compared to the idebenone-like analogue (**13**). The simplest way to modify L-phenylalanine methyl ester derivative **40** to obtain increased polarity in the side chain was to convert the amino ester to an amino acid derivative. With the use of the *t*-butyl ester this can be easily achieved. Therefore a variety of acid derivatives containing varying functionality were synthesised to prepare the next suite of

compounds for biological evaluation following the previously developed method (Table 5).[75]

Table 5: Synthesis of *t*-butyl ester analogues **61** – **68**.

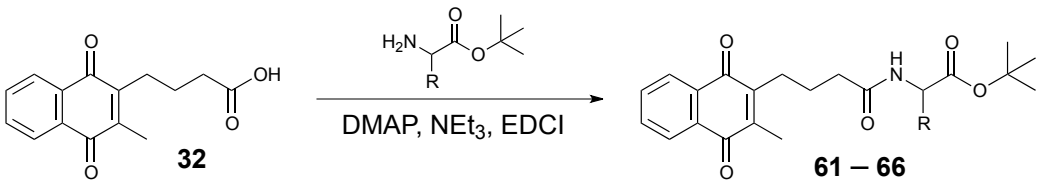

Entry	Amino Ester	Structure	Yield (%)
1	L-phenylalanine *t*-butyl ester	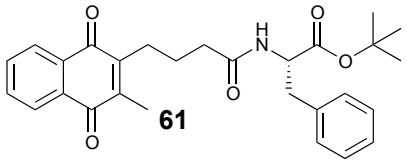 **61**	36
2	L-proline *t*-butyl ester	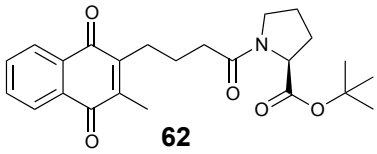 **62**	53
3	L-norvaline *t*-butyl ester	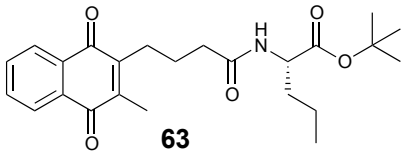 **63**	44
4	glycine *t*-butyl ester	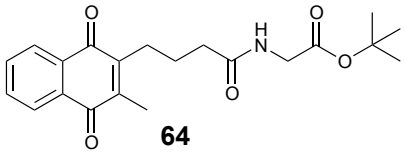 **64**	36
5	L-leucine *t*-butyl ester	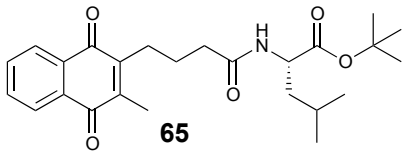 **65**	39
6	L-tyrosine *t*-butyl ester	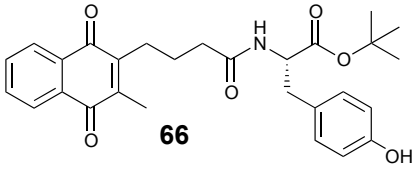 **66**	20

The successful formation of analogues (**61** – **66**) was consistent with spectroscopic data, particularly with ^{1}H NMR and ^{13}C NMR spectroscopy. The incorporation of the amide portion was supported by the ^{1}H NMR spectrum with a doublet present in all analogues at ~6.15 ppm integrating for one proton. This was identified as the proton attached to the nitrogen, which was shifted upfield due to the formation of the amide. In addition, all ^{1}H NMR spectra displayed characteristic singlets at ~1.40 ppm integrating for nine protons consistent with the presence of the *t*-butyl protecting group. In the ^{13}C NMR spectrum, the carbonyl of carboxylic acid derivative **32** experienced a shift from 179.3 to around ~172.0 ppm due to formation of the amide bond. However, in the case of analogue **66**, a second compound was identified. This compound was identified to be **68**, which was formed by coupling of a second equivalent of carboxylic acid **32** to the phenol of the tyrosine unit (Scheme 6).

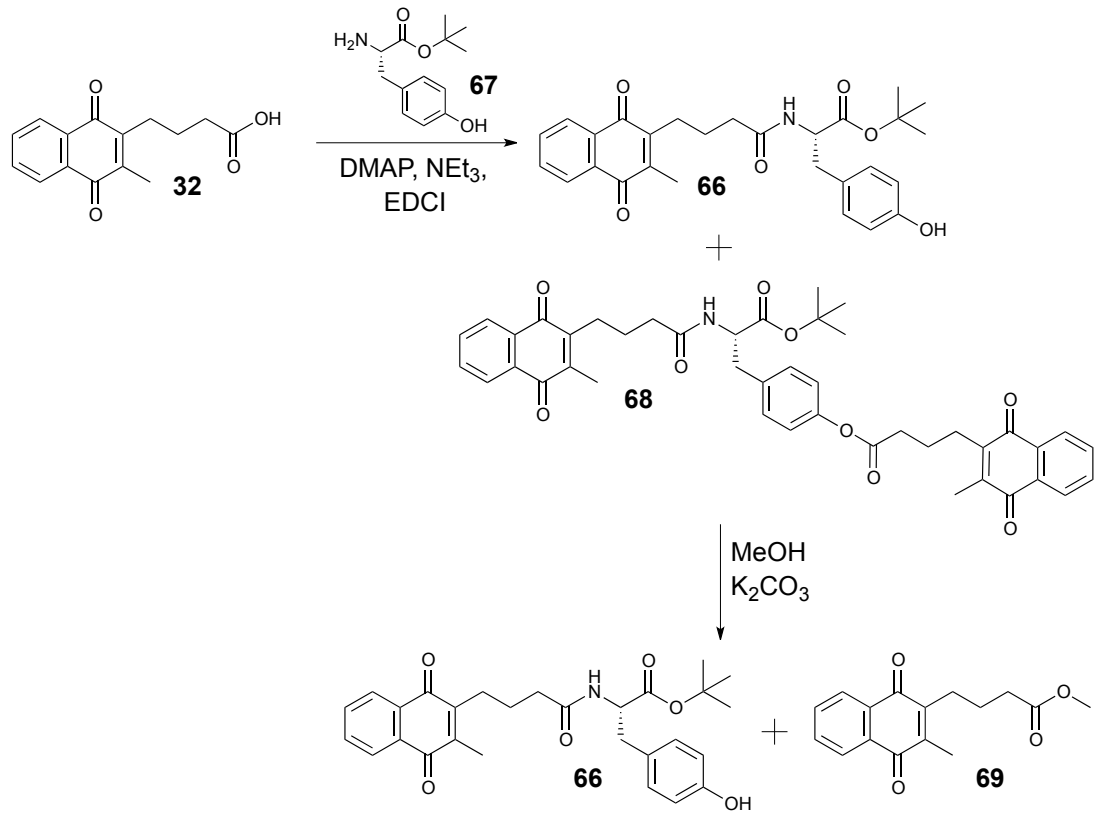

Scheme 6: Formation of analogues **66, 68** and **69**.

To prevent this occurrence, the phenol could have had a protecting group installed to avoid this unwanted side reaction. However, this issue was

overcome by performing a transesterification under mild conditions with potassium carbonate in methanol to cleave the ester group producing L-tyrosine *t*-butyl ester derivative **66** and methyl ester (**69**). This provided L-tyrosine *t*-butyl ester derivative **66** in a 20 % yield over the two reaction steps.

^{1}H NMR and ^{13}C NMR spectroscopy could easily distinguish between the tyrosine analogues. The ^{1}H NMR spectrum indicated the presence of the second quinone moiety of analogue **68** exhibiting two multiplet resonances at 7.66 – 7.71 ppm and 8.04 – 8.07 ppm for the quinone cores now integrating for four protons each with respect to the aromatic signals of the tyrosine which integrates for a total of four protons (Figure 24). In addition, a second set of resonances for the alkyl chain were present and an additional singlet at 2.22 ppm, that integrated for three protons was consistent with the second methyl substituent of the second quinone moiety.

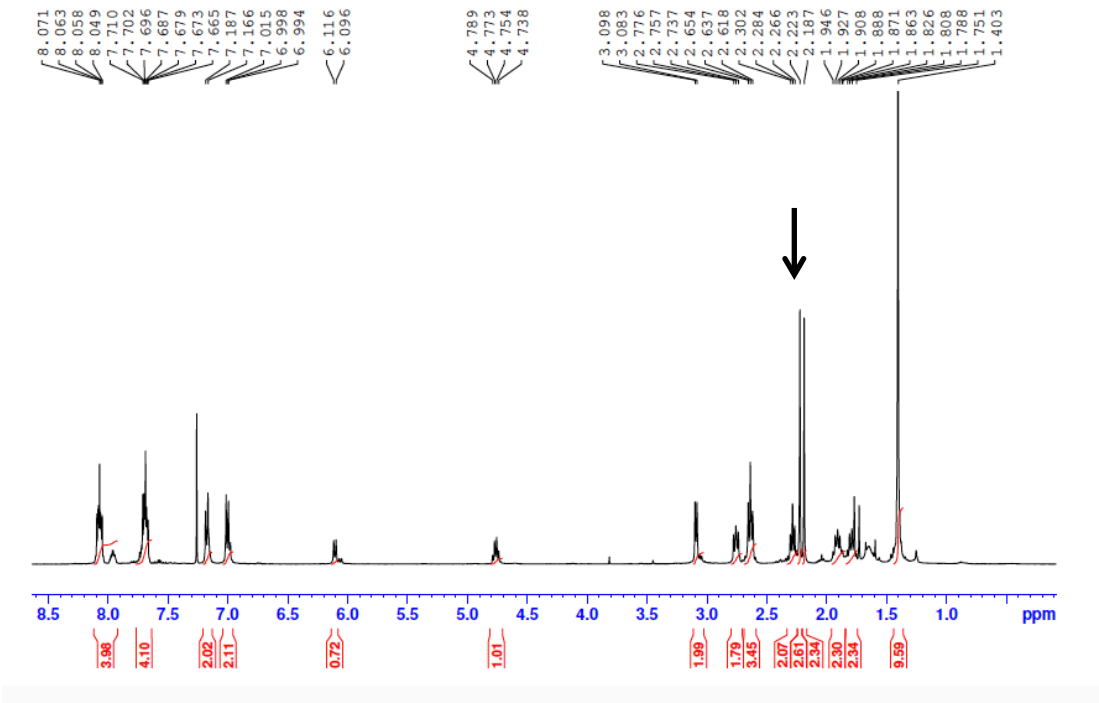

Figure 24: ^{1}H NMR spectrum of analogue **68** consistent with the formation of the ester linkage to the second quinone moiety.

Hydrolysis of the *t*-butyl ester analogues **61** – **66** revealed the carboxylic acid (Table 6). In addition to this, esters **61** – **66** were subjected to biological evaluation.

Table 6: Deprotection of *t*-butyl ester analogues **61** – **66** to produce analogues **70** - **75**.

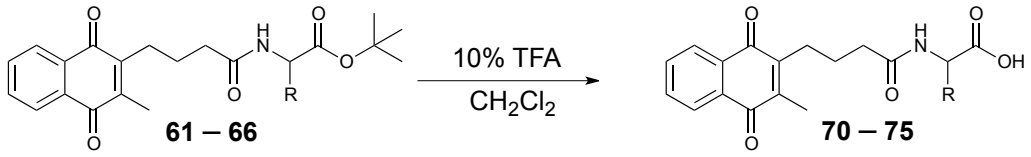

61 – 66 **70 – 75**

Entry	*t*-Butyl Ester	Structure	Yield (%)
1	**61**	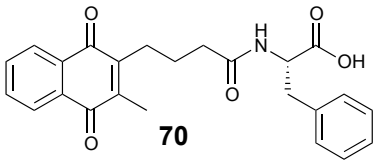 **70**	79
2	**62**	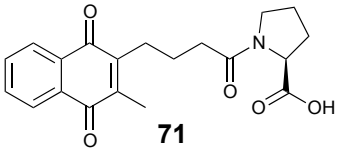 **71**	65
3	**63**	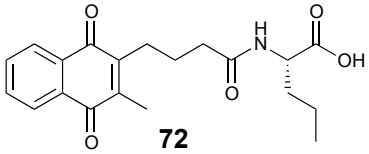 **72**	36
4	**64**	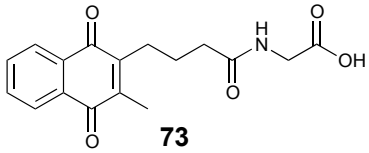 **73**	54
5	**65**	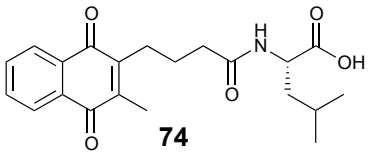 **74**	61
6	**66**	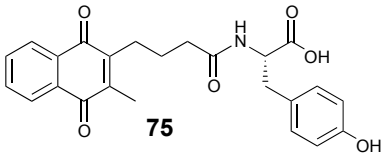 **75**	76

Successful removal of the *t*-butyl protecting groups was consistent with the ^{1}H NMR and ^{13}C NMR spectroscopic data. The absence of the *t*-butyl ester

was supported by the absence of the characteristic singlet at ~1.40 ppm integrating for nine protons in the ^{1}H NMR spectra. Similarly, the ^{13}C NMR spectra showed the absence of two signals, at ~82.0 and 28.0 ppm for the quaternary and methyl carbons respectively, which supports the loss of the *t*-butyl group. The ^{1}H NMR resonances for the quinone, propyl linker and amino acid portion remained within similar chemical shift ranges to their parent esters. However, there is one characteristic change that is seen in analogues containing a α-benzyl substituent in the amino acid fragment (L-phenylalanine derivatives **61** and **70** and the L-tyrosine derivatives **66** and **75)**. The two diastereotopic protons adjacent to the aromatic ring are part of an ABX type spin system and in the presence of the *t*-butyl group the proton signal presents as a apparent doublet of doublets. However, in the absence of the *t*-butyl group the splitting is more distinct with a downfield shift, giving two distinctive doublets of doublets (Figure 25).

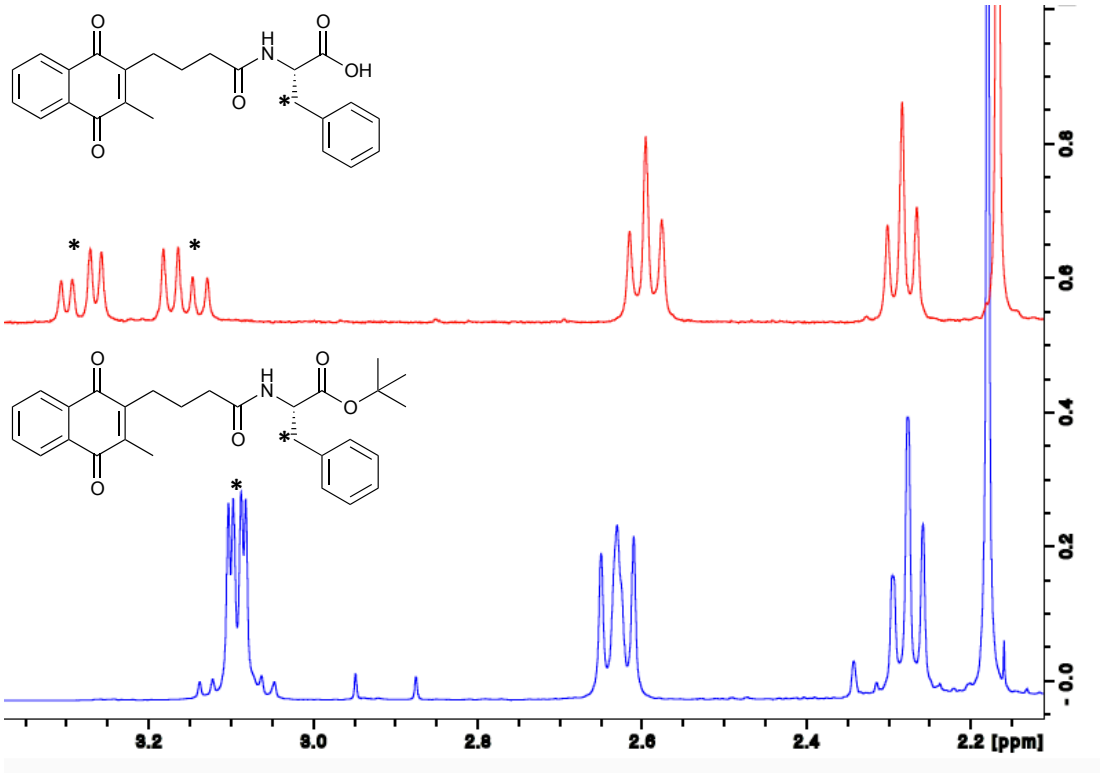

Figure 25: ^{1}H NMR of L-phenylalanine derivatives **61** and **70** illustrating the splitting of the diastereotopic protons.

With a new set of compounds in hand, Ms Monila Nadikudi at the University of Tasmania performed biological evaluation of both ester and acid analogues (Note: all biological evaluation of all analogues from this point forward were performed by Monila Nadikudi). Analogues were primarily analysed for both their ability to provide cytoprotection and rescue ATP levels (Figure 26).

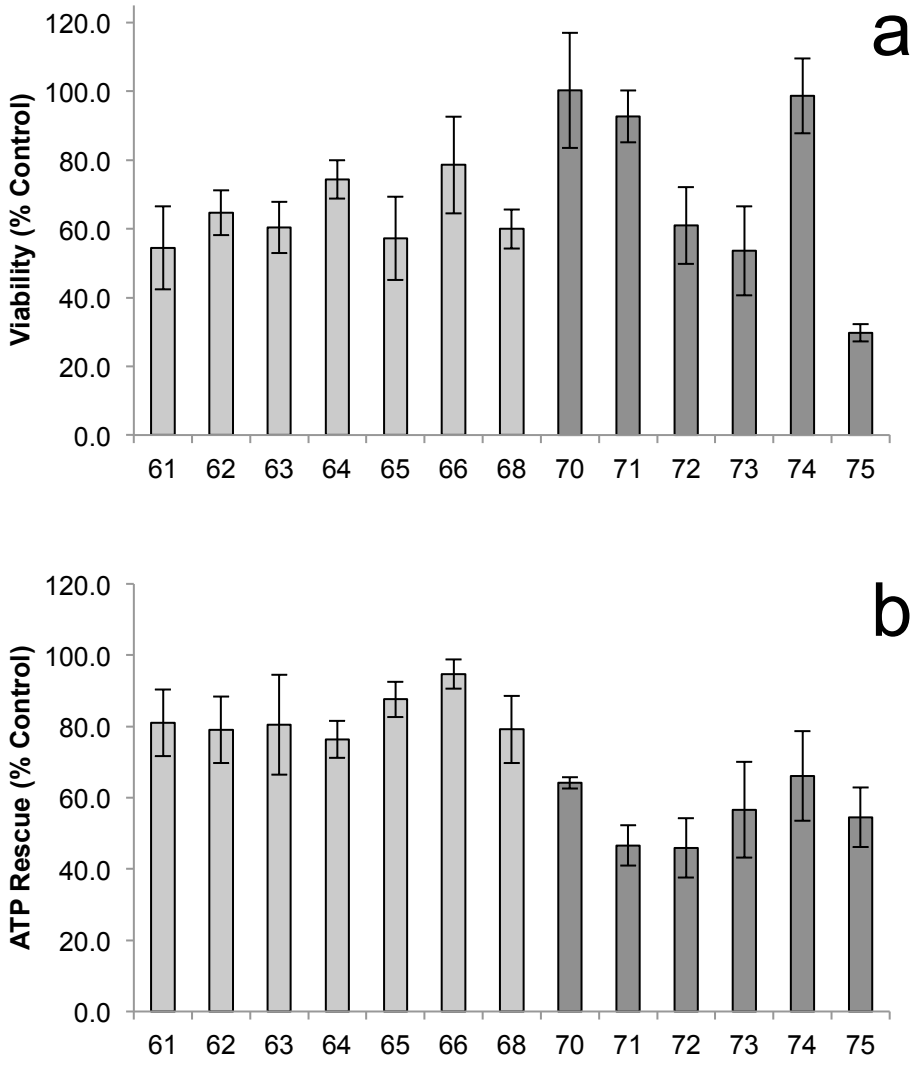

Figure 26: Biological evaluation of amino *t*-butyl esters (light grey) and amino acids (dark grey) in two assays (a) Cytoprotection against rotenone induced complex I dysfunction by quinones at 10μM given as a relative percentage of cell survival compared to untreated HepG2 cells (b) ATP rescue by quinones at 10μM in the presence of rotenone-induced complex I dysfunction as percentage of untreated HepG2 cells. Data represents the mean of n=3 independent experiments with 6 replicates each.

A sufficient number of analogues provided high levels of protection. The threshold for a compound to have a high level of activity is when the analogue restores ATP or viability to >80 % in the respective assay. Thus, indicating that L-phenylalanine methyl ester **40** represented a promising lead compound. Analogues containing amino esters excelled in their ability to restore ATP levels, with a number of analogues surpassing idebenone (**11**), however their cytoprotection levels were within range of idebenone (**11**) (Figure 26). Interestingly, the amino acids derivatives demonstrated the opposite trend, with some analogues greatly exceeding idebenone's (**11**) ability to provide cytoprotection. However, their capacity to provide ATP rescue was suboptimal with ATP rescue levels less than idebenone (**11**). ATP rescue and cytoprotection data of each analogue was plotted investigate correlations (Figure 27).

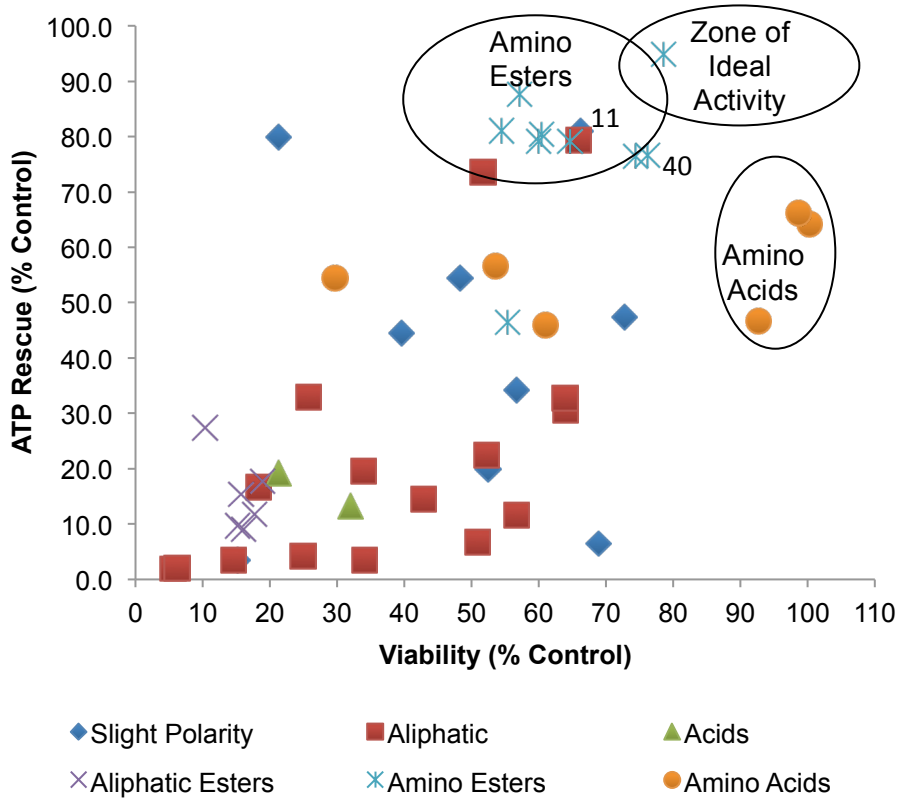

Figure 27: Protection of viability versus acute rescue of ATP levels against rotenone induced complex I dysfunction by naphthoquinones. Both cytoprotection and ATP rescue in HepG2 cells by naphthoquinones (10mM) are displayed as percentage of untreated control (no rotenone) with error bars omitted for clarity. Data represents the mean of n=3 independent experiments with 6 replicates each.

Interestingly, neither group of analogues (amino *t*-butyl esters or amino acid derivatives) showed activity within the zone of ideal activity. Although the amino ester analogues provided exceptional rescue of ATP levels, they did not provide high levels of cytoprotection. When converting the amino esters to amino acids, this trend was reversed. Specifically, their ability to provide cytoprotection greatly exceeds all other analogues, but their capacity to restore ATP levels is diminished once the ester functionality is removed. One analogue of interest was L-tyrosine *t*-butyl ester derivative **66** (Figure 28) which has obtained extremely high levels of ATP rescue, but still had the ability to increase cytoprotection levels that exceed idebenone (**11**) (Figure 27) and was the first analogue to fall within what is termed the zone of ideal activity.

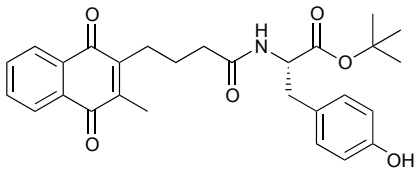

Figure 28: Stucture of L-tyrosine *t*-butyl ester derivative **66**.

The polarity of L-tyrosine *t*-butyl ester derivative **66** is between the two groups of analogues, with the phenolic residue providing greater polarity when compared to the other ester analogues. However, this analogue is less polar than the amino acid derivatives. This result indicated that amino acids may be too polar to provide activity that correlates to both ability to restore ATP levels and provide cytoprotection. For this reason, the next suite of analogues that were prepared contained amino alcohol residues or equivalent amine residues as this would provide compounds of intermediate polarity. Formation of the mid-polarity analogues followed the same amide coupling procedure utilised for synthesis of the amino ester derivatives (Table 7).

Table 7: Synthesis of analogues **76** – **87** containing mid-polarity (amino alcohols).

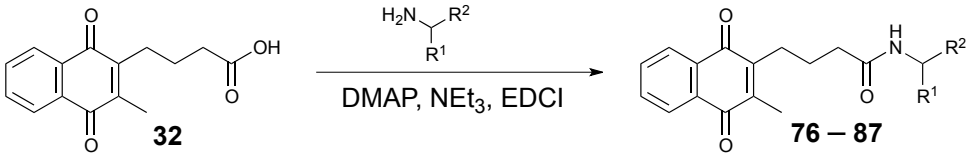

Entry	Amino Alcohol/Amine	Structure	Yield (%)
1	L-phenylalaninol	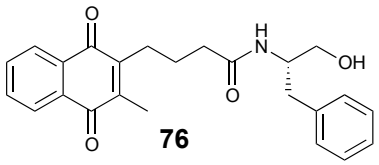 **76**	49
2	L-prolinol	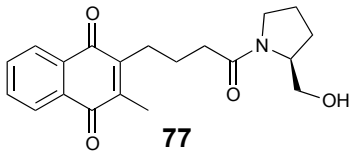 **77**	36
3	L-phenyl glycinol	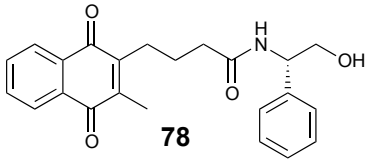 **78**	69
4	tyramine	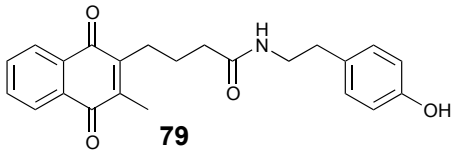 **79**	33
5	3,4-dimethoxy-phenethylamine	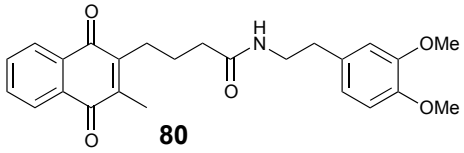 **80**	38
6	phenethylamine	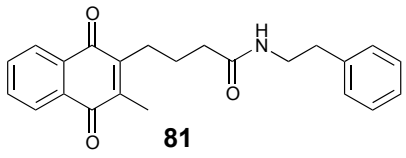 **81**	50
7	tryptamine	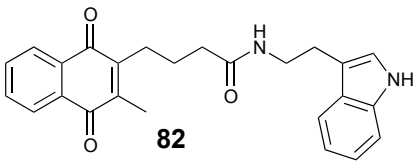 **82**	42

8	*trans*-4-hydroxy-L-proline	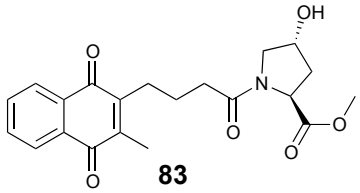 **83**	59
9	L-serine methyl ester	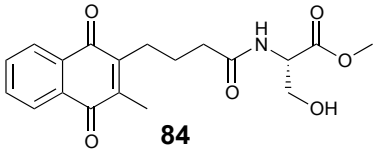 **84**	53
10	L-threonine methyl ester	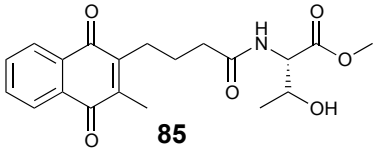 **85**	39
11	butylamine	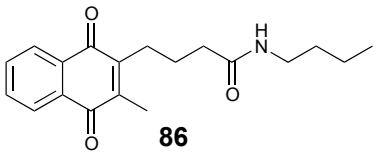 **86**	40
12	(*R*)-2-hydroxy-4-amino butyric acid methyl ester	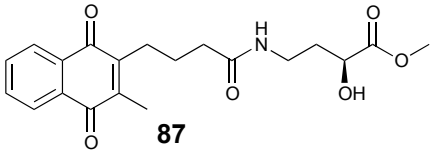 **87**	16

Formation of all analogues was consistent with spectrscopic data, particularly with the ^{1}H NMR and ^{13}C NMR data. Coupling of the amide portion is again supported by the ^{1}H NMR spectrum with a doublet or triplet present in all analogues around ~6.20 ppm integrating for one proton which was identified as the proton attached to the nitrogen. An additional multiplet resonating at ~4.15 – 4.30 ppm integrating for one proton was consistent with the proton alpha to the nitrogen in case of the amino alcohol derivatives **76** – **78** and **83** – **85** or at ~3.44 – 3.55 ppm in the cases of the amide derivatives **79** – **82**, **86** and **87**. In the ^{13}C NMR spectra associated with analogues (**76** – **87**) the carbonyl of the carboxylic acid of carboxylic acid **32** experiences a shift from 179.3 to ~173.0 ppm after formation of the amide bond. All remaining signals were consistent with the incorporation of the amine fragment into the product. Biological evaluation of the current suite of amino alcohol derivatives was

carried out, with primary analysis again studying the analogues ability to provide both cytoprotection and rescue ATP levels (Figure 29).

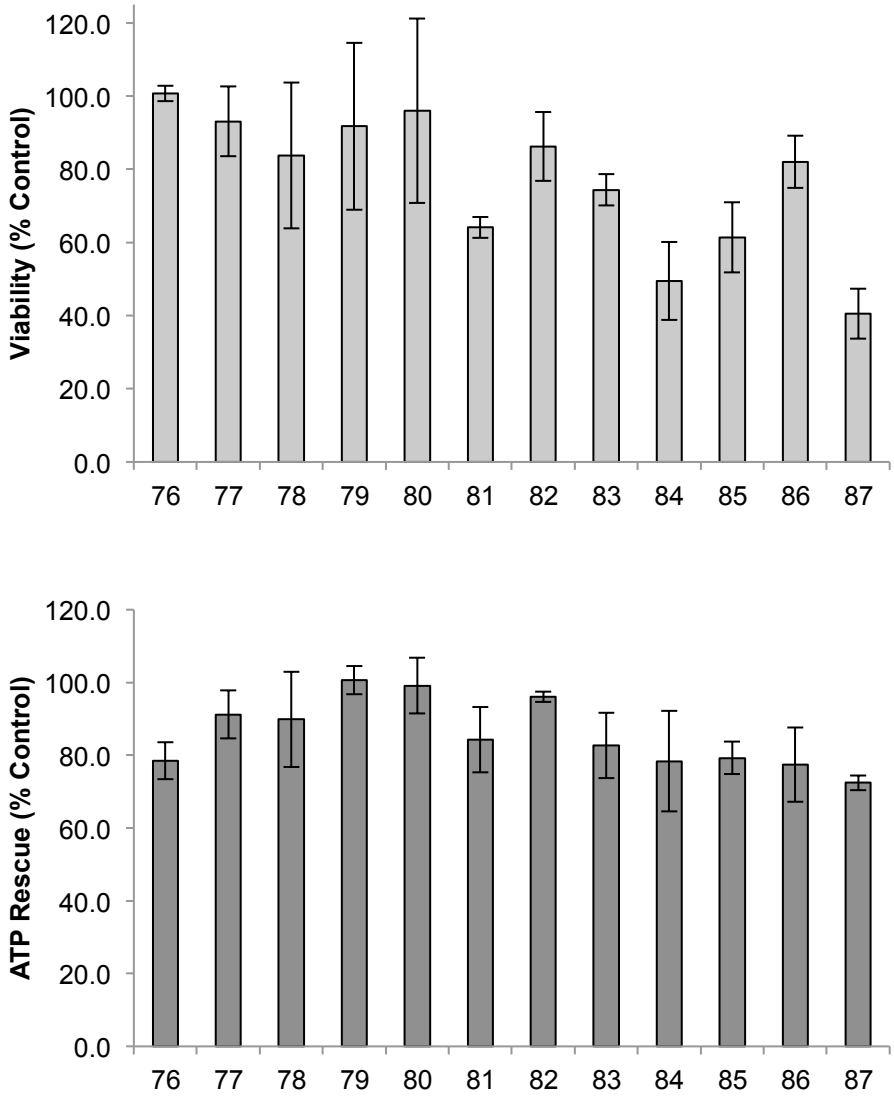

Figure 29: Biological evaluation of amino alcohol and amide derivatives in two assays (a) Cytoprotection against rotenone induced complex I dysfunction by quinones at 10μM given as a relative percentage of cell survival compared to untreated HepG2 cells (b) ATP rescue by quinones at 10μM in the presence of rotenone-induced complex I dysfunction as percentage of untreated HepG2 cells. Data represents the mean of n=3 independent experiments with 6 replicates each.

Pleasingly, a number of analogues provided the anticipated results. L-Phenylalaninol derivative **76**, L-prolinol derivative **77**, tyramine derivative **79** and 3,4-dimethoxyphenethylamine derivative **80** provided cytoprotection back to levels of the control. Where as tyramine derivative **79**,

dimethyoxyphenethylamine **80** and tryptamine derivative **82** restored ATP levels back to those of the control. These analogues are able to provide cytoprotection as well as restore ATP levels as correlated in Figure 30, with this being highly important in moving forward in research into LHON. Studies in the literature indicated that as long as a compound can restore ATP levels, it should also provide cytoprotection as proposed with idebenone (**11**). The current hypothesis is that idebenone (**11**) simply acts as a complex I by pass[4]. However, this research has shown this does not appear to be the case.

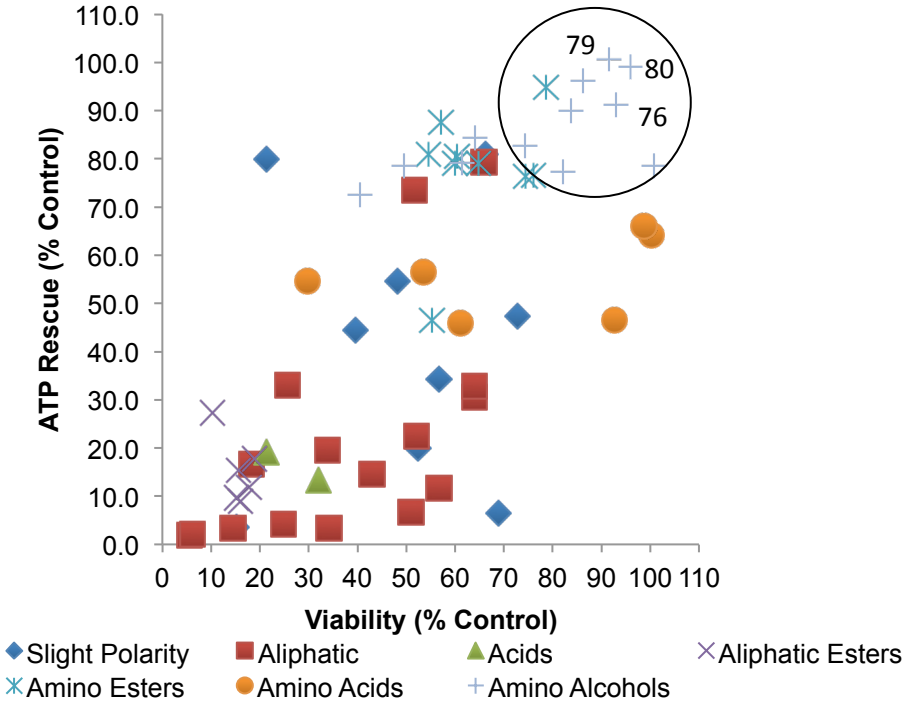

Figure 30: Protection of viability versus acute rescue of ATP levels against rotenone induced complex I dysfunction by naphthoquinones. Both cytoprotection and ATP rescue in HepG2 cells by naphthoquinones (10mM) are displayed as percentage of untreated control (no rotenone) with error bars omitted for clarity. Data represents the mean of n=3 independent experiments with 6 replicates each.

Structurally, the analogues that provided the highest level of protection through both ATP rescue and cytoprotection were analogues that contained some form of aromatic ring and a heteroatom (i.e. oxygen or nitrogen). Analogues **61**, **70** and **76** are all phenylalanine derivatives and all express high levels of activity, interesting analogue **76** is the amino alcohol derivative

and exhibits high levels of both ATP rescue and cytoprotection (Figure 31). In comparison, **61** which is the *t*-butyl ester of phenylalanine exhibited the highest level of ATP rescue but could not provide cytoprotection and analogue **70** as the phenylalanine acid exhibited the opposite trend.

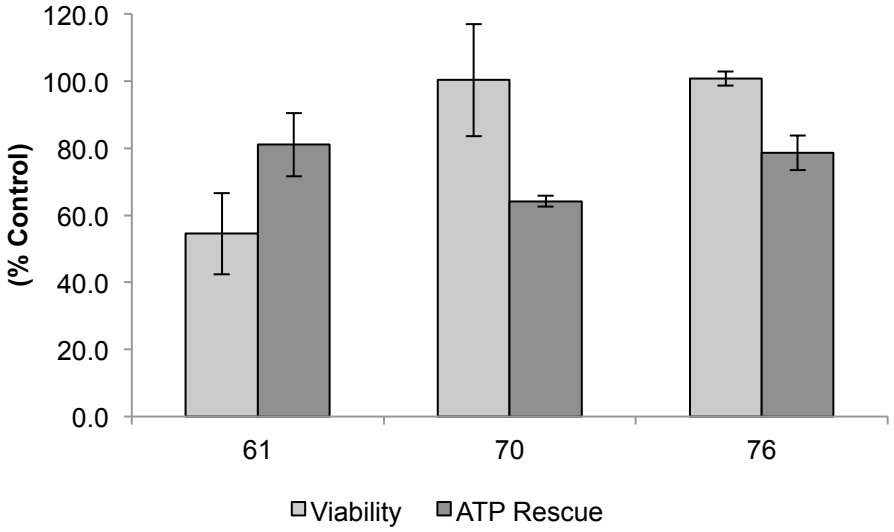

Figure 31: Biological evaluation of L-phenylalanine derivatives in two assays (a) Cytoprotection against rotenone induced complex I dysfunction by quinones at 10μM given as a relative percentage of cell survival compared to untreated HepG2 cells (b) ATP rescue by quinones at 10μM in the presence of rotenone-induced complex I dysfunction as percentage of untreated HepG2 cells. Data represents the mean of n=3 independent experiments with 6 replicates each.

In comparison, the other highly active amino alcohol/simple amide analogues all contain the phenethylamine core. The reasons for the high levels of activity are currently unknown, with both ATP rescue and cytoprotection levels in the prescence of the new naphthoquinone analogues adequately restored back to within error of the control. The top five analogues were selected to undergo further investigation into structure activity relationships (SAR) in relation to linker length and optimisation of the core. These analogues were selected for their ability to provide protection and due to synthetic processes. This process has included L-phenylalanine derivative **70** which was the analogue with the highest level of cytoprotection and L-phenylalanine *t*-butyl ester derivative **61** due to synthetic processes as well as its ability to restore ATP alone (Figure 32). Lastly, three of the top

analogues that were best able to restore both cytoprotection and rescue ATP levels (L-phenylalaninol derivative **76**, tyramine derivative **79** and 3,4-dimethoxyphenethylamine derivative **80**) were selected (Figure 32).

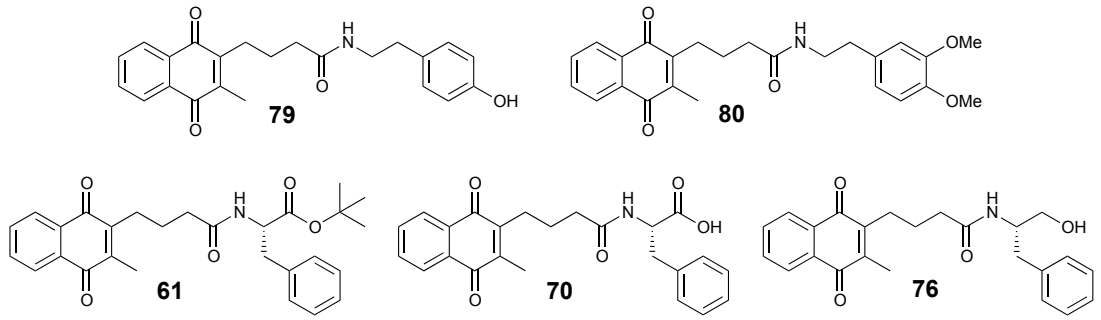

Figure 32: Structures of the top five analogues **61**, **70**, **76**, **79** and **80** which were selected to allow further structure activity relationship (SAR) studies.

Using these amino fragments, further investigation into other structural requirements were investigated. From the initial toxicity data it was proposed that the naphthoquinone core was ideal, providing significant less toxicity than the benzoquinone core. However, between the core and the amino fragment was a four-carbon linker. The impact the length of the linker had on the ability of the analogue to provide protection was unknown. For this reason analogues containing a three-, five- and six-carbon linkers were required to synthesise derivatives of the amino fragments that gave the best activity. Therefore, analogues of carboxylic acid **32** with differing linker lengths needed to be prepared on a multi-gram scale. These compounds were synthesised *via* the optimised conditions for the silver-mediated radical decarboxylation process (Table 8). Noteably, the synthesis of analogue **31** was low yielding when compared analogues **88** and **89**, this is a result of this reaction taking place with the bottle of ammion persulfate that was later identified to have decomposed.

Table 8: Synthesis of acid analogues **31**, **88** and **89** containing differing lengths of the acid side-chain.

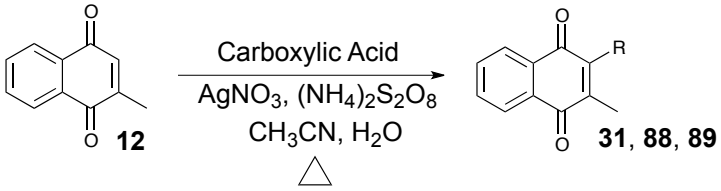

Entry	Carboxylic Acid	Structure	Yield (%)
1	succinic acid	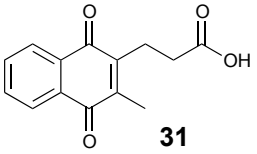 **31**	20
2	adipic acid	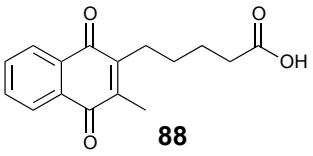 **88**	78
3	pimelic acid	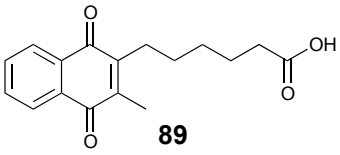 **89**	57

Formation of the analogues proceeded as expected although the yield of the reaction employing succinic acid was low. ^{1}H NMR and ^{13}C NMR spectroscopy supported their formation with the absence again of a singlet peak at 6.84 ppm consistent with the loss of the proton attached to the C3 position of the 2-methylnaphthoquinone (menadione, **12**) in the ^{1}H NMR spectrum. While the ^{13}C NMR spectrum showed characteristic resonances below 35.0 ppm correlating to the resonances of the aliphatic linker, whilst an additional diagnostic signal at 179.6 ppm was present corresponding the carboxylic acid group. These analogues were then coupled to the top five amino fragments previously identified as providing the most activity for comparison (Table 9) with the exception of the three-carbon linker. Due to the low yield obtained for the formation of the three-carbon carboxylic acid derivative **31**, L-phenylalanine *t*-butyl ester derivative **90** and L-phenylalanine

acid derivative **91** were synthesised. Two analogues and the carboxylic acid derivative **31** were deemed sufficient to determine if there was a difference in activity as a result of linker length. If there were any significant change in activity then the remaining analogues would be synthesised.

Table 9: Synthesis of analogues **90** – **101** containing the top five amino groups.

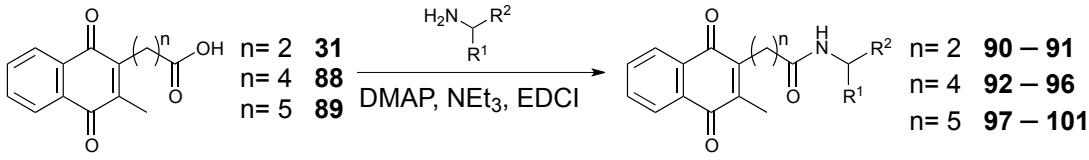

Entry	n=	Amino fragment	Structure	Yield (%)
1	2	L-phenylalanine *t*-butyl ester	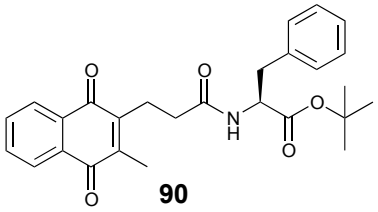 **90**	22
2#	2	L-phenylalanine	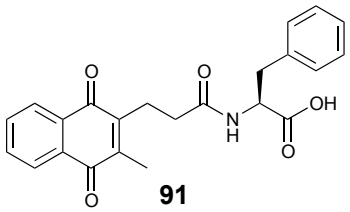 **91**	80
3	4	L-phenylalanine *t*-butyl ester	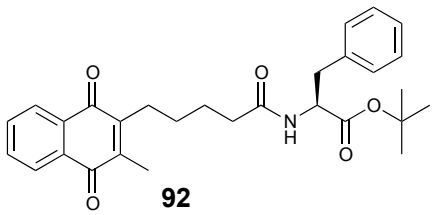 **92**	69
4#	4	L-phenylalanine	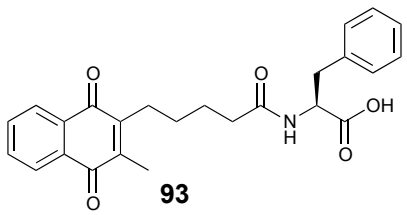 **93**	33

5	4	L-phenylalaninol	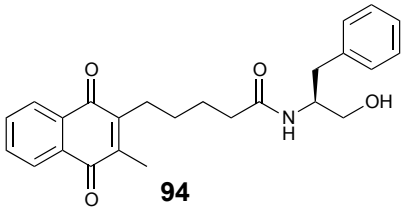 **94**	59
6	4	tyramine	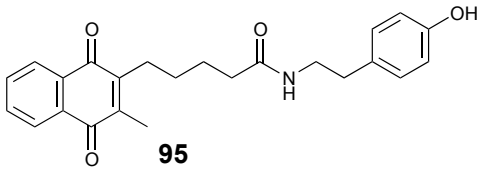 **95**	20
7	4	3,4-dimethoxy-phenethylamine	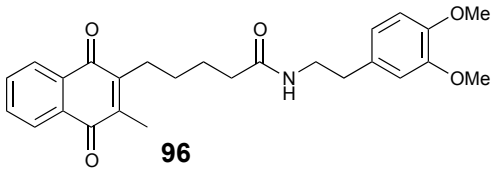 **96**	35
8	5	L-phenylalanine *t*-butyl ester	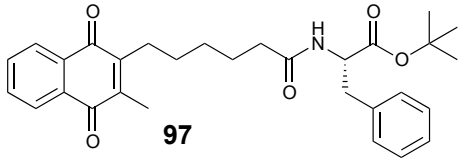 **97**	59
9[#]	5	L-phenylalanine	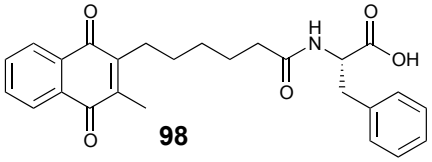 **98**	84
10	5	L-phenylalaninol	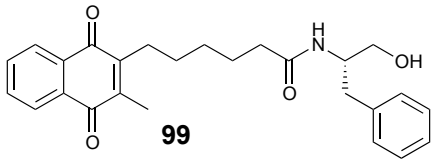 **99**	34
11	5	tyramine	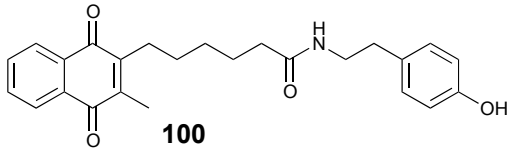 **100**	39
12	5	3,4-dimethoxy-phenethylamine	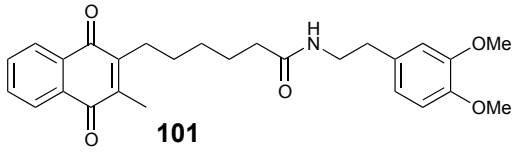 **101**	60

[#] analogue formed via deprotection of the *t*-butyl ester of the corresponding analogue.

Formation of all analogues was supported by NMR spectroscopy and Infared (IR) analysis. In the ^{1}H NMR and ^{13}C NMR spectra, the characteristic peaks observed previously with the four carbon chain linker were present in the case of the three-, five- and six-carbon linkers indicating attachment of the amine. Analogues were then subjected to the same biological evaluation as all other analogues and a comparison between the three-, four-, five- and six-carbon linkers made in relation to their ability to rescue ATP levels and provide cytoprotection (Figure 33).

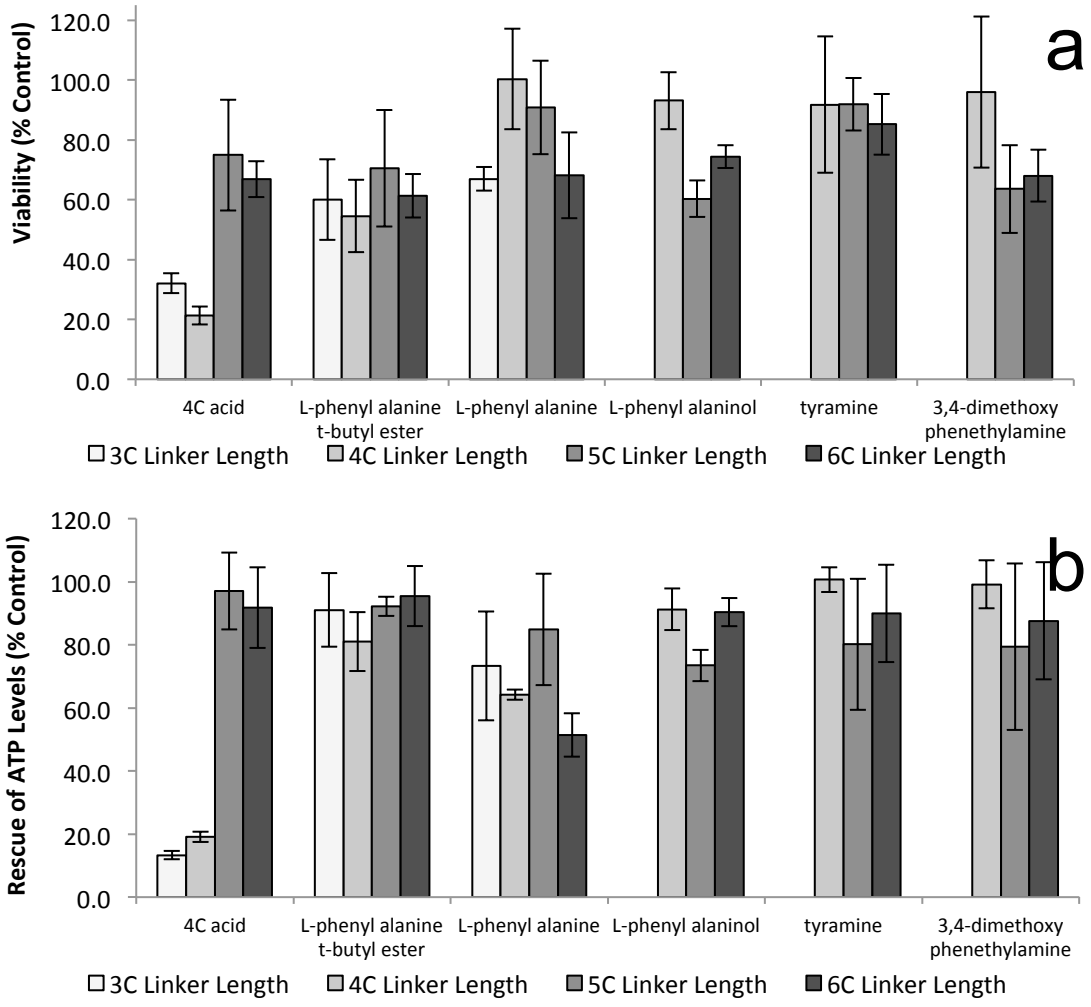

Figure 33: A comparison of linker length of top five analogues in assays (a) Cytoprotection against rotenone induced complex I dysfunction by quinones at 10μM given as a relative percentage of cell survival compared to untreated HepG2 cells (b) ATP rescue by quinones at 10μM in the presence of rotenone-induced complex I dysfunction as percentage of untreated HepG2 cells. Data represents the mean of n=3 independent experiments with 6 replicates each.

As seen in Figure 33, there was no significant difference between the three-, five- and six-carbon linkers with respect to the four-carbon linker. In general the four-carbon linker did provide the highest level of activity (Figure 33) with exception of the free carboxylic acid derivatives. Surprisingly, the free carboxylic acids showed a significant difference in activities. The five- and six-carbon carboxylic acid derivatives **88** and **89** had much improved activity in both ATP rescue and cytoprotection when compared to the three- and four- carbon carboxylic acid derivatives **31** and **32.** In fact, addition of the amine derivative to the side chain barely had any effect on activity in these cases. However, these straight chained carboxylic acid derivatives would be suseptible to the same degradation issues faced by idebenone (**11**) and are still not quite to the standard of the L-phenylalanine methyl ester derivative **40.**[4,63] This result combined with the fact that all initial analogues were sythesised from the four-carbon linker, suggested that there was no benefit to changing the linker length to explore any further structure activity relationships (SARs). Consequently, all subsequent work utilised the four-carbon linker.

It was proposed that if these analogues were not simply acting as a complex I bypass and their activity was in fact due to a particular interaction with an enzyme. Employing an amino fragment of the opposite enantiomeric series may provide some insight into molecular interactions. If polarity alone was responsible for activity, then no difference in activity would be expected. With this in mind, a series of analogues containing D-stereoisomers were synthesised. Of particular interest, were the two top five analogues, **70** and **76**.

The cost and availability of D-phenylalanine *t*-butyl ester dictated that an alternative synthetic pathway was required to produce the enantiomer of **71**. *N-N'*-Carbonyldiimidazole (**102**) is a common reagent for coupling carboxylic acids with amines to form amide bonds.[85] This method for amide bond formation can be utilized without the need for protecting groups. Generation and isolation of the active acyl imidazole intermediate (**103**) prior to coupling allows for selective coupling of an unprotected amino acid (Scheme 7). As the imidazole group provides an excellent leaving group that enables

nucelophilic attack by the amine to form the amide bond to generate analogue **105**. *N-N'*-Carbonyldiimidazole (**102**) is commonly used in place of aryl halides due to their ease of handling and greater stability.[86]

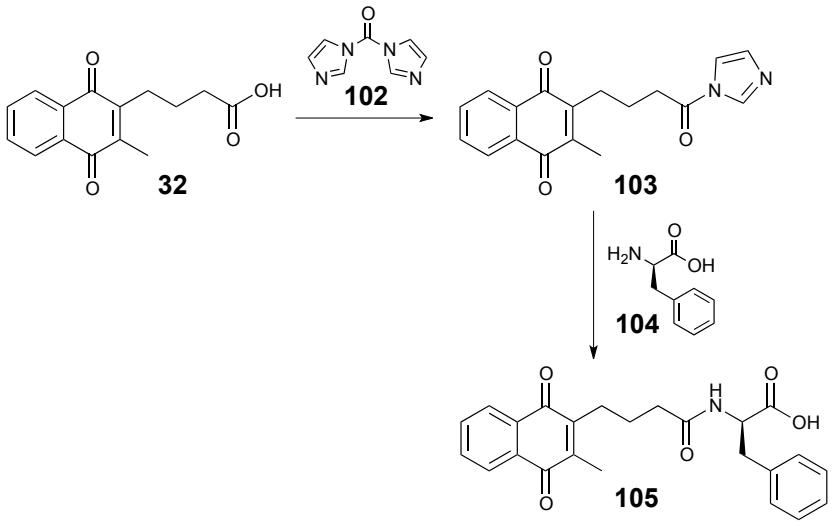

Scheme 7: Formation of D-phenylalanine derivative **105** through the use of an acyl imidazole intermidiate.

Formation of D-phenylalanine derivative **105** was supported by both ^{1}H NMR and ^{13}C NMR spectroscopy, with spectroscopic data identical to L-isomer **70**. Although this method was employed for the formation of analogue **105**, this reaction was low yielding with only a 14 % yield obtained over the two steps. Isolation and characterisation of the acyl imidazole intermediate indicated the initial step had proceeded in a 93 % yield. Formation of **103** was supported by ^{1}H NMR spectroscopy with three singlet resonances present at 6.99, 7.40 and 8.10 ppm all integrating for one proton each indicating the imidazole ring. Analysis by ^{13}C NMR spectroscopy showed a characteristic shift of the carbonyl of the carboxylic acid of derivative **32** from 179.3 ppm to 168.9 ppm consistent with the formation of the amide bond. Formation of intermediate **103** was also supported with a characteristic IR stretch at 1738 cm^{-1} for the carbonyl attached to the imidazole ring. The introduction of the amino acid resulted in the dramatic loss in yield. This is a clear indication that the reaction conditions for the second step, if used to prepare other analogues, would need significant optimisation. However, the quantity obtained was adequate for biological evaluation of **105**.

The synthesis of the remaining D-enantiomers employed standard amide coupling techniques using the methyl ester derivatives. Due to previous issues associated with hydrolysing esters in the presence of the quinone moiety, re-investigation of hydrolysis conditions was required to obtain the D-amino acid derivative to determine whether the stereochemistry would alter activity. The next suite of compounds prepared included both enantiomers of amino alcohols and unnatural amino ester residues such as D-phenylalaninol, D-phenyl glycinol and L- and D- phenyl glycine methyl ester (Table 10).

Table 10: Synthesis of D-analogues and unnatural amino derivatives.

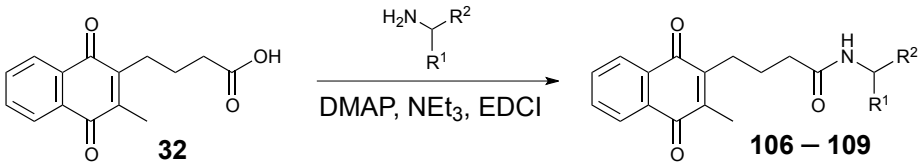

32 **106 – 109**

Entry	Amino derivative	Structure	Yield (%)
1	D-phenylalaninol	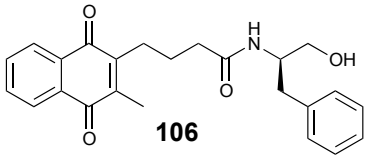 **106**	36
2	D-phenyl glycinol	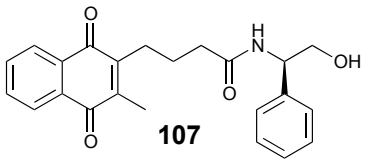 **107**	62
3	L-phenyl glycine methyl ester	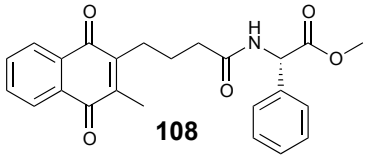 **108**	72
4	D-phenyl glycine methyl ester	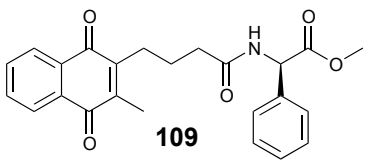 **109**	69

Standard NMR and IR spectroscopic analysis supported the successful synthesis of analogues **106** – **109.** The spectroscopic data for analogues **106** to **109** was identical to that obtained for the opposite enantiomer. To obtain the amino acid derivatives of both L- and D-phenyl glycine methyl ester, suitable hydrolysis conditions were re-investigated. In a relevant prior study by Woolley and co-workers,[75] base hydrolysis under standard conditions resulted in complete decomposition which was proposed to be due to the presence of the quinone moiety. Therefore both analogues were subjected to various acidic and basic hydrolysis conditions. Base hydrolysis was investigated with both lithium and potassium hydroxide. However, both reaction conditions resulted in rapid decomposition (Scheme 8).

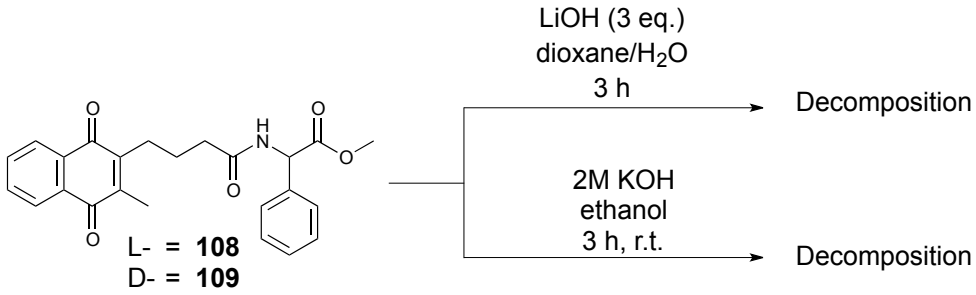

Scheme 8: Attempted base hydrolysis of methyl esters **108** and **109**.

Lithuim hydroxide is often used for deprotection of amino esters and as a result this base was utilised to optimise and screen the reaction conditions, including both solvent and temperature. Irrespective of the reaction temperature or time (Table 11), decomposition occurred. After the addition of base, the reaction mixture changed to black and when analysed by ^{1}H NMR spectroscopy, a complex mixture of products were observed.

Table 11: Attempted conditions for base hydrolysis with lithium hydroxide

Entry	Dioxane/H_2O	Temperature °C	Reaction Time (h)	Product
1	1:1	50	3	Decomposition
2	1:1	r.t.	1	Decompositon
3	2:1	50	3	Decomposition
4	3:1	50	5	Decompositon

Acid hydrolysis was then investigated. Reaction with 6 M hydrochloric acid with catalytic acetic acid was ultimately successful (Scheme 9). Purification of the respective acids was achieved by trituration with dichloromethane to yield L- and D- phenyl glycine analogues in 46 % and 14 % yields repectively.

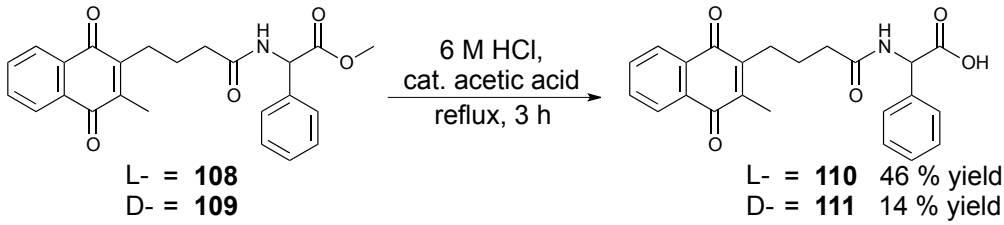

Scheme 9: Acid mediated hydrolysis of methyl esters **108** and **109** to form **110** and **111**.

The successful formation of analogues **110** and **111** was consistent with spectroscopic data, particularly the ^{1}H NMR and ^{13}C NMR spectrum. The ^{1}H NMR spectra associated with **110**/**111** showed a clear absence of a singlet at 3.71 ppm for the methyl ester. With all D-analogues synthesised, primary biological evaluation of the enantiomers was performed in order to assess their ability to rescue ATP levels and provide cytoprotection (Figure 34).

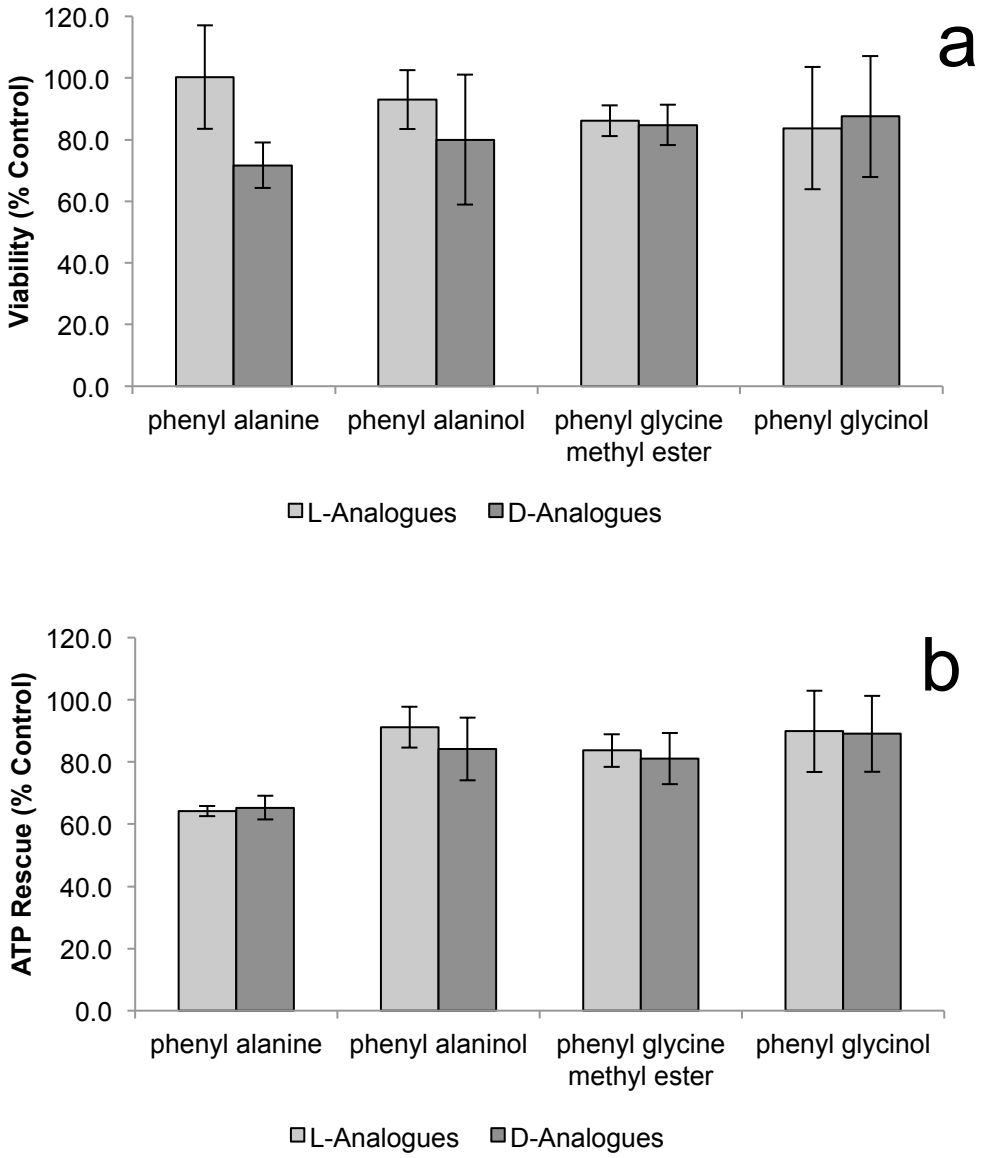

Figure 34: A comparison between L- and D-enantiomers of amino fragments in assays (a) Cytoprotection against rotenone induced complex I dysfunction by quinones at 10μM given as a relative percentage of cell survival compared to untreated HepG2 cells (b) ATP rescue by quinones at 10μM in the presence of rotenone-induced complex I dysfunction as percentage of untreated HepG2 cells. Data represents the mean of n=3 independent experiments with 6 replicates each.

Surprisingly, all analogues showed no difference in their ability to provide cytoprotection with the exception of the phenylalanine analogues (**70**/**105**) (Figure 34a). L- and D- enantiomers of phenylalanine provided remarkably different cytoprotective ability. Specifically, cytoprotection dropped almost 30 % by swapping to the D-isomer. However, the ability to restore ATP levels by

all analogues was independent of stereochemistry (Figure 34b). With these results in mind, in general it appears that the stereochemistry of the analogues is not significant and the differences between phenylalanine analogues (**70**/**105**) may be a result of rates of metabolism.

2.2.3 Synthesis of miscellaneous analogues *via* various methods

All structure activity relationships have demonstrated the need for a naphthoquinone core (**4**), a four-carbon linker, and an amino alcohol portion or amide group in the side chain to provide high levels of cytoprotection and ATP rescue. Investigation into whether replacing the carbon atom alpha to the quinone core in the four-carbon linker with a hetero atom was required. This represented only a small preliminary investigation, in which the carbon atom was substitueted for a nitrogen or sulfur atom.

Following the method of C. Chen and co workers,[87] the introduction of a sulfur chain was performed in a single step reaction from menadione (**12**) using mercapto-propanoic acid (**112**) to produce the sulfur-containing carboxylic acid derivative **113** (Scheme 10).

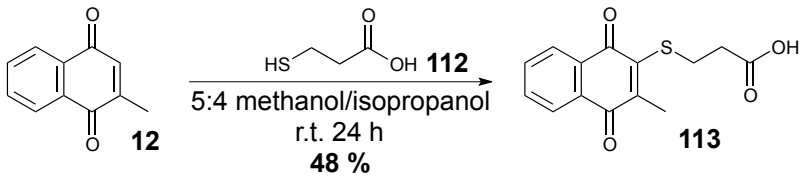

Scheme 10: Formation of analogue **113**.

Analogue **113** was synthesised *via* a 1,4-addition of mercapto-propanoic acid (**112**) to the menadione (**12**) core followed by air oxidation to form the desired analogue in 48 % yield.[88,89] ^{1}H NMR spectroscopic analysis of **113** was consistent with equivalient data reported in the literature, with the absence of a singlet peak at 6.84 ppm indicating the loss of the proton attached to the C3 position of menadione (**12**) in addition to new peaks visible in the aliphatic region.

After the formation of **113**, attempted coupling to L-phenylalanine *t*-butyl ester was performed (Scheme 11). A complex mixture of products was obtained

and isolation of the desired product **114** was not possible. It was postulated that the sulfur may act as a leaving group and this led to decomposition, however, this was not investigated further.

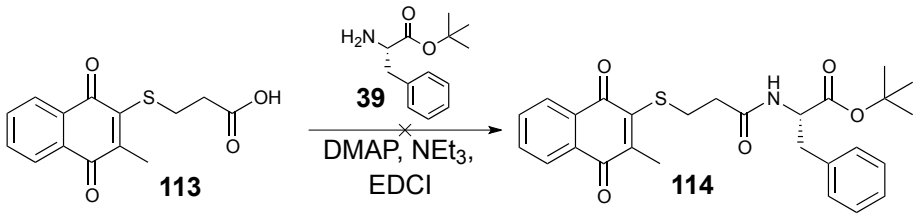

Scheme 11: Failed synthesis of analogue **114**.

Obtaining the top five amino fragments with the sulfur derivative was put on hold until biological evaluation of the sulfur naphthoquinone acid (**113**) could be obtained. As hetero-atoms within the linker were desired, focus moved on to obtaining a nitrogen analogue. Using a literature method by Bittner and coworkers,[90] formation of analogues on both the naphthoquinone (**4**) and menadione (**12**) was attempted (Scheme 12).

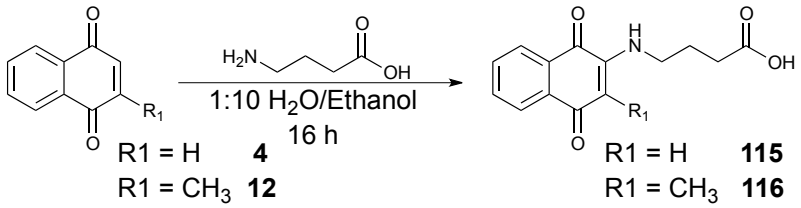

Scheme 12: Formation of nitrogen containing analogues **115** and **116**.

Similar to the sulfur analogue (**113**), this reaction proceeded with a 1,4-addition.[90] However, despite both cores **4** and **12** being used as substrates, only the formation of the naphthoquinone analogue (**115**) occurred. It is reported within the literature that a facile reaction occurs with the naphthoquionone (**4**). However, minimal reaction takes place on the menadione (**12**) core with the reaction being descibed in the literature as "sluggish".[90] It is proposed that both steric hinderance and electronic effects could be responsible for disfavouring the addition to menadione (**12**).[90] With this in mind, naphthoquinone analogue **115** was formed in a 20 % yield with all spectroscopic analysis consistent with the literature.[90] However, this is not ideal as the analogue does not contain a methyl substituent at the C3-

position to enable direct comparison to the top five analogues. The yield obtained was also significantly less than that reported in the literature, however, adequate quantites of analogue **115** were obtained for the purposes required. Analogue **115** was then subjected to coupling to L-phenylalanine methyl ester to give the product in a poor 18 % yield (Scheme 13).

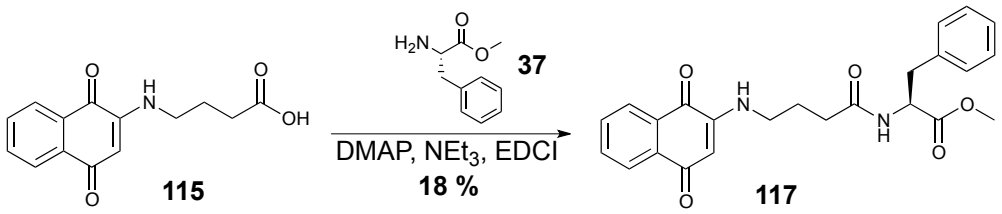

Scheme 13: Synthesis of analogue **117** *via* normal amide coupling methods.

Formation of analogue **117** was consistent with both ^{1}H and ^{13}C NMR spectroscopic analysis, with two exchangable proton signals present at 5.96 and 6.51 ppm indicating the prescence of two N-H's within the molecule. Again the characteristic doublet of doublet signals for the two diastereotopic protons alpha to the benzyl substituent were present at 3.06 and 3.09 ppm. Both sulfur and nitrogen-containing analogues were then subjected to biological evaluation (Figure 35).

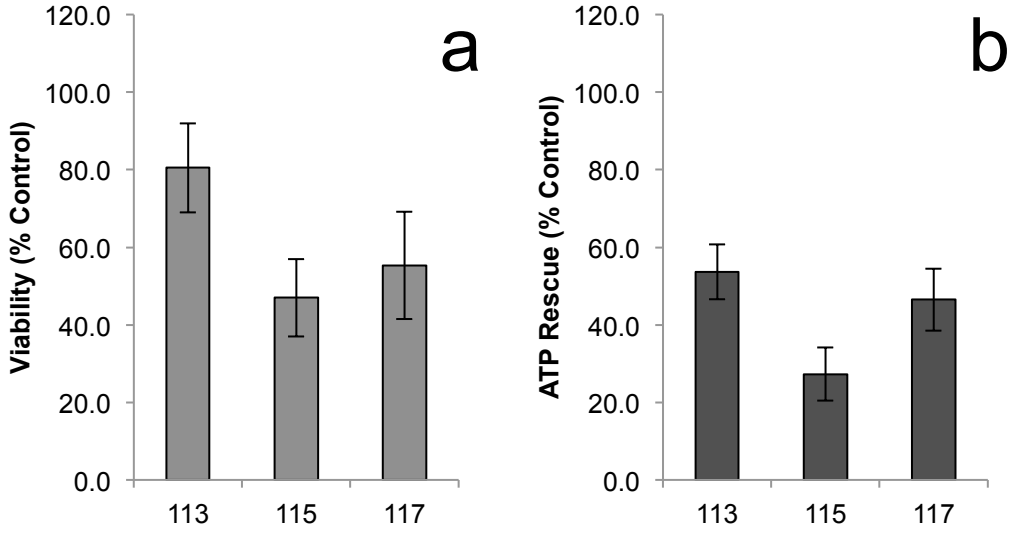

Figure 35: A comparison between analogues containing hetero-atoms within the linker (a) Cytoprotection against rotenone induced complex I dysfunction by quinones at 10μM given as a relative percentage of cell survival compared to

untreated HepG2 (b) ATP rescue by quinones at 10μM in the presence of rotenone-induced complex I dysfunction as percentage of untreated HepG2 cells. Data represents the mean of n=3 independent experiments with 6 replicates each.

As seen in Figure 35, the addition of the nitrogen atom in both **115** and **117** showed minimal ability to restore ATP levels or provide cytoprotection. The introduction of the sulfur atom had a positive influence on both ATP rescue and cytoprotection when compared to the straight carbon chain of carboxylic acid derivative **32**. However, as there is no viable method for introducing various amino groups into the side chain at this stage, this is not considered a viable route for further SAR investigation. Due to poor efficiency of these reactions, the preparation of other analogues containing heteroatoms was not pursued further at this time.

Investigation into the benefits of multiple amino acid fragments on activity was performed on the basis of SS-31 (**10**), which is a mitochondrial targeting peptide and contains four amino acid residues. Therefore, utilising analogue **70**, an additional amino acid residue was coupled *via* the normal amide coupling process before undergoing biological evaluation. L-Proline *t*-butyl ester was coupled to analogue **70** before undergoing the normal *t*-butyl ester deprotection with 10% TFA to reveal the dipeptide derivative **120** in 49 % yield (Scheme 14).

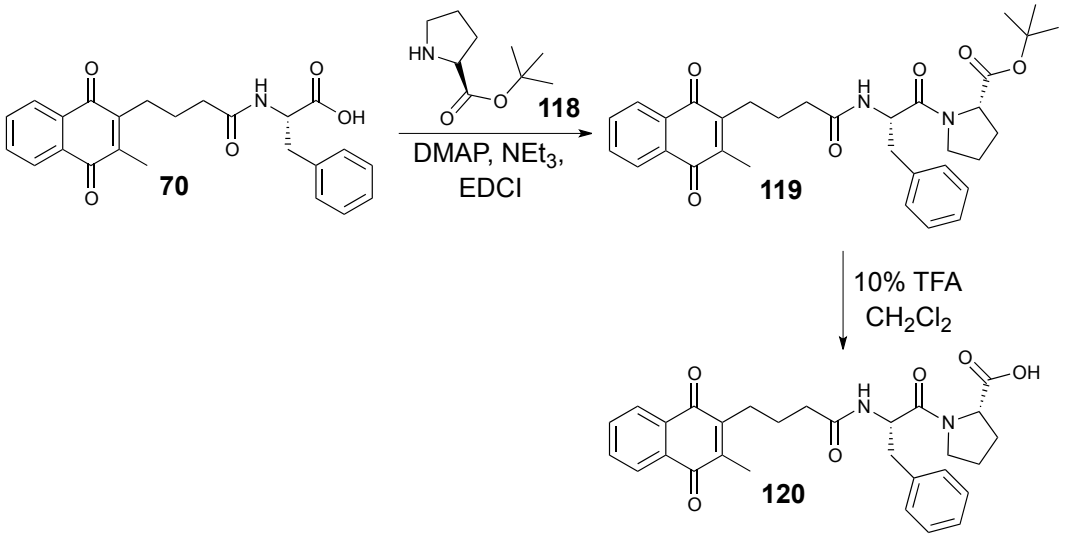

Scheme 14: Synthesis of analogue **120** containing two amino acid fragments.

The successful synthesis of compound **120** was supported primarily by high resolution electrospray ionisation mass spectroscopy (HR ESI MS). For $C_{29}H_{30}N_2NaO_6$, the predicted HRMS was 525.2002 and it was found to be 525.1990. The presence of amide rotamers or rotational isomers due to restricted rotation around the amide bond, complicated the analysis of the ^{1}H and ^{13}C NMR spectra in $CDCl_3$. Often these issues can be resolved for small peptides by variable-temperature (VT) NMR (which causes the proton NMR signals to coalesce), solvent switching or the introduction of a complexing agent.[91] However, these methods were not investigated as the amide coupling method was predictable and MS characterisation was satisfactory.

In addition to the peptide-containing analogue, a tetrapeptide that was available from a project on peptide opioid analogues was coupled. This peptide contained the dimethyltyrosine moiety that is present in the mitochondrial targeting SS-31 (**10**) peptide. Coupling of the carboxylic acid derivative **32** proceeded under standard conditions with DMT-Tic-Gly-Bnz (**121**) to give the tetrapeptide **122** in 27 % yield (Scheme 15). Formation of analogue **122** was also supported primarily by MS ESI showing a $(M+H)^+$ at 755 and {$(M+Na)^+$ peak} at 777. As for the dipeptides, the ^{1}H NMR and ^{13}C NMR spectra were even more complex due to the presence of amide rotamers.

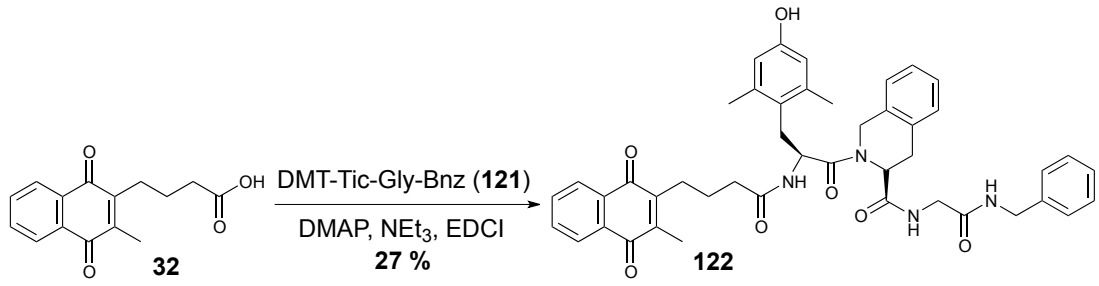

Scheme 15: Formation of the tetrapeptide analogue (**122**).

Both **120** and **122** were subjected to biological evaluation. Specifically, their ability to rescue ATP as well as their ability to provide cytoprotection was investigated. As seen in Figure 36, neither analogue showed any improvement on the already identified top five compounds and therefore no

other analogues were synthesised as the increase in polarity is consistent with a decrease in activity.

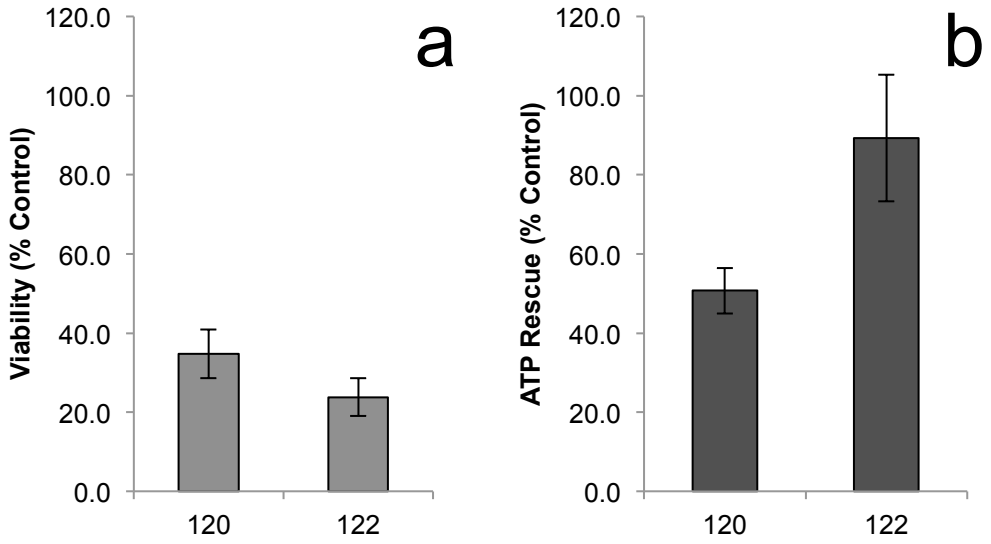

Figure 36: Biological evaluation of quinones containing multiple amino residues (a) Cytoprotection against rotenone induced complex I dysfunction by quinones at 10μM given as a relative percentage of cell survival compared to untreated HepG2 cells (b) ATP rescue by quinones at 10μM in the presence of rotenone-induced complex I dysfunction as percentage of untreated HepG2 cells. Data represents the mean of n=3 independent experiments with 6 replicates each.

Figure 36 indicates that the addition of the second amino acid residue results in a large reduction in their ability to provide cytoprotection. Although these analogues have not provided any significant activity, they have very little structural resemblance to SS-31 (**10**). Therefore, further investigation into tetrapeptides was conducted with the intention to provide a direct comparison to SS-31 (**10**). This resulted in the use of solid phase peptide synthesis (SPPS) to enable high-yielding and relatively simple construction of the peptide backbone with the advantage that the quinone portion can also be introduced into the standard protocol.

2.3 Solid Phase Peptide Synthesis (SPPS)

Solid phase peptide synthesis is a systematic process involving the stepwise addition of protected amino acids onto a growing peptide chain, which is bound to a resin (solid support). This allows for controlled peptide growth with exceptional yields. For the requirements of the analogues we proposed to synthesise, 2-chlorotrityl chloride resin was utilised as the solid support and 9-fluorenylmethyl carbonyl (Fmoc) protected amino acids were required for the coupling.[92] Fmoc protecting groups can be cleaved through the addition of base, with piperidine still the most commonly used reagent since first reported in the late 1970's.[93] This allows for orthogonal acid-labile protecting groups such as *N-tert*-butyloxycarbonyl (Boc) groups to be installed on additional fragments that require protection to ensure that unwanted side reactions do not occur. This allows for deprotection of the Fmoc groups in the presence of the acid-labile protecting groups without unwanted deprotection occurring.[94]

The SPPS process required the initial swelling of the resin in dichloromethane for 30 min before the first Fmoc-amino acid was coupled to the resin with diisopropylethylamine (DIPEA) and dimethylformamide (DMF). Deprotection of the Fmoc protecting group was then achieved with 10 % piperidine in DMF before a repetitive coupling/deprotection process occurred with amino acid fragments coupled to the growing peptide chain with PyBOP (**57**)/DIPEA. After the last amino acid had been deprotected, the peptide is normally cleaved from the resin using 10 % 1,1,1,3,3,3-hexaflouro-isopropanol in CH_2Cl_2 to yield the protected peptide. However, the quinone portion could also be incorporated into the solid phase synthesis to yield the desired derivatives directly and avoid lower yielding solution phase coupling. Once cleaved off the resin, the additional acid labile protecting groups can be removed with trifluoroacetic acid (TFA) before purification by trituration. SS-31 (**10**) features an alternating aromatic-cationic sequence of aromatic and basic residues, with investigation into this pattern being of initial interest (Figure 37).

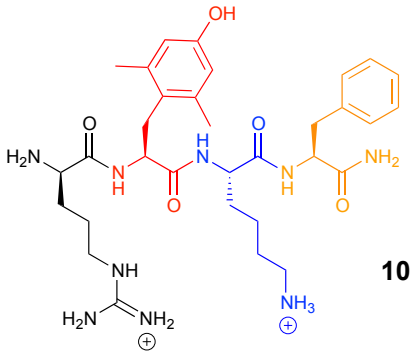

Figure 37: Primary structure of SS-31 (**10**)

The design of SS-31 (**10**) derivatives resulted in a rapid library of analogues required for synthesis. Design of a quinone-peptide conjugate was proposed to combine the SAR completed earlier and the published results of SS-31 (**10**). To develop a structure activity relationship, a variety of questions needed to be answered:

- Is the sequence of amino acids important? i.e. even though the literature indicates alternating aromatic cationic groups, can an analogue with aromatic-aromatic-cationic-cationic produce the same effect?
- As it is proposed that the dimethyltyrosine moiety is important for its antioxidant activities, can tyrosine without the dimethyl substituents provide a similar effect? How do other amino acids effect the acitivty?
- Which end of the peptide should the quinone be attached, the C-terminus or the N-terminus?

With these questions in mind, the first seven analogues were synthesised with the quinone peptides isolated in quantitative yields (Table 12). Upon addition of the quinone fragment, the resin went from clear to bright-yellow, indicating the successful attachment of the quinone moiety.

Table 12: Synthesis of the SPPS analogues **123** – **129**.

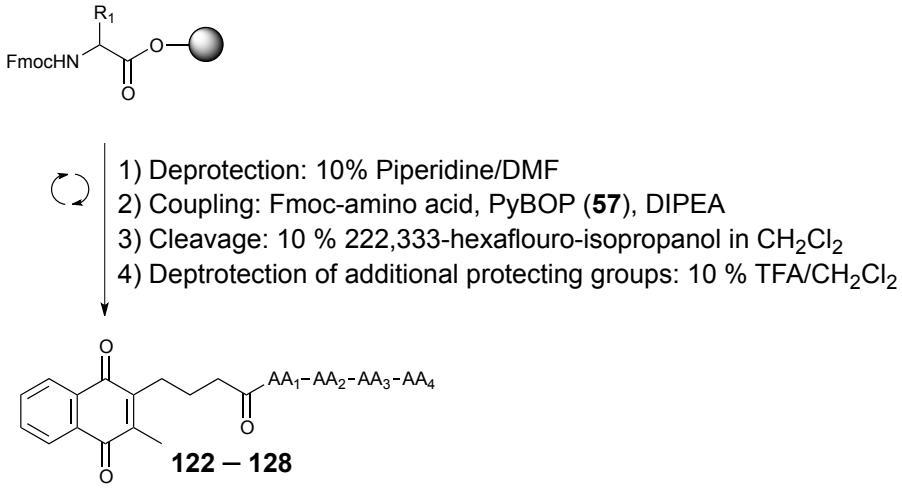

Entry	Amino Acid Sequence (AA_1-AA_2-AA_3-AA_4)	
1	Quin-N-Arg-Tyr-Lys-Phe-OH	**123**
2	Quin-N-Phe-Lys-Tyr-Arg-OH	**124**
3	Quin-N-Lys-Phe-Lys-Phe-OH	**125**
4	Quin-N-Lys-Phe-Phe-Lys-OH	**126**
5	Quin-N-Lys-Lys-Phe-Phe-OH	**127**
6	Quin-N-His-Phe-His-Phe-OH	**128**
7	Quin-N-Lys-Trp-Lys-Trp-OH	**129**

Arg = Arginine Lys = Lysine Trp = Tryptophan His = Histidine Tyr = Tyrosine Phe = Phenylalanine

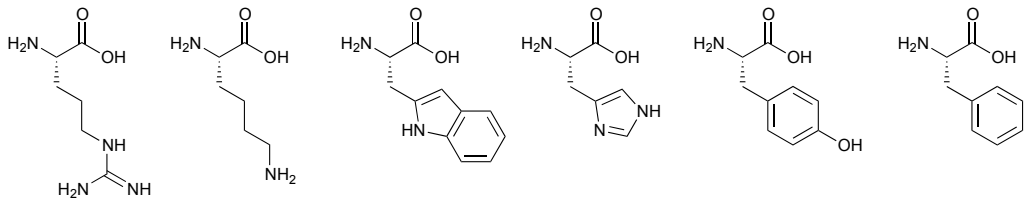

As seen in Table 12, various peptides were synthesised utilising a range of amino acid residues. The first analogue synthesised was a derivative of SS-31 (**10**), where the dimethyltyrosine (DMT) was simply swapped for tyrosine, to allow the effect of the dimethyl substituents to be investigated (**123** + **124**). Focus then shifted to the sequence of the amino acids residues. Although it

has been reported that the alternating aromatic-cationic feature is important, for the purposes of this study we decided to change the order of residues. This resulted in derivatives that contained grouped aromatic or cationic fragments. With analogues **125** – **127** synthesised, upon biological evaluation, a clear indication should be able to be obtained from these analogues. Lastly, SS-31 (**10**) requires charged amino acids, therefore swapping arginine and lysine for histidine and tryptophan will allow us to identify which charged unit will give the greatest activity (**128** and **129**). Unfortunately, due to time constraints, no biological testing has been performed on these analogues to date and therefore no comment in relation to either the order of amino acids or the type of amino acids used can be made on the modifications of the first suite of quinone-peptide conjugates.

2.4 SAR Conclusions

From the analogues investigated for SAR, a variety of important factors were identified. Through modification of the linker and the amide functionality, 31 analogues provided higher levels of cytoprotection than that of the current drug, idebenone (**11**) (Figure 38). Development of SAR has given a clear indication that although the quinone core is essential to be able to shuttle electrons through the electron transport chain, it does not influence the analogue's ability to provide cytoprotection or restore ATP levels. This was also supported by Erb *et al.* when investigating idebenone derivatives.[2]

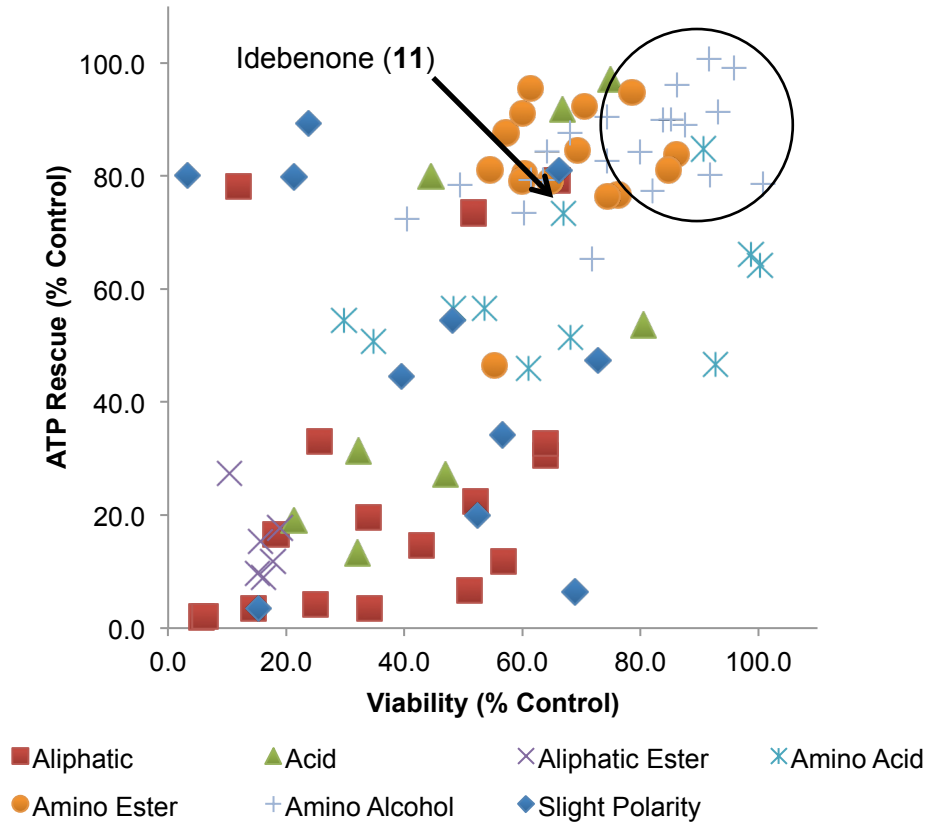

Figure 38: Protection of viability versus acute rescue of ATP levels against rotenone induced complex I dysfunction by naphthoquinones. Both cytoprotection and ATP rescue in HepG2 cells by naphthoquinones (10mM) are displayed as percentage of untreated control (no rotenone) with error bars omitted for clarity. Data represents the mean of n=3 independent experiments with 6 replicates each.

It was demonstrated that a naphthoquinone core in place of a benzoquinone core is essential to minimise toxicity levels. Similarly, a 4-carbon linker seems ideal, however, five- and six-carbon linkers can be utilised as well (Figure 39). The most significant outcome has been the effect that polar groups in the side-chain have on the ability for an analogue to provide both cytoprotection and restore ATP levels. Although previous literature indicates the importance of an analogue's ability to restore ATP levels as the key factor, little emphasis was placed on cytoprotection as it was assumed that increased ATP would result in cytoprotection. However, this study which represents the most in depth study on structure activity relationships (SAR's) suggests that this is not the case. While ATP rescue is a rapid two-hour assay, it is not a realistic measure if the cells do not survive over time with

cytoprotection being a five-day assay. This study has demonstrated the importance of the side-chain to tune/modify activity independently of the quinone core, with numerous examples demonstrating increased ATP but no increase in cytoprotection. However, this should not preclude further investigation of the quinone core, particularly novel quinone moieties.

Further investigation into modification of the naphthoquinone core is also required.

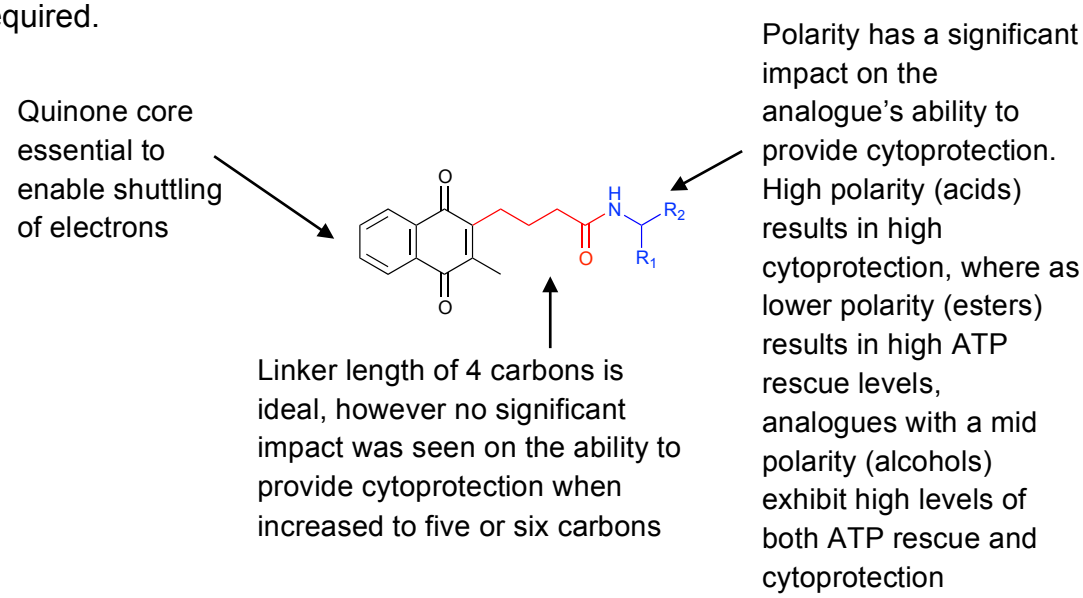

Figure 39: Identified fragments for Structure Activity Relationship (SAR).

Chapter 3: Quinone core optimisation

With the importance of the structure of the side-chain established in the two biological assays, the remaining portion of the active molecule to be investigated was the quinone core. Optimisation of the side-chain resulted in identification of the four-carbon linker and the requirement for an amino alcohol or equivalent amine fragment to provide cytoprotection and restore ATP levels. However, little investigation into the quinone moiety had been undertaken. The most readily available modification to perform on the quinone core was regarding the methyl substituent at the C3-position of the naphthoquinone core (Figure 40). The simplest modification to perform was to replace the methyl substituent with a proton. Therefore, analogues of the simple naphthoquinone core (**4**) with a proton at the-C3 position were synthesised.

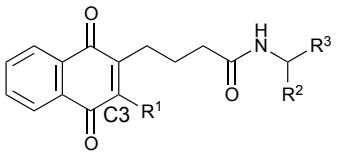

Figure 40: Structure of optimised analogue identifying the C3 position.

3.1 Synthesis of non-methyl naphthoquinone analogues

The preparation of analogues containing no methyl substituent in the C3-position required the initial synthesis of a carboxylic acid analogue containing the naphthoquinone core (**4**) with the four-carbon chain attached. Synthesis of this analogue proceeded *via* the optimised silver-mediated radical decarboxylation process described in Chapter 2.2, Scheme 2. In this way, analogue **130** (Scheme 16) was prepared in 42 % yield. However, di–alkylated analogue **131** was also formed in 9 % yield. The formation of the di–alkylated product was not ideal, however, di–alkylated analogue **131** could be separated from the desired product *via* chromatography. In this way, synthetically useful quantities of the mono–alkylated product were obtained to produce the suite of analogues required for analysis.

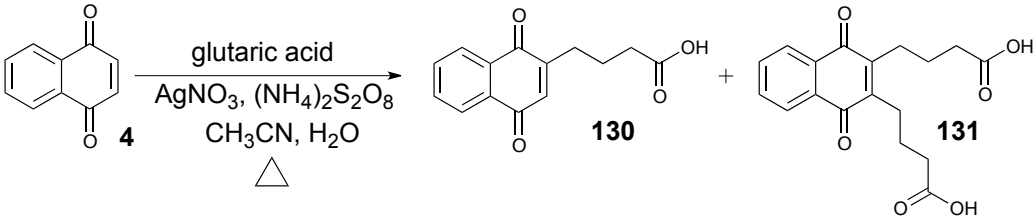

Scheme 16: Formation of analogue **130** and **131**.

Both ^{1}H NMR and ^{13}C NMR spectroscopy supported the formation of the mono– (**130**) and di–alkylated (**131**) products. Formation of the mono–alkylated (**130**) product was supported by ^{1}H NMR spectroscopy with a diagnostic shift of a singlet integrating for two protons at 6.98 ppm upfield to 6.85 ppm and now presenting as a triplet with integration of one (J = 1.1 Hz for allylic coupling). This was a key indication that there was an alkyl chain present at the C2-position, which was supported by three additional peaks within the aliphatic region integrating for two protons each. The presence of an additional carbonyl signal in the ^{13}C NMR at 176.8 ppm was consistent with a carboxylic acid.

In comparison, the ^{1}H NMR spectrum of the more polar di–alkylated derivative (**131**) did not feature signals at 6.85 or 6.98 ppm indicating there were no longer protons attached at the C2- or C3-position of the naphthoquinone core. There are nine carbon environments present in the ^{13}C NMR spectrum and five proton environments in the ^{1}H NMR spectrum (No –OH signal in CD_3OD), which is indicative of di–alkylation due to symmetry within the molecule. Carboxylic acid **130** was then coupled with each of the five lead-amido fragments that were previously identified as part of the SAR studies (Table 13).

Table 13: Synthesis of derivatives **132** – **136** containing the naphthoquinone core (**4**).

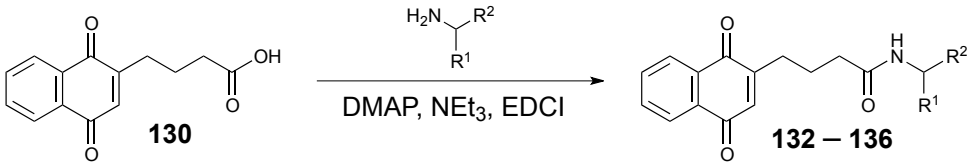

Entry	Amino Derivative	Structure	Yield %
1	L-phenylalanine *t*-butyl ester	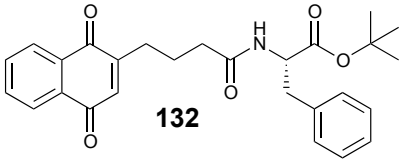 **132**	67
2[#]	L-phenylalanine	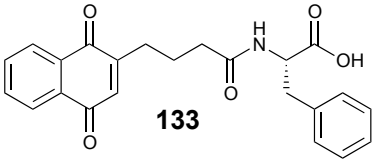 **133**	62
3	L-phenylalaninol	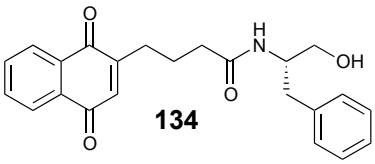 **134**	53
4	tyramine	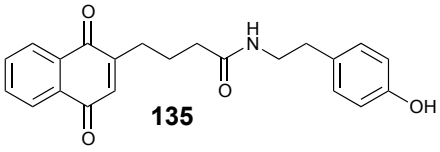 **135**	33
5	3,4-dimethoxy-phenethylamine	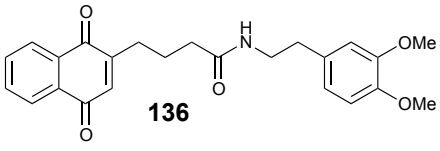 **136**	36

[#] Analogue formed *via* deprotection of the *t*-butyl ester **132**.

The successful synthesis of analogues **132** – **136** was supported by both ^{1}H and ^{13}C NMR spectroscopy. In each case, the respective NMR data was consistent with equivalent data obtained from analogues containing a methyl substituent at the C3-position. Coupling of the amide portion was supported by ^{1}H NMR spectroscopy with a triplet present around 5.63 and 5.89 ppm in analogues **135** and **136**, respectively. A doublet was present in the ^{1}H NMR

spectra associated with amino derivatives (**132** – **134**) at ~6.10 ppm integrating for one proton. This is consistent with the proton attached to the nitrogen.

Analogues **132** – **136** were subjected to biological evaluation to investigate their ability to restore ATP and provide cytoprotection in comparison to the analogues containing a methyl in the C3-position. As shown in Figure 41a, there was a significant decrease in the ability of two of the five analogues to provide cytoprotection when the methyl substituent was removed. However, as seen in Figure 41b, all analogues demonstrated a significant decrease in their capacity to restore ATP levels. This provided a clear indication that the presence of the methyl substituent enhanced activity, possibly by protection from oxidation or stopping other reactions occurring at the C3-position.

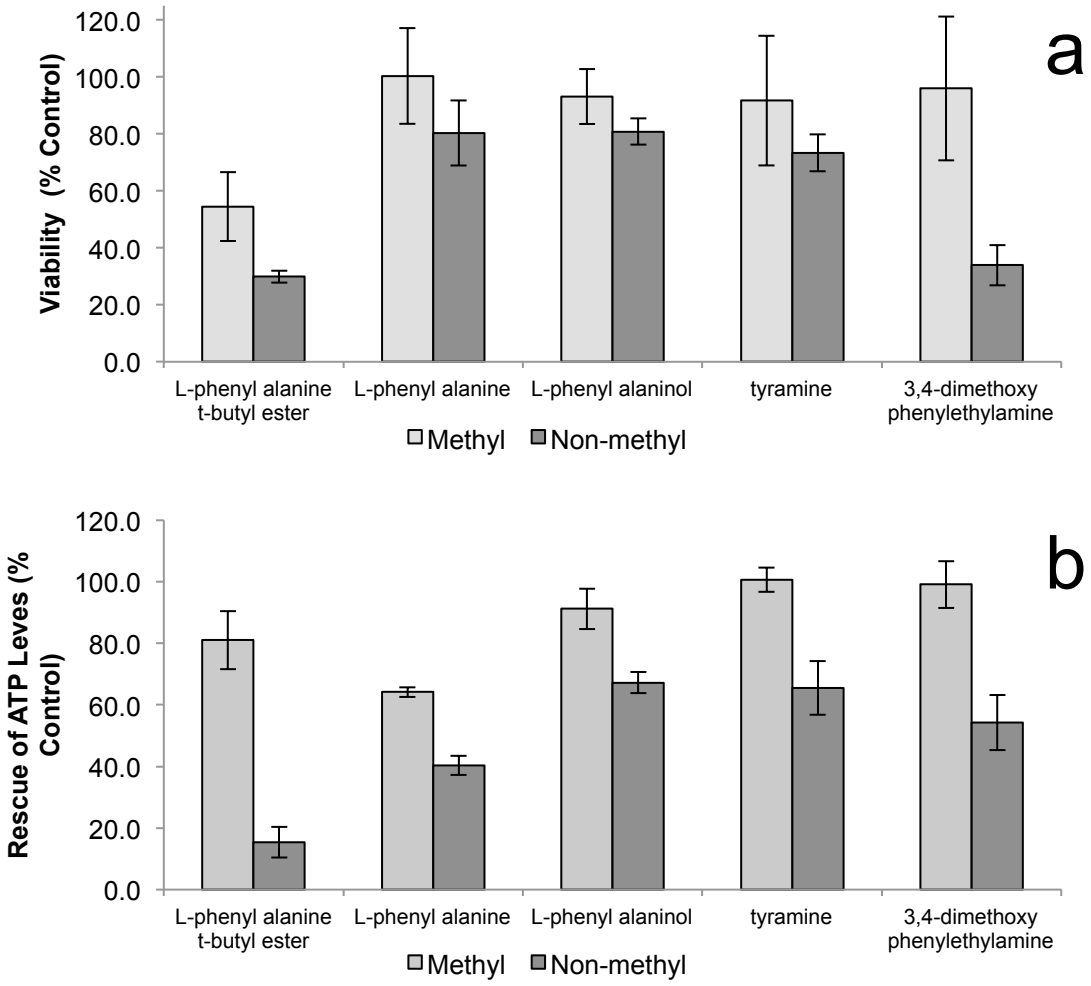

Figure 41: Biological evaluation of methyl and non-methyl naphthoquinones in two assays (a) Cytoprotection against rotenone induced complex I dysfunction by

quinones at 10μM given as a relative percentage of cell survival compared to untreated HepG2 cells (b) ATP rescue by quinones at 10μM in the presence of rotenone-induced complex I dysfunction as percentage of untreated HepG2 cells. Data represents the mean of n=3 independent experiments with 6 replicates each.

This effect was proposed to be due to metabolism by oxidation or conjugation of glutathione (Scheme 17). It is reported that menadione (**12**) readily forms a glutathione-S-conjugate *via* nucleophilic addition resulting in severe cytotoxicity.[95] The loss of viability of HepG2 cells upon exposure to menadione (**12**) was always preceded by a rapid depletion of intracellular glutathione.[96] This drop in glutathione is a result of either oxidation of glutathione to form the disulfide dimer or conjugation[96] with menadione (**12**) to form adducts which are then excreted directly into bile or undergo a series of biotransformations before excretion.[95]

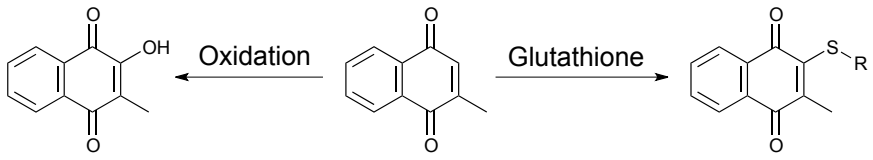

Scheme 17: Oxidation or conjugation of menadione with glutathione.

Thus, it was proposed that this same conjugation or oxidation by metabolism may be occurring with these naphthoquinone derivatives, and as a result the ability to restore ATP and provide cytoprotection would be diminished. As a consequence, the compound is no longer able to transport electrons through the electron transport chain and therefore a proton gradient cannot be maintained. To investigate this hypothesis, the synthesis of analogues containing hydroxyl substituents at the C3-position was undertaken in order to produce the structures that are proposed to result from metabolism (oxidation).

3.2 Synthesis of hydroxyl-naphthoquinone analogues

It was postulated that an epoxidation/hydrolysis sequence of analogues **132** – **136** could provide C3-hydroxy analogues as the synthesis of phthiocol (**138**) from menadione (**12**) has been reported in the literature (Scheme 18).[97] This sequence was successfully reproduced for menadione (**12**).

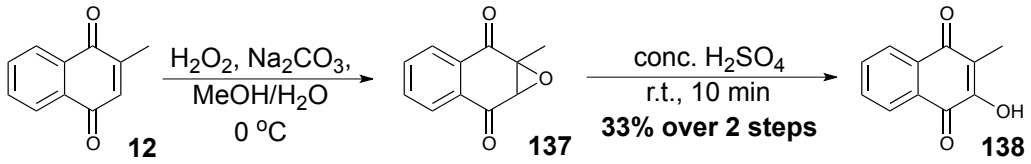

Scheme 18: Epoxidation and hydrolysis of menadione (**12**) to form phthiocol (**138**).

The successful synthesis of analogue **138** was consistent with the literature.[97] Analysis by ^{1}H NMR spectroscopy supported the formation of epoxide **137**,[98] with a diagnostic singlet at 3.86 ppm shifted downfield due to the presence of the epoxide. Similarly, the absence of a singlet peak at 6.84 ppm indicated the loss of the proton attached at the C3-position of menadione (**12**), supported the epoxidation. Hydrolysis of the epoxide **137** with conc. H_2SO_4 furnished analogue **138** as expected in a 33 % yield over the two steps. The yield obtained was lower than expected from the literature,[97] however, it was suitable as a proof-of-concept. Both ^{1}H NMR and ^{13}C NMR spectroscopy supported the formation of analogue **138**, with the diagnostic singlet from the epoxidation product **137** at 3.86 ppm absent and an exchangeable proton singlet present at 7.29 ppm consistent the hydroxyl group. This data was consistent with the literature.[97]

With the proof-of-concept reactions producing the desired compound, synthesis was focused on the transformation of analogues **132** – **136**. Although the initial epoxide formation was successful, hydrolysis of the epoxide for the amide analogues **132** – **136** did not proceed under the same conditions as demonstrated for the menadione (**12**) derivative (Scheme 19).

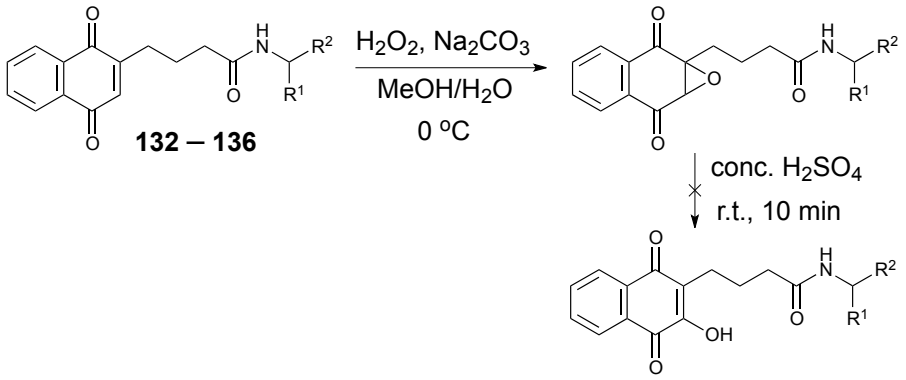

Scheme 19: Attempted epoxidation and hydrolysis of analogues **132** – **136**.

Surprisingly, concentrated sulfuric acid did not hydrolyse the epoxide even at elevated temperatures. Depending on the reaction conditions, either the epoxide was recovered or decomposition occurred. However, further optimisation of these conditions was not conducted as all material available for the various analogues was consumed in the initial attempts. Synthesis to regenerate sufficient amounts of these amide analogues would have been required. Therefore, an alternative synthetic route was investigated. Formation of a hydroxyl version of carboxylic acid analogue **130** prior to amide coupling would reduce the number of synthetic steps. However, when carboxylic acid **130** was reacted *via* the same two-step sequence, the rearrangement of the epoxide failed. Therefore, it was proposed to add the side chain to a hydroxynaphthoquinone.

The synthesis of hydroxy analogue of carboxylic acid derivative **32** was attempted by subjecting lawsone (**139**) to the standard silver-mediated radical decarboxylation method. However, this reaction was unsuccessful and likely due to the presence of the hydroxyl substituent. Concequently, a literature method by Kongkathip *et al.* who successfully *C*-alkylated lawsone (**139**) by α-bromoacetate ethyl ester (**140)** in DMF to form compound **141** in a 40 % yield (Scheme 20) was investigated.[99]

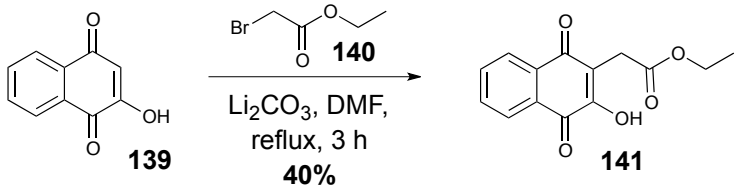

Scheme 20: Successful *C*-alkylation by of lawsone (**139**) by Kongkathip *et al.* [99]

The successful reaction conditions by Kongkathip *et al.* [99] suggested that the introduction of the side-chain could be achieved *via C*-alkylation using ethyl 4-bromobutyrate to form **142** followed a subsequent hydrolysis step to reveal the acid fragment. However, the reported reaction conditions resulted in the formation of analogue **143** by *O*-alkylation (Scheme 21).

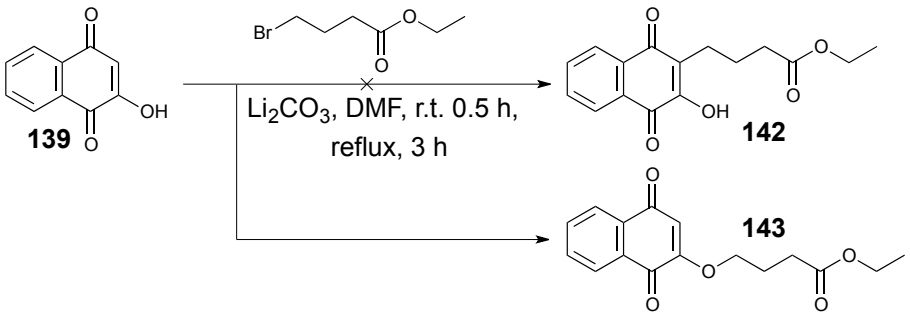

Scheme 21: Failed *C*-alkylation of lawsone (**147**) with Li_2CO_3.

Both ^{1}H NMR and ^{13}C NMR spectroscopy supported the formation of analogue **143** rather than **142**. The most compelling evidence that the *O*-alkylation had occurred in place of *C*-alkylation was the presence of a proton in the ^{1}H NMR spectrum at 6.14 ppm indicating the proton attached to the C3-position of lawsone (quinone) core (**139**). In addition to the diagnostic singlet, a resonance at 4.06 ppm integrating for two protons presenting as a triplet was a key indication that there was a -CH_2- fragment adjacent to oxygen as it was shifted downfield due to deshielding by the oxygen. As this synthetic method had resulted in an undesired *O*-alkylation, alternative reaction conditions were explored.

Although the silver-mediated radical decarboxylation method was unsuccessful for lawsone (**139**), there was literature precedence for the introduction of the alkyl chain through radical generation *via* an alternative silver-free method.[100] Generation of the radical *via* thermal cleavage of a peroxyacid intermediate was previously investigated for menadione (**12**) in the preliminary study by Woolley and co-workers.[75,77] Notably, Yakubovskaya and co-workers employed this same method for the successful introduction of alkyl chains onto the lawsone core (**139**) in 60 – 80 % yields (Scheme 22).

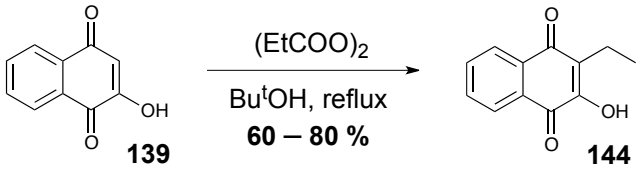

Scheme 22: Successful introduction of an alkyl chain by radical formation by Yakubovskaya *et al.*[100]

Although this method contains a number of drawbacks as discussed in Chapter 2.2, the scale of synthesis required to generate sufficient quantities of a hydroxy analogue of carboxylic acid derivative **32** for subsequent reactions meant this literature method was viable.

The nucleophilic attack of hydrogen peroxide of the carbonyl of the anhydride (**47b**) resulted in the formation of the peroxyacid **145** (Scheme 23). The oxygen of the peroxyacid then underwent the same nucleophilic attack on a second molecule of the anhydride (**47b**), to form the peroxide **48b**.[77] For safety reasons, this analogue was not scrupulously dried and was immediately subjected to the next step. Formation of the putative alkyl radical intermediate was generated through the slow addition of the peroxide to a solution of lawsone (**139**) in refluxing *t*-butanol.

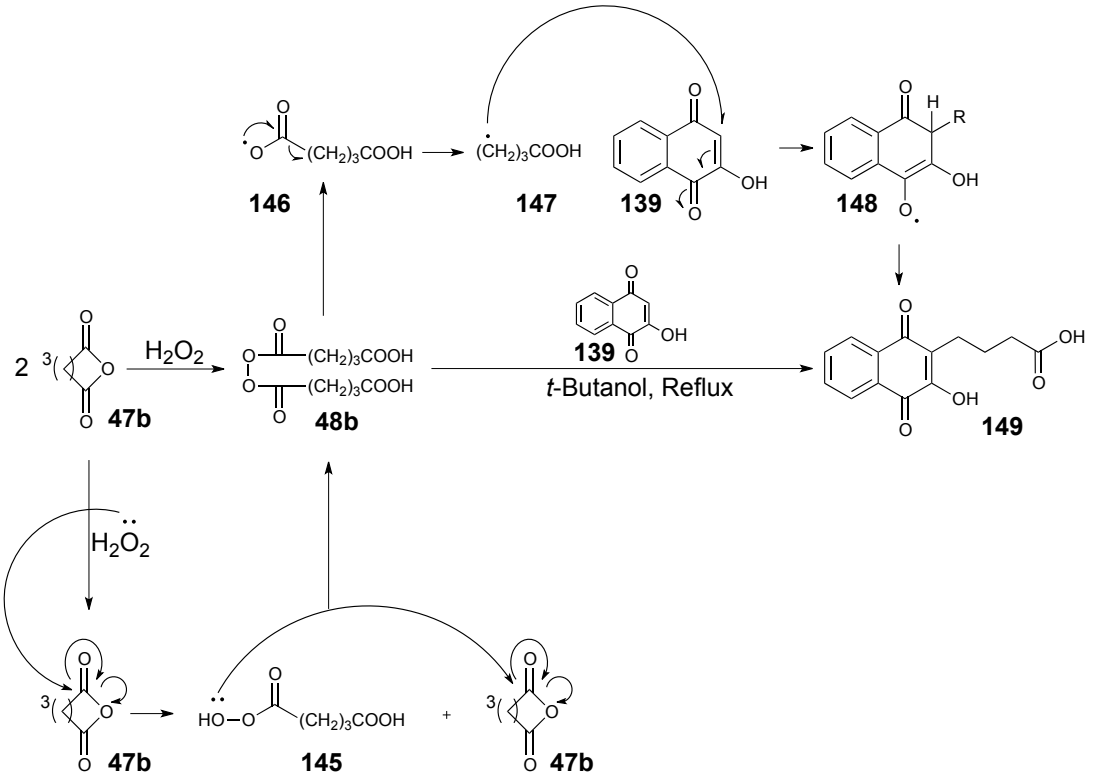

Scheme 23: Synthesis of analogues **149** *via* a peroxyacid intermediate to generate the carbon-centred radical.

The formation of acid **149** was supported by ^{1}H NMR and ^{13}C NMR spectroscopic analysis. However, acid **149** could not be separated from a by-product by either flash column chromatography or recrystallisation. Although

a small amount was obtained in pure form for characterisation purposes, it was decided that analogue **158** would be used as a crude mixture and purified after the amide coupling step. The crude mixture was subjected to amide bond formation with the five key amine fragments (Table 14).

Table 14: Synthesis of derivatives **150** – **154** containing hydroxyl substituents.

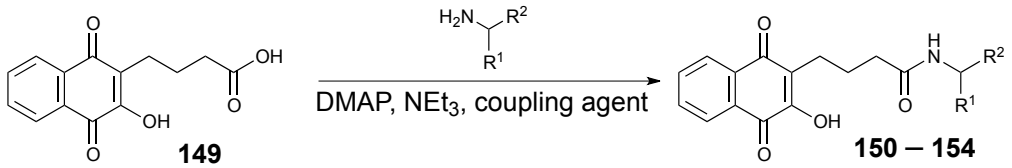

Entry	Amino Derivative	Structure	Yield (%)
1	L-phenylalanine *t*-butyl ester	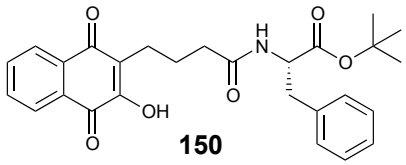 **150**	9*
2[#]	L-phenylalanine	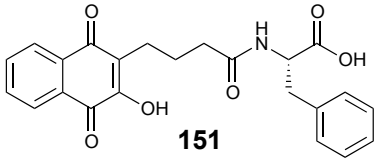 **151**	74
3	L-phenylalaninol	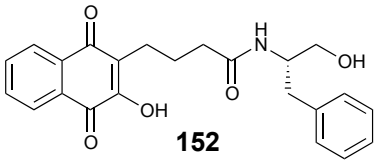 **152**	0
4	tyramine	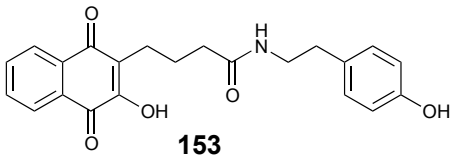 **153**	4*
5	3,4-dimethoxy-phenethylamine	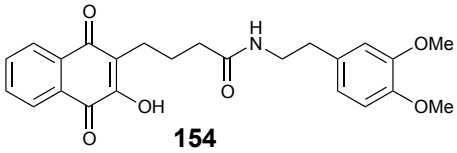 **154**	5*

[#] Analogue formed *via* deprotection of the *t*-butyl ester **150**.
* Yield was calculated as if acid **149** was a pure compound.

With the exception of phenylalaninol derivative **152**, all of the compounds were successfully prepared and characterised by ^{1}H and ^{13}C NMR spectroscopy. The yields of these analogues (**150**, **153** and **154**) were very low (<10 %) but sufficient material was formed for biological evaluation. The ^{1}H NMR spectra associated with analogues **150**, **151**, **153** and **154** were consistent with the equivalent ^{1}H NMR spectroscopic data associated with the respective non-methylated analogues (**132**, **133**, **135** and **136**). A key diagnostic shift at ~155.0 ppm in the ^{13}C NMR spectrum associated with all analogues was consistent with the presence of the hydroxyl substituent on the quinone core. In the other C3-derivatives (Me or H), this carbon signal was present at ~145.0 ppm.

Unfortunately, the formation of phenylalaninol derivative **152** was not successful when PyBOP (**59**) was used as the coupling agent. Analysis of the crude mixture by ^{1}H NMR spectroscopy could not determine whether the amide coupling was successful. It is not clear if the alcohol was interfering with the coupling. Attempts using different coupling agents all proved fruitless and no products were isolated. Due to time constraints, biological evaluation was performed without L-phenylalaninol derivative **152** and synthesis of analogue **152** was no longer pursued. All successfully synthesised analogues were subjected to biological evaluation and compared against the methyl and non-methyl analogues as indicated in Figure 42.

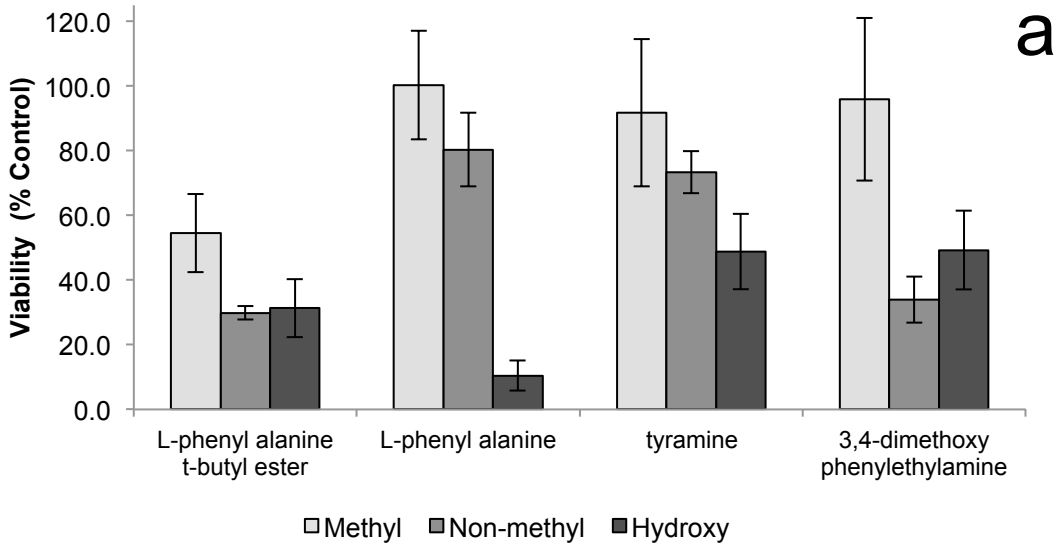

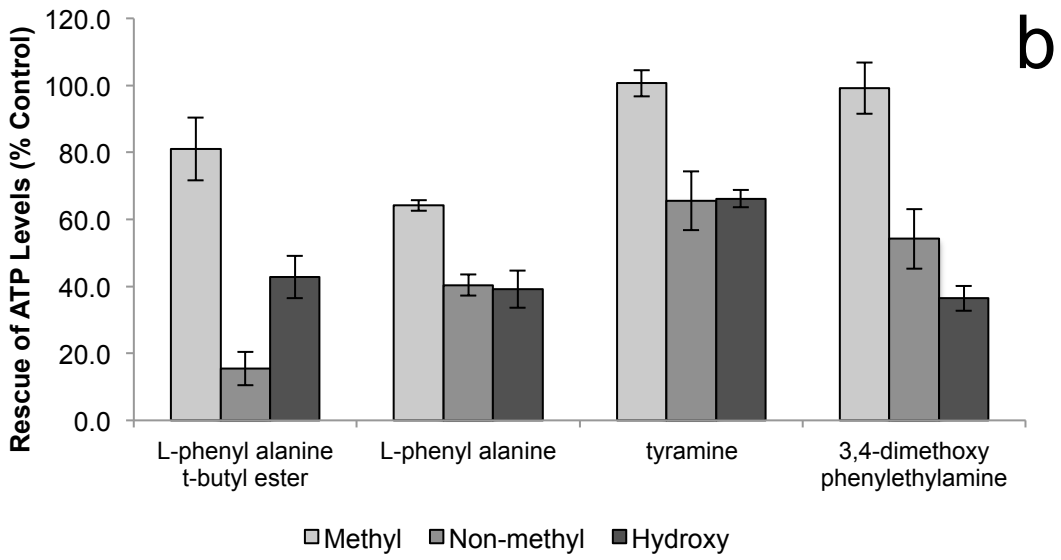

Figure 42: Biological evaluation of methyl, non-methyl and hydroxyl substituted naphthoquinones in two assays (a) Cytoprotection against rotenone induced complex I dysfunction by quinones at 10μM given as a relative percentage of cell survival compared to untreated HepG2 cells (b) ATP rescue by quinones at 10μM in the presence of rotenone-induced complex I dysfunction as percentage of untreated HepG2 cells. Data represents the mean of n=3 independent experiments with 6 replicates each.

As observed with the non-methyl derivatives (**132** – **136**), the analogues containing a hydroxyl substituent showed a decrease in their ability to provide cytoprotection and restore ATP levels compared to the methyl derivatives (**61**, **70**, **76**, **79** and **80**). A decrease in cytoprotection indicates the hydroxyl quinone derivatives **150**, **151**, **153** and **154** are more cytotoxic. Not only does this evidence support the hypothesis that the methyl substituent blocks metabolism or prevents some form of conjugation, it also highlights the need for further investigation into modifications of the quinone core.

These results indicated the need for a substituent at the C3-position of the naphthoquinone core. However, quinones containing hydroxyl substituents such as embelin (**155**) and plumbagin (**156**) (Figure 43) are both found to induce apoptosis in various human cancer cells and increase ROS production.[101-105] As these are undesirable characteristics for analogues that provide protection against mitochondrial dysfunction, hydroxyl groups should not be considered for further core modifications.

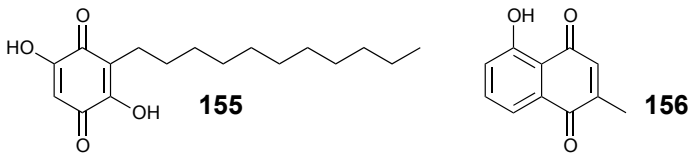

Figure 43: Structure of Embelin (**155**) and Plumbagin (**156**).

Prior to further core modifications occurring such as halogenation in the C3-position, it was proposed more evidence was required to determine if the naphthoquinone core was in fact optimal. All prior hypotheses were based of toxicity data and the comparison of idebenone (**11**) and the idebenone-like naphthoquinone derivative (**13**). Therefore, further evidence was required for a direct comparison of benzoquinones before additional core modifications were to be conducted. Therefore, the synthesis of analogues containing the plastiquinone and benzoquinone cores was required for comparison. This was attempted using the silver-mediated addition of an alkyl group to the corresponding quinone.

3.3 Synthesis of plastiquinone analogues

Synthesis of analogues containing the plastiquinone core required the oxidation of trimethylhydroquinone (**157**). The oxidation of hydroquinone was effected using a mixture of iodine, sulfuric acid and aqueous hydrogen peroxide at room temperature to afford 2,3,5-trimethyl-*p*-benzoquinone (plastiquinone) (**5**) in an 80% yield as reported in the literature (Scheme 24).[18]

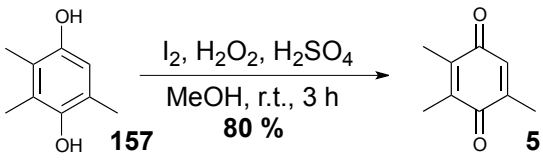

Scheme 24: Formation of the plastiquinone core (**5**) *via* oxidation.

The successful synthesis of the plastiquinone core (**5**) was consistent with the literature.[18] Two diagnostic carbonyl signals present in the ^{13}C NMR spectrum at 187.3 and 187.7 ppm indicated that oxidation to the quinone had occurred. With the formation of sufficient quantities of the plastiquinone core

(**5**), it was then subjected to the silver-mediated radical decarboxylation reaction to introduce the four-carbon chain as seen in Scheme 25.

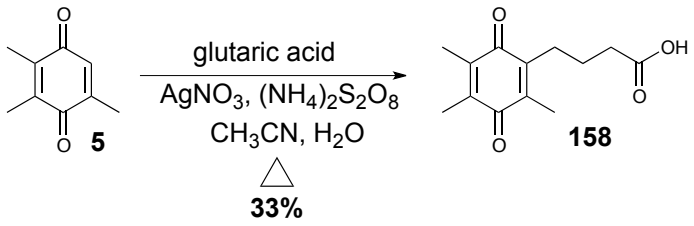

Scheme 25: Formation of analogue **158**.

Alkylation of the plastoquinone core **5** gave the desired analogue **158** in a moderate 33 % yield. This was not ideal, however, in order to prevent the formation of a by-product similar to that observed when synthesising the naphthoquinone carboxylic acid derivative **32**, the reaction time was limited to 0.5 h with sufficient quantities obtained to prepare subsequent compounds. The unreacted plastiquinone core (**5**) was recovered *via* chromatography and reused in subsequent reactions. Formation of analogue **158** was supported by both ^{1}H and ^{13}C NMR spectroscopic analysis, with no spectral data available in the literature for comparison. The diagnostic absence of a singlet in the ^{1}H NMR at 6.46 ppm indicated that the proton at the C3-position of the plastiquinone core (**5**) was no longer present. Additional resonances in the aliphatic region of the ^{1}H NMR spectrum indicated the successful introduction of the four-carbon chain. An additional carbonyl resonance in the ^{13}C NMR spectrum at 179.2 ppm supported the presence of the carboxylic acid fragment of the new alkyl chain. The plastiquinone derivative containing the four-carbon chain (**158**) was then subjected to amide coupling of the top five fragments as seen in Table 15.

Table 15: Synthesis of plastiquinone derivatives **159** – **163**.

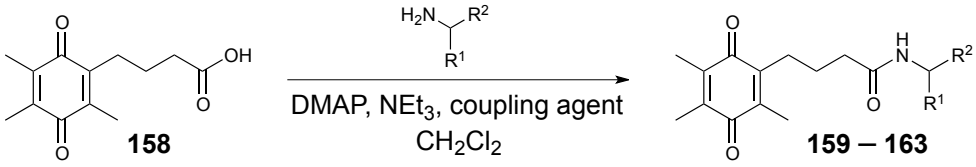

Entry	Amino Derivative	Structure	Yield %
1	L-phenylalanine *t*-butyl ester	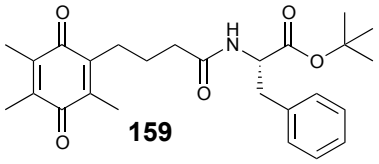 **159**	24
2[#]	L-phenylalanine	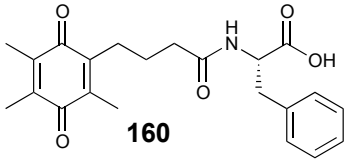 **160**	>95
3	L-phenylalaninol	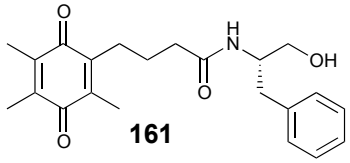 **161**	11
4	tyramine	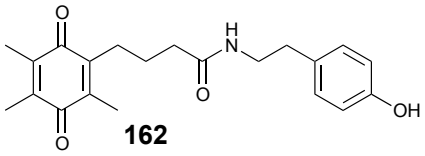 **162**	51
5	3,4-dimethoxy-phenethylamine	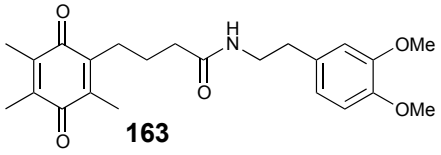 **163**	42

[#] Analogue formed *via* deprotection of the *t*-butyl ester **168**.

The successful synthesis of analogues **159** – **163** was supported by ^{1}H NMR and ^{13}C NMR spectroscopy. The NMR spectra associated with analogues **159** – **163** were consistent with the equivalent NMR spectroscopic data associated with the respective naphthoquinone derivatives (**61**, **70**, **76**, **79** and **80**). However, the yield of **161** was exceptionally low, prompting investigation as to why amide coupling had not been high yielding for the phenylalaninol. A second compound (**164**) (Figure 44) was isolated from the

reaction mixture; however, no yield for **164** was obtained. The formation of analogue **164** was proposed to be a result of decomposition of the coupling agent BOP (**59**) due to age, which allowed for amide coupling to the dimethylamine fragments.

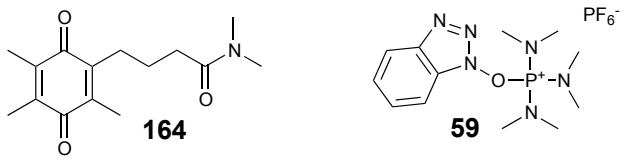

Figure 44: Structure of the by-product (**164**) and BOP (**59**).

Formation of the by-product (**164**) was identified by ^{1}H NMR spectroscopy with two very distinctive singlets at 2.92 and 2.98 ppm integrating for three protons each. The formation of the by-product (**164**) resulted in a decrease of the amount of the plastiquinone derivative (**158**) and accounted for the reduced yield of phenylalaninol derivative **161**. Although the yields for all analogues were low, sufficient quantities were synthesised for the purpose of biological evaluation. However, before all plastiquinone analogues were subjected to biological evaluation, synthesis of the benzoquinone derivatives were required for comparison.

3.4 Synthesis of 2,3-dimethoxy-5-methyl-1,4-benzoquinone analogues

Synthesis of analogues containing the 2,3-dimethoxy-5-methyl-1,4-benzoquinone core (**6**) required the synthesis of the core itself, which was achieved through a four-step synthesis (Scheme 26).

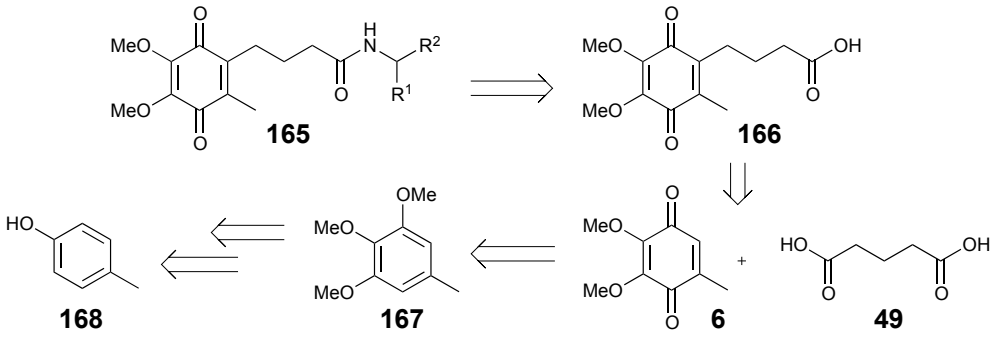

Scheme 26: Retrosynthetic analysis of analogues containing the 2,3-dimethoxy-5-methyl-*para*-benzoquinone core (**6**).

Synthesis of the benzoquinone core (**6**) required commercially available 2,3,4-trimethoxytoluene (**167**) as a precursor. However, due to difficulties sourcing this compound, the key starting material was synthesised in the first instance.

Synthesis of 3,4,5-trimethoxytoluene (**167**)

2,3,4-Trimethoxytoluene (**167**) was synthesised by the literature method[106] starting from *p*-cresol (**168)**, through bromination followed by *O*-methylation to produce 3,5-dibromo-4-methoxytoluene (**170**) before subsequent methoxylation to produce 3,4,5-trimethoxytoluene (**167**) (Scheme 27).[106]

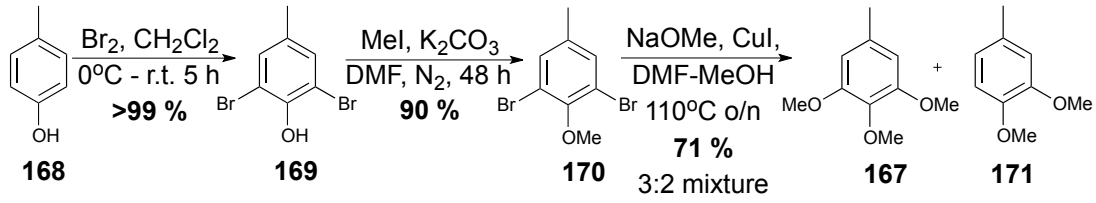

Scheme 27: Synthesis of 3,4,5-trimethoxytoluene (**167**).

Formation of 2,6-dibromo-*p*-cresol (**169**) was consistent with the literature and required no purification.[107] ^{1}H NMR spectroscopy supported the formation of the product with a lone singlet present in the aromatic region at 7.20 ppm integrating for two protons indicating successful dibromonation with no proton signal splitting due to symmetry. *O*-Methylation of 2,6-dibromo-*p*-cresol (**169**) with methyl iodide produced 3,5-dibromo-4-methoxytoluene (**170**) as a pale yellow oil in 90 % yield (Figure 45). The copper-catalysed C–

O coupling of dibromide **170** provided 3,4,5-trimethoxytoluene (**167**) and 3,4-dimethoxytoluene (**171**) in a 3:2 ratio respectively.[108]

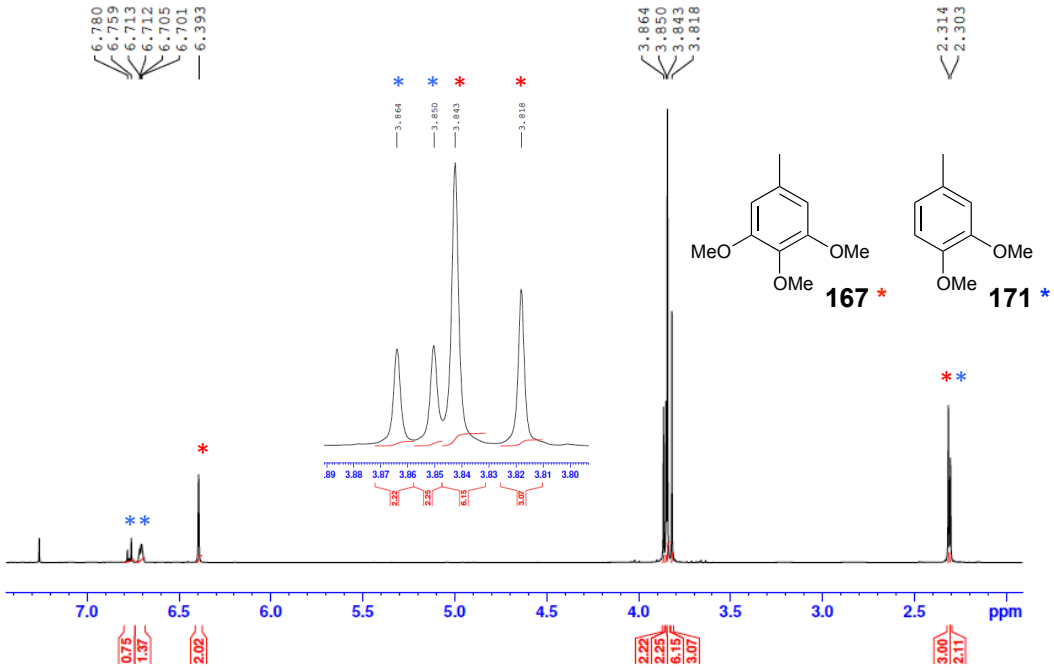

Figure 45: ^{1}H NMR of a 3:2 mixture of 3,4,5-trimethoxytolune (**167**) and 3,4-dimethoxytoluene (**171**).

The two analogues were clearly distinguished by ^{1}H NMR spectroscopy with two singlets present at 3.81 and 3.84 ppm integrating for three and six protons respectively, which is consistent with 3,4,5-trimethoxytoluene (**167**). In comparison, two singlets present at 3.85 and 3.86 ppm integrating for three protons each is consistent with 3,4-dimethoxytoluene (**171**). These two analogues co-eluted *via* column chromatography and although separation would have been possible by distillation, the mixture was not purified but was used in the next step as a crude mixture. The formation of the 3,4-dimethoxytoluene (**171**) through de-halogenation was proposed to be a result of the quality of copper (I) iodide used. However, due to sufficient quantities of 3,4,5-trimethoxytoluene (**167**) obtained, further reactions with fresh copper (I) iodide were not pursued.

Synthesis of the 2,3-dimethoxy-5-methyl-benzoquinone core (6) and analogues

2,3-Dimethoxy-5-methyl-benzoquinone core (**6**) was prepared according to a literature procedure by Wang and co-workers,[109] who screened and optimised conditions for the conversion of 3,4,5-trimethoxytoluene (**167**) to 2,3-dimethoxy-5-methyl-1,4-benzoquinone (**6**). Formation of **6** occured in metal-free conditions utilising hydrogen peroxide as an oxygen atom donor. The choice of solvent, formic acid/acetic acid, is reported to play an important role in the transformation.[109] Formation of the benzoquinone core (**6**) proceeded in a 55 % yield and was easily purified by chromatography from the 3,4-dimethoxytoluene (**171**) (Scheme 28).

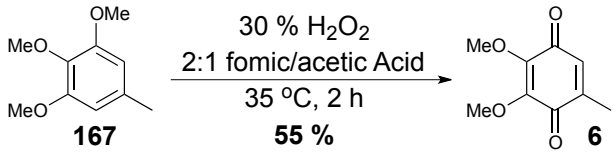

Scheme 28: Synthesis of 2,3-dimethoxy-5-methyl-1,4-benzoquinone (**6**).

Formation of the benzoquinone core (**6**) was consistent with the literature[109] and supported by both ^{1}H NMR and ^{13}C NMR spectroscopy. With the formation of the core complete, this analogue was subjected to the silver-mediated radical decarboxylation process to install the four-carbon chain (Scheme 29).

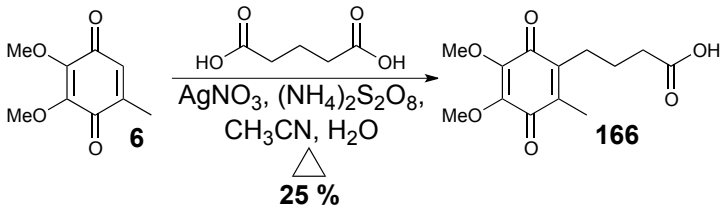

Scheme 29: Formation of analogue **166**.

Reaction of benzoquinone **6** under the standard conditions gave the desired benzoquinone carboxylic acid **166** in a low 25 % yield. Despite the yield, the unreacted benzoquinone core **6** was recovered after column chromatography and re-used in subsequent reactions. Both ^{1}H NMR and ^{13}C NMR spectroscopy supported formation of analogue **166**, with the absence of the

diagnostic peak at 6.42 ppm, indicating the proton attached to the C3-position of the core was no longer present. Similarly, the presence of a third carbonyl signal at 178.5 ppm and additional aliphatic carbon signals in the ^{13}C NMR spectrum indicated the successful installation of the alkyl chain. The benzoquinone derivative containing the four-carbon chain (**166**) was then subjected to amide coupling of the top five fragments (Table 16).

Table 16: Synthesis of benzoquinone derivatives **172** – **176**.

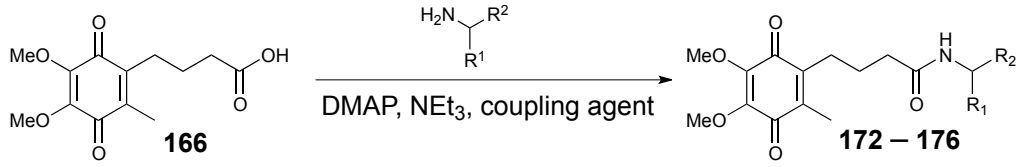

Entry	Amino Derivative	Structure	Yield (%)
1	L-phenylalanine *t*-butyl ester	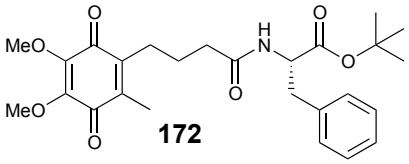 **172**	12
2[#]	L-phenylalanine	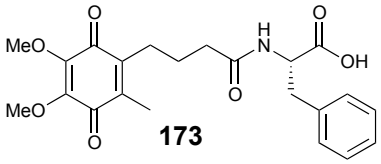 **173**	84
3	L-phenylalaninol	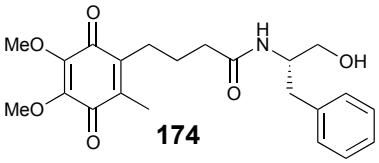 **174**	17
4	tyramine	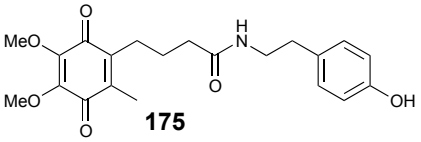 **175**	13
5	3,4-dimethoxy-phenethylamine	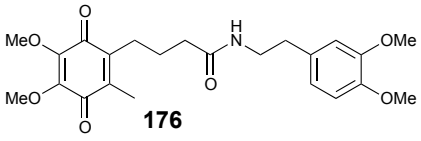 **176**	11

[#] Analogue formed *via* deprotection of the *t*-butyl ester **172**.

Synthesis of the analogues proceeded as expected, albeit in low yields. These yields and reactions occurred prior to the knowledge that the integrity of the BOP (**59**) coupling agent was compromised. Therefore, a large percentage of the mass contained the dimethyl amide. Co-elution of this impurity was also an issue and the isolation of the pure product required multiple chromatographic attempts, which contributed to the low yields. Both ^{1}H NMR and ^{13}C NMR spectroscopy supported the formation of all analogues, with characteristic signals associated with both the plastiquinone and naphthoquinone analogues also observed for the benzoquinone analogues (**172** – **176**).

With both the plastiquinone and benzoquinone analogues synthesised, biological evaluation was undertaken to compare the three quinone cores with identical side-chains (Figure 46). In all but one case, the activity of the benzoquinone and plastoquinones was significantly less than the naphthoquinone. Notably, L-phenylalanine, L-phenylalaninol, tyramine and 3,4-dimethoxyphenethylamine analogues containing either the plastiquinone or benzoquinone core showed no ability to provide cytoprotection or restore ATP levels.

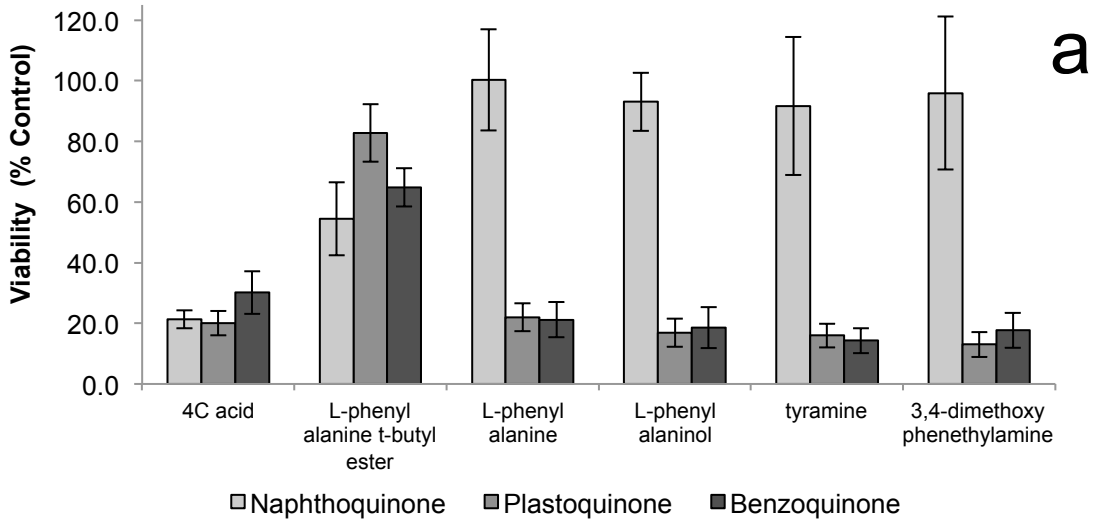

Figure 46a: Biological evaluation of naphthoquinone, plastoquinone and benzoquinone. Cytoprotection against rotenone induced complex I dysfunction by quinones at 10μM given as a relative percentage of cell survival compared to untreated HepG2 cells Data represents the mean of n=3 independent experiments with 6 replicates each.

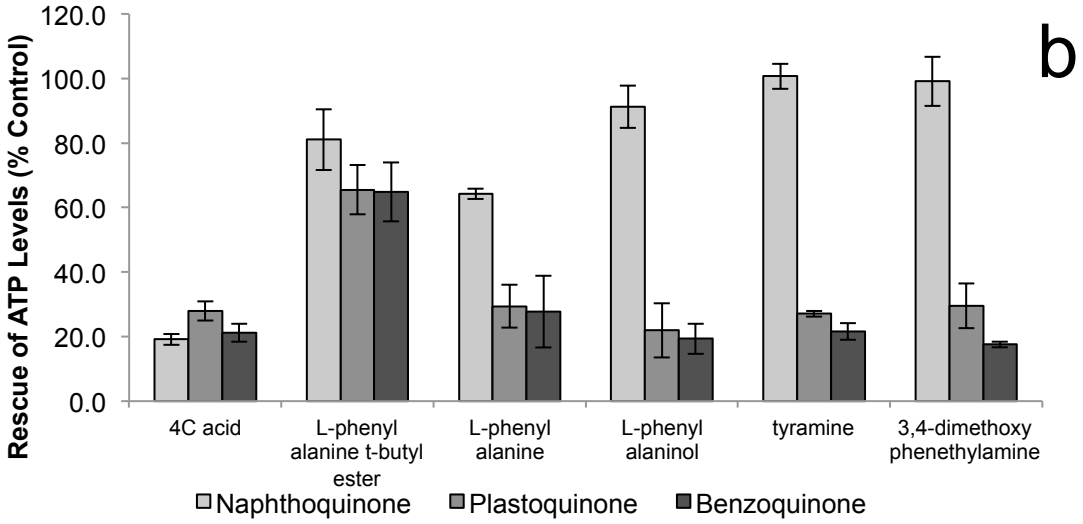

Figure 46b: Biological evaluation of naphthoquinone, plastoquinone and benzoquinone. ATP rescue by quinones at 10μM in the presence of rotenone-induced complex I dysfunction as percentage of untreated HepG2 cells. Data represents the mean of n=3 independent experiments with 6 replicates each.

The comparison of the four-carbon acid analogues of all three quinone cores showed no difference in their ability to provide cytoprotection or restore ATP levels with all showing little activity in ATP rescue or cytoprotection. Within the top five optimised analogues, the naphthoquinone core was superior to both the plastiquinone and benzoquinone derivatives indicating the combination of the naphthoquinone core and side-chain provide superior activity. Both plastiquinone and benzoquinone derivatives were unable to provide cytoprotection or restore ATP levels with the exception of the L-phenylalanine *t*-butyl ester derivatives, which provided unexpected results as all three quinone cores produced similar levels of protection. Although the naphthoquinone L-phenylalanine *t*-butyl ester analogue **61** did not provide excellent cytoprotection, it was expected that both the plastiquinone and benzoquinone analogues would still show a significant difference. This result prompted the question as to whether the quinone moiety was actually required or was a simple aryl group sufficient for this substrate. Therefore an analogue containing phenyl butyric acid coupled to L-phenylalanine *t*-butyl ester was synthesised (Scheme 30) to determine if ATP rescue and cytoprotection could be restored in the absence of a quinone moiety.

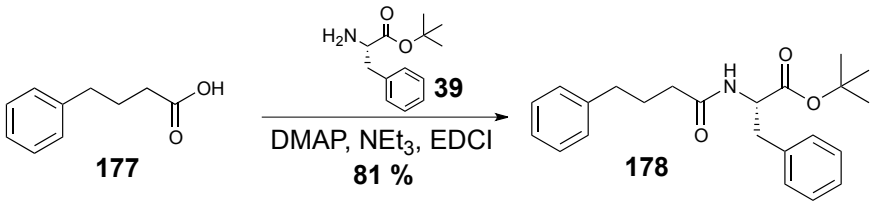

Scheme 30: Synthesis of analogue **178**.

The successful synthesis of analogue **178** from phenylbutyric acid and L-phenylalanine *t*-butyl ester occurred in an 81 % yield. Both ^{1}H NMR and ^{13}C NMR spectroscopy supported the formation of the analogue with the characteristic doublet at 6.13 ppm integrating for one proton which was identified as the proton attached to the nitrogen. Biological evaluation of phenyl derivative **178** indicated it had no ability to restore ATP or provide cytoprotection, which was vastly different from the quinone derivatives. Therefore this indicated the requirement of the quinone core for activity was essential. The likely explanation for the results seen for the L-phenylalanine *t*-butyl analogues with all three cores is the effect of polarity of the residues. There is potential that the less polar *t*-butyl esters resemble the types of compounds investigated by Erb *et al*.[2] Nevertheless, this result does not affect the outcome of this research, as the L-phenylalanine *t*-butyl ester analogues do not provide the highest level of cytoprotection or ATP rescue levels seen by the other four fragments and the L-phenylalanine, L-phenylalaninol, tyramine and 3,4-dimethoxyphenethylamine derivatives remain the most active.

Therefore, core optimisation studies indicated the importance of the naphthoquinone core and the requirement for a substituent in the C3-position. This potentially prevents metabolism of the naphthoquinone core. The methyl group represented the optimal C3-substituent investigated. The comparison of the three quinone cores illustrated the ineffectiveness of all potential therapeutics currently being investigated for mitochondrial dysfunction. Notably, to date no analogues contain the naphthoquinone core. Initial investigations into the phosphonium cation analogues MitoQ (**8**) and SKQ1 (**9**) have shown potential as therapeutics for mitochondrial dysfunction but again both have neglected to investigate the core properties. Similarly

with idebenone (**11**), a simple modification to the naphthoquinone has shown dramatic results. Therefore this result indicates that studies investigating quinone analogues for mitochondrial dysfunction should also include derivatives featuring naphthoquinone core for comparison.

3.5 Synthesis of Indoloquinone analogues

The idea of investigating novel organic cores was attempted with the introduction of the indoloquinone core (**179**) as a substitute for the naphthoquinone (Figure 47). Various indoloquinones are naturally occurring and are known to contain antifungal, antitumour activity and cytotoxic activities.[110] One well known indoloquinone is Mitomycin C (MMC, **180**) (Figure 47), which is an antitumour antibiotic (chemotherapeutic agent) and has been widely used for the treatment of various cancers.[111,112] Since the discovery of MMC (**180**) and its clinical applications, a large number of synthetic indoloquinones have been developed. A synthetic analogue of MMC (**180**), apaziquone (EO9, **181**) is currently in advanced clinical trials as a treatment for bladder cancer (Figure 47).[113]

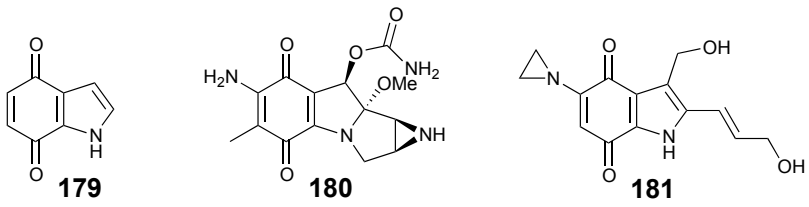

Figure 47: Structure of the indoloquinone core (**179**), Mitomycin C (MMC, **180**) and synthetic analogue apaziquone (EO9, **181**).

Although the bioactive characteristics of Mitomycin C (**180**) are not ideal for analogues to treat mitochondrial dysfunction, it is important to note that the majority of indoloquinones within the literature are highly functionalised, which is vastly different from the application under investigation. The compounds proposed would be simple substrates with an alkyl chain at one of the four positions (Figure 48).

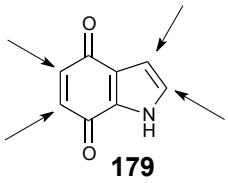

179

Figure 48: Structure if the indoloquinone core **179** with the four sites of modification highlighted.

Initially, a propyl chain attached to the C3-position of the indoloquinone core would be required, which could be prepared by the proposed sequence in Scheme 31. The 4,7-dimethoxyindole (**182**) was required, which upon oxidation yields the indoloquinone core. The key step in the synthesis of indole **182** was a Hemetsberger–Knittel reaction meaning that 2,5-dimethoxybenzaldehyde was required.

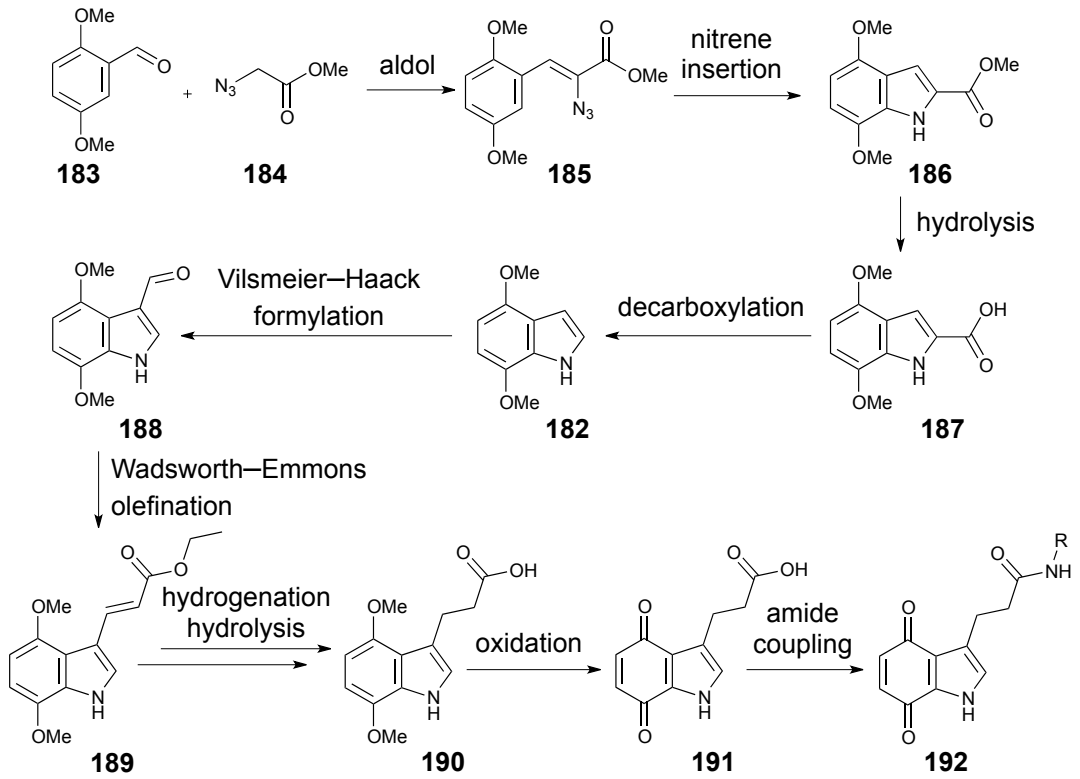

Scheme 31: Proposed multi-step reaction route to obtain analogue **192**.

Synthesis of 2,5-dimethoxybenzaldehyde (**183**) proceeded according to literature methods *via* bromination of hydroquinone (**193**) to give **194**.[114-116] Subsequent *O*-methylation of the hydroxyl groups with methyl iodide provided **195**, then a bromine–lithium exchange and reaction with DMF

produced 2,5-dimethoxybenaldehyde (**183**)[117] in ~62 % yield over the three steps (Scheme 32).

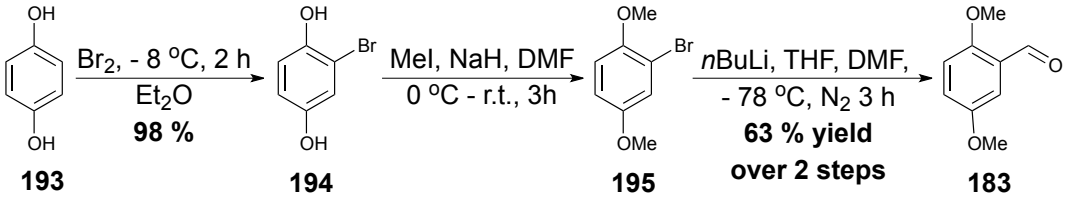

Scheme 32: Synthesis of 2,5-dimethoxybenaldehyde (**183**).

The successful synthesis of **183** was consistent with the literature and supported by both ^{1}H NMR and ^{13}C NMR spectroscopy.[118] 2,5-Dimethoxybenzaldehyde (**183**) underwent a modified aldol condensation reaction (Knoevenagel condensation[119]) with methyl-2-azidoacetate (**184**) (Scheme 33) to form analogue **185.** Compound **185** was subjected to thermal ring closure to form the indole core (**186**) *via* a Hemetsberger–Knittel reaction which involves insertion of a nitrene.[120] Hydrolysis of ester of **186** revealed the carboxylic acid fragment in **187** in a 60 % yield.

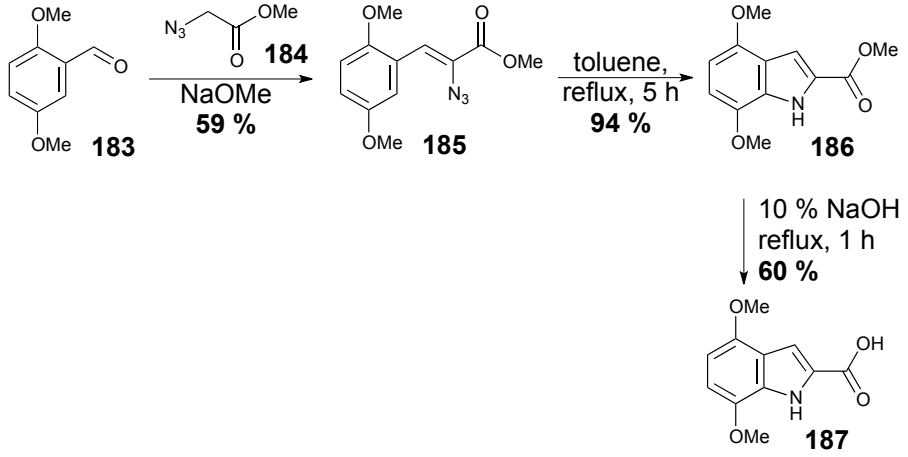

Scheme 33: Formation indole core **187**.

The ^{1}H NMR and ^{13}C NMR spectra of **185**, **186** and **187** were consistent with equivalent data reported previously.[121] The ^{1}H NMR spectrum of indole **186** showed two distinct doublets at 6.33 and 6.59 ppm each integrating for one proton, which was consistent with the protons attached to the C5 and C6 position. The proton attached at the C3 position of the indole was consistent with a doublet at 7.44 ppm (J = 2.3 Hz). Hydrolysis to form **187** was

consistent with literature[121] and in comparison to the ^{1}H NMR spectrum of **186**, did not feature a singlet at 3.90 ppm, which previously integrated for three protons, suggesting the loss of the methyl substituent.

Decarboxylation of **187** was problematic with the literature method resulting in a poor yield and therefore reaction conditions were optimised (Table 17). Optimisation of the literature method (Table 17, Entry 1) featured an investigation into copper loading, temperature and reaction time. In addition to optimisation of the reaction conditions, the work-up procedure was also altered. The literature method[121] featured the evaporation of quinoline under reduced pressure followed by chromatography, however, difficulties of removing the quinoline prior to chromatography proved problematic. Instead, an aqueous extraction was effective in removing the quinoline before indole **182** was purified by chromatography.

Table 17: Optimisation of reaction conditions for the decarboxylation of **187** to yield **182**.

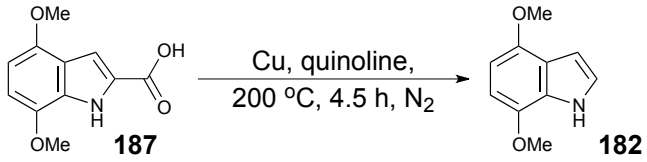

Entry	Copper Bronze (eq.)	Reaction Time (h)	Temperature (°C)	Work up Procedure	Yield %
1	0.7	3	160	filtration	6
2	0.7	18	160	filtration	22
3	5	2.5	200	aqueous extraction	44
4	**5**	**4.5**	**200**	**aqueous extraction**	**60**
5	5	6	200	aqueous extraction	22

Note: Yield % is the pure mass after purification.

Spectroscopic analysis of the decarboxylation of 4,7-dimethoxy-1*H*-indole-2-carboxylic acid (**187**) to yield 4,7-dimethoxyindole (**182**) was consistent with that reported in the literature.[121] However, an inability to replicate the results

(table 17, Entry 4) was a significant issue as yields varied from 19 – 60 %. A subsequent Vilsmeier–Haack formylation provided aldehyde **188**[122-124] and a Wadsworth–Emmons olefination was then performed to install the alkyl side chain (Scheme 34).

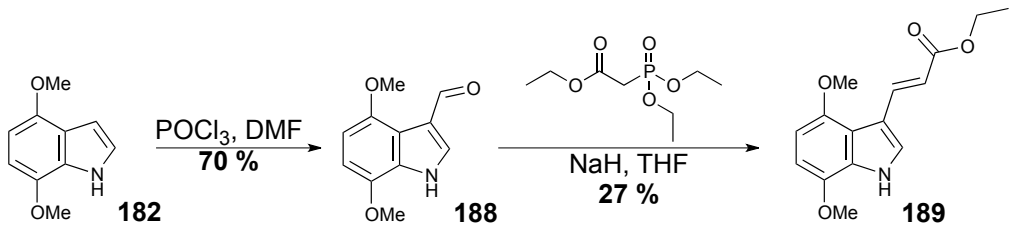

Scheme 34: Formation of analogue **188** and **189**.

Formylation of 4,7-dimethoxyindole **182** gave aldehyde **188** in good yield (70 %) according to the literature procedure.[124] A diagnostic resonance at 10.30 ppm in the ^{1}H NMR spectrum was consistent with the introduction of an aldehyde while a singlet at 7.89 ppm was consistent with the proton attached to the C2-position, therefore supporting formylation at C3. This was further supported by an additional carbonyl resonance at 186.3 ppm indicating the successful installation of the aldehyde functionality. However, when subjected to the Wadsworth–Emmons olefination to produce novel compound **189,** the reaction proceeded in a low 27 % yield. Both ^{1}H NMR and ^{13}C NMR spectra supported the successful conversion to analogue **189**. The ^{1}H NMR spectrum showed key diagnostic features for the introduction of an ethyl ester functionality with a distinct triplet at 1.33 ppm integrating for three protons and a quartet at 4.26 ppm integrating for two protons which was shifted downfield due to deshielding by the ester. In addition, two doublets were present at 6.41 and 8.30 ppm with a coupling of 14.0 Hz. This indicated the presence of a *trans*-alkene as expected from a Wadsworth–Emmons olefination.

The low yields obtained for the key steps such as the formation of **182** by decarboxylation and the Wadsworth–Emmons olefination of **188** to form **189** dictated that the structure of the target molecule should be revised. A more synthetically accessible molecule was identified in order to evaluate the biological activity of an indoloquinone moiety as a Complex I bypass prior to

committing to prepare a more complex target. Therefore a new synthetic route was devised to utilise indoloquinone **197** to introduce side-chains to make compounds such as **198** (Scheme 35). This would require far fewer synthetic steps and used indole ester **186** already in-hand.

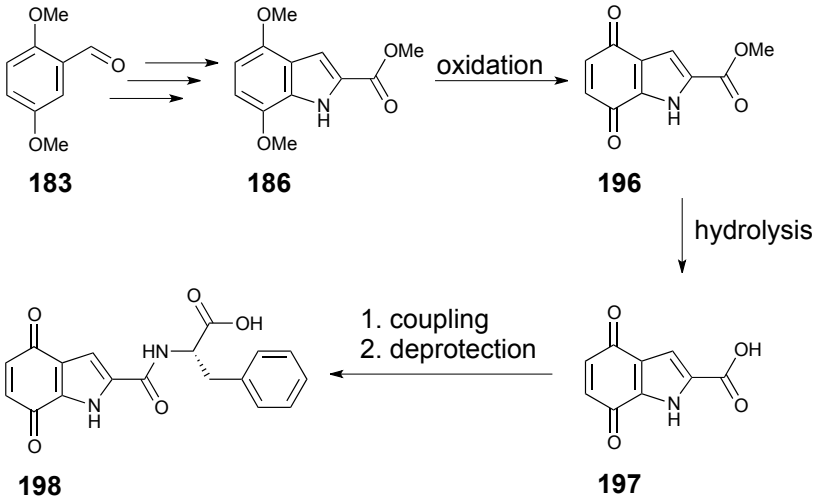

Scheme 35: Proposed formation of analogue **198**.

Initial oxidation attempts were performed using ceric ammonium nitrate (CAN) as it is the most frequently used oxidant for formation of quinones. Oxidation of the indole methyl ester **186** to the indoloquinone core of **196** was performed following a literature method with reported quantitative conversion of derivative **199** to **200** (Scheme 36).[125]

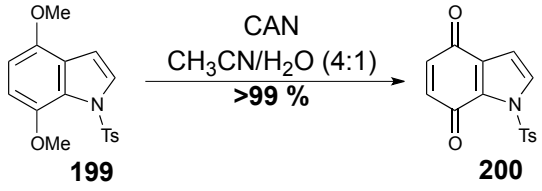

Scheme 36: Literature example of oxidation of an indole core **199** to the corresponding indoloquinone **200**.[125]

However, oxidation of the indole methyl ester **186** to the indoloquinone core of **196** using the literature method proved difficult. An unidentified product was obtained in high yield. Initially this was proposed to be over oxidation of the C3-position of the indole ring or introduction of a nitro (NO_2) substituent through radical formation as no signal for H3 could be observed in the ^1H

NMR spectrum. Therefore supporting a structure consistent with **201a**. Optimisation of the reaction conditions focused on shortening of the reaction time, avoiding light to prevent the formation of nitro radicals and decreasing the reaction temperature (Table 18). Unfortunately, in all cases the desired product was not formed.

Table 18: Oxidation of **186** using CAN.

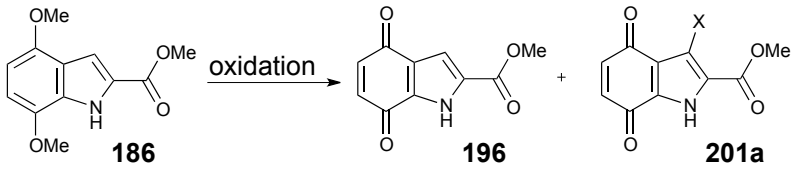

Entry	Temperature (°C)	CAN (Eq.)	Light/Dark	Reaction Time (h)	**196**	**201a**
1	r.t.	3	Light	2	✗	✓
2	r.t.	3	Dark	1	✗	✓
3	0	3	Dark	1	✗	✓

Formation of the indoloquinone portion of the oxidation product **201a** was supported by two doublets present in the ^{1}H NMR spectrum at 6.57 and 6.70 ppm integrating for one proton each with a coupling of 10.3 Hz indicating H5 and H6 protons. In addition to this, two carbonyl signals at 179.1 and 184.2 ppm for C4 and C5 indicated the successful oxidation to the indoloquinone core. The structural assignment of the molecule could be determined with the exception of the C3-substituent. Analysis of the sample by MS indicated that a dimer had formed and therefore the structure of the oxidation was bispyrrole **201** (Figure 49). The predicted HRESIMS for $C_{20}H_{12}N_2NaO_8$ was 431.0486 and it was found to be 431.0487 for analogue **201**.

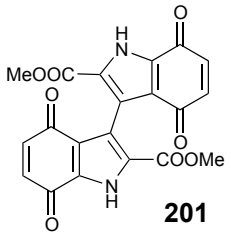

201

Figure 49: Structure of by-product **201**.

This suggests that the desired product was formed but reacted further and therefore alternative oxidants were investigated. A literature method for oxidising indoles to indoloquinones *via* silver oxide and nitric acid was employed, however, decomposition occurred.[126] Therefore alternative conditions were explored. Hypervalent iodine (III) oxidant, PIFA (phenyliodine (III) bis(trifluoroacetate)), was shown to oxidise indoles to indoloquinones in aqueous reaction conditions in good yields (Scheme 37).[127]

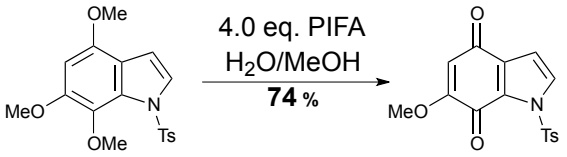

202 **203**

Scheme 37: Literature example of oxidation of an indole (**202**) to the corresponding indoloquinone (**203**) using PIFA.[127]

Utilising PIFA under the reported conditions, the desired product (**196**) was obtained (Table 19, Entry 1), but the undesired bisindoloquinone **201** formed in the CAN reactions was observed as the major product in a 1:2 ratio of **196**:**201**. Therefore the reaction conditions for PIFA oxidation were optimised to increase conversion of the desired product (**196**) and minimise formation of the undersired bispyrrole **201** (Table 19).

Table 19: Oxidation of analogue **186** using PIFA.

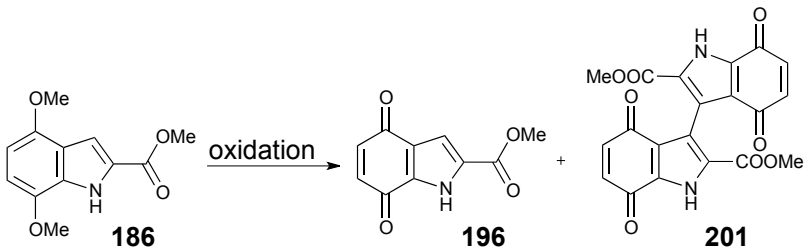

186 **196** **201**

Entry	PIFA (Eq.)	Reaction Time (h)	Temperature (°C)	**186** : **196** : **201**
1	4	2	r.t.	0 : 1: 2
2	4	0.75	r.t.	0 : 1 : 2
3	1.5	1	0	3.5 : 5 : 4.5
4	**1.5**	**1**	**r.t.**	**1 : 1 : 0.2**
5	1.5	1	40	1 : 1 : 0.5

Decreasing the reaction time from 2 h to 0.75 h did not alter the product ratio. However, decreasing the equivalents of PIFA from 4 to 1.5 resulted in a decrease in the formation of the undesired bispyrrole **201**. A decrease in reaction temperature resulted in both **196** and **201** forming at similar rates. The reaction conditions (Table 19, Entry 4) were deemed to be the conditions for future oxidation as minimal by-product was formed. Notably there is starting material present, however chromatography enabled the separation and recovery of both materials. Thus, the recovered starting material could be reused.

The structure of the desired indoloquinone **196** was supported by both ^{1}H NMR and ^{13}C NMR spectroscopy and was consistent with the spectral data reported in the literature.[128] The successful oxidation to indoloquinone **196** was supported by ^{13}C NMR spectroscopy with the presence of two new carbonyl signals at 177.7 and 182.3 ppm. A doublet at 7.23 ppm with a coupling for 1.7 Hz and an integration of one was consistent with the presence of the C3 proton in the ^{1}H NMR spectrum.

The formation of the bisindoloquinone **201** was proposed to result from an Scholl oxidation, which is the dimerization of an aryl, however, electron rich heteroarenes such as pyrroles and indoles have also been reported to undergo such reactions.[129,130] Specifically, Kita and co-workers developed the use of PIFA and a Lewis acid additive in the oxidative coupling of pyrroles (**204**) to give bipyrroles (**205**) (Scheme 38).[127,131]

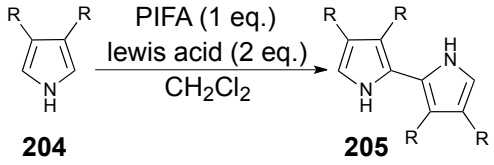

204 **205**

Scheme 38: Oxidative coupling of pyrroles using PIFA to give bipyrroles.[129,130]

Therefore, it is not surprising that an indoloquinone dimer was obtained in the presence of PIFA. In the literature examples of **200** and **203** with CAN and PIFA respectively, the bispyrrole is likely not formed due to an electron-withdrawing group present on the nitrogen of the pyrrole. Notably, it appears that there are no reports in the literature of CAN effecting this type of reaction. With sufficient quantities of **196** now available, an attempted hydrolysis of the methyl ester to reveal the acid moiety was performed as indicated in Scheme 39.

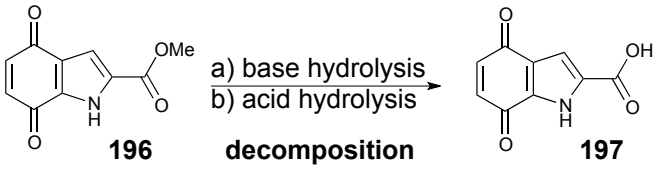

196 **decomposition** **197**

Scheme 39: Attempted hydrolysis of **196** to form **197**, (a) 10 % NaOH (b) H_2SO_4, AcOH, H_2O.

However, both base and acid hydrolysis under standard conditions resulted in rapid decomposition. Therefore it was proposed that changing the reaction sequence to the hydrolysis of the methyl ester, oxidation to the indoloquinone and then subsequent amide coupling was one potential synthetic pathway or hydrolysis followed by amide coupling and then oxidation to the indoloquinone as the alternative pathway to investigate. Oxidation of the 4,7-dimethoxy-1*H*-indole-2-carboxylic acid **187** to the resulting indoloquinone *via*

the optimised PIFA reaction conditions resulted in complete decomposition. Therefore, coupling of L-phenylalanine *t*-butyl ester to 4,7-dimethoxy-1*H*-indole-2-carboxylic acid **187** prior to oxidation was investigated. Coupling of 4,7-dimethoxy-1*H*-indole-2-carboxylic acid **187** with L-phenylalanine *t*-butyl ester resulted in the formation of analogue **206** in a 50 % yield (Scheme 40).

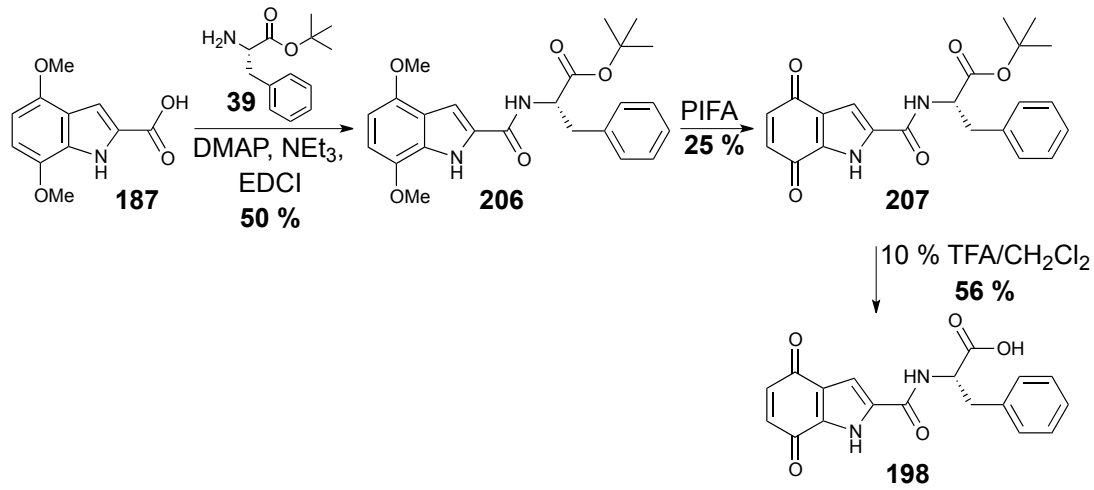

Scheme 40: Formation of analogue **198**.

Formation of the coupled product **206** was supported by ^{1}H NMR and ^{13}C NMR spectroscopy. The ^{1}H NMR spectrum featured a doublet present at 6.77 ppm integrating for one proton with a coupling of 7.7 Hz, which is consistent with the proton attached to the nitrogen. The presence of the C3 proton was supported by a doublet at 6.97 ppm with a coupling of 1.7 Hz. Analogue **207** was then oxidised to the indoloquinone following the optimised PIFA conditions, producing the indoloquinone analogue **207** in a 25 % yield. Notably, the undesired dimer of **207** was also present. Formation of **207** was supported by both ^{1}H NMR and ^{13}C NMR spectroscopy. The key diagnostic signals that suggested that the successful oxidation had occurred were the two carbonyl signals at 177.4 and 182.6 ppm in the ^{13}C NMR spectrum. Additional support for this was the absence of the singlet at 3.89 ppm, which integrated for 6 protons and had previously been attributed to the methoxy substituents. Lastly, a singlet at 6.93 indicated the proton attached to the C3-position had been retained throughout the oxidation process.

In the final step, deprotection of the *t*-butyl ester revealed acid **198**. Successful removal of the protecting group was supported by both ^{1}H NMR and ^{13}C NMR spectroscopy. In the ^{1}H NMR spectrum, the absence of a singlet at 1.44 ppm integrating for nine protons was consistent with this. Furthermore, the ^{13}C NMR spectrum displayed the loss two signals at 83.2 and 28.1 ppm for the quaternary and methyl carbons respectively, which supports the loss of the *t*-butyl group.

The successful synthesis of indoloquinone **198** clearly was inefficient and required a large number of synthetic steps. Most importantly it indicated this was not a viable route to obtain a library of compounds containing the indoloquinone core moiety for SAR. Thus, due to the significant synthetic challenges encountered and the exceptionally low yields for a number of reaction steps, a new synthetic pathway was required. A possible alternative may employ a synthetic method developed by Eastabrook *et al.* which utilises a C–H borylation method (Scheme 41).[128]

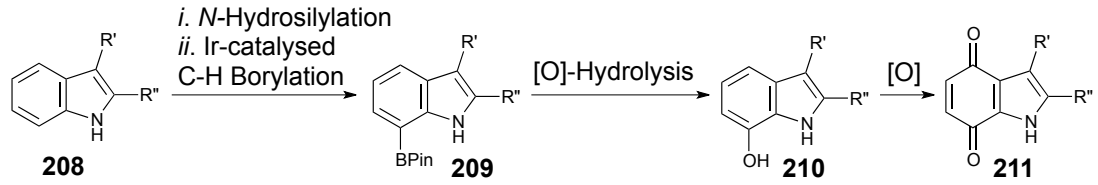

Scheme 41: Literature method by Eastabrook *et. al.* for rapid three step synthesis of indoloquinones.[128]

However, due to time restraints no other indoloquinone analogues were synthesised until the results of biological testing on analogue **198** were obtained.

3.6 Conclusions

In summary, in this chapter a number of important factors were identified:-

1. The methyl substituent at the C3-position of the naphthoquinone core was identified as highly important, as removal of this substituent resulted in a decrease in cytoprotection and the ability to restore ATP levels.

2. This effect was proposed to be due to oxidation or conjugation with glutathione that prevented the analogues to shuttle in and out of the mitochondria.

3. The superiority of the naphthoquinone core over both plastiquinone and benzoquinone analogues was determined. It was demonstrated that both the plastiquinone and benoquinone derivatives were unable to rescue ATP levels and provide cytoprotection under identical conditions in a comparative analysis featuring five common side-chains.

4. Therefore, the identified analogues that are superior to idebenone require a naphthoquinone core with a methyl substituent in the C3-position, a side chain containing a four-carbon linker and an amino alcohol or equivalent amine attached through an amide linkage (Figure 50).

With the SAR complete, the next stage will be to select compounds for *in vivo* analysis.

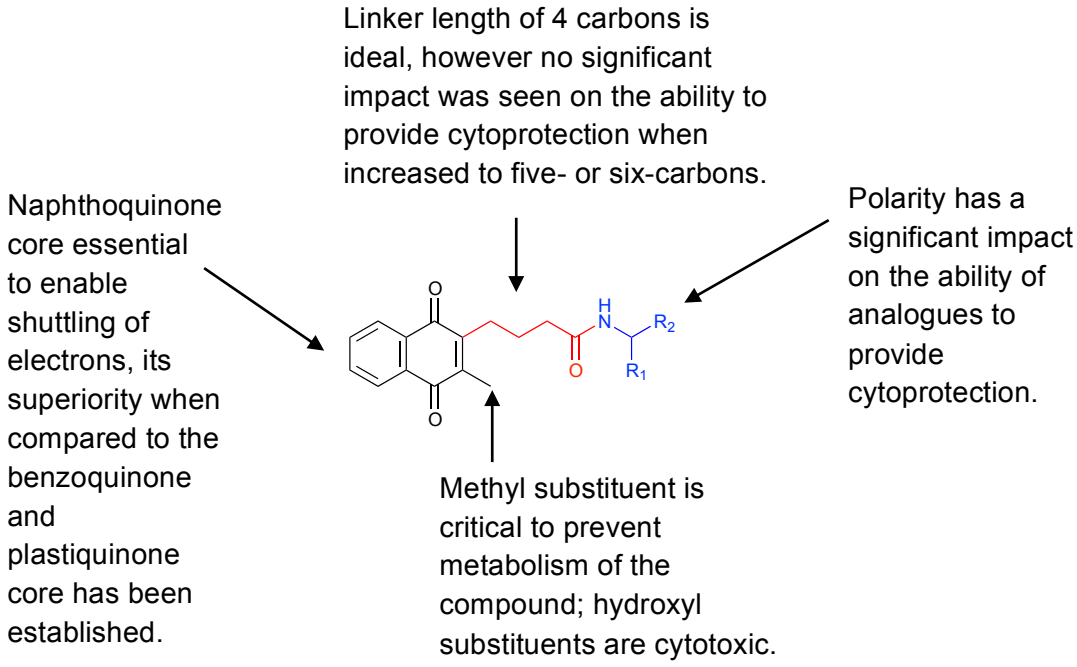

Figure 50: Identified fragments for structure activity relationship (SAR).

Chapter 4: Redox active dye synthesis

A molecular probe that provides a fluorescent reporter signal upon enzyme activation is highly sought after for many biological applications. This group of molecules are often referred to as optical contrast agents and are currently being explored by researchers for visualizing biological processes at the molecular level within living systems.[132,133] In the literature, there are many examples of quinones coupled to profluorescent molecules that upon reduction with NQO1 release fluorophores resulting in fluorescence.[134] One such example by Silvers and co-workers, employs compound **212** (Scheme 42) as a rapid and selective tool for visualising and detecting human cancer cells that over express NQO1.[134] In the context of this project, the monitoring of enzymes that can reduce quinones may be beneficial.

For example, a profluorophore would be highly beneficial for identifying patients that have an inactivating NQO1 polymorphism, which are described in the general population, such as 609C>T polymorphism that results in decreased or even absent enzymatic activity of NQO1.[14,64,65] If there is decreased or absent enzymatic activity, no fluorescence would be observed using such a probe. Identifying patients who have a NQO1 inactivation is of high importance as failure to reduce the quinone can lead to cytotoxicity.[2] Therefore, synthesis of a probe utilising the well-known naphthalimide dyes was investigated (Scheme 42).

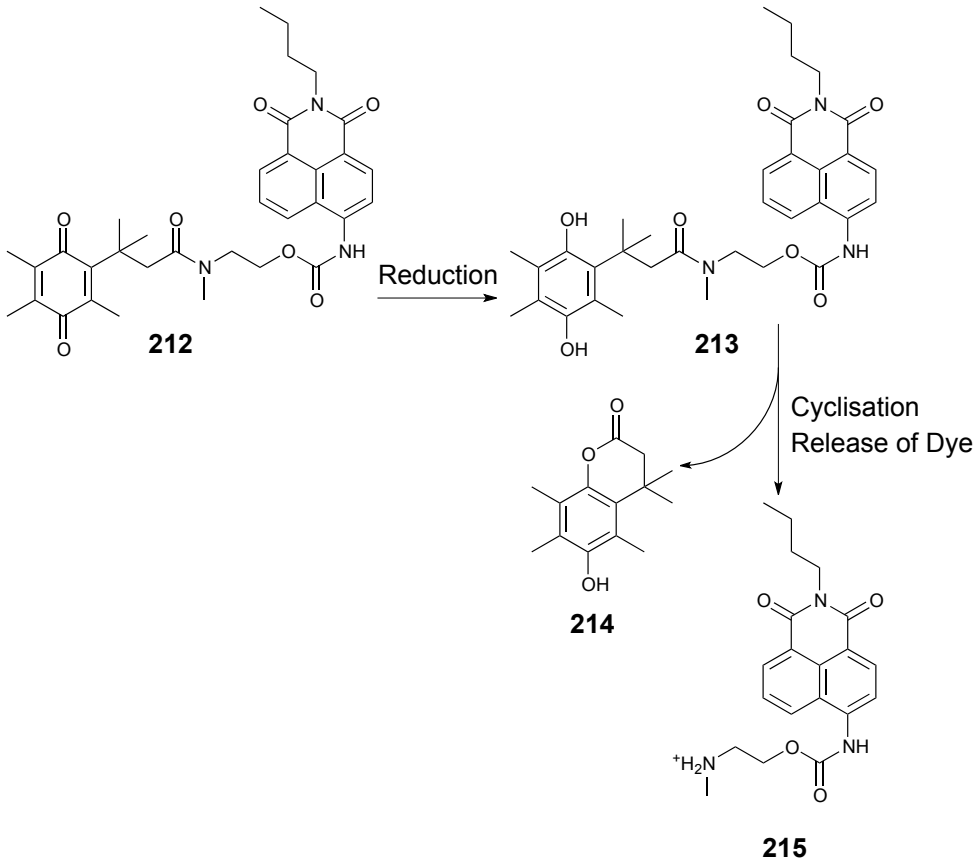

Scheme 42: Representative reduction of a profluorophore **212** to release dye **215**.

This probe will be designed such that the fluorescence of the naphthalimide portion is quenched by being in close proximity to the quinone motif.[133,134] Upon reduction of the quinone to the hydroquinone, the molecule will undergo lactonisation and release of the fluorophore resulting in a fluorescence signal. Structural modifications to the profluorophore can be broken down into three sections, the quinone acid, the linker and lastly the dye itself (Figure 51). It has been demonstrated previously that the carbon-chain between the quinone and the carbonyl need *gem*-dimethyl substituents.[134] This exploits the Thorpe–Ingold effect and cyclisation is >10^3 faster than analogues without the *gem*-dimethyl substituents.[134]

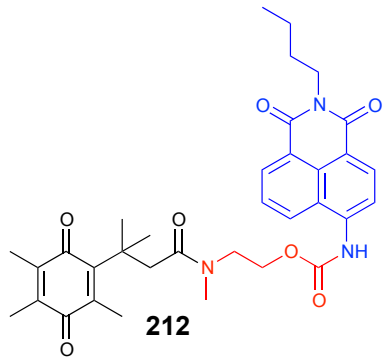

Figure 51: Identified portions of the profluorophore **212** for modification.

While probe **212** has been reported for NQO1, a new probe was designed based on the SAR developed in the previous chapters. After establishing the superiority of the naphthoquinone core over benzoquinones in Chapter 3, the design of the new probe contained the naphthoquinone core attached to the *gem*-dimethyl propionic chain. However, to develop an accurate SAR, comparison to the plastiquinone and benzoquinone core was required. The design of the linker portion of **212** was not discussed[134] and is not clear that all the elements are necessary. To allow a methodical approach to developing a SAR, the linker portion of the new probe will contain the minimal amount of functionality possible in the first suite of compounds. Additional functionality would be introduced into the linker in the next suite of compounds if required. To reduce the number of structural changes in the first suite of probes, the proof of concept was performed without modification to the dye portion. In the future, the butyl chain of the naphthalimide can be altered for solubility reasons or to introduce polarity.

The first suite of compounds proposed contained the unaltered naphthalimide portion directly to the quinone acid. Therefore, the first suite of compounds will remove the extra amino ethanol linker. For comparative reasons, three probes will be synthesised with each containing a different core.

4.1 Synthesis of the quinone acid moieties

Synthesis of the plastiquinone propionic acid (**216**) was performed according to the literature as reported by Borchardt *et al.* (Scheme 43).[135] 2,3,5-

Trimethylhydroquinone (**157**) readily underwent Friedel–Crafts alkylation/ lactonisation under acidic conditions to form lactone **214** in 38 % yield. The successful synthesis of **214** was supported by both ^{1}H NMR and ^{13}C NMR spectroscopy, which was consistent with that reported in the literature.[136]

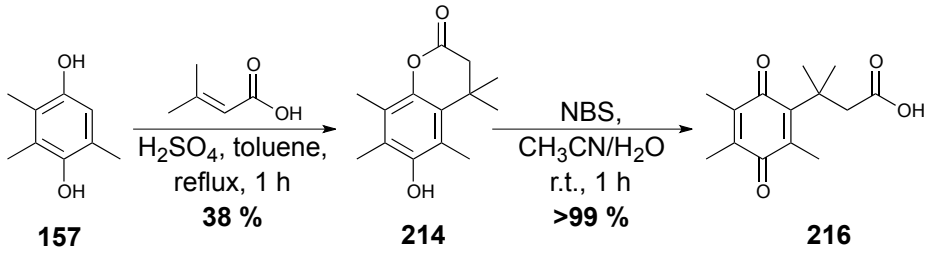

Scheme 43: Synthesis of plastiquinone *gem*-dimethyl propanioc acid derivative **216**.

Oxidation and hydrolysis to the quinone was performed using NBS in quantitative yield.[135] The formation of quinone **216** was supported by ^{13}C NMR spectroscopy with shift in the carbonyl signal of the lactone from 168.9 to 178.8 ppm consistent with a carboxylic acid moiety, along with two additional carbonyl signals present at 187.4 and 190.8 ppm indicating oxidation to the quinone. With formation of the plastiquinone derivative complete, focus shifted to the naphthoquinone moiety. Reduction of menadione (**12**) to menadiol (**217**) by sodium dithionite provided the hydroquinone (**217**) in a quantitative yield (Scheme 44).[137-139]

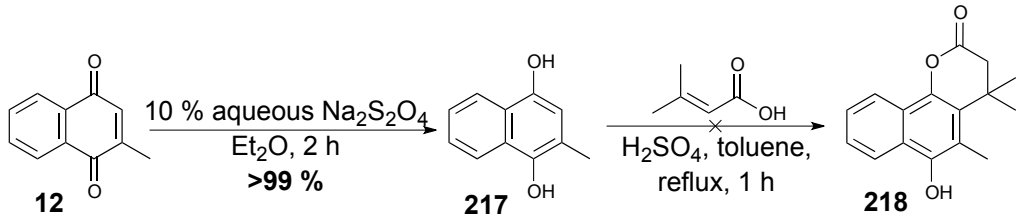

Scheme 44: Reduction of menadione (**12**) to menadiol (**217**) followed by failed Friedel–Crafts alkylation/ lactonisation to yield **218**.

Attempts to lactonise menadiol (**217**) using the previously successful conditions failed to provide compound **218**, with complete decomposition being observed. Therefore focus moved to a literature method specifically reported for the naphthoquinone moiety.[140] However, these conditions did not yield the desired compound (Table 20, Entry 1).[140] Screening of reaction

conditions by altering the reaction temperature, reaction time and the acid percentage did not improve the reaction outcome (Table 20).

Table 20: Attempted lactonization of menadiol (**217**) to form **218**.

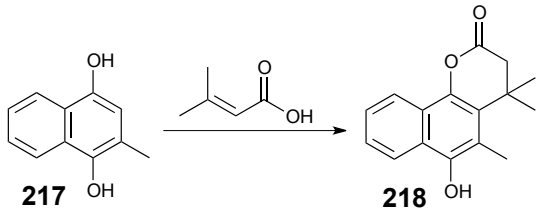

217 **218**

Entry	Reaction Mixture	Temperature (°C)	Reaction time (h)	Outcome
1	CH_3SO_2H	70	2	Decomposition
2	CH_3SO_2H	Reflux	2	Decomposition
3	CH_3SO_2H	40	2	Decomposition
4	CH_3SO_2H	r.t.	2	Decomposition
5	10 % CH_3SO_2H/ CH_2Cl_2	Reflux	1.5	Decomposition
6	Toluene (Microwave)	170 (300 watts)	1	Starting material + menadione (**12**)
7	Neat (Microwave)	100 (100 watts)	0.5	Starting material + menadione (**12**)

The addition of methanesulfonic acid to menadiol (**217**) resulted in an immediate colour change to dark purple then black, suggesting possible acid-promoted decomposition. However, attempts to form lactone **218** in acid-free conditions at high temperature under microwave irradiation resulted in the return of starting material and menadione (**12**). Therefore, it was proposed that forming the *gem*-dimethyl acid of naphthoquinone could be achieved *via* the silver-promoted decarboxylation process (Scheme 45). 2,2-

Dimethylsuccinic anhydride (**219**) was converted to mono-ester **220** in order to enable the introduction to the quinone core selectively. Ethanol opened the anhydride by attack at the least hindered carbonyl group.

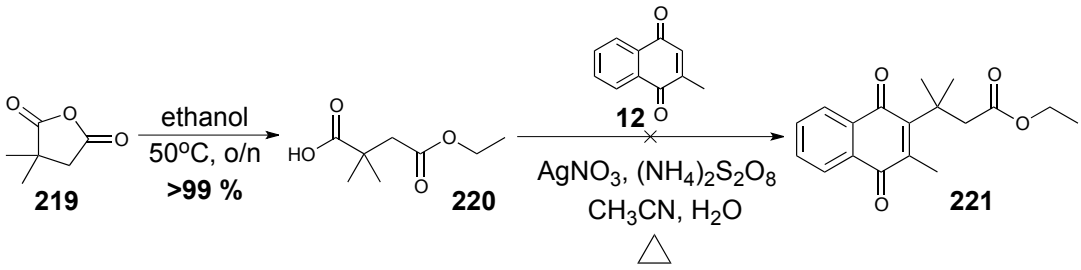

Scheme 45: Attempted formation of **221** *via* the silver-catalysed decarboxylation method.

Formation of mono-ester **220** was supported by both ^{1}H NMR, ^{13}C NMR and HMBC spectroscopy. In the HMBC, the hydrogen of the -CH_2- of the ethyl ester displayed a three-bond correlation to the ester carbonyl. Where as the hydrogens of the *gem*-dimethyl substituents showed a correlation to the carbonyl of the carboxylic acid. Because these two groups did not show correlations to the same carbonyl group, this supported the ethyl ester formation at the least hindered carbonyl group (Figure 52).

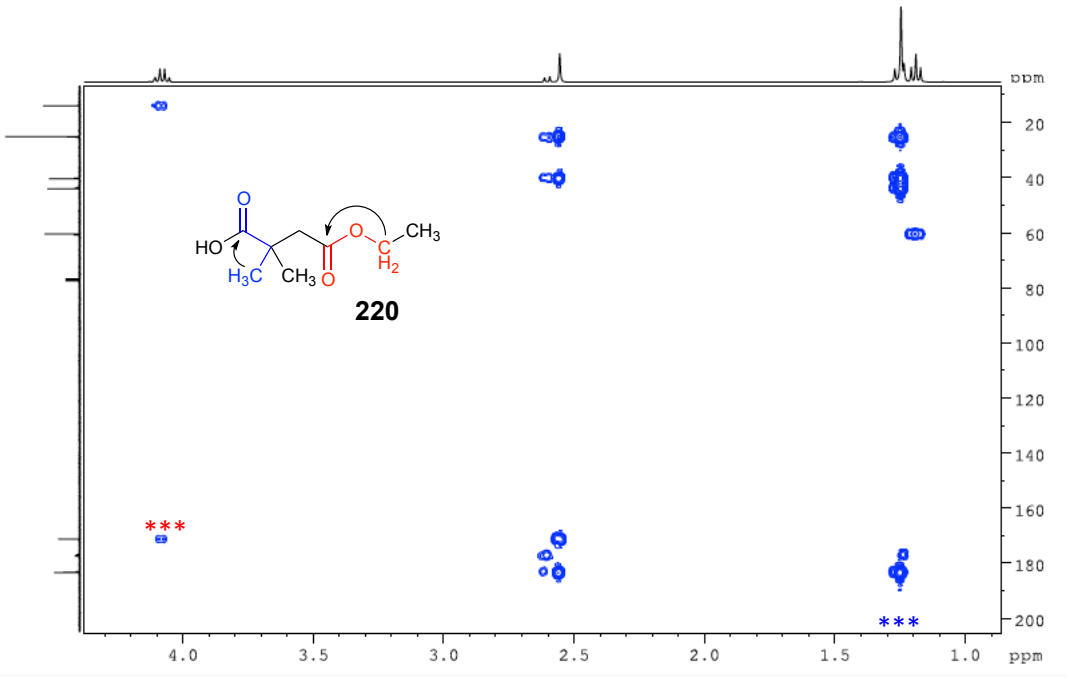

Figure 52: HMBC spectrum of **220**.

With acid **220** in hand, the synthesis of compound **221** *via* the silver-mediated decarboxylation process was attempted. However, only menadione (**12**) was recovered. With the failure to obtain the naphthoquinone lactone **218** or to form ester **221**, focus shifted to synthesising the benzoquinone derivative. As the synthesis of 2,3-dimethoxy-5-methylbenzoquinone core (**6**) features the oxidised quinone moiety, reduction to the hydroquinone was required. The 2,3-dimethoxy-5-methyl-benzoquinone core (**6**) was reduced to the hydroquinone **222** in a 54 % yield *via* a sodium borohydride reduction, utilising a biphasic solvent mixture (Scheme 46).[140]

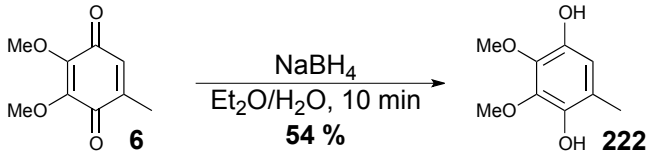

Scheme 46: Sodium borohydride reduction of **6** to form **222**.

Hydroquinone **222** was then subjected to the Friedel–Crafts alkylation/ lactonisation reaction under acidic conditions as seen with the plastiquinone derivative (Scheme 47). Lactone **223** was formed under these conditions, in low yield (20 %). The literature indicates use of methanesulfonic acid as both the solvent and the catalyst for the synthesis of the benzoquinone derivative as seen with the naphthoquinone.[140] However, due to decomposition observed with the naphthoquinone derivative and sufficient material obtained by this approach, no further optimisation was required.

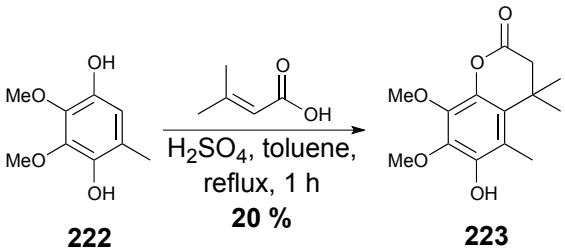

Scheme 47: Synthesis of *gem*-dimethyl lactone derivative **223**.

Lactonisation to form **223** was consistent with both ^{1}H NMR and ^{13}C NMR spectroscopy. Two additional singlets in the ^{1}H NMR spectrum at 1.44 ppm integrating for six protons indicating the two *gem*-dimethyl substituents and a

singlet at 2.56 ppm integrating two protons which is consistent with the protons adjacent to the carbonyl group is consistent with formation of **223**. A diagnostic carbonyl signal was now present in the ^{13}C NMR spectrum at 167.8 ppm for the lactone carbonyl. The lactone was also supported by IR spectroscopy with a carbonyl stretch observed at 1767 cm^{-1}.

The subsequent oxidation and ring-opening of compound **223** led to significant decomposition. The same reaction conditions that produced plastiquinone **216** resulted in complete decomposition of the benzoquinone derivative **224**. Visual observation of the reaction mixture upon dropwise addition of NBS indicated a rapid colour change from clear to bright yellow indicating the successful formation of the quinone moiety. However, after 10 min the bright yellow-coloured solution turned black. Therefore, the reaction was repeated with immediate quenching after the addition of NBS to prevent further decomposition (Scheme 48). Under these conditions the desired quinone **224** was formed in 18 % yield and unreacted lactone could be recovered and re-subjected to the reaction conditions.

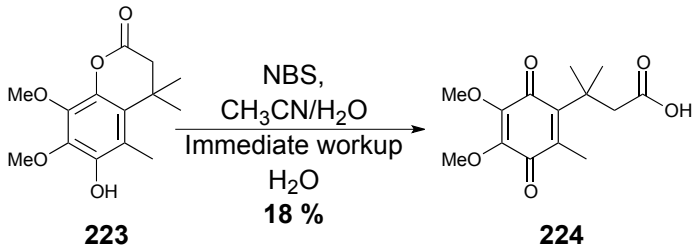

223 **224**

Scheme 48: Ring opening and oxidation of **223** to yield **224**.

The successful formation of **224** was indicated by ^{1}H NMR and ^{13}C NMR spectroscopy.[84] A diagnostic shift of the lactone carbonyl signal from 167.8 ppm to 177.8 ppm was consistent with the presence of a carboxylic acid and the presence of two additional carbonyl signals at 184.5 and 186.4 ppm indicating successful oxidation to the quinone. The IR also showed absorptions at 1711 and 1684 cm^{-1} for the carboxylic acid and 1,4-quinone respectively.

With two of the three quinone acid moieties synthesised, focus moved on to synthesising the simplified probes from the plastiquinone carboxylic acid

216. This would illustrate whether the fluorescence would be quenched due to the proximity of the quinone moiety. And therefore demonstrate proof-of-concept before any further attempts to synthesise the naphthoquinone derivative.

The first quinone-dye analogue proposed was the quinone moiety coupled directly to the amino-naphthalimide dye with no linker fragment (Figure 53). This would enable the importance of the linker fragment and what influence it has on the probes ability to act as a profluorophore to be determined.

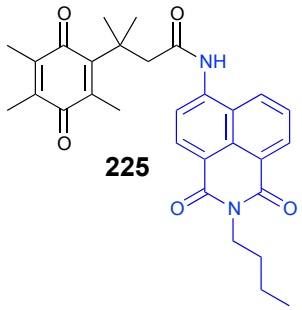

Figure 53: Structure of the first proposed profluorophore (**225**).

4.2 Synthesis of the dye fragment

Formation of the probe consisted of a multi-step synthesis following literature procedures (Scheme 49). Commercially available 4-bromo-1,8-naphthalic anhydride (**226**) was reacted with sodium azide at 100 °C to provide the azido compound **227** in 72 % yield (Scheme 49).[141] Upon hydrogenation with Pd/C the 4-amino-1,8-naphthalic anhydride (**228**) was obtained in moderate yield.[141] Formation of amine **228** was supported by ^{1}H NMR spectroscopy with an exchangeable proton signal present at 7.08 ppm integrating for two protons, consistent with the presence of the amine. Introduction of the N-butyl chain was achieved by heating the anhydride and *N*-butylamine in ethanol to deliver probe fragment **229**. The ^{1}H and ^{13}C NMR spectroscopic data was consistent with equivalent data reported in the literature.[134,142]

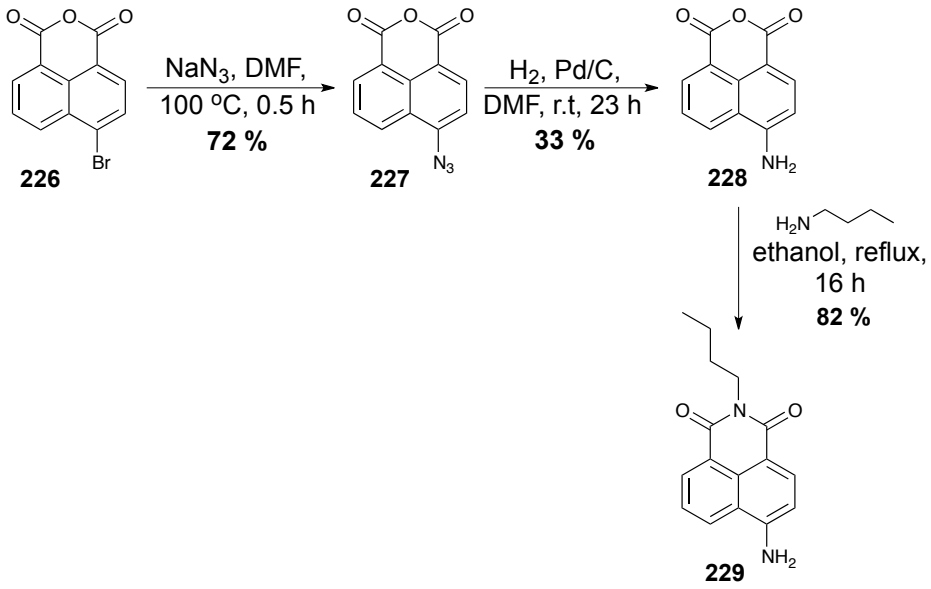

Scheme 49: Formation of the dye fragment **229**.

The successful introduction of the butyl chain in **229** was consistent with both ^{1}H NMR and ^{13}C NMR spectra. In the ^{1}H NMR spectrum, four proton signals are present in the aliphatic region, with three of those signals located between 0.5 and 2.0 ppm and the fourth signal shifted upfield to 4.09 ppm as a triplet indicating its attachment to the nitrogen of the naphthalimide. These same trends were observed in the ^{13}C NMR spectrum with four signals below 45.0 ppm indicating the presence of four sp^{3}-hybridised carbons. With the dye portion successfully prepared and synthetically useful amounts of the *gem*-dimethyl plastiquinone acid (**216**) readily available, coupling of the two portions *via* amide coupling as previously used for all naphthoquinone derivatives was attempted (Scheme 50).

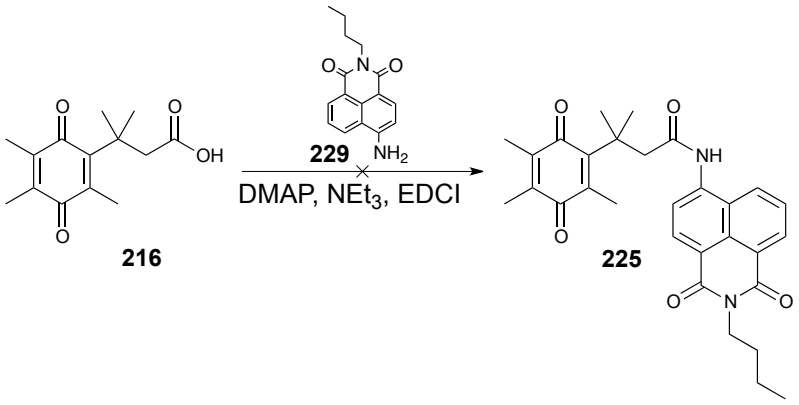

Scheme 50: Attempted amide coupling of **216** and **229** to yield **225**.

With many successful amide couplings performed with the scope of this project, it was surprising to realise that this coupling was not successful. The inability to form the amide bond is attributed to the amine of the probe being a poor nucleophile due to its location on the naphthalene ring and the greater delocalisation of the nitrogen lone pair due to the presence of the imide. While no desired product was obtained, both starting materials were recovered from the reaction mixture. To support this hypothesis that probe **229** is a poor nucleophile, L-phenyl glycinol and L-phenylalaninol were each successfully coupled to the *gem*-dimethyl plastiquinone acid (**216**) (Scheme 51). The successful coupling of the two amine fragments indicate the coupling agent was active and the inability to couple the probe to the *gem*-dimethyl plastiquinone acid (**216**) was a result of the poor nucleophilicity of compound **229**.

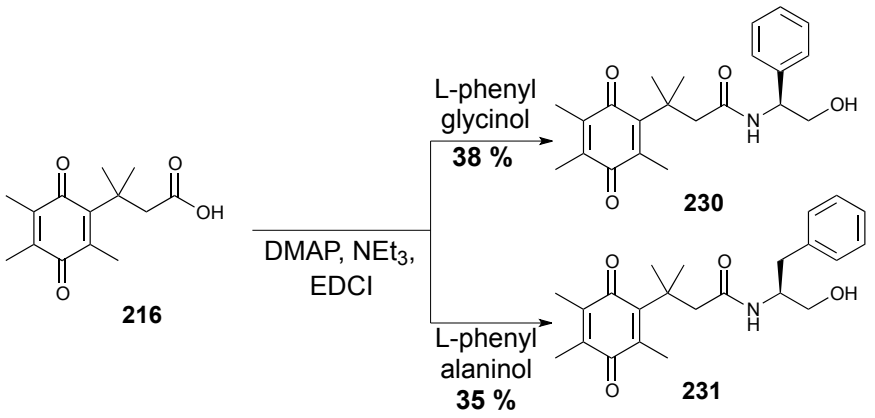

Scheme 51: Successful amide coupling of L-phenyl glycinol derivative (**230**) and L-phenylalaninol derivative (**231**) to the *gem*-dimethyl plastiquinone acid (**216**).

The successful synthesis of analogues **230** and **231** was supported by both ^{1}H and ^{13}C NMR spectroscopy. An exchangeable proton signal was present in both analogues at 6.15 ppm and 5.63 ppm for analogue **230** and **231** respectively, with both integrating for one proton, which was identified as the proton attached to the nitrogen. Similarly, in the ^{13}C NMR, a shift of the carbonyl due to the formation of amide bond is seen from 178.8 ppm to 172.4 ppm.

With support for the hypothesis that the amine fragment is a poor nucleophile, an alternative method was sought. It was proposed that a

Staudinger-type reaction would allow successful coupling of an azide and carboxylic acid in anhydrous conditions.[143] Because the Staudinger reaction employs azide substrates, formation of the probe fragment **232** was synthesised (Scheme 52). Therefore, azido-napthalimide **232** was obtained from 4-azido-1,8-naphthalic anhydride and *n*-butylamine in a low 22 % yield.

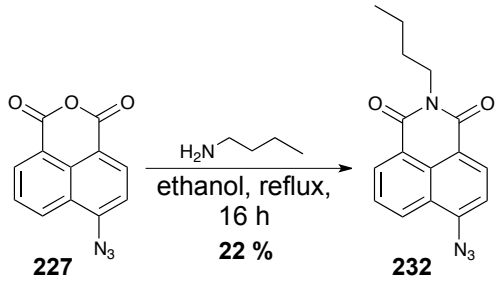

Scheme 52: Synthesis of dye portion **232**.

Formation of the naphthalimide **232** was consistent ^{1}H NMR, ^{13}C NMR and infrared spectroscopy (IR).[144] A strong IR band was present at 2127 cm^{-1} in the IR spectrum, which is indicative of an azide group. Similarly, both ^{1}H NMR and ^{13}C NMR spectroscopy supported the introduction of the butyl chain with analogous signals to those of the amine **229** present. With successful formation of the azide **232** the Staudinger reaction was attempted. Surprisingly, no amide was formed and, instead, the stable iminophosphorane (**233**) intermediate was isolated (Scheme 53).

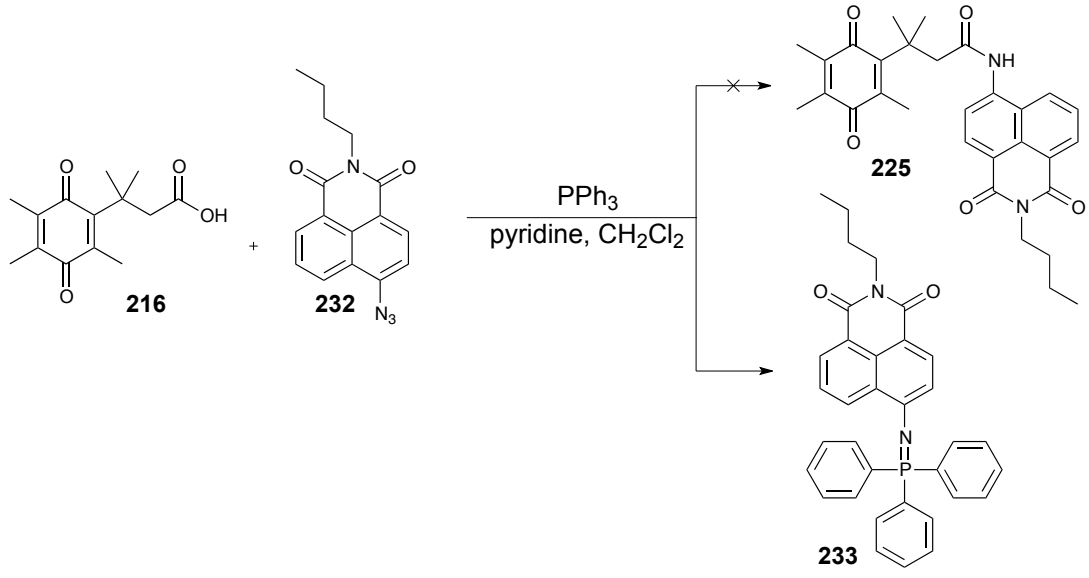

Scheme 53: Attempted Staudinger reaction to form **225**.

^{1}H NMR spectroscopy supported the formation of **233** with multiplets present between 7.50 ppm and 7.90 ppm integrating for a total of fifteen protons indicating the presence of the three phenyl groups, which was also consistent with data reported in the literature.[145] Iminophosphorane (**233**) is a known compound and, surprisingly, synthesised *via* the same conditions that were utilised in the Staudinger reaction.[145] After purification and isolation of intermediate **233**, additional *gem*-dimethyl plastiquinone acid (**216**) was added and the mixture refluxed in toluene overnight. However, all attempts failed to cleave the nitrogen – phosphorous double bond. Therefore, it was decided that this was not a viable way to form the profluorophore.

Recently it was reported that the amide bond of a naphthalimide could be formed by a palladium-mediated protocol from a primary amide and 4-bromo-1,8-naphthalic anhydride (**226**) (Scheme 54). This would avoid the problems of nucleophilicity of the amine attached to the naphthalimide. Therefore the synthesis of the quinone primary amide **234** was required (Scheme 54). Initially, the optimistic approach was taken with using excess ammonium chloride as the ammonia source and subjecting this to the normal amide coupling reaction previously optimised (Scheme 54).

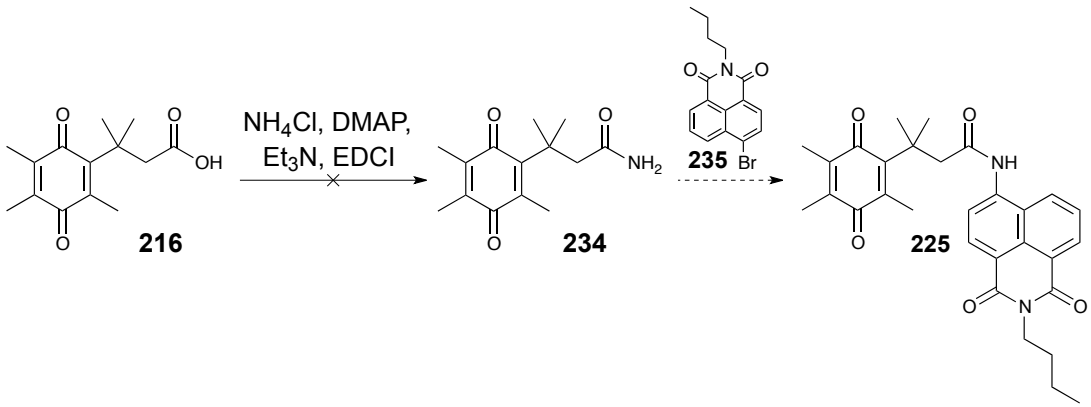

Scheme 54: Attempted synthesis of **234**.

Unfortunately, no product was obtained with a complex mixture of undesired products observed when analysed by ^{1}H NMR spectroscopy. Therefore, the synthesis of amide **234** was investigated *via* acid chloride **236** (Scheme 55).

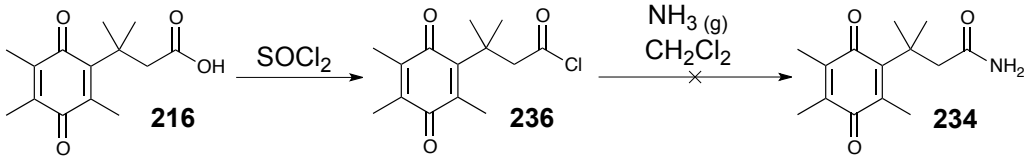

Scheme 55: Formation of acid chloride intermediate **236** before failed attempts of obtaining **234**.

The synthesis of **234** was not successful when subjecting the acid chloride intermediate **236** to bubbling ammonia gas. A possible explanation for no formation of **234** was insufficient removal of excess thionyl chloride. Formation of intermediate **236** was expected, however, it was difficult to isolate and sufficiently characterise the intermediate. Therefore, an alternative active intermediate was sought. An *N*-acyl imidazole intermediate would allow for isolation and characterisation prior to reaction with ammonia (Scheme 56).

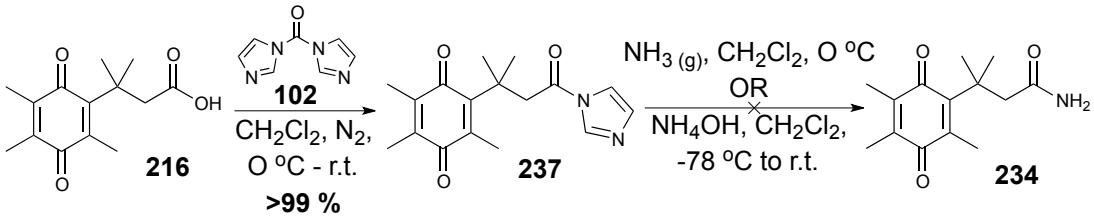

Scheme 56: Formation of the carbonyl imidazole intermediate **237** before failed attempts of obtaining **234**.

^{1}H NMR spectroscopy supported the successful synthesis of intermediate **237**. Three singlets present in the ^{1}H NMR spectrum at 7.03, 7.39 and 8.11 ppm each integrating for one proton were consistent with the incorporation of the imidazole in compound **237**. With evidence supporting the formation of the intermediate, **237** was then subjected to either liquid ammonia in CH_2Cl_2 at –78°C and then warmed to room temperature or ammonia gas bubbled through the reaction mixture at 0°C. Surprisingly, no product was obtained by employing either set of reaction conditions. In both cases, the lactone **214** was recovered upon purification of the reaction mixtures, indicating that a reduction of the quinone had unexpectedly occurred. This result in itself is odd, as a reduction must occur for formation of the lactone and, currently, there is no logical explanation for this.

With various unsuccessful attempts at forming the amide portion, it was decided that coupling the dye directly to the quinone moiety was no longer a viable option. Instead, it was proposed that the linker portion might be essential to coupling the two fragments together. The initial carbamate linkage was not initially investigated as it adds a significant number of synthetic steps to the sequence. Therefore, a new quinone coupled probe was proposed that featured a simple linker fragment and the smallest number of carbon atoms (Figure 54). In this way, profluorophore **238** which features an ethylenediamine linker was identified.

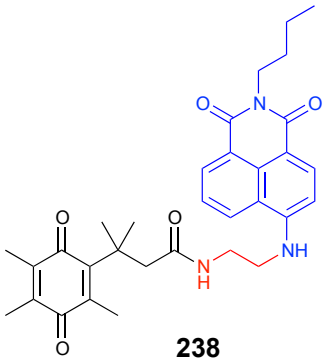

238

Figure 54: Structure of the newly proposed profluorophore **238**.

Due to the addition of the linker, formation of the dye fragment **239** was synthesised from 4-bromo-1,8-naphthalic anhydride **227**. The installation of the *N*-butylamine chain occurred prior to the installation of the ethylenediamine fragment (Scheme 57).

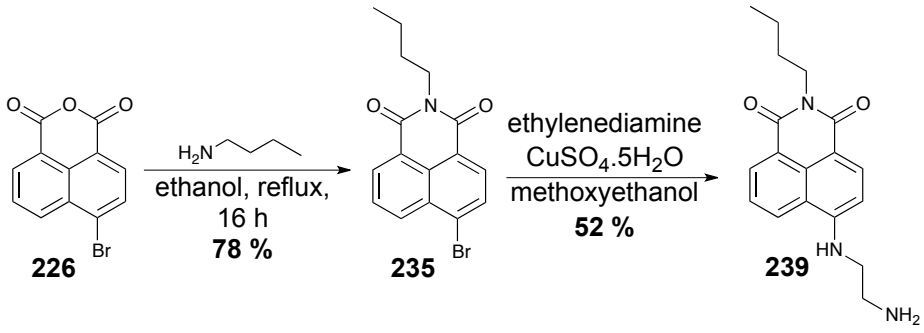

226 **235** **239**

Scheme 57: Formation of the new dye portion **239** containing the ethylenediamine linker.

Installation of the butyl chain to form **235** occurred in a good yield, with spectral data matching that reported in the literature.[146] Naphthalimide **235**

was then subjected to ethylenediamine in 2-methoxyethanol to produce the desired probe **239** in 52 % yield. Formation of **239** was consistent with data reported in the literature with both ^{1}H NMR and ^{13}C NMR spectroscopy supporting the addition of the ethylenediamine fragment.[147] An additional triplet and quartet were present in the ^{1}H NMR spectrum at 3.20 and 3.55 ppm respectively both integrating for two protons with a coupling of 5.6 Hz indicated the addition of the ethylenediamine fragment. This successful addition was supported by ^{13}C NMR spectroscopy with six carbon signals below 45.0 ppm indicating the presence of six sp^{3}-hybridised carbons. With the successful formation of the probe (**239**), amide coupling was attempted with the *gem*-dimethyl plastiquinone acid **216** (Scheme 58).

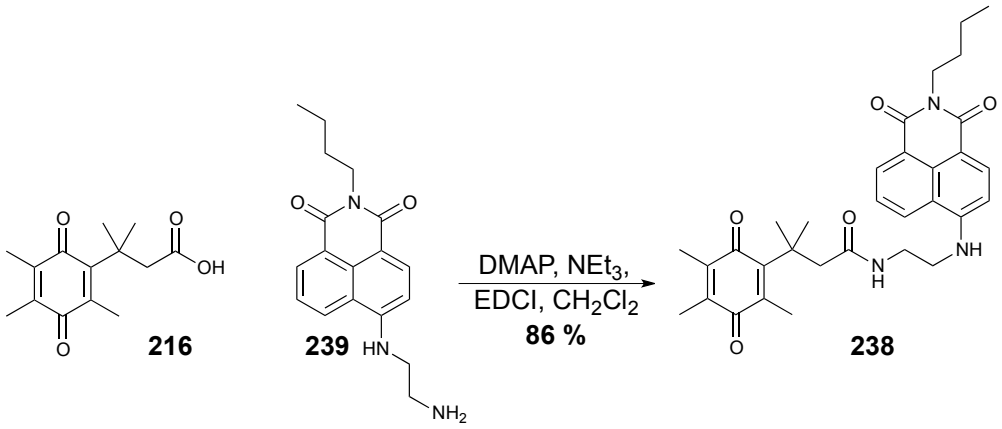

Scheme 58: The successful coupling the probe (**239**) to the *gem*-dimethyl quinone acid (**216**) to form **238**.

The successful coupling of the two fragments to produce **238** proceeded in an excellent 86 % yield. Formation of **238** was supported by full analysis, including ^{1}H NMR, ^{13}C NMR, IR and high resolution mass spectroscopy (HRMS). HRESIMS for $C_{32}H_{37}N_3O_5Na$ gave a predicted value of 566.2631 and analogue **238** was found to have a mass of 566.2646. Significant support for **238** was obtained from the ^{1}H NMR with two exchangeable proton signals present at 6.22 ppm presenting as a triplet and a broad singlet at 7.03 ppm both integrating for one proton each indicating the two N–H bonds (Figure 55). Similarly, five singlets are present between 1.35 and 3.00 ppm indicating the presence of the five methyl groups and the -CH_2- of the *gem*-dimethyl plastiquinone core fragment. This is also supported in the ^{13}C NMR spectrum

with three carbonyl resonances of the quinone core and amide bond present at 175.5, 187.2 and 191.1 ppm as well as the two carbonyls of the naphthalimide present at 164.4 and 164.7 ppm.

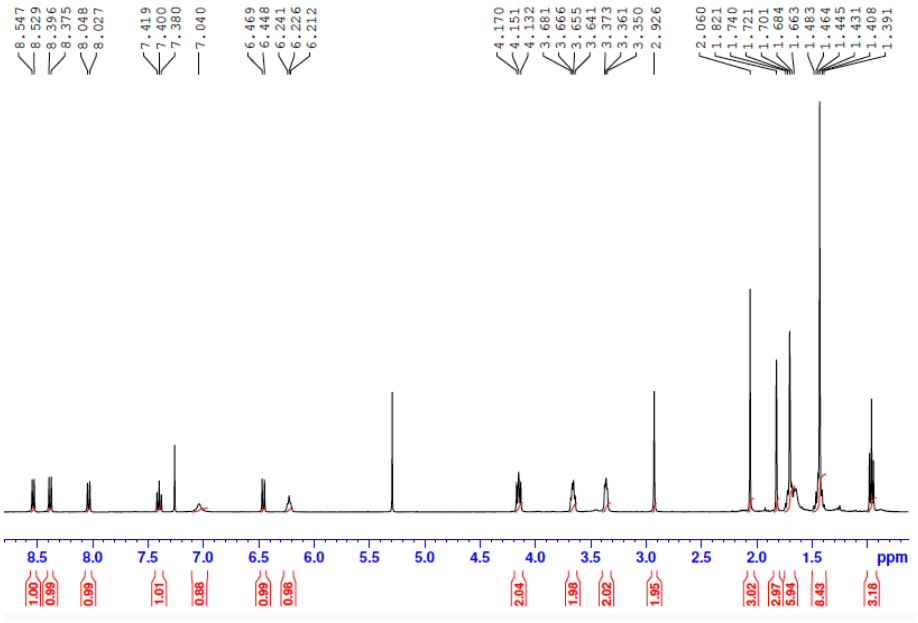

Figure 55: ^{1}H NMR spectrum of the probe **238**.

With the successful formation of the probe **238**, investigation into the probe's ability to act as a profluorophore was performed. Probe **238** was designed with the intention that the proximity of the quinone moiety would quench the fluorescence of the naphthalimide portion. Upon reduction of the quinone moiety to the hydroquinone, elimination of the naphthalimide dye **239** would then lead to a rapid increase in fluorescence due to the liberation of naphthalimide portion. Comparison of the fluorescence of the probe **238** compared to the dye **239** can been observed in Figure 56.

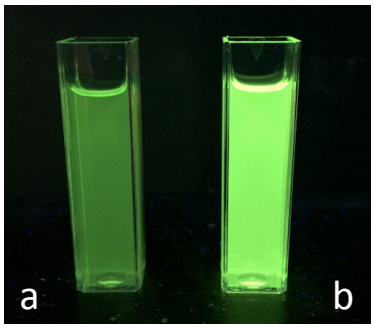

Figure 56: Fluorescence of 1.0 x 10^{-4} M solutions of a) probe (**238**) and b) dye (**239**) in ethanol at λ_{ex} = 365 nm.

The fluorescence is significantly brighter when the naphthalimide is not attached to the quinone (i.e. **239** vs. **238**) (Figure 56). There is highly effective proximity-induced quenching of the naphthalimide **239** when coupled to the plastiquinone acid **216**. Therefore, supporting the hypothesis that conjugation quenches fluorescence, although not completely. As a result the fluorescence and emission spectra were obtained (Figure 57).

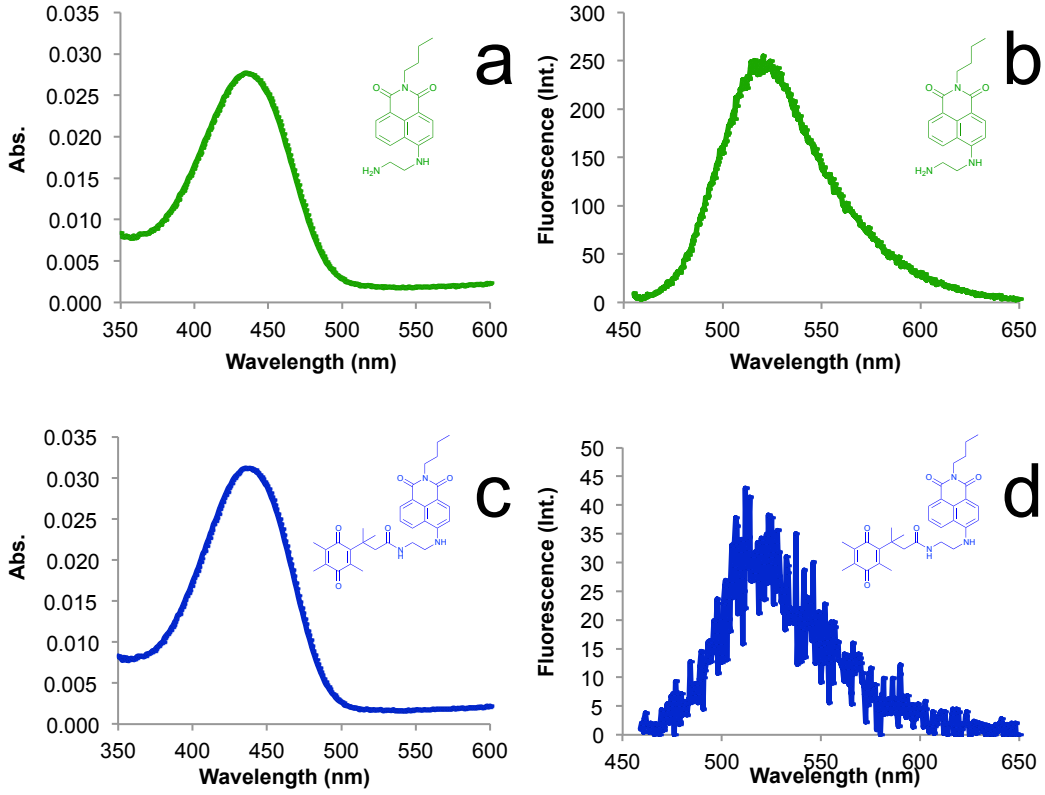

Figure 57: Absorption and emission spectra of 2.0 x 10^{-6} M probe (**238**) and dye (**239**) in ethanol. Absorption (A and C); fluorescence emission spectra (B and D) at λ_{ex} = 445 nm.

Figure 57a,c illustrates that probe **238** absorbs over the range of 360–500 nm with a λ_{max} at 438 nm. In comparison, dye **239** absorbs over 360–510 nm with a λ_{max} at 435 nm. The emission energy maxima are 514 and 524 nm for probe **238** and dye **239** respectively. This large Stokes shift observed when comparing absorption and emission maxima is reported by Prasai and co-workers[133] and is characteristic of the naphthalimide dyes. The increase in fluorescence of Figure 57.b when compared to Figure 57.d supported the fluorescence quenching ability of the quinone moiety. The literature indicates that the quenching by the quinone moiety of probe **238** will be drastically

increased due to the decreased length of the linker portion.[133] Unfortunately, as seen in Figure 56, complete quenching of the coupled probe at high concentrations is not observed. However, upon application to cells or chemically induced reduction, a high degree of contrast should be observed.

With this data, the ability of probe **238** to release the free dye **239** through chemically induced reduction of the quinone core to the hydroquinone was investigated. Probe **238** was subjected to reduction by sodium dithionite with the fluorescence measured every ten seconds over an 8 min period to monitor the formation of the dye **239** (Figure 58).

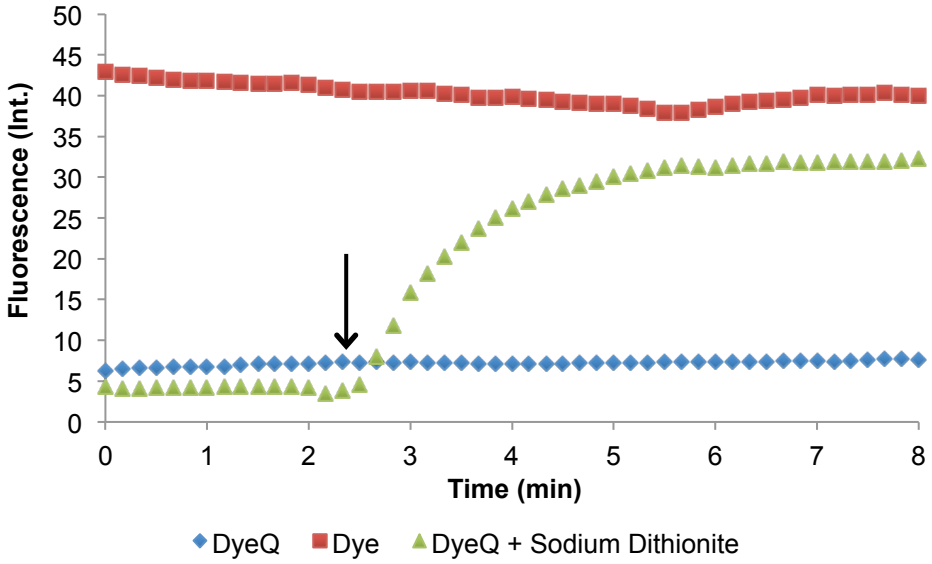

Figure 58: Comparing the sodium dithionite initiated formation of Dye **239** from Probe **238**. The fluorescence (λ_{ex} = 445, λ_{em} = 525) from 3 mL solution of 2.0 x 10^{-6} M of probe **238** in pH 7.5, 0.1 M PBS buffer was monitored after reduction of probe **238** by the addition of 0.5 mg of sodium dithionte (denoted by arrow). Probe **238** and Dye **239** as controls in analogous conditions in the absence of sodium dithionite.

As indicated in Figure 58, rapid fluorescence was observed over a 1.5 min period after the addition of sodium dithionite, with maximum fluorescence achieved with in 3 min. This result provides proof-of-concept and gives a clear indication that fluorescence is quenched due to the proximity of the quinone core to the naphthalimide. With evidence that the reduction triggered cyclisation is occurring, it is expected that this probe could proceed in a

similar manner in the presence of enzymes such as NQO1 as initially hypothesised.

The potential of probe **238** to be reduced by NQO1 was investigated in a cell free assay. A solution of the probe **238** with NADPH and NQO1 and dye **239** with NADPH and NQO1 were compared against probe **238** with NADPH over a 30 min period (Figure 59).

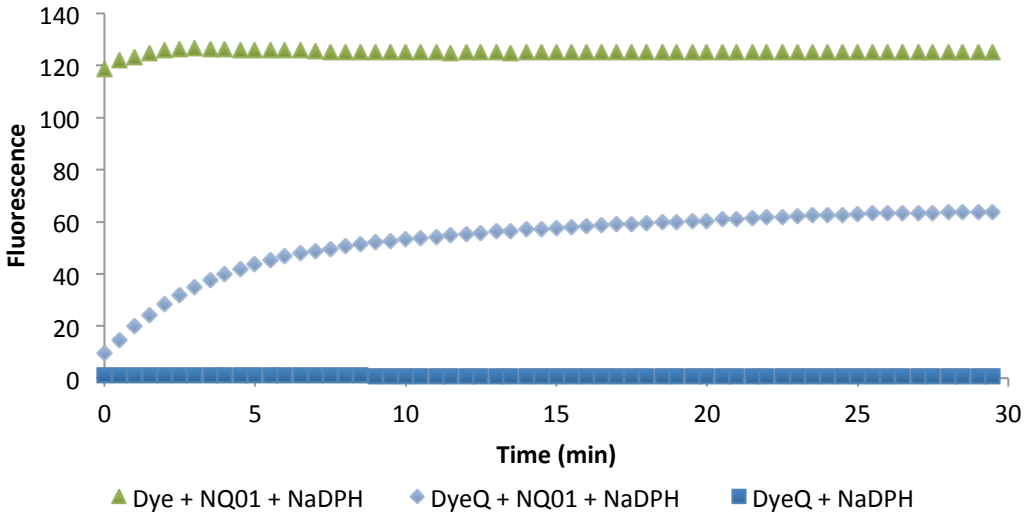

Figure 59: The fluorescence (λ_{ex} = 460 nm, λ_{em} = 538 nm) from total volume of 100 µL solution of 1.0 x 10^{-5} M of probe **238** or dye **239**, 10mM NADPH (10 µL) + 0.5 mg/mL NQO1 (10 µL), probe **238** in pH 7.4, 0.1 M PBS was monitored after the addition of NQO1.

As seen in Figure 59, in the presence of NAPH, probe **238** only showed base line fluorescence indicating no reduction of the quinone. However, upon the addition of NQO1, fluorescence rapidly increased over the first 10 min before plateauing. Although this did not reach the full level of fluorescence of the uncoupled probe, this can be attributed to all the NADPH being consumed and therefore unable to provide the energy NQO1 required to reduce the quinone moiety further. However, in a biological setting such as a cellular assay, this would not be an issue and would give an on/off response. This would provide a yes or no answer to NQO1 activity in the cells accordingly.

With proof of concept illustrated by both chemical and enzyme reduction resulting in a dramatic increase in fluorescence, further investigation into

SAR is required to develop a probe that has no background fluorescence. Although the proposed benzoquinone moiety **224** was synthesised, due to time constraints coupling of the probe did not occur. However, the proposed naphthoquinone moiety is required, such that the potential reducing power of the cells can be investigated. In addition to this, further investigation into the linker fragment may be required, as particular functional groups attached to the naphthalimide can shift the region of absorption and emission to prevent back ground fluorescence being a problem.[133] Potential optimisation of probe **238** are summarised in Figure 60. Due to time constraints, these optimisations and investigations are work for the future.

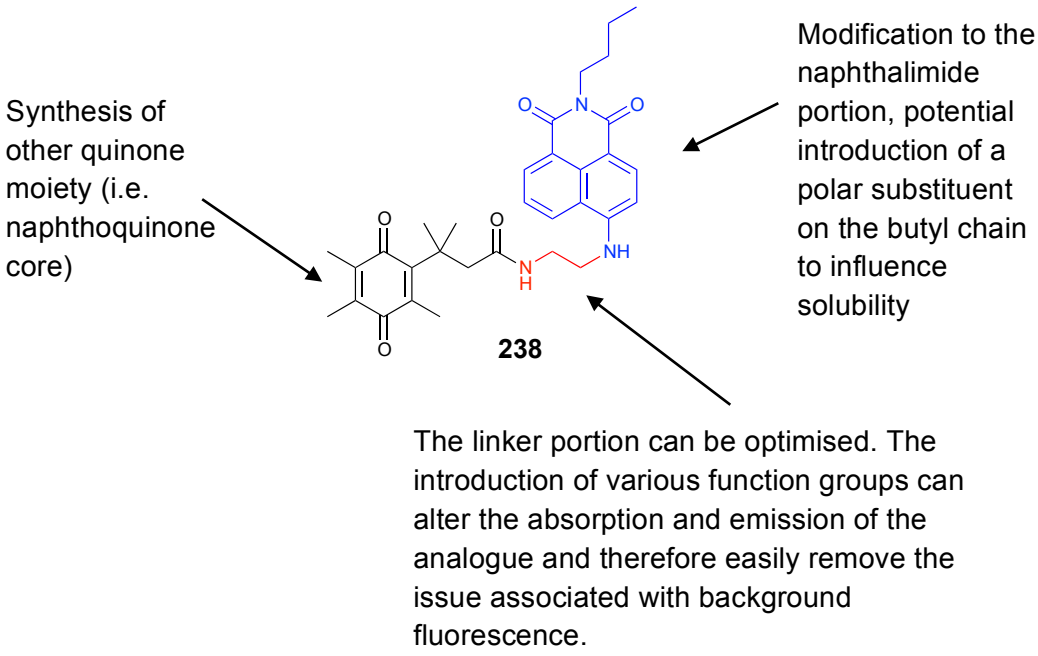

Figure 60: Identified modifications to the three fragments of coupled probe **238**.

Chapter 5: *In vivo Studies*

After extensively analysing the *in vitro* activity of the top five analogues (L-phenylalanine *t*-butyl ester derivative **61**, L-phenylalanine derivative **70**, L-phenylalaninol derivative **76**, tyramine derivative **79** and 3,4-dimethoxyphenethylamine derivative **80**) two analogues were identified to progress to the *in vivo* studies (Figure 61).

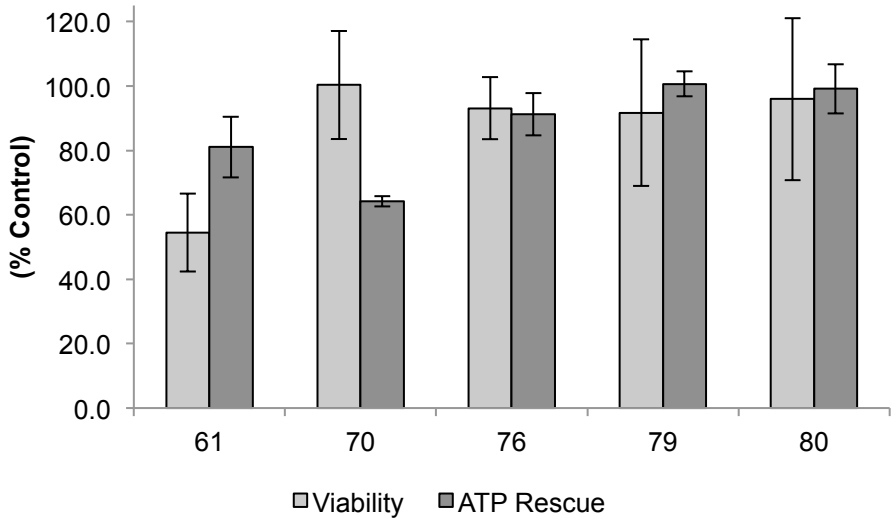

Figure 61: Biological evaluation of the top five analogues (**61**, **70**, **76**, **79**, **80**). (a) Cytoprotection against rotenone induced complex I dysfunction by quinones at 10μM given as a relative percentage of cell survival compared to untreated HepG2 cells (b) ATP rescue by quinones at 10μM in the presence of rotenone-induced complex I dysfunction as percentage of untreated HepG2 cells.

From the data shown in Figure 61, L-phenyl derivative **70** was selected due to its dramatic ability to provide cytoprotection and increased solubility due to the acid fragment. The decrease in ATP activity of analogue **70** was proposed not to be an issue as over time cytoprotection is extensive. In addition, 3,4-dimethoxyphenethylamine derivative **80** was selected due to its ability to restore both ATP levels and provide cytoprotection. With these two selected derivatives, *in vivo* studies were conducted in two different disease models.

5.1 *In vivo* studies in a mouse model LHON

Collaborators in the School of Medicine – Pharmacy at the University of Tasmania (PhD candidate Ms. Monila Nadikudi) tested both L-phenylalanine derivative **70** and 3,4-dimethoxyphenethylamine derivative **80** in a mouse model of LHON. Mice were treated according to a previously described method by Heitz *et al.*.[3] The mice were pre-treated with the selected compounds at 200 mg/kg *via* their diet for one week prior to commencement and subsequently for the entire time period of the study as previously described.[3] The animals received an injection of the synthetic complex I inhibitor rotenone (1 µl of a 5 mM solution) directly into the left eye over a two minute period. Over the next seventy days, visual acuity was evaluated by placing the mice on a stationary platform, surrounded by an optomotor drum with black and white stripes (1cm thick). The number of stimulus-induced reflex-head-turns by the mice were counted, while the optomotor drum was rotated at 2 rpm for 2 min each in both clockwise and anticlockwise direction (Figure 62). Head-turns were also monitored 1 to 3 times before injection of rotenone to establish a baseline for visual acuity of each animal. Head-turns in a clockwise direction indicate the visual acuity of the left (injected) eye, whereas head-turns in the counter-clockwise direction represent the visual acuity of the right (control) eye.

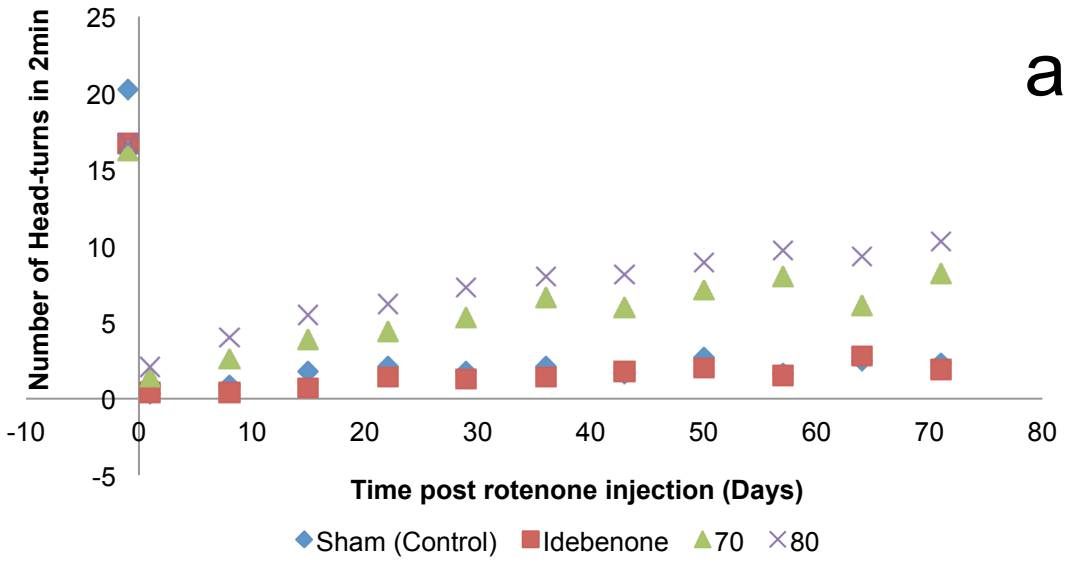

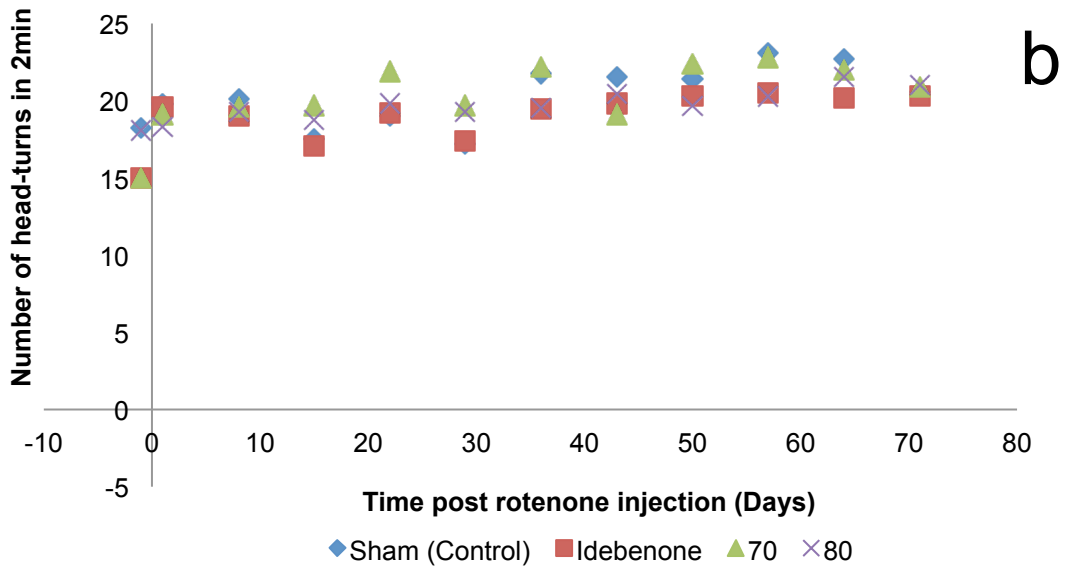

Figure 62: Novel short-chain quinones restore visual acuity under conditions of mitochondrial dysfunction-induced blindness. Visual acuity was evaluated by placing the mice on a stationary platform, surrounded by an optomotor drum with black and white stripes (1 cm thick). The number of head-turns made by the mice was counted while the optomotor drum was rotated at 2 rpm for 2min each in both clockwise and anticlockwise direction. All mice were treated with the respective compounds at a dosage equivalent to 200mg/kg body weight of idebenone. a) Quantification of clockwise head-turns, b) Quantification of counter-clockwise head-turns. .

As shown in Figure 62, animals showed a time-dependent recovery of sight when subjected to both **70** and **80**, up to ~50 % of baseline level. Noticeable restoration of vision occurred at 10 days post treatment. In contrast, idebenone (**11**) treated animals showed no recovery of vision in this study. Interestingly, when Heitz *et al.*[3] described recovery of vision in this animal model using idebenone (**11**) alone; idebenone was administered at ten times the concentration used in the current study and required ~70 days of treatment to show a noticeable recovery. Therefore, analogues **70** and **80** restored sight at significantly lower concentrations that the lead compound, which represented a significant increase in drug potency and could facilitate their therapeutic use.

5.2 *In vivo* studies into diabetic retinopathy

In further testing at the School of Medicine – Pharmacy at the University of Tasmania both L-phenyl derivative **70** and 3,4-dimethoxyphenethylamine derivative **80** were also tested in a rat model of diabetic retinopathy. Diabetic retinopathy is a leading cause of progressive vision loss.[40] There is growing recognition that retinal dysfunction and impaired visual behaviour is present prior to permanent damage occurring.[40] Diabetic complications in the first phase of diabetic retinopathy are associated with many metabolic processes that are upregulated. These metabolic processes are linked by mitochondrial production of reactive oxygen species (ROS) and evidence within the literature suggests that normalising mitochondrial dysfunction can mitigate the damage.[148,149] Therefore, it was suggested that early intervention and normalising of mitochondrial dysfunction prior to permanent damage occurring in diabetes patients may provide an effective treatment.

In a study by Alam *et al*., the effect of SS-31 (**10**) on diabetic retinopathy was evaluated. In this mouse model, SS-31 (**10**) reversed visual decline without effecting the diabetes.[40] With this promising result, L-phenylalanine derivative **70** and 3,4-dimethoxyphenethylamine derivative **80** were subjected to a rat model to determine if these analogues could have a similar effect on diabetic retinopathy compared to SS-31 (**10**). This work was performed by UTAS PhD candidate Mr. Abraham Daniels. Prior to inducing diabetes, each rat had its sight and blood sugar levels monitored for four weeks to establish robust basal levels. At week four, an osmotic pump was implanted on the rats' backs that administered streptozotocin (STZ) at a level of 125 mg/kg over a two week period. STZ kills the pancreatic beta cells (insulin producing cells), which is a common technique for studies into hyperglycaemia and it typically provides in a model for type I diabetes. In addition, the animals were also fed a high fat diet for the period of the study, which results in a mixed model of type I and II diabetes. As seen in Figure 63, the visual response of all animals (measured by the same rotating drum as in the previous LHON model) dropped dramatically over the next weeks. After ten weeks of being severely diabetic, the rats received the test compounds formulated as eye drops to their right eye. Due to vision loss in both eyes and being able to

locally treat the right eye only, the left eye was used as an internal control. As seen in Figure 63, both analogues as well as idebenone (**11**) restored vision over only a very short treatment period as indicated by a rapid increase in head turns towards the treated eye.

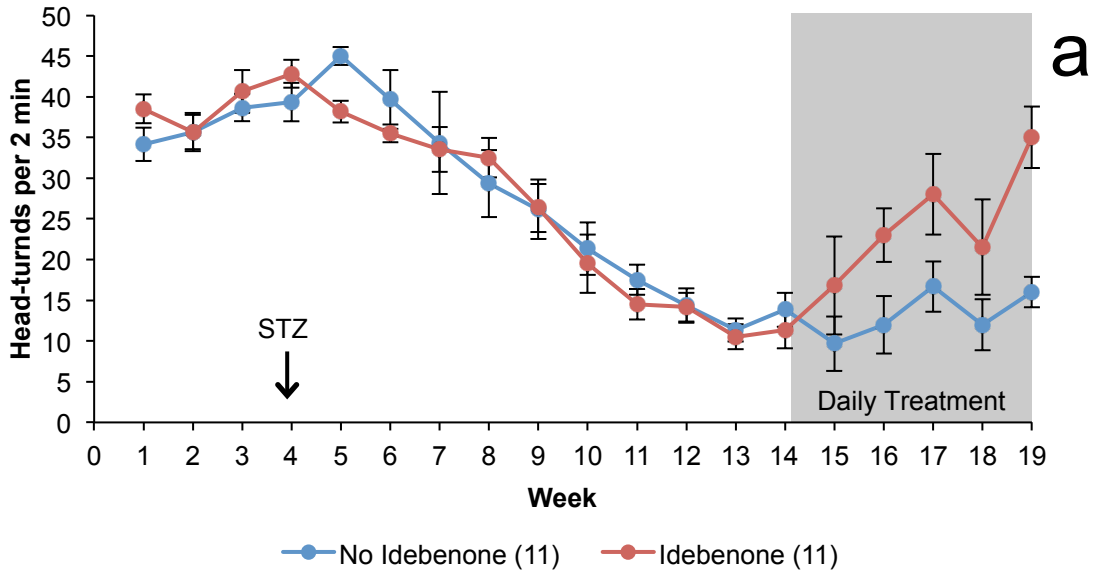

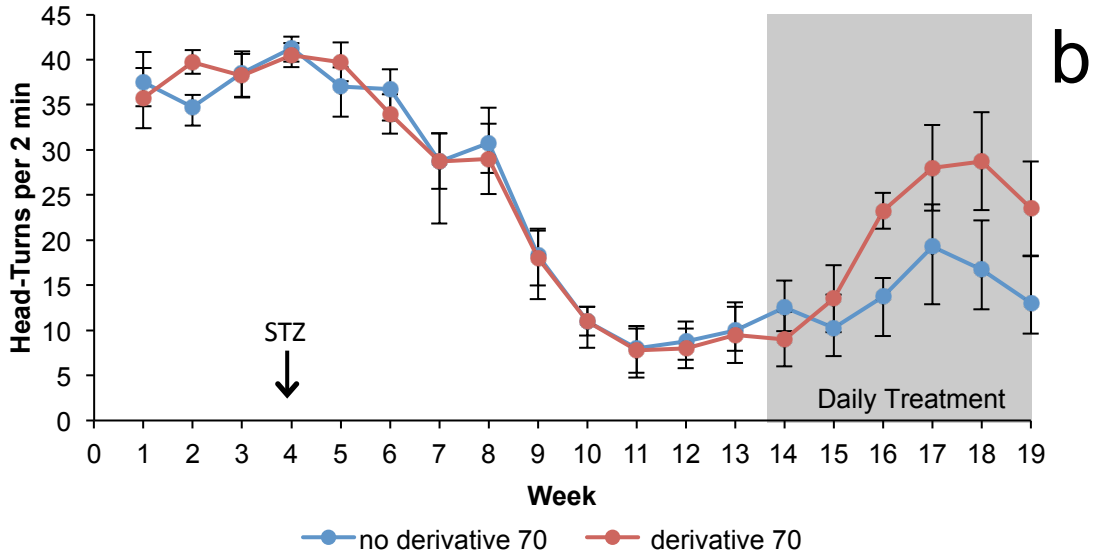

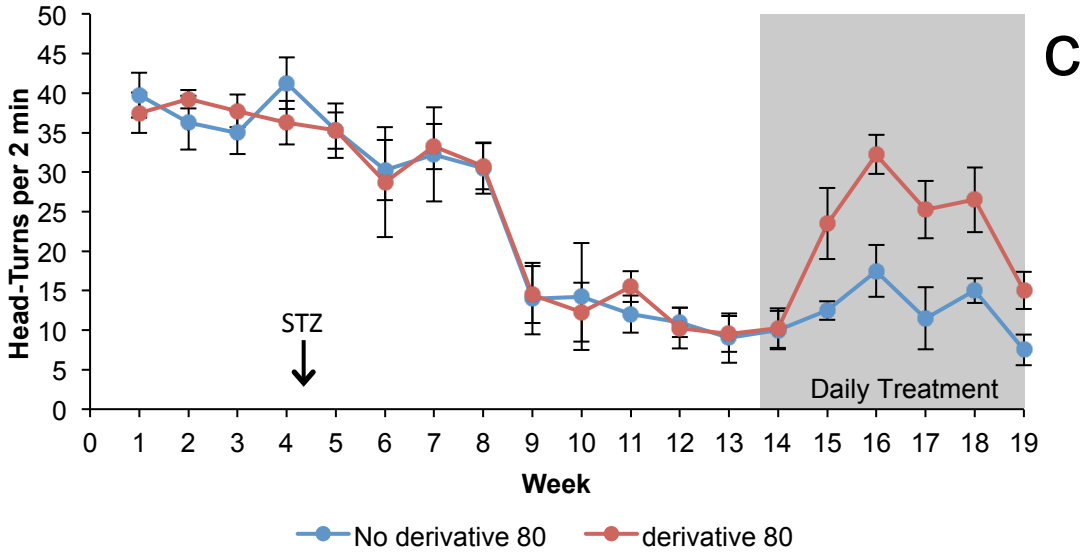

Figure 63: Visual response following daily eye drop treatment with test-compounds in diabetic Long Evans (LE) Rats. Using 0.1 cycle per degree optokinetic drum, visual acuity testing was performed for both the left and right eyes of LE rats at a speed of 2.61 rpm for 2 minutes over a period of 19 weeks. Upon administration of STZ (week 4), a significant drop in reflex head movement was evident by week 9, with further reduction by week 14. **a)** Daily idebenone (**11**) (10 mg/ml) treatment of the right eyes (shaded area), significantly improved head tracking score within 3 weeks of treatment. n = 6, **b)** Daily L-phenylalanine analogue **70** (>2 mg/ml) treatment on right eyes alone which is indicated by shading, resulted in significant improvement of head tracking score within two weeks of treatment on the right eyes. n = 4, **c)** Daily 3,4-dimethoxyphenethylamine **80** (>2 mg/ml) treatment on right eyes alone which is indicated by shading, resulted in significant improvement of head tracking score within one week of treatment on the right eyes. n = 4, Error bars = SEM, $P < 0.05$ (using one-way ANOVA, Dunnett's multiple comparison test). Left eye vision (Blue = No treatment), Right eye vision (Red = treatment).

Both L-phenylalanine derivative **70** and 3,4-dimethoxyphenethylamine derivative **80** as well as idebenone (**11**) showed promising ability to restore sight in the diabetic animals. Figure 63 indicates L-phenylalanine derivative **70** and 3,4-dimethoxy phenethylamine derivative **80** provide the same effect as idebenone (**11**) even though they were administered at five times less concentration due to solubility issues associated with novel derivatives in the eye drop formulation. It is worth mentioning that the slight increase in the control (left eye) is due to the increase of sight in the right eye. A recent study showed that in contrast to mice, the optokinetic reflex (OKR) in rats is not fully separated for the left vs right eye and that there is some cross over in

sight from the opposite eye.[150] This effect is likely responsible for the partial response of the untreated eye observed in this study. Over the course of this study, blood glucose levels were analysed and, notably, irrespective of the treatment-induced recovery of visual response, all animals remained extremely diabetic over the entire course of the study (Figure 64).

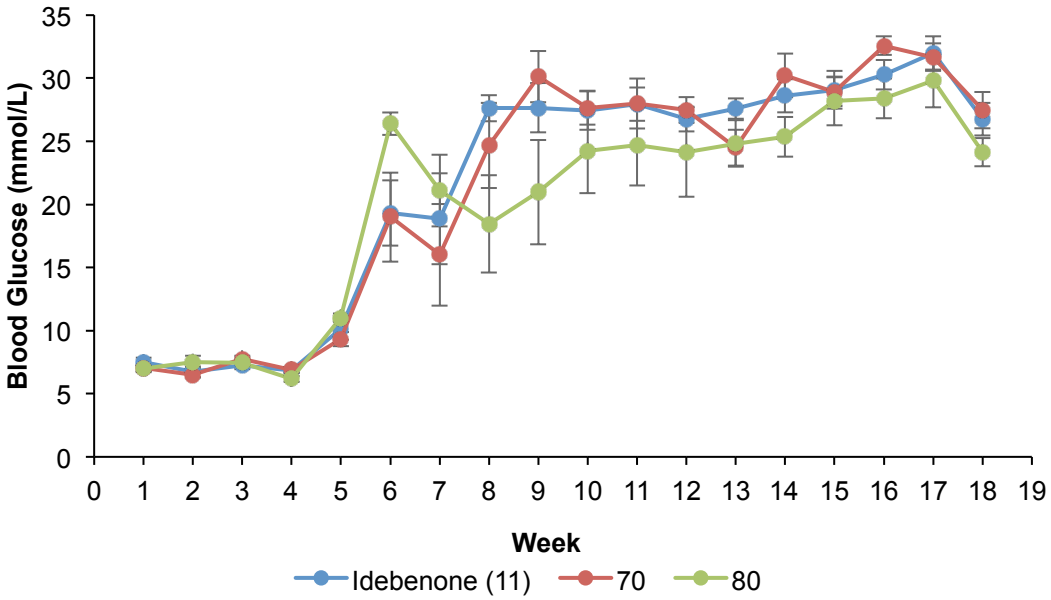

Figure 64: STZ at 125 mg/kg induces severe hyperglycemia in all 3 groups of Long Evans rats 2 weeks after administration and this high blood glucose level was sustained throughout out the experiment.

This evidence (Figure 64) indicates that local treatment of vision loss does not affect the diabetic state of the animals. These results are also consistent with a previous study that also described improvements in visual acuity using SS-31 (**10**) with no improvement in the diabetic state of the animals.[40] Therefore, this positive outcome leads to further investigation into *in vivo* diabetic retinopathy studies, with future work moving to oral treatment with the lead compounds in order to ascertain their capacity to positively affect the diabetic state of the animals. Notably, oral treatment will remove any uncertainty associated with the solubility issue of the novel naphthoquinone derivatives when formulating the eye drops.

5.3 Conclusions of *in vivo* studies

Both *in vivo* studies into LHON and diabetic retinopathy showed promising preliminary results. The extensive structure activity relationship (SAR) developed in Chapter 2 demonstrated an adequate representation of responses *in vivo*. Both analogues provided exceptional levels of activity. The most significant outcome from the LHON study was the superiority of the naphthoquinone derivatives over idebenone (**11**). At the concentration used (200 mg/kg), idebenone (**11**) was unable to restore visual acuity, with the novel compounds having an effect after 10 days. Similarly, in the diabetic retinopathy study, the novel derivatives provided a similar response to idebenone when administered at one fifth of the concentration. Therefore further investigations into these analogues ability to act as a therapeutic in other disease models associated with mitochondrial dysfunction needs to be undertaken.

Chapter 6: Experimental Details

6.1 General Experimental Details

Nuclear Magnetic Resonance Spectroscopy

Proton (^{1}H) and carbon (^{13}C) nuclear magnetic resonance spectra were recorded in deuterated chloroform ($CDCl_3$), methanol (CD_3OD), dimethylsulfoxide (DMSO-D_6) or acetone-D6 on a Bruker Avance III operating at 400 MHz for ^{1}H and 100 MHz for ^{13}C. Chemical shifts were recorded as δ values in parts per million (ppm) and referenced to the solvent used. In the case of $CDCl_3$ solvent references were at 7.26 ppm and 77.16 ppm for ^{1}H and ^{13}C respectively, For CD_3OD solvent references were 3.31 ppm and 49.3 ppm for ^{1}H and ^{13}C respectively, DMSO-D_6 solvent references were at 2.50 ppm and 39.52 ppm for ^{1}H and ^{13}C respectively, similarly for acetone-D_6 solvent references were at 2.05 ppm for ^{1}H and 29.84 and 206.26 for ^{13}C[151]. The following abbreviations were used to describe ^{1}H spectra peak splitting patterns; s = singlet, bs = broad singlet, d = doublet, bd = broad doublet, dd = doublet of doublets, t = triplet, ddt = doublet of doublets of triplets, qd = quartet of doublets, q = quartet, quin = quintet, sex = sextet, m = multiplet.

Cyclic Voltammetry

Cyclic voltammetry (CV) studies were carried out using a Metrohm 797 VA potentiostat fitted with a glassy carbon working electrode, a platinum auxiliary electrode and a saturated calomel reference electrode (SCE). Measurements were performed at room temperature in 20 mL of a 0.1 M tetrabutylammonium perchlorate solution in acetonitrile containing the naphthoquinones at a concentration of 1 mM. The electrochemical cell was deoxygenated by purging with N_2 for 2 min before scanning between –0.850 and 0.500 V (vs SCE) at a scan rate of 100 mV/s. The electrodes and measurement cell were rinsed with acetonitrile between each experiment.

Infrared Spectroscopy

Infrared spectroscopy was performed on a Shimadzu FTIR 8400s spectrometer, using NaCl plates. Liquids and solids were recorded as thin films from CH_2Cl_2 in cm^{-1}.

Mass Spectrometry

Mass spectrometry was performed on Kratos Concept ISQ using electron ionisation with 70eV electrons with an accelerating voltage of 5.3 kV or a Water Xero Triple Quadrupole using 2.5 kV needle voltage with direct infusion electrospray ionisation measuring positive ions. Accurate mass was also measured by 'peak matching' at 10,000 resolution against perfluorokerosene.

Analytical analyses were performed by the Central Science Laboratory at the University of Tasmania. The molecular ions and fragments are quoted with the relative intensities of the peaks referenced to the most intense taken as 100 %.

Column Chromatography

Merck flash grade silica (32-63 μm) was used for column and flash chromatography and were performed according to the general method of Still *et al.*[152]

Thin Layer Chromatography (TLC)

Merck Silica gel 60 F254 aluminium backed sheets were used for analytical thin layer chromatography. TLC plates were visualised under a 254 nm UV lamp and/or by treatment with a phosphomolybdic acid (37.5 g), ceric acid (7.5 g), sulfuric acid (37.5 mL), water (720 mL) dip or a potassium permanganate dip (3 g, $KMnO_4$, 20 g K_2CO_3, 5 mL 5 % aqueous NaOH, 300 mL), followed by heating.

Solvents and Reagents

All standards and reagents were purified by standard laboratory procedures.[153] Anhydrous magnesium sulfate was used as the drying agent for organic extracts unless otherwise stated and solvents removed under reduced pressure on a rotary evaporator.

Melting Points

Melting points were obtained with a Stuart Scientific melting point SMP1 apparatus and are uncorrected.

Optical Rotation

Optical rotations were obtained using a Rudolph research analytical Autopol III automatic polarimeter.

Spectroscopic Methods

UV-Vis absorption spectra were recorded in a 1.0 cm path length cuvette on a UV-1800 Shimadzu UV spectrophotometer. All fluorescence experiments were performed with a PerkinElmer LS55 spectrofluormeter in a 1.0 cm x 0.2 cm quartz cuvette.

6.2 Chapter 2 Experimental Details

6.2.1 General Procedures

General Procedure A: Silver-mediated radical decarboxylation general method:

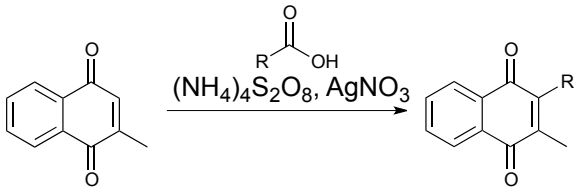

Carboxylic acid (2 equiv.) was added to a solution of menadione (1 equiv.) in CH_3CN/H_2O (3:1) and the mixture was heated to 75 °C. To this solution, $AgNO_3$ (0.1 equiv.) was added followed by the slow addition of $(NH_4)_2S_2O_8$ (2.5 equiv.) in H_2O (5 mL) over 10 min. The resulting mixture was stirred for a further 1 h. The mixture was cooled to room temperature, extracted with

CH_2Cl_2 and the organic extract washed with sat. $NaHCO_3$ and H_2O. The organic layer was dried over $MgSO_4$, filtered and the solvent removed under reduced pressure to give the crude product, which was purified by flash chromatography (silica gel).

General Procedure B: Quinone amide coupling general method:

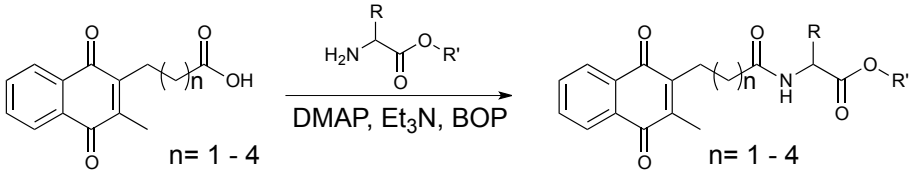

Quinone acid (1 equiv.) was added to anhydrous dichloromethane (5–10ml) under an atmosphere of N_2 and cooled to 0 °C. Amino acid (1 equiv.), dimethylaminopyridine (DMAP, 0.1 equiv.), triethylamine (Et_3N, 2.5 equiv.) and either EDCI, BOP or PyBOP (1.4 equiv.) were added successively and the reaction mixture warmed slowly to room temperature before leaving overnight. The reaction was quenched with H_2O (20mL) and the organic layer washed with sat. $KHSO_4$ solution, sat. $NaHCO_3$ solution and H_2O. The organic layer was dried with $MgSO_4$, filtered and the solvent removed under reduced pressure to give a crude product, which was purified by flash chromatography (silica gel) to give the amide.

General Procedure C: *t*-butyl ester deprotection method:

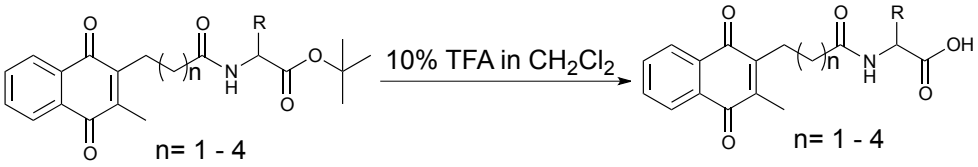

The *t*-butyl esters were added to 10% TFA in dichloromethane (5.0 mL) and the reaction mixture stirred at room temperature overnight and the solvent removed under reduced pressure. The crude product was obtained and purified by flash chromatography (silica gel) to give the pure carboxylic acid.

6.2.2 Synthesis of Compounds for SAR

4-(3-methyl-naphthoquione-2-yl)butanoic acid and 3,3'-(propane-1,3-diyl)bis(2-methyl-1,4-naphthoquinone) (**32** and **52**)

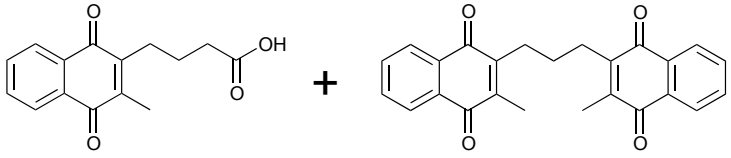

32 was prepared according to general procedure A from menadione (**12**) (5.998 g, 34.83 mmol) and glutaric acid (**49**) (4.611 g, 34.89 mmol) and the product purified by flash chromatography (100 % dichloromethane followed by 100% ethyl acetate) to give **32** as a bright yellow crystalline solid in 62 % yield (5.579 g, 21.67 mmol).

Modified General Procedure A: Glutaric acid (**49**) (4.368 g, 0.0331 mol) was added to a solution of menadione (2.984g, 0.0173 mol) in CH_3CN/H_2O (3:1, 50 mL) and the mixture was heated to 75 °C. To this solution, $AgNO_3$ (321 mg, 1.891 mmol) was added followed by the slow addition of $(NH_4)_2S_2O_8$ (9.897 g, 0.0434 mol) in H_2O (20 mL) over 1.5 h. The resulting mixture was stirred for a further 2 h, before being left o/n at room temperature. The mixture was extracted with CH_2Cl_2 (3 x 50 mL) and the organic extract washed with H_2O (4 x 50 mL). The organic layer was dried over $MgSO_4$, filtered and the solvent removed under reduced pressure to give the crude product, which was purified by a Reveleris ® X2 automated flash chromatography system (Eluent: gradient 100 % Hexanes - 100 % ethyl acetate, Column: Reveleris ® Silica 40 g, Flow rate: 30 mL/min) to two products, identified as **52** as a yellow needle crystals in <1 % yield (10 mg, 0.0.0260 mmol) and **32** in as a yellow solid in 18 % yield (791 mg, 0.3063 mmol).

4-(3-methyl-naphthoquione-2-yl)butanoic acid (**32**)

Melting point: 75-77 °C

^{1}H NMR δ ($CDCl_3$, 400 MHz): 1.82 (quin, *J* =7.4 Hz, 2H), 2.20 (s, 3H), 2.46 (t, *J* =7.4 Hz, 2H), 2.69 (t, *J* = 7.4 Hz,

2H), 7.66 – 7.69 (m, 2H), 8.04 - 8.06 (m, 2H)

^{13}C NMR δ ($CDCl_3$, 100 MHz): 12.8, 23.5, 26.4, 33.8, 126.4, 126.5, 132.2, 132.28, 133.61, 133.62, 144.1, 146.2, 179.3, 184.7, 185.3

IR V_{max}: 3064, 2938, 1706 (C=O), 1695 (C=O), 1658, 1616, 1595, 1412, 1379, 1295, 1260, 717, 660 cm^{-1}

3,3'-(propane-1,3-diyl)bis(2-methyl-1,4-naphthoquinone) (**52**)

^{1}H NMR δ ($CDCl_3$, 400 MHz): 1.66 – 1.74 (m, 2H), 2.20 (s, 6H), 2.76 (t, *J* = 8.0 Hz, 4H), 7.66 – 7.70 (m, 2H), 8.02 – 8.07 (m, 2H)

^{13}C NMR δ ($CDCl_3$, 100 MHz): 12.8, 27.3, 27.4, 126.3, 126.4, 132.22, 132.26, 133.53, 133.54, 143.7, 146.6, 184.7, 185.2

IR V_{max}: 1658 (C=O), 1618, 1595, 1377, 1325, 1296, 711 cm^{-1}

2-Methyl-3-(3,3,3-trifluoropropyl)-1,4-naphthoquinone (**41**)

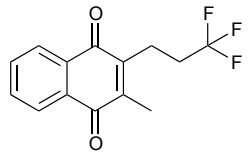

41 was prepared according to general procedure A from menadione (**12**) (910 mg, 5.284 mmol) and trifluorobutyric acid (268 mg, 1.883 mmol) and the product purified by flash chromatography (70 % CH_2Cl_2/hexanes) to give **41** as a bright yellow crystalline solid in 59 % yield (299 mg, 1.115 mmol) with a melting point of 61–62 °C.

^{1}H NMR δ ($CDCl_3$, 400 MHz): 2.13 (s, 3H) 2.21 – 2.33 (m, 2H), 2.81 (t, *J* = 7.8Hz, 2H), 7.60 – 7.62 (m, 2H), 7.93 – 7.95 (m, 2H)

^{13}C NMR δ ($CDCl_3$, 100 MHz): 12.4, 20.1 (q, J_{C-F} = 3.5 Hz), 32.2 (q, J_{C-F} = 29.1 Hz), 126.2, 126.3, 126.6 (q, J_{C-F} = 277.6 Hz), 131.8, 131.9, 133.56, 133.59, 143.6, 144.6, 184.0, 184.6

IR V_{max}: 1660 (C=O), 1622, 1595, 1456, 1381, 1294, 1251, 1238, 1138, 991, 717 cm^{-1}

2-Methyl-3-(3,3,3-trifluoro-2-hydroxy-2-methylpropyl)-1,4-naphthoquinone (**42**)

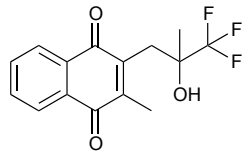

42 was prepared according to general procedure A from menadione (**12**) (7478 mg, 4.342 mmol) and 3-(trifluoro)-3-hydroxybutyric acid (245 mg, 1.425 mmol) and the product purified by flash chromatography (90 % CH_2Cl_2/hexanes) to give **42** as a crystalline yellow solid in 14 % yield (60 mg, 0.201 mmol) with a melting point of 42–44 °C.

^{1}H NMR δ ($CDCl_3$, 400 MHz): 1.32 (s, 3H), 2.25 (s, 3H), 2.94 (d, *J* = 14.0 Hz, 1H), 3.23 (d, *J* = 14.0 Hz, 1H), 4.12 (bs, 1H), 7.72 – 7.74 (m, 2H), 8.07 – 8.10 (m, 2H)

^{13}C NMR δ ($CDCl_3$, 100 MHz): 14.2, 20.8, 3.28, 74.1 (q, J_{C-F} = 28.2 Hz), 126.2 (q, J_{C-F} = 285.0 Hz), 126.7, 126.9, 131.7, 132.0, 133.9, 134.3, 140.8, 148.0, 184.6, 187.6

IR V_{max}: 3462 (-OH), 1662 (C=O), 1618, 1539, 1462, 1381, 1332, 1286, 1153, 1097, 779 cm^{-1}

2-Isopentylnaphthoquinone and 2,3-Diisopentyl-1,4-naphthoquinone (**43** and **44**)

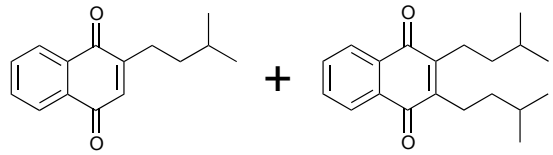

43 was prepared according to general procedure A from naphthoquinone (0.530 g, 3.351 mmol) and 4-methyl valeric acid (1.476 g, 12.71 mmol). Purification by flash column chromatography (50 % CH_2Cl_2/hexanes) resulted in two products being identified, **44** as a yellow viscous in a 10% yield (10 mg, 0.0322 mmol) and **43** as a yellow crystalline solid in 35 % yield (271 mg, 1.188 mmol).

2-Isopentylnaphthoquinone (**43**)

MP:	35 – 38 °C
^{1}H NMR δ ($CDCl_3$, 400 MHz):	0.95 (d, *J* = 6.7 Hz, 6H), 1.42 – 1.48 (m, 2H), 1.65 (septet, *J* = 6.7 Hz, 1H), 2.57 (td, *J* = 8.1, 1.4 Hz, 2H), 6.78 (t, *J* = 1.4 Hz, 1H), 7.70 – 7.73 (m, 2H), 8.04 – 8.06 (m, 1H), 8.08 – 8.10 (m, 1H)
^{13}C NMR δ ($CDCl_3$, 100 MHz):	22.5, 27.6, 28.1, 37.2, 126.1, 126.7, 132.2, 132.5, 133.72, 133.75, 134.7, 152.4, 185.3, 185.7
IR V_{max}:	2956, 2928, 2870, 1662 (C=O), 1620, 1595, 1467, 1367, 1329, 1301, 1265, 779 cm^{-1}

2,3-Diisopentyl-1,4-naphthoquinone (**44**)

^{1}H NMR δ ($CDCl_3$, 400 MHz):	1.00 (d, *J* = 6.7 Hz, 12H), 1.36 – 1.41 (m, 4H), 1.72 (ap. Octet, *J* = 6.6 Hz, 2H), 2.59 – 2.64 (m, 4H), 7.69 – 7.71 (m, 2H), 8.07 – 8.09 (m, 2H)

^{13}C NMR δ ($CDCl_3$, 100 MHz): 22.5, 25.1, 28.9, 38.7, 126.2, 132.4, 133.3, 147.5, 185.2

IR V_{max}: 2956, 2924, 2852, 1660 (C=O), 1597, 1465, 1367, 1317, 1284, 1259, 1103, 719 cm^{-1}

(*S*)-*tert*-Butyl-2-(4-(3-methyl-1,4-naphthoquinone-2-yl)butanamido)-3-phenylpropanoate (**61**)

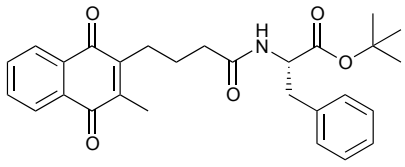

61 was prepared according to general procedure B from 4-(3-Methyl-1,4-naphthalen-2-yl)-butanoic acid (**32**) (504 mg, 1.952 mmol) and L-phenylalanine *t*-butyl ester.HCl (489 mg, 1.902 mmol) and the product purified by flash chromatography (40 % ethyl acetate/hexanes) to give **61** as yellow oil in 36 % yield (317 mg, 0.687 mmol).

^{1}H NMR δ ($CDCl_3$, 400 MHz): 1.40 (s, 9H), 1.78 (quin, *J* = 7.6 Hz, 2H), 2.17 (s, 3H), 2.27 (t, *J* = 7.6 Hz, 2H), 2.60 – 2.62 (m, 2H), 3.04 – 3.13 (m, 2H), 4.74 – 4.79 (m, 1H), 6.09 (d, *J* = 7.8 Hz, 1H), 7.14 – 7.27 (m, 5H), 7.66 – 7.69 (m, 2H), 8.04 – 8.07 (m, 2H)

^{13}C NMR δ ($CDCl_3$, 100 MHz): 12.8, 24.3, 26.3, 28.0, 36.1, 38.2, 53.5, 82.4, 126.3, 126.4, 127.0, 128.4 (2 x C), 129.5 (2 x C), 132.21, 132.26, 133.4, 133.5, 136.3, 144.0, 146.4, 170.9, 171.8, 184.8, 185.3

$[\alpha]_D^{20}$: +36.24° (*c* 0.91, $CHCl_3$)

IR V_{max}: 3420 (N-H), 2978, 1732 (C=O), 1658 (C=O), 1595, 1525, 1367, 1329, 1294, 1257, 1226, 1155, 700 cm^{-1}

HRMS [M+Na]: For $C_{28}H_{31}N_1O_5Na$, predicted 484.2100, found 484.2110

(*S*)-*tert*-Butyl-1-(4-(3-methyl-1,4-naphthoquinone-2-yl)butanoyl)pyrrolidine-2-carboxylate (**62**)

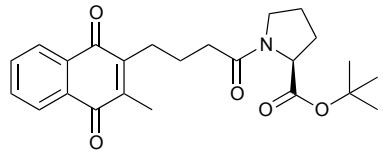

62 was prepared according to general procedure B from 4-(3-Methyl-1,4-naphthalen-2-yl)-butanoic acid (**32**) (197 mg, 0.7623 mmol) and L-proline *t*-butyl ester.HCl (140 mg, 0.6716 mmol) and the product purified by flash chromatography (60 % ethyl acetate/hexanes) to give **62** as yellow oil in 53 % yield (146 mg, 0.3543 mmol).

^{1}H NMR δ ($CDCl_3$, 400 MHz): 1.44 (s, 9H), 1.82 – 1.88 (m, 2H), 1.90 – 1.96 (m, 2H), 2.04 – 2.13 (m, 2H), 2.21 (s, 3H), 2.36 – 2.48 (m, 2H), 2.67 – 2.71 (m, 2H), 3.47 – 3.52 (m, 1H), 3.59 – 3.64 (m, 1H), 4.37 (dd, *J* = 8.5, 3.9 Hz, 1H), 7.66 – 7.68 (m, 2H), 8.03 – 8.07 (m, 2H)

^{13}C NMR δ ($CDCl_3$, 100 MHz): 12.8, 23.7, 24.7, 26.5, 28.0, 29.3, 34.1, 47.1, 59.5, 81.2, 126.2 (2 x C), 132.23, 132.26, 133.3 (2 x C), 144.0, 146.7, 171.0, 171.6, 184.7, 185.3

$[\alpha]_D^{20}$: +48.70 ° (*c* 0.97, $CHCl_3$)

IR V_{max}: 2976, 2935, 1735 (C=O), 1654 (C=O), 1618, 1595, 1456, 1425, 1367, 1294, 1153, 719 cm^{-1}

(*S*)-*tert*-Butyl-2-(4-(3-methyl-1,4-naphthoquinone-2-yl)butanamido) pentanoate (**63**)

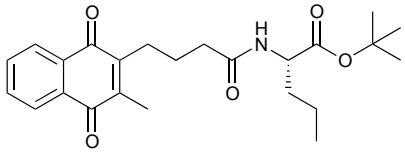

63 was prepared according to general procedure B from 4-(3-Methyl-1,4-naphthalen-2-yl)-butanoic acid (**32**) (209 mg, 0.8096 mmol) and L-norvaline *t*-butyl ester.HCl (159 mg, 0.7587 mmol) and the product purified by flash chromatography (50 % ethyl acetate/hexanes) to give **63** as yellow oil in 44 % yield (140 mg, 0.3376 mmol).

^{1}H NMR δ ($CDCl_3$, 400 MHz): 0.90 (t, *J* = 7.3 Hz, 3H), 1.29 – 1.33 (m, 2H), 1.43 (s, 9H), 1.58 – 1.65 (m, 2H), 1.77 -1.84 (m, 2H), 2.17 (s, 3H), 2.31 (t, *J* = 7.2 Hz, 2H), 2.64 – 2.68 (m, 2H), 4.45 – 4.50 (m, 1H), 6.27, d, *J* = 8.0 Hz, 1H), 7.64 – 7.67 (m, 2H), 8.01 – 8.03 (m, 2H)

^{13}C NMR δ ($CDCl_3$, 100 MHz): 12.8, 13.9, 18.6, 24.4, 26.4, 28.1, 34.9, 36.2, 52.6, 82.0, 126.40, 126.45, 132.23, 132.29, 133.51, 133.55, 144.1, 146.4, 171.9, 172.2, 184.9, 185.3

$[\alpha]_D^{20}$: -3.43° (*c* 0.17, $CHCl_3$)

IR V_{max}: 3354 (N-H), 3296, 2962, 1734 (C=O), 1660 (C=O), 1595, 1521, 1458, 1367, 1329, 1294, 1149, 717 cm^{-1}

***tert*-Butyl 2-(4-(3-methyl-1,4-naphthoquinone-2-yl)butanamido)acetate** (**64**)

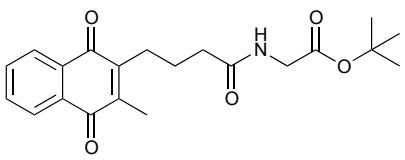

64 was prepared according to general procedure B from 4-(3-Methyl-1,4-naphthalen-2-yl)-butanoic acid (**32**) (165 mg, 0.6381 mmol) and glycine *t*-butyl ester (148 mg, 0.8852 mmol) and the product purified by flash chromatography (50 % ethyl acetate/hexanes) to give **64** as yellow viscous oil in 36 % yield (85 mg, 0.2294 mmol).

^{1}H NMR δ ($CDCl_3$, 400 MHz): 1.41 (s, 9H), 1.79 (quin, *J* = 7.2 Hz, 2H), 2.15 (s, 3H), 2.31 (t, *J* = 7.2 Hz, 2H), 2.62 – 2.62 (m, 2H), 3.89 (d, *J* = 5.1 Hz, 2H), 6.27 – 6.29 (m, 1H), 7.60 – 7.65 (m, 2H), 7.98 – 8.01 (m, 2H)

^{13}C NMR δ ($CDCl_3$, 100 MHz): 12.7, 24.3, 26.3, 28.0, 35.8, 42.0, 82.2, 126.25, 126.29, 132.13, 132.17, 133.3, 133.4, 144.0, 146.3, 169.2, 172.4, 184.7, 185.1

IR V_{max}: 3369 (N-H), 2978, 1743 (C=O), 1660 (C=O), 1595, 1521, 1369, 1329, 1294, 1224, 1157, 717 cm^{-1}

(*S*)-*tert*-butyl-4-methyl-2-(4-(3-methyl-1,4-naphthoquinone-2-yl)butanamido)pentanoate (**65**)

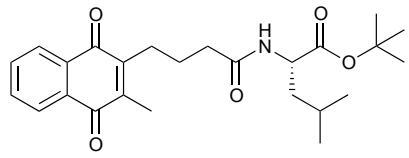

65 was prepared according to general procedure B from 4-(3-Methyl-1,4-naphthalen-2-yl)-butanoic acid (**32**) (194 mg, 0.7496 mmol) and L-Leucine *t*-butyl ester.HCl (168 mg, 0.7509 mmol) and the product purified by flash chromatography (40 % ethyl acetate/hexanes) to give **65** as yellow oil in 39 % yield (124 mg, 0.2898 mmol).

^{1}H NMR δ ($CDCl_3$, 400 MHz): 0.90 (d, *J* = 6.5 Hz, 6H), 1.42 (s, 9H), 1.46 – 1.65 (m, 2H), 1.79 (quin, *J* = 7.4 Hz, 2H), 2.16 (s, 3H), 2.29 (t, *J* = 7.4 Hz, 2H), 2.62 –

2.66 (m, 2H), 4.49 (td, *J* = 8.6, 5.3 Hz, 1H), 6.16 (d, *J* = 8.3 Hz, 1H), 7.62 – 7.66 (m, 2H), 7.98 – 8.03 (m, 2H)

^{13}C NMR δ ($CDCl_3$, 100 MHz): 12.7, 22.1, 22.8, 24.3, 25.0, 26.4, 28.07, 36.1, 41.9, 51.4, 81.8, 126.2, 126.3, 132.1, 132.2, 133.40, 133.43, 144.0, 146.4, 171.9, 172.5, 184.8, 185.2

$[\alpha]_D^{20}$: -2.62 ° (*c* 1.06, $CHCl_3$)

IR V_{max}: 3354 (N-H), 2958, 2870, 1734 (C=O), 1718 (C=O), 1660 (C=O), 1595, 1541, 1521, 1456, 1367, 1329, 1294, 1149, 717 cm^{-1}

(*S*)-*tert*-butyl-3-(4-hydroxyphenyl)-2-(4-(3-methyl-1,4-naphthoquinone-2-yl)butanamido)propanoate and (*S*)-4-(3-(*tert*-butoxy)-2-(4-(3-methyl-1,4-naphthoquinone-2-yl)butanamido)-3-oxopropyl)phenyl-4-(3-methyl-1,4-naphthoquinone-2-yl)butanoate (**66** and **68**)

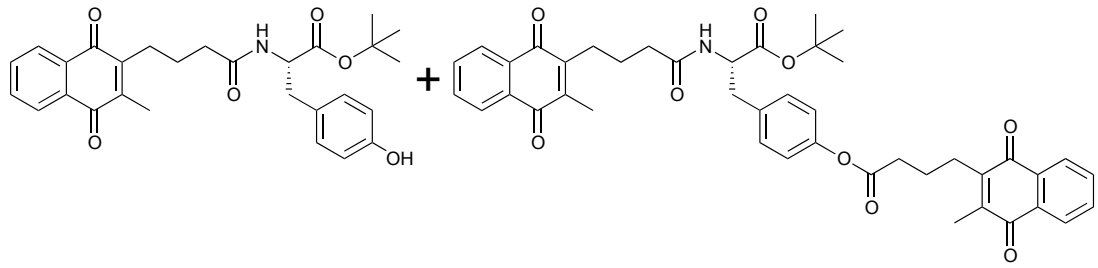

66 were prepared according to general procedure B from 4-(3-Methyl-1,4-naphthalen-2-yl)-butanoic acid (**32**) (225 mg, 0.8727 mmol) and L-tyrosine *t*-butyl ester.HCl (188 mg, 0.7902 mmol). Purification by flash chromatography (60 % ethyl acetate/ hexanes) resulted in the identification of **66** and **68**. Compounds were combined and dissolved in 10 mL methanol, excess potassium carbonate added and the reaction left stirring at r.t for 1hour. The mixture was extracted with dichloromethane 3x 30 mL and the organic layer dried over $MgSO_4$, filtered and the solvent removed under reduced pressure to give crude **66** which was purified by flash chromatography (50 % ethyl

acetate/ hexanes) to give **66** as yellow oil in 20 % yield (42 mg, 0.0871 mmol).

Note: **68** (14.9 mg, 0.0208 mmol) was kept for analysis (yellow viscous oil).

(*S*)-*tert*-butyl-3-(4-hydroxyphenyl)-2-(4-(3-methyl-1,4-naphthoquinone-2-yl)butanamido)propanoate

^{1}H NMR δ ($CDCl_3$, 400 MHz): 1.42 (s, 9H), 1.78 (quin, *J* = 7.5 Hz, 2H), 2.17 (s, 3H), 2.27 (t, *J* = 7.5 Hz, 2H), 2.61 – 2.65 (m, 2H), 2.98 (dd, *J* = 14.1, 6.1 Hz, 1H), 3.05 (dd, *J* = 14.1 Hz, 6.1 Hz, 1H), 4.72 – 4.76 (m, 1H), 6.09 (d, *J* = 8.0 Hz, 1H), 6.72 (d, *J* = 8.2 Hz, 2H), 7.01 (d, *J* = 8.2 Hz, 2H), 7.67 – 7.72 (m, 2H), 8.05 – 8.08 (m, 2H)

^{13}C NMR δ ($CDCl_3$, 100 MHz): 12.8, 24.3, 26.4, 28.1, 36.2, 37.4, 77.3, 82.5, 115.4 (2 x C), 126.42, 126.47, 130.7 (2 x C), 132.3, 133.5, 144.2, 146.5, 154.9, 171.1, 171.9, 184.9, 185.3

$[\alpha]_D^{20}$: +14.86. $^{\circ}$ (*c* 0.18, $CHCl_3$)

IR V_{max}: 3367 (N-H), 2987, 2931, 1732 (C=O), 1654 (C=O), 1616, 1695, 1516, 1506, 1369, 1330, 1294, 1259, 1153, 734 cm^{-1}

(*S*)-4-(3-(*tert*-butoxy)-2-(4-(3-methyl-1,4-naphthoquinone-2-yl)butanamido)-3-oxopropyl)phenyl 4-(3-methyl-1,4-naphthoquinone-2-yl)butanoate

^{1}H NMR δ ($CDCl_3$, 400 MHz): 1.40 (s, 9H), 1.78 (quin, *J* = 7.8 Hz, 2H), 1.90 (quin, *J* = 7.8 Hz, 2H), 2.18 (s, 3H), 2.22 (s 3H), 2.28 (t, *J* = 7.8 Hz, 2H), 2.61 – 2.65 (m, 4H), 2.73 – 2.77 (m, 2H), 3.09 (d, *J* = 6.1 Hz, 2H), 4.73 – 4.78 (m, 1H), 6.10 (d, *J* = 7.7 Hz, 1H), 7.00 (d, *J* = 8.4 Hz,

2H), 7.17 (d, *J* = 8.4 Hz, 2H), 7.66 – 7.71 (m, 4H), 8.04 – 8.09 (m, 4H)

^{13}C NMR δ ($CDCl_3$, 100 MHz): 12.84, 12.87, 23.7, 24.3, 26.3, 26.4, 28.1, 34.1, 36.1, 37.6, 53.5, 82.6, 121.5, 126.3, 126.43, 126.45, 126.47, 130.5 (2 x C), 132.23, 132.25, 132.29, 132.3, 133.51, 133.52, 133.59 (2 x C), 134.0, 144.1, 146.2, 146.4, 149.7, 170.8, 171.6, 172.8, 184.7, 184.9, 185.31, 185.35

$[\alpha]_D^{20}$: +17.91° (*c* 0.34, $CHCl_3$)

IR V_{max}: 3366 (N-H), 2978, 2933, 1734 (C=O), 1654 (C=O), 1595, 1506, 1456, 1369,1296, 1259, 1201, 1153, 734 cm^{-1}

(*S*)-2-(4-(3-Methyl-1,4-naphthoquinone-2-yl)butanamido)-3-phenylpropanoic acid (**70**)

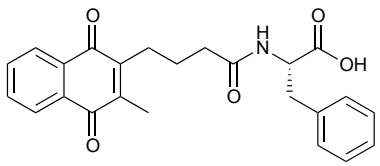

70 was prepared from the deprotection of **61** (317 mg, 0.6875 mmol), using general procedure C. The product was purified by flash chromatography (5 % methanol/ethyl acetate) to give **70** as brown viscous oil in 79 % yield (220 mg, 0.542 mmol).

^{1}H NMR δ ($CDCl_3$, 400 MHz): 1.72 – 1.79 (m, 2H), 2.14 (s, 3H), 2.29 (t, *J* = 7.2 Hz, 2H), 2.58 (t, *J* = 7.8 Hz, 2H), 3.12 (dd, *J* = 14.0, 7.0 Hz, 1H), 3.26 (dd, *J* = 14.0, 5.4 Hz, 1H), 4.90 (m, 1H), 6.54 (d, *J* = 7.7 Hz, 1H), 7.17 – 7.28 (m, 5H), 7.66 – 7.69 (m, 2H), 8.02 – 8.05 (m, 2H), 8.92 (bs, 1H)

^{13}C NMR δ ($CDCl_3$, 100 MHz): 12.8, 24.2, 26.2, 35.8, 37.3, 53.4, 126.4, 127.2, 128.7 (2 x C), 129.4 (2 x C), 132.0, 132.2, 133.5, 133.6, 135.9, 144.3, 146.2, 173.5, 174.7, 185.1, 185.2

$[\alpha]_D^{20}$: +35.83 ° (*c* 0.24, $CHCl_3$)

IR V_{max}: 3491 (N-H), 2931, 1716 (C=O), 1660 (C=O), 1616, 1595, 1521, 1456, 1332, 1296, 1267, 1217, 702 cm^{-1}

HRMS [M+Na]: For $C_{24}H_{23}N_1O_5Na$, predicted 428.1474, found 428.1484

(*S*)-1-(4-(3-Methyl-1,4-naphthoquinone-2-yl)butanoyl)pyrrolidine-2-carboxylic acid (**71**)

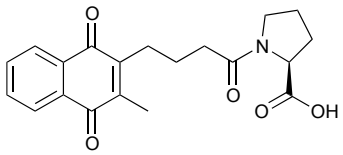

71 was prepared from the deprotection of **62** (114 mg, 0.2766 mmol), using general procedure C. The product was purified by flash chromatography (3 % methanol/ethyl acetate) to give **71** as brown viscous oil in 65 % yield (64 mg, 0.1798 mmol).

^{1}H NMR δ ($CDCl_3$, 400 MHz): 1.82 – 1.90 (m, 2H), 2.02 – 2.08 (m, 2H), 2.21 (s, 3H), 2.13 – 2.33 (m, 2H), 2.45 – 2.50 (m, 2H), .68 – 2.72 (m, 2H), 3.49 – 3.53 (m, 1H), 3.60-3.63 (m, 1H), 4.55 – 4.58 (m, 1H), 7.53 bs, 1H), 7.68 – 7.07 (m, 2H), 8.04 – 8.08 (m, 2H)

^{13}C NMR δ ($CDCl_3$, 100 MHz): 12.8, 23.3, 24.8, 26.4, 28.0, 34.1, 47.8, 59.7, 126.34, 126.38, 132.1, 132.2, 133.51, 133.56, 144.2, 146.3, 173.4, 173.9, 184.8, 185.3

$[\alpha]_D^{20}$: -65.80° (*c* 1.69, $CHCl_3$)

IR V_{max}: 2976, 2956, 1716 (C=O), 1658 (C=O), 1616, 1595, 1456, 1329, 1294, 1188, 717 cm^{-1}

(*S*)-2-(4-(3-Methyl-1,4-naphthoquinone-2-yl)butanamido)pentanoic acid (72)

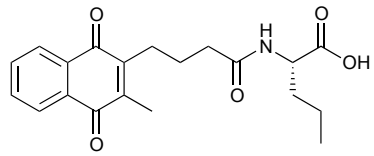

72 was prepared from the deprotection of **63** (140 mg, 0.3376 mmol), using general procedure C. The product was purified by silica plug (gradient 5-10 % methanol/ethyl acetate) to give **72** as yellow/brown viscous oil in 36 % yield (44 mg, 0.1223 mmol).

^1H NMR δ (CD_3OD, 400 MHz): 0.92 (t, *J* = 7.3 Hz, 3H), 1.35 – 1.45 (m, 2H), 1.61 – 1.70 (m, 2H), 1.78 (quin, *J* = 7.4 Hz, 2H), 2.14 (s, 3H), 2.34 (t, *J* = 7.4, 2H), 2.64 (m, 2H), 4.29 – 4.32 (m, 1H), 7.68 – 7.72 (m, 2H), 7.94 – 7.98 (m, 2H)

^{13}C NMR δ (CD_3OD, 100 MHz): 12.7, 14.0, 20.1, 25.7, 27.3, 35.0, 36.6, 54.6, 127.00, 127.08, 133.3, 134.5, 144.9, 147.5, 175.3 (2 x C) 185.6, 186.2

$[\alpha]_D^{20}$: -24.44° (*c* 0.09, $CHCl_3$)

IR V_{max}: 3336 (N-H), 3296, 2960, 2874, 1681 (C=O), 1660 (C=O), 1595, 1558, 1456, 1296, 1205, 1139, 1026, 721 cm^{-1}

2-(4-(3-methyl-1,4-naphthoquinone-2-yl)butanamido)acetic acid (**73**)

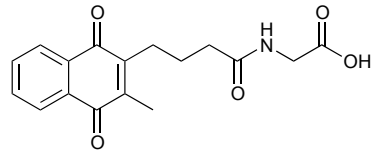

73 was prepared from the deprotection of **64** (75 mg, 0.1952 mmol), using general procedure C. The product purified by precipitation from dichloromethane and the solvent was decanted to give **73** as brown solid in 54 % yield (34 mg, 0.1062 mmol) with a melting point of 62 – 66 °C.

^{1}H NMR δ ($CDCl_3$, 400 MHz): 1.82 (quin, *J* = 7.2 Hz, 2H), 2.16 (s, 3H), 2.41 (t, *J* = 7.2 Hz, 2H), 2.64 – 2.68 (m, 2H), 4.09 (d, *J* = 5.2 Hz, 2H), 6.96 – 6.99 (m, 1H), 7.65 – 7.68 (m, 2H), 7.99 – 8.04 (m, 2H)

^{13}C NMR δ ($CDCl_3$, 100 MHz): 12.8, 24.3, 26.3,35.7, 41.6, 126.45, 126.48, 132.0, 132.2, 133.6, 133.7, 144.5, 146.0, 172.6, 174.7, 185.2, 185.3

IR V_{max}: 3296 (N-H), 2939, 1734 (C=O), 1718 (C=O), 1654 (C=O), 1595, 1533, 1330, 1296, 1024, 717 cm^{-1}

(*S*)-4-methyl-2-(4-(3-methyl-1,4-naphthoquinone-2-yl)butanamido)pentanoic acid (**74**)

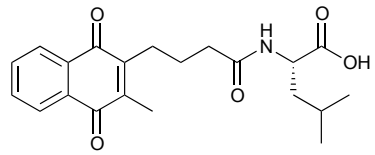

74 was prepared from the deprotection of **65** (109 mg, 0.2559 mmol), using general procedure C. The product purified by flash chromatography (5 % methanol/ethyl acetate) to give **74** as a dark yellow viscous oil in 61 % yield (58 mg, 0.1612 mmol).

^{1}H NMR δ ($CDCl_3$, 400 MHz): 0.93 – 0.95 (m, 6H), 1.61 – 1.73 (m, 2H) 1.82 (quin, *J* = 7.4 Hz, 2H), 2.17 (s, 3H), 2.38 (t, *J* = 7.4 Hz, 2H), 2.64 – 2.68 (m, 2H), 4.59 – 4.64 (m, 1H), 6.73 (d, *J* = 8.0 Hz, 1H), 7.65 – 7.67 (m, 2H), 7.99 – 8.03 (m, 2H)

^{13}C NMR δ ($CDCl_3$, 100 MHz): 12.7, 21.8, 22.9, 24.3, 25.0, 26.3, 35.9, 41.0, 51.0, 126.3 (2 x C), 132.0, 132.1, 133.5, 133.6, 144.3, 146.2, 173.5, 176.2, 185.1, 185.2

$[\alpha]_D^{20}$: -5.35 ° (*c* 0.93, $CHCl_3$)

IR V_{max}: 3321 (N-H), 1716 (C=O), 1660 (C=O), 1618, 1595, 1539, 1506, 1330, 1294, 1207, 717 cm^{-1}

(*S*)-3-(4-hydroxyphenyl)-2-(4-(3-methyl-1,4-naphthoquinone-2-yl)butanamido)propanoic acid (**75**)

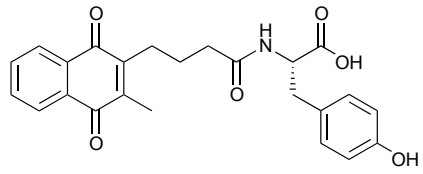

75 was prepared from the deprotection of **66** (30 mg, 0.06213 mmol), using general procedure C. The product purified by precipitation from dichloromethane and the solvent decanted to give **75** as a dark yellow viscous oil in 76 % yield (20 mg, 0.0479 mmol).

^{1}H NMR δ (CD_3OD, 400 MHz): 1.67 (quin, *J* = 7.7 Hz, 2H), 2.08 (s, 3H), 2.23 – 2.30 (m, 2H), 2.37 – 2.45 (m, 1H), 2.52 – 2.59 (m, 1H), 2.82 (dd, *J* = 14.0, 9.5 Hz, 1H), 3.12 (dd, *J* = 14.0, 4.9 Hz, 1H), 4.60 – 4.64 (m,1H), 6.65 (d, *J* = 8.3 Hz, 2H), 7.04 (d, *J* = 8.3 Hz, 2H), 7.71 – 7.73 (m, 2H), 7.99 – 8.02 (m, 2H)

^{13}C NMR δ (CD_3OD, 100 MHz): 12.6, 25.6, 27.1, 36.5, 37.6, 55.2, 116.1 (2 x C), 127.0, 127.1, 129.1, 131.2 (2 x C), 133.4, 134.56, 134.57, 145.0, 147.5, 157.2, 174.9, 175.3, 185.7, 186.3

$[\alpha]_D^{20}$: +2.21 ° (*c* 0.81, $CHCl_3$)

IR V_{max}: 3365 (N-H), 2937, 1734 (C=O), 1716 (C=O), 1647 (C=O), 1616, 1595, 1516, 1456, 1296, 1232 cm^{-1}

(*S*)-*N*-(1-hydroxy-3-phenylpropan-2-yl)-4-(3-methyl-1,4-naphthyoquinone-2-yl)butanamide (**76**)

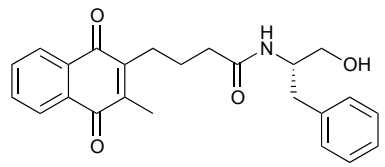

76 was prepared according to general procedure B from 4-(3-Methyl-1,4-naphthalen-2-yl)-butanoic acid (**32**) (134 mg, 5169 mmol) and L-phenyl analinol (76 mg, 0.5053 mmol) and the product purified by flash chromatography (100 % ethyl acetate) to give **76** as yellow/orange oil in 49 % yield (98 mg, 0.2496 mmol).

^{1}H NMR δ ($CDCl_3$, 400 MHz): 1.70 – 1.78 (m, 2H), 2.15 (s, 3H), 2.25 (t, *J* = 7.2 Hz, 2H), 2.55 (t, *J* = 8.0 Hz, 2H), 2.83 – 2.94 (m, 2H), 3.03 (bs, 1H), 3.59 (dd, *J* = 11.2, 5.4 Hz, 1H), 3.71 (dd, *J* = 11.2, 3.8 Hz, 1H), 4.21 – 4.29 (m, 1H), 6.31 (d, *J* = 8.0 Hz, 1H), 7.15 – 7.27 (m, 5H), 7.64 – 7.69 (m, 2H), 8.00 – 8.05 (m, 2H)

^{13}C NMR δ ($CDCl_3$, 100 MHz): 12.7, 24.3, 26.2, 36.2, 37.0, 52.9, 64.1, 126.35, 126.36, 126.6, 128.6 (2 x C), 129.2 (2 x C), 132.0, 132.1, 133.5, 133.6, 137.9, 144.2, 146.2, 173.1, 185.12, 185.13

$[\alpha]_D^{20}$: -21.33 ° (*c* 1.57, $CHCl_3$)

IR V_{max}: 3369 (N-H), 3296 (-OH), 2933, 1658 (C=O), 1595, 1539, 1456, 1377, 1330, 1296, 1043, 717, 702 cm^{-1}

HRMS [M+Na]: For $C_{24}H_{25}N_1O_4Na$, predicted 414.1676, found 414.1667

(*S*)-2-(4-(2-(hydroxymethyl)pyrrolidin-1-yl)-4-oxobutyl)-3-methyl-1,4-naphthoquinone (**77**)

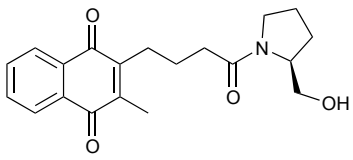

77 was prepared according to general procedure B from 4-(3-Methyl-1,4-naphthalen-2-yl)-butanoic acid (**32**) (117 mg, 0.4522 mmol) and L-Prolinol (159 mg, 0.7587 mmol) and the product purified by flash chromatography (100 % ethyl acetate) to give **77** as yellow oil in 36 % yield (50 mg, 1459 mmol).

^1H NMR δ ($CDCl_3$, 400 MHz): 1.60 (quin, *J* = 6.2 Hz, 2H), 1.82 – 2.02 (m, 6H), 2.21 (s, 3H), 2.39 (t, *J* = 7.2 Hz, 2H), 2.67 – 2.72 (m, 2H), 3.50 – 3.55 (m, 1H), 3.66 (dd, *J* = 11.3, 2.8 Hz, 1H), 4.15 – 4.22 (m, 1H), 7.66 – 7.68 (m, 2H), 8.03 – 8.07 (m, 2H).

^{13}C NMR δ ($CDCl_3$, 100 MHz): 12.8, 23.6, 24.5, 26.4, 28.3, 34.6, 48.1, 61.2, 67.3, 126.33, 126.37, 132.1, 132.2, 133.4, 133.5, 144.1, 146.6, 173.6, 184.9, 185.3

$[\alpha]_D^{20}$: -35.12 ° (*c* 0.41, $CHCl_3$)

IR V_{max}: 3367 (N-H), 2953, 2877, 1695, 1654, 1616, 1595, 1454, 1329, 1296, 1047, 732, 719 cm^{-1}

(*S*)-*N*-(2-hydroxy-1-phenylethyl)-4-(3-methyl-1,4-naphthoquinone-2-yl)butanamide (**78**)

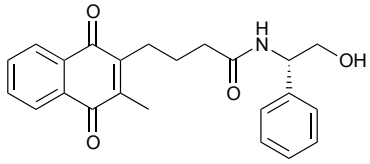

78 was prepared according to general procedure B from 4-(3-Methyl-1,4-naphthalen-2-yl)-butanoic acid (**32**) (187 mg, 0.7252 mmol) and L-phenyl glycinol (106 mg, 0.7690 mmol) and the product purified by dissolving in dichloromethane and adding hexanes dropwise until a precipitate was formed to give **78** as yellow crystaline solid in 69 % yield (188 mg, 0.4992 mmol) with a melting point of 140 – 144 °C.

^{1}H NMR δ ($CDCl_3$, 400 MHz): 1.80 – 1.90 (m, 2H), 2.19 (s, 3H), 2.37 (t, *J* = 7.1 Hz, 2H), 2.65 – 2.72 (m, 2H), 3.92 (d, *J* = 5.0 Hz, 2H), 5.09 – 5.14 (m, 1H), 6.53 (d, *J* = 6.3 Hz, 1H), 7.27 – 7.38 (m, 5H), 7.68 – 7.70 (m, 2H), 8.04 – 8.08 (m, 2H)

^{13}C NMR δ ($CDCl_3$, 100 MHz): 128, 24.4, 26.3, 36.1, 56.2, 66.7, 126.4, 126.9, 128.0, 128.9 (2 x C), 132.1, 132.3, 133.5, 133.7, 139.0, 144.4, 146.3, 173.0, 185.2, 185.3

$[\alpha]_D^{20}$: $+18.01^{\circ}$ (*c* 0.66, $CHCl_3$)

IR V_{max}: 3294 (C=O), 2937, 1656 (C=O), 1595, 1535, 1454, 1377, 1330, 1294, 1070, 700 cm^{-1}

***N*-(4-hydroxyphenethyl)-4-(3-methyl-1,4-naphthoquinone-2-yl) butanamide** (**79**)

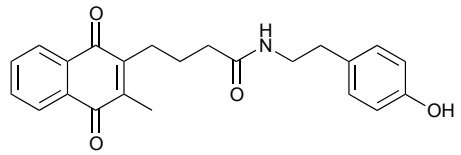

79 was prepared according to general procedure B from 4-(3-Methyl-1,4-naphthalen-2-yl)-butanoic acid (**32**) (236 mg, 0.9122 mmol) and tyramine (119 mg, 0.8675 mmol) and the product purified by flash chromatography (80 % ethyl acetate/hexanes) to give **79** as yellow solid in 33 % yield (109 mg, 0.2885 mmol) with a melting point of 116 – 118 °C.

^{1}H NMR δ ($CDCl_3$, 400 MHz): 1.76 (quin, *J* = 7.5 Hz, 2H), 2.12 (s, 3H), 2.24 (t, *J* = 7.2 Hz, 2H), 2.56 – 2.60 (m, 2H), 2.71 (t, *J* = 7.0 Hz, 2H), 3.44 – 3. 49 (m, 2H), 6.22 (t, *J* = 5.5 Hz, 1H), 6.75 (d, *J* = 8.4 Hz, 2H), 6.96 (d, *J* = 8.4 Hz, 2H), 7.62 – 7.65 (m, 2H), 7.97 – 8.00 (m, 2H)

^{13}C NMR δ ($CDCl_3$, 100 MHz): 12.7, 24.4, 16.3, 34.7, 36.1, 41.1, 115.7, 126.3, 129.8 (2 x C), 129.9, 132.0, 132.1, 133.53, 133.59, 144.2, 146.2, 155.3, 173.1, 185.0, 185.2

IR V_{max}: 3365 (N-H), 3306 (-OH), 2935, 1654 (C=O), 1616, 1595, 1541, 1516, 1375, 1330, 1296, 715 cm^{-1}

HRMS [M+Na]: For $C_{23}H_{23}N_1O_4Na$, predicted 400.1519, found 400.1510

***N*-(3,4-dimethoxyphenethyl)-4-(3-methyl-1,4-naphthoquinone-2-yl) butanamide** (**80**)

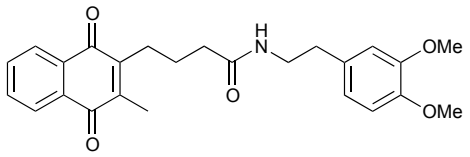

80 was prepared according to general procedure B from 4-(3-Methyl-1,4-naphthalen-2-yl)-butanoic acid (**32**) (188 mg, 0.7260 mmol) and 3,4-dimethoxyphenylethylamine (147 mg, 0.8088 mmol) and the product purified by flash chromatography (90 % ethyl acetate/hexanes) to give **80** as pale orange crystalline solid in 38 % yield (117 mg, 0.2776 mmol) with a melting point of 105 – 108 °C.

^{1}H NMR δ ($CDCl_3$, 400 MHz): 1.77 (quin, *J* = 7.2 Hz, 2H), 2.16 (S, 3H), 2.22 (t, *J* = 7.2 Hz, 2H), 2.58 – 2.62 (m, 2H), 2.74 (t, *J* = 7.2 Hz, 2H), 3.46 – 3.51 (m, 2H), 3.79 (s, 3H), 3.81 (s, 3H), 5.94 (t, *J* = 5.6 Hz, 1H), 6.68 – 6.76 (m, 3H), 7.63 – 7.66 (m, 2H), 7.98 – 8.02 (m, 2H)

^{13}C NMR δ ($CDCl_3$, 100 MHz): 12.7, 24.3, 26.3, 35.2, 36.1, 40.7, 55.8, 55.9, 111.4, 111.9, 120.7, 126.25, 126.29, 131.4, 132.0, 132.1, 133.4, 133.5, 144.0, 146.2, 147.7, 149.0, 172.3, 184.8, 185.1

IR V_{max}: 3377 N-H), 3296, 2935, 1656 (C=O), 1595, 1516, 1462, 1329, 1294, 1261, 1236, 1157, 1141, 1028, 717 cm^{-1}

HRMS [M+Na]: For $C_{25}H_{27}N_1O_5Na$, predicted 444.1781, found 444.1773

4-(3-methyl-1,4-naphthoquinone-2-yl)-*N*-phenethylbutanamide (**81**)

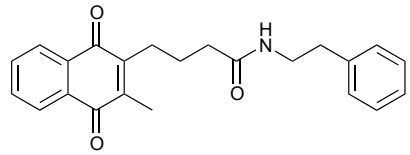

81 was prepared according to general procedure B from 4-(3-Methyl-1,4-naphthalen-2-yl)-butanoic acid (**32**) (179 mg, 0.6942 mmol) and phenethylamine (98 mg, 0.8088 mmol) and the product purified by flash chromatography (70 % ethyl acetate/hexanes) to give **81** as yellow solid in 59 % yield (148 mg, 0.4086 mmol) with a melting point of 106 – 107 °C.

^{1}H NMR δ ($CDCl_3$, 400 MHz): 1.80 (quin, *J* = 7.3 Hz, 2H), 2.20 (s, 3H), 2.25 (t, *J* = 7.3 Hz, 2H), 2.62 – 2.66 (m, 2H), 2.85 (t, *J* = 7.0 Hz, 2H), 3.53 – 3.58 (m, 2H), 5.92 (bs, 1H),7.20 – 7.23 (m, 3H), 7.28 – 7.32 (m, 2H), 7.67 (m, 2H), 7.71 (m, 2H), 8.03 – 8.09 (m, 2H)

^{13}C NMR δ ($CDCl_3$, 100 MHz): 12.8, 24.4, 26.4, 35.7, 36.1, 40.7, 126.3, 126.4, 126.6, 128.7 (2 x C), 128.8 (2 x C), 132.1, 132.2, 133.5, 133.6, 138.9, 144.2, 146.3, 172.4, 185.0, 185.2

IR V_{max}: 3298 (N-H), 3064, 2933, 1714 (C=O), 1653 (C=O), 1595, 1541, 1456, 1377, 1329, 1294, 717 cm^{-1}

***N*-(2-(1*H*-indol-3-yl)ethyl)-4-(3-methyl-1,4-naphthoquinone-2-yl) butanamide** (**82**)

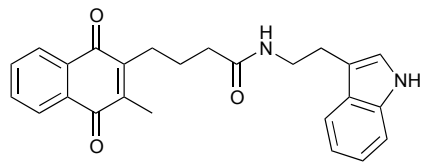

82 was prepared according to general procedure B from 4-(3-Methyl-1,4-naphthalen-2-yl)-butanoic acid (**32**) (194 mg, 0.7507 mmol) and tryptamine

(124 mg, 0.7708 mmol) and the product purified by flash chromatography (80 % ethyl acetate/hexanes) to give **82** as a brown viscous oil in 42 % yield (127 mg, 0.3178 mmol).

^{1}H NMR δ ($CDCl_3$, 400 MHz): 1.77 (quin, *J* = 7.4 Hz, 2H), 2.14 (s, 3H), 2.22 (t, *J* = 7.4 Hz, 2H), 2.57 – 2.61 (m, 2H), 2.97 (t, *J* = 6.8 Hz, 2H), 3.58 – 3.63 (m, 2H), 6.13 (t, *J* = 5.2 Hz, 1H), 7.01 (bs, 1H), 7.04 – 7.08 (m, 1H), 7.11 – 7.15 (m, 1H), 7.32 (d, *J* = 8.0 Hz, 1H), 7.56 (d, *J* = 8.0 Hz, 1H), 7.64 – 7.67 (m, 2H), 7.99 – 8.04 (m, 2H), 8.69 (bs, 1H)

^{13}C NMR δ ($CDCl_3$, 100 MHz): 12.7, 24.3, 25.2, 26.3, 36.1, 39.9, 111.4, 112.7, 118.6, 119.3, 122.0, 122.2, 126.2 (2 x C), 127.3, 132.02, 132.09, 133.42, 133.47, 136.4, 143.9, 146.2, 172.6, 184.8, 185.1

IR V_{max}: 3392 (N-H), 3294, 2935, 1705 (C=O), 1653 (C=O), 1595, 1527, 1458, 1332, 1296, 740, 715 cm^{-1}

(2*S*,4*R*)-methyl-4-hydroxy-1-(4-(3-methyl-1,4-dioxo-1,4-dihydronaphthalen-2-yl)butanoyl)pyrrolidine-2-carboxylate (**83**)

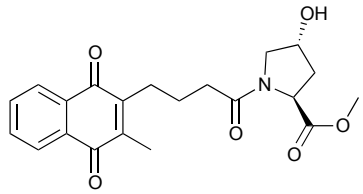

83 was prepared according to general procedure B from 4-(3-Methyl-1,4-naphthalen-2-yl)-butanoic acid (**32**) (143 mg, 0.5536 mmol) and *trans*-4-Hydroxy-L-proline methyl ester.HCl (103 mg, 0.5693 mmol) and the product purified by flash chromatography (90 % ethyl acetate/hexanes) to give **83** as yellow viscous oil in 59 % yield (126 mg, 0.3256 mmol).

^{1}H NMR δ ($CDCl_3$, 400 MHz): 1.77 – 1.85 (m, 2H), 2.05 (ddd, *J* = 13.3, 8.1, 5.0 Hz, 1H), 2.18 (s, 3H), 2.25 – 2.31 (m, 1H), 2.41 (t, *J* = 7.2 Hz, 2H), 2.64 – 2.68 (t, *J* = 7.9 Hz, 2H), 3.47 (bs, 1H), 3.54 – 3.56 (m, 1H), 3.69 (s, 3H), 3.73 – 3.76 (m, 1H), 4.56 (t, *J* = 8.0 Hz, 2H), 7.63 – 7.67 (m, 2H), 7.99 – 8.04 (m, 2H)

^{13}C NMR δ ($CDCl_3$, 100 MHz): 12.8, 23.5, 26.3, 34.0, 37.8, 52.4, 55.3, 57.7, 70.3, 126.3 (2 x C, 132.1, 132.2, 133.4, 133.5, 144.2, 146.5, 172.0, 172.8, 184.9, 185.3

$[\alpha]_D^{20}$: -58.57° (*c* 1.33, $CHCl_3$)

IR V_{max}: 3396 (N-H), 2951, 1747 (C=O), 1716 (C=O), 1653 (C=O), 1622, 1595, 1456, 1437, 1327, 1296, 1199, 1084, 717 cm^{-1}

(*S*)-methyl-3-hydroxy-2-(4-(3-methyl-1,4-naphthoquinone-2-yl)butanamido)propanoate (**84**)

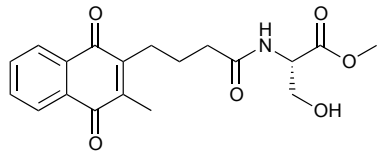

84 was prepared according to general procedure B from 4-(3-Methyl-1,4-naphthalen-2-yl)-butanoic acid (**32**) (149 mg, 0.5777 mmol) and L-serine methyl ester.HCl (98 mg, 0.6286 mmol) and the product purified by flash chromatography (100 % ethyl acetate) to give **84** as yellow crystalline needles in 53 % yield (110 mg, 0.3069 mmol) with a melting point of 94 – 98 °C.

^{1}H NMR δ ($CDCl_3$, 400 MHz): 1.78 – 1.94 (m, 2H), 2.21 (s, 3H), 2.37 (td, *J* = 7.0, 2.7 Hz, 2H), 2.46 (bs, 1H), 2.62 – 2.77 (m, 2H), 3.79 (s, 3H), 4.02 (d, *J* = 3.5 Hz, 2H), 4.70 (dt, *J* = 7.1, 3.5 Hz, 1H), 6.64

(d, *J* = 7.1 Hz, 1H), 7.68 – 7.70 (m, 2H), 8.03 – 8.08 (m, 2H)

^{13}C NMR δ ($CDCl_3$, 100 MHz): 12.8, 24.2, 26.1, 35.8, 53.9, 54.9, 63.4, 126.4, 126.5, 132.0, 132.2, 133.6, 133.7, 144.5, 146.3, 171.1, 172.7, 185.2, 185.3

$[\alpha]_D^{20}$: +6.17 ° (*c* 0.75, $CHCl_3$)

IR V_{max}: 3280 (N-H), 2955, 1734 (C=O), 1716 (C=O), 1645 (C=O), 1616, 1558, 1521, 1506, 1456, 1338, 1296 cm^{-1}

(2*S*,3*S*)-methyl-3-hydroxy-2-(4-(3-methyl-naphthoquione-2-yl)butanamido)butanoate (**85**)

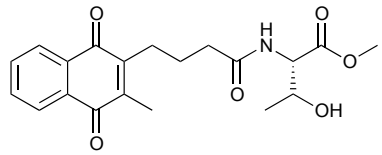

85 was prepared according to general procedure B from 4-(3-Methyl-1,4-naphthalen-2-yl)-butanoic acid (**32**) (151 mg, 0.5827 mmol) and L-threonine methyl ester.HCl (103 mg, 0.6102 mmol) and the product purified by flash chromatography (90 % ethyl acetate/hexane) to give **85** as yellow crystalline solid in 39 % yield (84 mg, 0.2252 mmol) with a melting point of 50 – 52 °C.

^{1}H NMR δ ($CDCl_3$, 400 MHz): 1.25 (d, *J* = 6.5 Hz, 3H), 1.81 – 1.89 (m, 2H), 2.20 (s, 3H), 2.39 (t, *J* = 7.1 Hz, 2H), 2.67 – 2.72 (m, 2H), 3.76 (s, 3H), 4.36 (dq, *J* = 6.5, 2.5 Hz, 1H), 4.63 (dd, *J* = 8.8, 2.5 Hz, 1H), 6.50 (d, *J* = 8.8 Hz, 1H), 7.67 – 7.70 (m, 2H), 8.02 – 8.08 (m, 2H)

^{13}C NMR δ ($CDCl_3$, 100 MHz): 12.8, 20.2, 24.3, 26.3, 36.0, 52.6, 57.4, 68.1, 126.3, 126.4, 132.0, 132.2, 133.5, 133.6, 144.2, 146.3, 171.7, 173.0, 185.0, 185.2

$[\alpha]_D^{20}$: -2.42° (*c* 1.60, $CHCl_3$)

IR V_{max}: 3358 (N-H), 2974, 1743 (C=O), 1658 (C=O), 1595, 1529, 1437, 1379, 1329, 1294, 1209, 717 cm^{-1}

_N_-butyl-4-(3-methyl-1,4-naphthoquione-2-yl)butanamide (**86**)

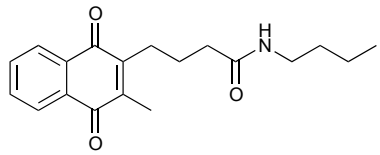

86 was prepared according to general procedure B from 4-(3-Methyl-1,4-naphthalen-2-yl)-butanoic acid (**32**) (149 mg, 0.5533 mmol) and butylamine (67 mg, 0.9106 mmol) and the product purified by flash chromatography (70 % ethyl acetate/hexanes) to give **86** as yellow solid in 40 % yield (73 mg, 0.2336 mmol) with a melting point of 136 – 138 °C.

^1H NMR δ ($CDCl_3$, 400 MHz): 0.91 (t, *J* = 7.3 Hz, 3H), 1.35 (sextet, *J* = 7.3 Hz, 2H), 1.49 (quin, *J* = 7.3 Hz, 2H), 1.83 (quin, *J* = 7.3 Hz, 2H), 2.21 (s, 3H), 2.27 (t, *J* = 7.3 Hz, 2H), 2.65 – 2.69 (m, 2H), 3.24 – 3.29 (m, 2H), 5.78 (bs, 1H), 7.67 – 7.69 (m, 2H), 8.04 – 8.08 (m, 2H)

^{13}C NMR δ ($CDCl_3$, 100 MHz): 12.8, 13.8, 20.2, 24.5, 26.5, 31.8, 36.2, 39.4, 126.40, 126.43, 132.2, 132.3, 133.5, 133.6, 144.2, 146.4, 172.2, 185.1, 185.2

IR V_{max}: 3302 (N-H), 2931, 2862, 1660 (C=O), 1639, 1595, 1554, 1458, 1323, 1296, 717 cm^{-1}

(*S*)-methy-2-hydroxy-4-(4-(3-methyl-1,4-naphthoquinone-2-yl)butanamido)butanoate (**87**)

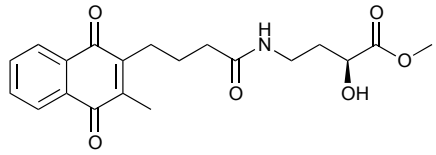

87 was prepared according to general procedure B from 4-(3-Methyl-1,4-naphthalen-2-yl)-butanoic acid (**32**) (153 mg, 0.5905 mmol) and (R)-2-hydroxy-4-aminobutyric acid methyl ester.HCl (103 mg, 0.6073 mmol) and the product purified by a Reveleris ® X2 automated flash chromatography system (Eluent: gradient 50 – 80% ethyl acetate/hexanes, Column: Reveleris ® Silica 4 g, Flow rate: 18 mL/min) to give **87** as a bright yellow oil in 16 % yield (34 mg, 0.0921 mmol).

^{1}H NMR δ ($CDCl_3$, 400 MHz): 1.74 – 1.81 (m, 2H), 2.16 (s, 3H), 2.28 (t, *J* = 7.2 Hz, 2H), 2.60 – 2.64 (m, 2H), 3.32 – 3.39 (m, 2H), 3.47 – 3.53 (m, 2H), 3.73 (s, 3H), 4.25 (dd, *J* = 8.8, 3.7 Hz, 1H), 6.54 (t, *J* = 5.7 Hz, 1H), 7.64 – 7.67 (m, 2H), 7.99 – 8.03 (m, 2H)

^{13}C NMR δ ($CDCl_3$, 100 MHz): 12.7, 24.3, 26.4, 33.7, 36.0, 36.2, 52.6, 69.0, 126.3 (2 x C), 132.0, 132.1, 133.5, 133.6, 144.2, 146.2, 173.4, 174.0, 185.0, 185.1

$[\alpha]_D^{20}$: -2.47. ° (*c* 0.97, $CHCl_3$)

IR V_{max}: 3367 (N-H), 3306, 2953, 2929, 1739 (C=O), 1658 (C=O), 1595, 1539, 1456, 1437, 1329, 1294, 1215, 1122, 846, 717 cm^{-1}

3-(3-methyl-1,4-naphthoquinone-2-yl)propanoic acid (**31**)

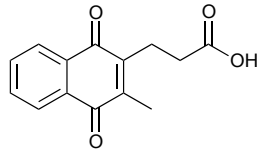

31 was prepared according to general procedure A from menadione (**12**) (1.995 g, 11.59 mmol) and succinic acid (2.757 g, 23.34 mmol) and the product purified by flash chromatography (100% dichloromethane followed by 100% ethyl acetate) to give **31** as a crystalline yellow solid in 20 % yield (0.5607 g, 2.296 mmol) with a melting point of 68 – 72 °C.

^{1}H NMR δ ($CDCl_3$, 400 MHz): 2.23 (s, 3H), 2.60 (t, *J* = 7.9 Hz, 2H), 2.98 (t, *J* = 7.9 Hz, 2H), 7.69 – 7.71 (m, 2H), 8.06 – 8.09 (m, 2H)

^{13}C NMR δ ($CDCl_3$, 100 MHz): 12.9, 22.7, 32.6, 126.5, 126.5, 132.2, 132.3, 133.75, 133.76, 144.7, 144.9, 177.8, 184.6, 185.2

IR V_{max}: 2932 (-OH), 1738 (C=O), 1706 (C=O), 1658 1595, 1379, 1330, 1296, 716

5-(3-methyl-1,4-naphthoquinone-2-yl)pentanoic acid (**88**)

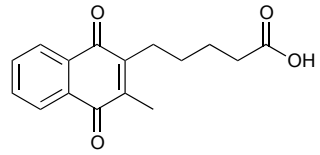

88 was prepared according to general procedure A from menadione (**12**) (2.164 g, 12.566 mmol) and adipic acid (3.724 g, 25.484 mmol) and the product purified by flash chromatography (100% dichloromethane followed by 100% ethyl acetate) to give **88** as a crystalline yellow solid in 78 % yield (2.653 g, 9.7422 mmol) with a melting point of 66 – 70 °C.

^{1}H NMR δ ($CDCl_3$, 400 MHz): 1.49 – 1.57 (m, 2H), 1.70 – 1.77 (m, 2H), 2.17 (s, 3H), 2.40 (t, *J* = 7.4 Hz, 2H), 2.64

(t, *J* = 7.9 Hz, 2H), 7.66 – 7.68 (m, 2H), 8.03 – 8.05 (m, 2H)

^{13}C NMR δ ($CDCl_3$, 100 MHz): 12.7, 24.9, 26.7, 28.1, 33.8, 126.3, 126.4, 132.20, 132.21, 133.4, 133.5, 143.5, 146.8, 179.6, 184.7, 185.3

IR V_{max}: 2939 (-OH), 1705 (C=O), 1658 (C=O), 1618, 1595, 1379, 1327, 1294, 1261, 715 cm^{-1}

6-(3-methyl-1,4-naphthoquinone-2-yl)hexanoic acid (**89**)

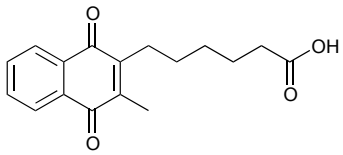

89 was prepared according to general procedure A from menadione (**12**) (2.010 g, 11.676 mmol) and pimelic acid (3.720 g, 23.229 mmol) and the product purified by flash chromatography (100% dichl;oromethane followed by 100% ethyl acetate) to give **89** as a crystalline yellow solid in 57 % yield (1.921 mg, 6.710 mmol) with a melting point of 49 – 51 °C.

^{1}H NMR δ ($CDCl_3$, 400 MHz): 1.45 – 1.51 (m, 4H), 1.69 (quin, *J* = 7.4 Hz, 2H), 2.18 (s, 3H), 2.36 (t, *J* = 7.4 Hz, 2H), 2.63 (t, *J* = 7.4 Hz, 2H), 7.66 – 7.69 (m, 2H), 8.05 – 8.07 (m, 2H)

^{13}C NMR δ ($CDCl_3$, 100 MHz): 12.7, 24.5, 26.9, 28.4, 29.4, 33.9, 126.3, 126.4 132.2, 132.3, 133.46, 133.49, 143.4, 147.2, 179.6, 184.8, 185.4

IR V_{max}: 2937 (-OH), 1707 (C=O), 1658 (C=O), 1595, 1327, 1294, 1259, 715 cm^{-1}

(*S*)-*tert*-butyl-2-(3-(3-methyl-1,4-naphthoquinone-2-yl)propanamido)-3-phenylpropanoate (**90**)

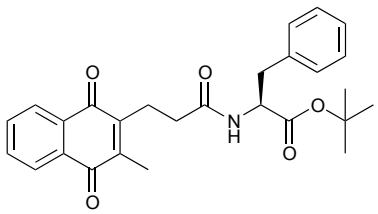

90 was prepared according to general procedure B from 3-(3-Methyl-1,4-naphthalen-2-yl)-propanoic acid (**31**) (119 mg, 0.4876 mmol) and L-phenylalanine *t*-butyl ester.HCl (115 mg, 0.4462 mmol) and the product purified by flash chromatography (30 % ethyl acetate/hexanes) to give **90** as yellow oil in 22 % yield (45 mg, 0.0997 mmol).

^{1}H NMR δ ($CDCl_3$, 400 MHz):	1.37 (s, 9H), 2.94 (s, 3H), 2.37 – 2.41 (m, 2H), 2.92 (t, *J* = 7.8 Hz, 2H), 3.05 (d, *J* = 6.1 Hz, 2H), 4.71 – 4.76 (m, 1H), 6.08 (d, *J* = 7.7 Hz, 1H), 7.09 – 7.21 (m, 5H), 7.66 – 7.68 (m, 2H), 8.02 – 8.05 (m, 2H)
^{13}C NMR δ ($CDCl_3$, 100 MHz):	12.8, 23.4, 28.0, 34.9, 38.1, 53.5, 82.4, 126.33, 126.39, 127.0, 128.4 (2 x C), 129.5 (2 x C), 132.1, 132.2, 133.50, 133.54, 136.2, 144.5, 145.4, 170.7, 171.0, 184.7, 185.0
$[\alpha]_D^{20}$:	+29.91° (*c* 0.54, $CHCl_3$)
IR V_{max}:	3365 (N-H), 2978, 1732(C=O), 1718 (C=O), 1660 (C=O), 1595, 1521, 1456, 1367, 1294, 1153, 700 cm^{-1}

(*S*)-2-(3-(3-methyl-1,4-naphthoquinone-2-yl)propanamido)-3-phenyl propanoic acid (**91**)

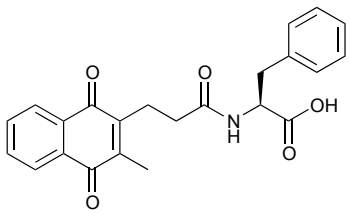

91 was prepared from the deprotection of **90** (18 mg, 0.0407 mmol), using general procedure C. The product purified by flash chromatography (5 % methanol/ethyl acetate) to give **91** as a yellow oil in 80 % yield (13 mg, 0.0327 mmol).

^{1}H NMR δ (CD_3OD, 400 MHz):	2.08 (s, 3H), 2.37 (td, *J* = 7.6, 3.5 Hz, 2H), 2.82 (t, *J* = 7.6 Hz, 2H), 2.89 (dd, *J* = 13.9, 9.3 Hz, 1H), 3.17 (dd, *J* = 13.9, 4.9 Hz, 1H), 4.64 (dd, *J* = 9.3, 5.0 Hz, 1H), 7.11 – 7.17 (m, 5H), 7.72 – 7.75 (m, 2H), 8.00 – 8.02 (m, 2H)
^{13}C NMR δ (CD_3OD, 100 MHz):	12.7, 24.3, 35.1, 38.4, 55.0, 127.0, 127.7, 129.3 (2 x C), 130.1 (2 x C), 133.4, 134.590, 134.598, 138.4, 145.5, 146.4, 174.4, 185.6, 186.1
$[\alpha]_D^{20}$:	-3.95 ° (*c* 0.45, $CHCl_3$)
IR V_{max}:	3306 (N-H), 2926, 1732 (C=O), 1714 (C=O), 1658 (C=O), 1595, 1454, 1330, 1296, 1195, 734, 702 cm^{-1}

(*S*)-*tert*-butyl-2-(5-(3-methyl-1,4-naphthoquinone-2-yl)pentanamido)-3-phenylpropanoate (**92**)

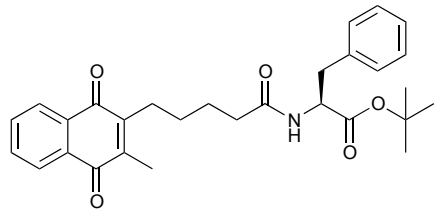

92 was prepared according to general procedure B from 5-(3-methyl-1,4-naphthoquinone-2-yl)pentanoic acid (**88**) (205 mg, 0.7525 mmol) and L-phenylalanine *t*-butyl ester.HCl (188 mg, 0.7308 mmol) and the product purified by flash chromatography (40 % ethyl acetate/hexanes) to give **92** as bright yellow oil in 69 % yield (240 mg, 0.5055 mmol).

^{1}H NMR δ ($CDCl_3$, 400 MHz): 1.35 (s, 9H), 1.39 - 1.47 (m, 2H), 1.67 (quin, *J* = 7.5 Hz, 2H), 2.11 (s, 3H), 2.20 (t, *J* = 7.5 Hz, 2H), 2.58 (t, *J* = 7.9 Hz, 2H), 2.98 – 3.08 (m, 2H), 4.70 – 4.75 (m, 1H), 6.09 (d, *J* = 7.6 Hz, 1H), 7.09 – 7.12 (m, 5H), 7.60 – 7.64 (m, 2H), 7.98 – 8.02 (m, 2H)

^{13}C NMR δ ($CDCl_3$, 100 MHz): 12.6, 25.6, 26.5, 27.9 28.0, 36.0, 38.0, 53.4, 82.2, 126.1, 126.2, 126.8, 128.3 (2 x C), 129.4 (2 x C), 132.11, 132.12, 133.3 (2 x C), 136.2, 143.4, 146.8, 170.8, 172.1, 184.6, 185.1

$[\alpha]_D^{20}$: +37.83° (*c* 0.92, $CHCl_3$)

IR V_{max}: 3306 (N-H), 2978, 2933, 1732 (C=O), 1658 (C=O), 1595, 1531, 1367, 1329, 1257, 1294, 1155, 715 cm^{-1}

(*S*)-2-(5-(3-methyl-1,4-naphthoquinone-2-yl)pentanamido)-3-phenylpropanoic acid (**93**)

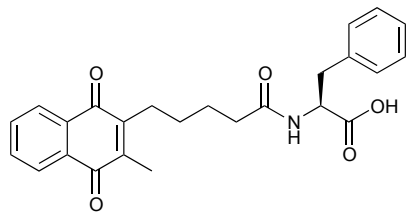

93 was prepared from the deprotection of **92** (215 mg, 0.4517 mmol), using general procedure C. The product purified by flash chromatography (35 % ethyl acetate/hexane) to give **93** as a brown oil in 85 % yield (161 mg, 0.3843 mmol).

^{1}H NMR δ (CD_3OD, 400 MHz): 1.26 – 1.40 (m, 2H), 1.58 (quin, *J* = 7.6 Hz, 2H), 2.09 (s, 3H), 2.17 – 2.22 (m, 2H), 2.55 (t, *J* = 7.9 Hz, 2H), 2.90 (dd, *J* = 14.0, 9.6 Hz, 1H), 3.19 (dd, *J* = 14.0, 4.8 Hz, 1H), 4.67 (dd, *J* = 9.6, 4.8 Hz, 2H), 7.14 – 7.21 (m, 5H), 7.70 – 7.74 (m, 2H), 7.99 – 8.02 (m, 2H)

^{13}C NMR δ (CD_3OD, 100 MHz): 12.7, 26.9, 27.4, 28.9, 36.4, 38.3, 54.8, 127.0, 127.1, 127.6, 129.3 (2 x C), 130.1 (2 x C), 133.40, 133.42, 134.5 (2 x C), 138.5, 144.5, 148.0, 174.7, 175.7, 185.7, 186.3

$[\alpha]_D^{20}$: +25.16° (*c* 1.06, $CHCl_3$)

IR V_{max}: 3316 (N-H), 2939, 1734 (C=O), 1716 (C=O), 1656 (C=O), 1595, 1525, 1456, 1294, 1190, 736, 702 cm^{-1}

(*S*)-*N*-(1-hydroxy-3-phenylpropan-2-yl)-5-(3-methyl-1,4-naphthoquinone-2-yl)pentanamide (**94**)

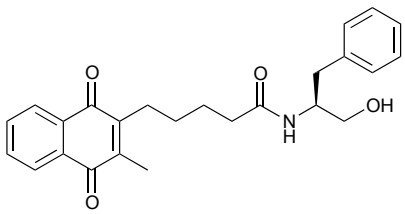

94 was prepared according to general procedure B from 5-(3-methyl-1,4-naphthoquinone-2-yl)pentanoic acid (**88**) (149 mg, 0.5483 mmol) and L-phenylalaninol (88 mg, 0.5800 mmol) and the product purified by flash chromatography (2 % methanol/ethyl acetate) to give **94** as bright yellow/brown oil in 59 % yield (131 mg, 0.3236 mmol).

^{1}H NMR δ ($CDCl_3$, 400 MHz): 1.43 (quin, *J* = 7.7 Hz, 2H), 1.66 – 1.75 (m, 2H), 2.17 (s, 3H), 2.24 – 2.28 (m, 2H), 2.56 – 2.64 (m, 2H), 2.83 – 2.94 (m, 2H), 3.39 (bs, 1H), 3.58 (dd, *J* = 11.2, 5.1 Hz, 1H), 3.70 (dd, *J* = 11.2, 3.5 Hz, 2H), 4.19 – 4.23 (m, 1H), 6.26 (d, *J* = 7.7 Hz, 1H), 7.15 – 7.28 (m, 5H), 7.68 – 7.72 (m, 2H), 8.03 – 8.09 (m, 2H)

^{13}C NMR δ ($CDCl_3$, 100 MHz): 12.8, 25.8, 26.5, 27.7, 36.0, 37.0, 53.0, 64.1, 126.32, 126.39, 126.6, 128.6 (2 x C), 129.2 (2 x C), 132.1, 132.2, 133.5, 133.6, 137.7, 143.7, 146.7, 173.7, 185.0, 185.2

$[\alpha]_D^{20}$: -16.60° (*c* 2.12, $CHCl_3$)

IR V_{max}: 3296 (N-H), 2935, 1656 (C=O), 1595, 1531, 1456, 1377, 1329, 1294, 702 cm^{-1}

***N*-(4-hydroxyphenethyl)-5-(3-methyl-1,4-naphthoquinone-2-yl)pentanamide** (**95**)

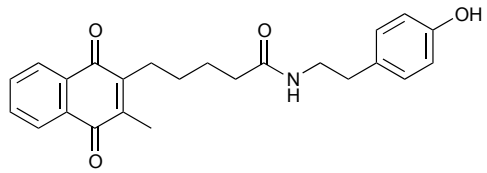

95 was prepared according to general procedure B from 5-(3-methyl-1,4-naphthoquinone-2-yl)pentanoic acid (**88**) (159 mg, 0.5831 mmol) and tyramine (77 mg, 0.5628 mmol) and the product purified by flash chromatography (85 % ethyl acetate/hexanes) to give **95** as orange solid in 20 % yield (45 mg, 0.1137 mmol) with a melting point of 136 – 138 °C.

^{1}H NMR δ (CD_3OD, 400 MHz): 1.42 – 1.50 (m, 2H), 1.66 (quin, *J* = 7.5 Hz, 2H), 2.15 (s, 3H), 2.19 (t, *J* = 7.3 Hz, 2H), 2.62 – 2.68 (m, 4H), 3.33 (t, *J* = 7.2 Hz, 2H), 6.67 (d, *J* = 8.5 Hz, 2H), 7.00 (d, *J* = 8.5 Hz, 2H), 7.72 – 7.74 (m, 2H), 8.01 – 8.04 (m, 2H)

^{13}C NMR δ (CD_3OD, 100 MHz): 12.7, 27.1, 27.4, 29.1, 35.6, 36.8, 42.2, 116.1, 127.0, 127.1, 130.7 (2 x C), 131.2, 133.4, 134.5 (2 x C), 144.6, 148.0, 156.8, 175.8, 185.8, 186.3

IR V_{max}: 3369 (N-H), 3296, 2937, 1755 (C=O), 1693 (C=O), 1653 (C=O), 1616, 1595, 1516, 1329, 1294, 1197, 734, 715 cm^{-1}

***N*-(3,4-dimethoxyphenethyl)-5-(3-methyl-1,4-naphthoquinone-2-yl)pentanamide** (**96**)

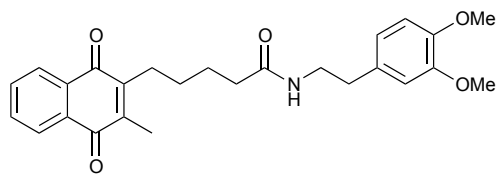

96 was prepared according to general procedure B from 5-(3-methyl-1,4-naphthoquinone-2-yl)pentanoic acid (**88**) (170 mg, 0.6243 mmol) and 3,4-dimethoxyphenylethylamine (105 mg, 0.5777 mmol) and the product purified by flash chromatography (90 % ethyl acetate/hexanes) to give **96** as bright yellow solid in 35 % yield (95 mg, 0.2170 mmol) with a melting point of 106 – 108 °C.

^{1}H NMR δ ($CDCl_3$, 400 MHz): 1.46 (quin, *J* = 7.5 Hz, 2H), 1.70 (quin, *J* = 7.6 Hz, 2H), 2.14 (s, 3H), 2.18 (t, *J* = 7.5 Hz, 2H), 2.58 – 2.62 (m, 2H), 2.73 (t, *J* = 7.1 Hz, 2H), 3.44 – 3.49 (m, 2H), 3.80 (s, 3H), 3.82 (s, 3H), 5.75 (t, *J* = 5.4 Hz, 1H), 6.66 – 6.68 (m, 2H), 6.73 – 6.73 (m, 1H), 7.64 – 7.67 (m, 2H), 7.99 – 8.04 (m, 2H)

^{13}C NMR δ ($CDCl_3$, 100 MHz): 12.7, 25.8, 26.5, 28.0, 35.3, 36.3, 40.7, 55.90, 55.94, 111.3, 111.8, 120.6, 126.25, 126.29, 131.4, 132.14, 132.17, 133.43, 133.47, 143.5, 146.8, 147.7, 149.0, 172.8, 184.7, 185.2

IR V_{max}: 3381 (N-H), 3292, 2935, 1658 (C=O), 1595, 1516, 1462, 1329, 1294, 1261, 1236, 1157, 1141, 1028, 715 cm^{-1}

(*S*)-*tert*-butyl-2-(6-(3-methyl-1,4-naphthoquinone-2-yl)hexanamido)-3-phenylpropanoate (**97**)

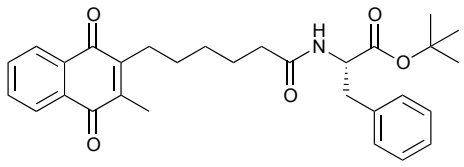

97 was prepared according to general procedure B from 6-(3-methyl-1,4-naphthoquinone-2-yl)hexanoic acid (**89**) (240 mg, 0.8396 mmol) and L-phenylalanine *t*-butyl ester.HCl (180 mg, 0.7001 mmol) and the product

purified by flash chromatography (40 % ethyl acetate/hexanes) to give **97** as yellow oil in 48 % yield (166 mg, 0.3383 mmol).

^{1}H NMR δ ($CDCl_3$, 400 MHz): 1.40 (s, 9H), 1.41 – 1.47 (m, 4H), 1.64 (quin, *J* = 7.5 Hz, 2H), 2.16 (s, 3H), 2.18 – 2.29 (m, 2H), 2.60 (t, *J* = 7.8 Hz, 2H), 3.02 – 3.10 (m, 2H), 4.73 – 4.78 (m, 1H), 6.05 (d, *J* = 7.7 Hz, 1H), 7.13 – 7.15 (m, 2H), 7.21 – 7.28 (m, 3H), 7.65 – 768 (m, 2H), 8.03 – 8.06 (m, 2H)

^{13}C NMR δ ($CDCl_3$, 100 MHz): 12.6, 25.2, 26.8, 27.9, 28.3, 29.4, 36.3, 38.1, 53.3, 82.3, 126.20, 126.28, 126.9, 128.3 (2 x C), 129.5 (2 x C), 132.17, 132.19, 133.32, 133.35, 134.18, 136.3, 143.2, 147.2, 170.9, 172.3, 184.6, 185.3

$[\alpha]_D^{20}$: +23.33° (*c* 0.66, $CHCl_3$)

IR V_{max}: 3290 (N-H), 2978, 2933, 1734 (C=O), 1718 (C=O), 1695 (C=O), 1653, 1595, 1521, 1456, 1369, 1294, 1155, 702 cm^{-1}

(*S*)-2-(6-(3-methyl-1,4-naphthoquinone-2-yl)hexanamido)-3-phenylpropanoic acid (**98**)

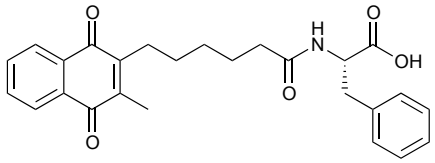

98 was prepared from the deprotection of **97** (166 mg, 0.3382 mmol), using general procedure C. The product purified by precipitation from dichloromethane and the solvent was decanted to give **98** as brown solid in 84 % yield (124 mg, 0.2854 mmol) with a melting point of 72 – 76 °C.

^{1}H NMR δ (CD_3OD, 400 MHz): 1.30 – 1.35 (m, 2H), 1.39 – 1.46 (m, 2H), 1.56 (quin, *J* = 7.5 Hz, 2H), 2.16 (s, 3H),

2.17 – 2.20 (m, 2H), 2.58 – 2.62 (m, 2H), 2.93 (dd, *J* = 14.0, 9.5 Hz, 1H), 3.22 (dd, *J* = 14.0, 4.9 Hz, 1H), 4.69 (dd, *J* = 9.5, 4.9 Hz, 1H), 7.20 – 7.28 (m, 5H), 7.74 – 7.76 (m, 2H), 8.03 – 8.05 (m, 2H)

^{13}C NMR δ (CD_3OD, 100 MHz): 12.7, 26.5, 27.6, 29.3, 30.2, 36.5, 38.4, 54.8, 127.02, 127.09, 127.7, 129.4, 130.2, 133.46, 133.49, 134.57, 134.58, 138.5, 144.4, 148.3, 174.7, 175.9, 185.8, 186.3

$[\alpha]_D^{20}$: +24.71 ° (*c* 0.78, $CHCl_3$)

IR V_{max}: 3288 (N-H), 2937, 1732 (C=O), 1716 (C=O), 1660 (C=O), 1595, 1531, 1456, 1377, 1330, 1294, 1172, 736, 702 cm^{-1}

(*S*)-*N*-(1-hydroxy-3-phenylpropan-2-yl)-6-(3-methyl-1,4-naphthoquione-2-yl)hexanamide (**99**)

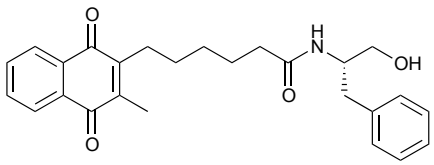

99 was prepared according to general procedure B from 6-(3-methyl-1,4-naphthoquinone-2-yl)hexanoic acid (**89**) (148 mg, 0.5176 mmol) and L-phenylalaninol (92 mg, 0.6071 mmol) and the product purified by flash chromatography (2 % methanol/ethyl acetate) to give **99** as yellow semi solid in 34 % yield (74 mg, 0.1759 mmol).

^{1}H NMR δ ($CDCl_3$, 400 MHz): 1.34 – 1.48 (m, 4H), 1.62 (quin, *J* = 7.4 Hz, 2H), 2.16 (s, 3H), 2.17 (t, *J* = 7.5 Hz, 2H), 2.56 – 2.60 (m, 2H), 2.78 (bs, 1H), 2.81 – 2.92 (m, 2H), 3.59 (dd, *J* = 11.1, 5.2 Hz, 1H), 3,69 (dd, *J* = 11.1, 3.5 Hz, 1H), 4.16 – 4.20 (m, 1H), 5.97 (d, *J* = 7.0 Hz, 1H), 7.19

– 7.23 (m, 3H), 7.27 - 7.31 (m, 2H), 7.67 – 7.70 (m, 2H), 8.03 – 8.07 (m, 2H)

^{13}C NMR δ ($CDCl_3$, 100 MHz): 12.8, 25.4, 26.9, 28.3, 29.3, 36.4, 37.1, 53.1, 64.4, 126.3, (2 x C), 126.8, 128.7, 129.3, 132.26, 132.28, 133.51, 133.53, 137.7, 143.4, 147.2, 174.1, 184.9, 185.4 cm^{-1}

$[\alpha]_D^{20}$: +15.15° (*c* 2.31, $CHCl_3$)

IR V_{max}: 3336 (N-H), 2935, 1695 (C=O), 1658 (C=O), 1595, 1541, 1456, 1377, 1329, 1296, 715, 702 cm^{-1}

***N*-(4-hydroxyphenethyl)-6-(3-methyl-1,4-naphthoquinone-2-yl) hexanamide** (**100**)

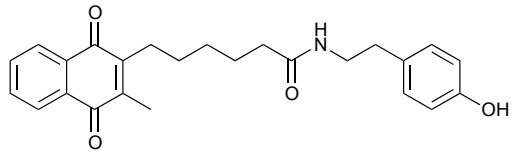

100 was prepared according to general procedure B from 6-(3-methyl-1,4-naphthoquinone-2-yl)hexanoic acid (**89**) (1367 mg, 0.4778 mmol) and tyramine (74 mg, 0.5423 mmol) and the product purified by flash chromatography (90 % ethyl acetate/hexanes) to give **100** as orange crystalline solid in 39 % yield (75 mg, 0.1842 mmol) with a melting point of 90 – 92 °C.

^{1}H NMR δ (CD_3OD, 400 MHz): 1.33 – 1.42 (m, 2H), 1.45 – 1.54 (m, 2H), 1.62 (quin, *J* = 7.4 Hz, 2H), 2.13 – 2.16 (m, 2H), 2.17 (s, 3H), 2.62 – 2.69 (m, 2H), 3.34 (t, *J* = 7.3 Hz, 2H), 6.68 – 6.70 (m, 2H), 6.99 – 7.03 (m, 2H), 7.72 – 7.78 (m, 2H), 8.02 – 8.05 M, 2H)

^{13}C NMR δ (CD_3OD, 100 MHz): 12.6, 26.6, 27.6, 29.2, 30.3, 35.7, 36.9, 42.0, 116.3, 127.00, 127.08, 130.6 (2 x C),

131.3, 133.55, 134.52, 134.54, 144.5, 148.4, 156.8, 175.9, 185.9, 186.4

IR V_{max}: 3369 (N-H), 3296, 2935, 1695 (C=O), 1654 (C=O), 1595, 1541, 1516, 1329, 1296, 734, 713 cm^{-1}

***N*-(3,4-dimethoxyphenethyl)-6-(3-methyl-1,4-naphthoquinone-2-yl)hexanamide** (**100**)

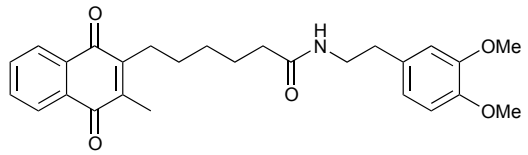

101 was prepared according to general procedure B from 6-(3-methyl-1,4-naphthoquinone-2-yl)hexanoic acid (**89**) (165 mg, 0.5773 mmol) and 3,4-dimethoxyphenyletheylamine (126 mg, 0.6932 mmol) and the product purified by flash chromatography (90 % ethyl acetate/hexanes) to give **101** as yellow solid in 60 % yield (155 mg, 0.3457 mmol) with a melting point of 98 – 100 °C.

^{1}H NMR δ ($CDCl_3$, 400 MHz): 1.39 – 1.48 (m, 4H), 1.65 (quin, *J* = 7.4 Hz, 2H), 2.14 (t, *J* = 7.7 Hz, 2H), 2.16 (s, 3H), 2.57 – 2.61 (m, 2H), 2.74 (t, *J* = 7.0 Hz, 2H), 3.46 – 3.51 (m, 2H), 3.83 (s, 3H), 3.84 (s, 3H), 5.61 (bs, 1H), 6.70 – 6.72 (m, 2H), 6.77 – 6.80 (m, 1H), 7.65 – 7.68 (m, 2H), 8.02 – 8.06 (m, 2H)

^{13}C NMR δ ($CDCl_3$, 100 MHz): 12.7, 25.4, 26.9, 28.3, 29.5, 35.3, 36.5, 40.7, 55.9, 56.0, 111.4, 112.0, 120.7, 126.31, 126.32, 131.4, 132.2, 133.44, 133.45, 143.3, 147.2, 147.8, 149.1, 173.0, 184.8, 185.3

IR V_{max}: 3369 (N-H), 3304, 2935, 1656 (C=O), 1595, 1516, 1456, 1329, 1294, 1261, 1236, 1028, 715 cm^{-1}

(*R*)-2-(4-(3-methyl-1,4-naphthoquinone-2-yl)butanamido)-3-phenylpropanoic acid (**105**)

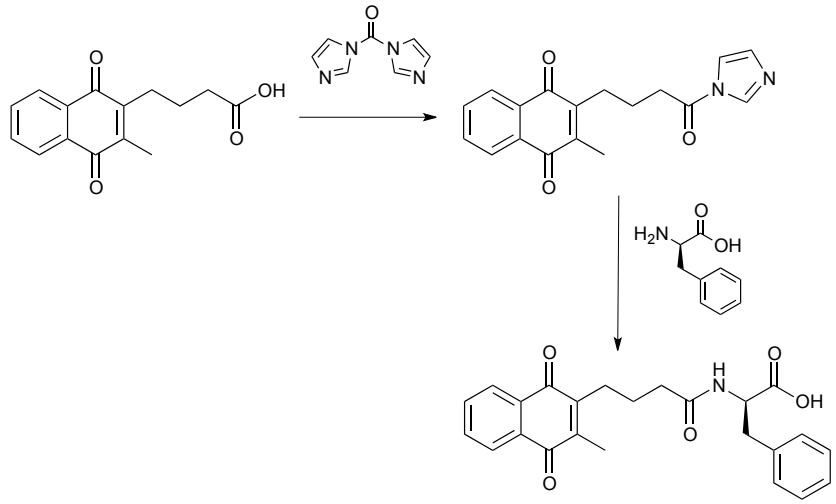

4-(3-Methyl-1,4-naphthalen-2-yl)-butanoic acid (**32**) (200 mg, 0.7736 mmol) was added to anhydrous dichloromethane (10 mL) under an atmosphere of N_2. Carbonyl diimidazole (145 mg, 0.8930 mmol) was added and the resulting mixture stirred for 3.5 h at room temperature. The reaction was quenched with H_2O (20mL) and the organic layer washed with H_2O (2 x 20 mL). The organic layer was dried with $MgSO_4$, filtered and the solvent removed under reduced pressure to give the crude intermediate **103** as a yellow oil (221.7 mg, 0.7190 mmol). To the crude intermediate in THF (5 mL) a solution of D-phenylalanine (650 mg, 3.937 mmol) and pyridine (0.28 mL, 3.6084 mmol) in H_2O (15 mL) was added and the reaction stirred under an atmosphere of nitrogen for 6 h. The reaction mixture was quenched with 20 mL 2M HCl and extracted DCM (3 x 20 mL) and the organic layer was dried with $MgSO_4$, filtered and the solvent removed under reduced pressure to give a crude product, which was purified by flash chromatography (7 % methanol/ethyl acetate) to give **105** as yellow oil in 14 % yield (44 mg, 0.1080 mmol).

(2-(4-(1*H*-imidazol-1-yl)-4-oxobutyl)-3-methylnaphthalene-1,4-dione)
Intermediate (**103**)

^{1}H NMR δ ($CDCl_3$, 400 MHz): 1.90 (quin, *J* = 7.6 Hz, 2H), 2.13 (s, 3H), 2.65 – 2.29 (m, 2H), 2.94 (t, *J* = 7.0 Hz, 2H), 6.99 (s, 1H), 7.40 (s, 1H), 7.57 – 7.60 (m, 2H), 7.90 – 7.93 (m, 2H), 8.10 (s, 1H)

^{13}C NMR δ ($CDCl_3$, 100 MHz): 12.5, 22.4, 25.8, 34.6, 126.1, 130.9, 131.7, 131.8, 133.3, 133.4, 144.0, 145.5, 168.9, 184.4, 184.8

IR V_{max}: 1738 (C=O), 1695 (C=O), 1658, 1595, 1472, 1390, 1295, 1222, 717

(*R*)-2-(4-(3-methyl-1,4-naphthoquinone-2-yl)butanamido)-3-phenylpropanoic acid (**105**)

^{1}H NMR δ ($CDCl_3$, 400 MHz): 1.72 – 1.79 (m, 2H), 2.15 (s, 3H), 2.30 (t, *J* = 7.3 Hz, 2H), 2.57 – 2.61 (m, 2H), 3.13 (dd, *J* = 14.1, 7.0 Hz, 2H), 3.27 (dd, *J* = 14.1, 5.5 Hz, 2H), 4.88 – 4.93 (m, 1H), 6.51 (d, *J* = 7.5 Hz, 1H), 7.18 – 7.29 (m, 5H), 7.67 – 7.71 (m 2H), 8.03 – 8.07 (m, 2H)

^{13}C NMR δ ($CDCl_3$, 100 MHz): 12.8, 24.2, 26.2, 35.9, 37.4, 53.4, 126.4, 127.2, 128.7 (2 x C), 129.4 (2 x C), 132.1, 132.2, 133.5, 133.6, 135.9, 144.3, 146.2, 173.3, 174.8, 185.0, 185.2

$[\alpha]_D^{20}$: -38.75° (*c* 0.16, $CHCl_3$)

IR V_{max}: 3370 (N-H), 2928, 1732 (C=O), 1716 (C=O), 1658 (C=O), 1595, 1527, 1456, 1330, 1294, 734, 717, 702 cm^{-1}

(*R*)-*N*-(1-hydroxy-3-phenylpropan-2-yl)-4-(3-methyl-1,4-naphthoquione-2-yl)butanamide (**106**)

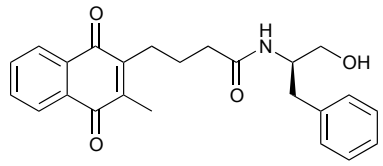

106 was prepared according to general procedure B from 4-(3-Methyl-1,4-naphthalen-2-yl)-butanoic acid (**32**) (180 mg, 0.6954 mmol) and D-phenylalaninol (117 mg, 0.7731 mmol) and the product purified by flash chromatography (100 % ethyl acetate) to give **106** as a brown oil in 55 % yield (186 mg, 0.4300 mmol).

^{1}H NMR δ ($CDCl_3$, 400 MHz): 1.72 – 1.78 (m, 2H), 2.17 (s, 3H), 2.25 (t, *J* = 6.9 Hz, 2H), 2.56 – 2.60 (m, 2H), 2.86 – 2.91 (m, 2H), 3.60 (dd, *J* = 11.2, 5.2 Hz, 1H), 3.74 (dd, *J* = 11.2, 3.5 Hz, 1H), 4.21 – 4.25 (m, 1H), 6.09 (d, *J* = 7.7 Hz 1H), 7.19 – 7.29 (m, 5H), 7.68 – 7.71 (m, 2H), 8.03 – 8.08 (m, 2H)

^{13}C NMR δ ($CDCl_3$, 100 MHz): 12.8, 24.3, 26.2, 36.2, 37.1, 53.0, 64.4, 126.45, 126.47, 126.7, 128.7, 129.3, 132.1, 132.2, 133.5, 133.7, 137.8, 144.3, 146.3, 173.0, 185.22, 185.27

$[\alpha]_D^{20}$: -13.88° (*c* 0.25, $CHCl_3$)

IR V_{max}: 3369, 3306, 3064, 2933, 1653, 1595, 1533, 1456, 1377, 1330, 1294, 1041, 734, 702 cm^{-1}

(*R*)-*N*-(2-hydroxy-1-phenylethyl)-4-(3-methyl-1,4-naphthoquinone-2-yl)butanamide (**107**)

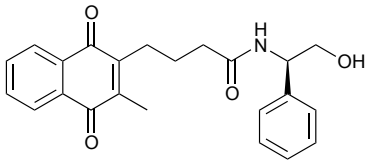

107 was prepared according to general procedure B from 4-(3-Methyl-1,4-naphthalen-2-yl)-butanoic acid (**32**) (178 mg, 0.6877 mmol) and D-phenyl glycinol (109 mg, 0.7953 mmol) and the product purified by dissolving in dichloromethane and adding hexanes dropwise until a precipitate was formed to give **107** as yellow crystaline solid in 62 % yield (161 mg, 0.4266 mmol) with a melting point of 150 – 154 °C.

^{1}H NMR δ ($CDCl_3$, 400 MHz):	1.80 – 1.90 (m, 2H) 2.29 (s, 3H), 2.36 (t, *J* = 7.1 Hz, 2H), 2.65 – 2.73 (m, 2H), 3.92 (d, *J* = 5.0 Hz, 2H), 5.10 – 5.14 (m, 1H), 6.50 (d, *J* = 6.8 Hz, 1H), 7.27 – 7.38 (m, 5H), 7.67 – 7.72 (m, 2H), 8.03 – 8.10 (m, 2H)
^{13}C NMR δ ($CDCl_3$, 100 MHz):	12.8, 24.4, 26.3, 36.2, 56.1, 66.8, 126.4, 126.9, 128.0, 129.0 (2 x C), 132.1, 132.3, 133.5, 133.7, 139.0, 144.4, 146.3, 172.9, 185.2, 185.3
$[\alpha]_D^{20}$:	-31.81° (*c* 0.64, $CHCl_3$)
IR V_{max}:	3296 (N-H), 2935, 1658 (C=O), 1595, 1541, 1456, 1377, 1330, 1294, 719, 700 cm^{-1}

(*S*)-methyl-2-(4-(3-methyl-1,4-naphthoquinone-2-yl)butanamido)-2-phenylacetate (**108**)

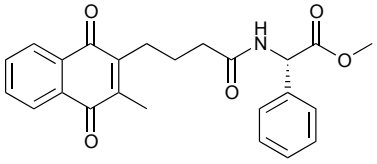

108 was prepared according to general procedure B from 4-(3-Methyl-1,4-naphthalen-2-yl)-butanoic acid (**32**) (209 mg, 0.8100 mmol) and S-(+)-phenyl glycine methyl ester.HCl (169 mg, 0.8396 mmol) and the product purified by flash chromatography (45 % ethyl acetate/hexanes) to give **108** as yellow solid in 72 % yield (236 mg, 0.5826 mmol) with a melting point of 100 – 102 °C.

^{1}H NMR δ ($CDCl_3$, 400 MHz):	1.78 – 1.85 (m, 2H), 2.13 (s, 3H), 2.35 (td, *J* = 7.3, 3.2 Hz, 2H), 2.63 – 2.67 (m, 2H), 3.70 (s, 3H), 5.59 (d, *J* = 7.2 Hz, 1H), 6.87 (d, *J* = 7.2 Hz, 1H), 7.28 – 7.37 (m, 5H), 7.63 – 7.66 (m, 2H), 7.99 – 8.03 (m, 2H)
^{13}C NMR δ ($CDCl_3$, 100 MHz):	12.7, 24.2, 26.3, 35.8, 52.8, 56.5, 126.3, 126.4, 127.4, 128.6, 129.1, 132.1, 132.2, 133.4, 133.5, 136.5, 144.1, 146.3, 171.5, 171.7, 184.9, 185.2
$[\alpha]_D^{20}$:	+99.11° (*c* 1.13, $CHCl_3$)
IR V_{max}:	3306 (N-H), 3030, 2953, 1743 (C=O), 1647 (C=O), 1597, 1597, 1537, 1456, 1379, 1330, 1296, 1213, 1127, 754, 717, 698 cm^{-1}

(*R*)-methyl-2-(4-(3-methyl-1,4-naphthoquinone-2-yl)butanamido)-2-phenylacetate (**109**)

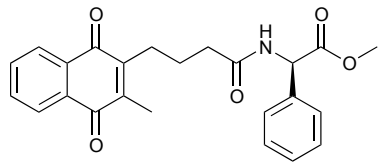

109 was prepared according to general procedure B from 4-(3-Methyl-1,4-naphthalen-2-yl)-butanoic acid (**32**) (202 mg, 0.7810 mmol) and R-(-)-phenyl glycine methyl ester.HCl (161 mg, 0.8396 mmol) and the product purified by flash chromatography (45 % ethyl acetate/hexanes) to give **109** as yellow solid in 69 % yield (219 mg, 0.5394 mmol) with a melting point of 90 – 92 °C.

^{1}H NMR δ ($CDCl_3$, 400 MHz): 1.78 – 1.86 (m, 2H), 2.15 (s, 3H), 2.35 (td, *J* = 7.3, 3.0 Hz, 2H), 2.46 – 2.68 (m, 2H), 3.71 (s, 3H), 5.60 (d, *J* = 7.2 Hz, 1H), 6.79 (d, *J* = 7.2 Hz, 1H), 7.30 – 7.36 (m, 5H), 7.64 – 7.69 (m, 2H), 8.00 – 8.06 (m, 2H)

^{13}C NMR δ ($CDCl_3$, 100 MHz): 12.7, 24.3, 26.3, 35.9, 52.9, 56.5, 126.3, 126.4, 127.4 (2 x C), 128.7, 129.1 (2 x C), 132.20, 132.27, 133.50, 133.54, 136.6, 144.1, 146.4, 171.5, 171.7, 184.9, 185.3

$[\alpha]_D^{20}$: -93.58° (*c* 0.78, $CHCl_3$)

IR V_{max}: 3304 (N-H), 3032, 2953, 1743 (C=O), 1656 (C=O), 1647, 1597, 1521, 1456, 1435, 1379, 1323, 1296, 1259, 1213, 1172, 754, 717, 696 cm^{-1}

(*S*)-2-(4-(3-methyl-1,4-naphthoquinone-2-yl)butanamido)-2-phenylacetic acid (**110**)

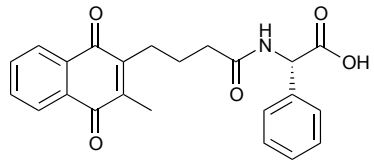

108 (76 mg, 0.1877 mmol) was added to 6M HCl (4 mL) with a catalytic amount of glacial acetic acid. Solution was refluxed for 2h and reaction quenched with the addition of H_2O (20 mL) and dichloromethane (20 mL), and the aqueous layer extracted with a further 2 x 20 mL dichloromethane. The organic layer dried with $MgSO_4$ and the solvent removed under reduced pressure to give a crude product, which was purified by precipitation from dichloromethane and the solvent decanted to give **110** as pale yellow solid in 46 % yield (34 mg, 0.0869 mmol) with a melting point of 168 – 170 °C.

^{1}H NMR δ (CD_3OD, 400 MHz): 1.81 (quin, *J* = 7.6 Hz, 2H), 2.14 (s, 3H), 2.35 – 2.40 (m, 2H), 2.65 – 2.70 (m, 2H),

5.42 (s, 1H), 7.31 – 7.42 (m, 5H), 7.72 – 7.75 (m, 2H), 8.02 – 8.04 (m, 2H)

^{13}C NMR δ (CD_3OD, 100 MHz): 12.7, 25.6, 27.2, 36.2, 58.2, 127.0, 127.1, 128.8 (2 x C), 129.3, 129.7 (2 x C), 133.50, 133.51, 134.5, 134.6, 138.1, 145.9, 147.5, 175.1, 185.8, 186.3 (Note: one carbon signal missing or overlapped)

$[\alpha]_D^{20}$: +90.34° (*c* 0.74, $CHCl_3$)

IR V_{max}: 3350 (N-H), 3030, 2933, 1732 (C=O), 1658 (C=O), 1647, 1597, 1533, 1456, 1379, 1330, 1296, 1259, 1219, 754, 717, 698 cm^{-1}

(*R*)-2-(4-(3-methyl-1,4-naphthoquinone-2-yl)butanamido)-2-phenylacetic acid (**111**)

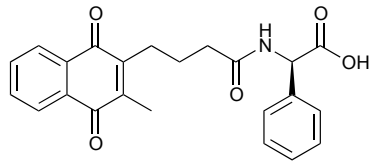

109 (49 mg, 0.1208 mmol) was added to 6M HCl (4 mL) with a catalytic amount of glacial acetic acid. Solution was refluxed for 2h and reaction quenched with the addition of H_2O (20 mL) and dichlormethane (20 mL), and the aqueous layer extracted with a further 2 x 20 mL dichloromethane. The organic layer dried with $MgSO_4$ and the solvent removed under reduced pressure to give a crude product, which was purified by precipitation from dichloromethane and the solvent decanted to give **111** as pale yellow solid in 14 % yield (7 mg, 0.0169 mmol) with a melting point of 128 – 130 °C.

^{1}H NMR δ (CD_3OD, 400 MHz): 1.81 (quin, *J* = 7.5 Hz, 2H), 2.14 (s, 3H), 2.35 – 2.40 (m, 2H), 2.65 – 2.70 (m, 2H), 5.42 (s, 1H), 7.31 – 7.42 (m, 5H), 7.73 – 7.75 (m, 2H), 8.02 – 8.04 (m, 2H)

^{13}C NMR δ (CD_3OD, 100 MHz): 12.7, 25.6, 27.2, 36.2, 58.3, 127.0, 127.1, 128.8 (2 x C), 129.3, 129.7 (2 x C), 133.50, 133.52, 134.57, 134.59, 138.2, 145.0, 147.5, 175.1, 185.8, 186.3 (Note: one carbon signal missing or overlapped)

$[\alpha]_D^{20}$: -127.41° (*c* 0.14, $CHCl_3$)

IR V_{max}: 3348 (N-H), 3066, 2928, 1732 (C=O), 1658 (C=O), 1647, 1597, 1496, 1456, 1379, 1330, 1296, 1259, 1217, 1178, 754, 717, 698 cm^{-1}

3-((3-Methyl-1,4-naphthoquinone-2-yl)thio)propanoic acid (**113**)

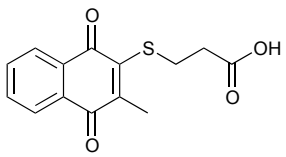

Mercapto-propanoic acid (**112**) (1.4 mL, 10.829 mmol) was added to a solution of menadione (**12**) (536 mg, 3.1119 mmol) in methanol (50 mL) and isopropanol (40 mL) and the reaction mixture stirred at room temperature for 24 h. The solvent was removed under reduced pressure and re-dissolved in dichloromethane and washed with 10% copper sulfate solution (2 x 25 mL) and H_2O (3 x 25 mL) The organic layer was dried with $MgSO_4$, filtered and the solvent removed under reduced pressure to give a crude product which was purified by flash chromatography (30 % ethyl acetate/hexanes) to give **113** as red solid oil in 48 % yield (387 mg, 1.4021 mmol).

^{1}H NMR δ ($CDCl_3$, 400 MHz): 2.34 (s, 3H), 2.75 (t, *J* = 7.0 Hz, 2H), 3.42 (t, *J* = 7.0 Hz, 2H), 7.69 – 7.71 (m, 2H), 8.06 – 8.09 (m, 2H)

^{13}C NMR δ ($CDCl_3$, 100 MHz): 15.4, 28.9, 35.4, 126.7, 126.9, 132.1, 132.9, 133.5, 133.8, 145.8, 147.6, 176.2, 181.3, 182.2

Spectral data consistent with data reported in the literature.[64]

4-((1,4-naphthoquinone-2-yl)amino)butanoic acid (**115**)

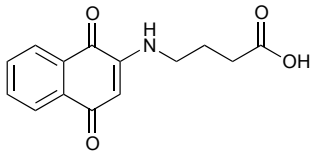

A solution of gamma amino butyric acid (170 mg, 1.6466 mmol) in H_2O (5 mL) was added to a hot solution of 1,4-naphthoquinone (**4**) (525 mg, 3.317 mmol) in ethanol (50 mL) and the mixture stirred at room temperature for 16 h. The solvent removed under reduced pressure and the product purified by a Reveleris ® X2 automated flash chromatography system (Eluent: gradient 0 – 10 % methanol in dichloromethane, Column: Reveleris ® Silica 4 g, Flow rate: 18 mL/min) to give **115** as a burgundy red solid in 22 % yield (92 mg, 0.3560 mmol).

^{1}H NMR δ ($CDCl_3$, 400 MHz): 2.04 (quin, *J* = 7.0 Hz, 2H), 2.50 (t, *J* = 7.0 Hz, 2H), 3.29 (q, *J* = 7.0 Hz, 2H), 5.78 (s, 1H), 6.07 – 6.10 (m, 1H), 7.61 (td, *J* = 7.5, 1.3 Hz, 1H), 7.72 (td, *J* = 7.5, 1.3 Hz, 1H), 8.03 (dd, *J* = 7.7, 1.0 Hz, 1H), 8.09 (dd, *J* = 7.7, 1.0 Hz, 1H)

^{13}C NMR δ (d_6-DMSO, 100 MHz): 22.6, 30.9, 41.22, 99.3, 125.2, 125.8, 130.4, 132.0, 133.1, 134.7, 148.5, 174.1, 181.2, 181.5

Spectral data consistent with data reported in the literature.[90]

(*S*)-methyl-2-(4-((1,4-naphthoquinone-2-yl)amino)butanamido)-3-phenylpropanoate (**117**)

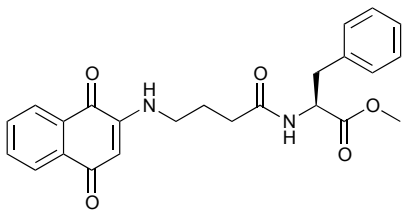

117 was prepared according to general procedure B from 4-((1,4-naphthoquinone-2-yl)amino)butanoic acid (**115**) (63 mg, 0.2416 mmol) and L-phenylalanine methyl ester.HCl (60 mg, 0.2791 mmol) in DMF. The reaction was quenched with H_2O (20mL) and the aqueous layer was extracted with 1:1 ethyl acetate/hexanes. The organic layer was combined and washed with 2x 25 mL H_2O, dried with $MgSO_4$, filtered and the solvent removed under reduced pressure to give a crude product. The product was purified by flash chromatography (90 % ethyl acetate/hexanes) to give **117** as bright red solid in 18 % yield (19 mg, 0.0445 mmol) with a melting point of 105 – 107 °C.

^{1}H NMR δ ($CDCl_3$, 400 MHz):	1.97 – 2.04 (m, 2H), 2.29 – 2.33 (m, 2H), 3.08 (dd, *J* = 14.0, 6.2 Hz, 1H), 3.18 (dd, *J* = 14.0, 5.8 Hz, 1H), 3.19 – 3.23 (m, 2H), 3.73 (s, 3H), 4.90 – 4.95 (m, 1H), 5.82 (s, 1H), 5.96 (d, *J* = 7.6 Hz, 1H), 6.51 (bs, 1H), 7.07 – 7.09 (m, 2H), 7.22 – 7.29 (m, 3H), 7.61 (td, *J* = 7.6, 1.3 Hz, 1H), 7.72 (td, *J* = 7.6, 1.3 Hz), 8.05 (dd, *J* = 7.7, 1.0 Hz, 1H), 8.09 (dd, *J* = 7.7, 1.0 Hz, 1H)
^{13}C NMR δ ($CDCl_3$, 100 MHz):	23.4, 33.6, 37.9, 42.4, 52.5, 53.2, 100.5, 126.4, 126.6, 127.3, 128.7 (2 x C), 129.3 (2 x C), 130.6, 132.2, 133.5, 134.9, 135.8, 148.6, 171.6, 172.1,181.6, 182.8
$[\alpha]_D^{20}$:	-46.67° (*c* 0.06, $CHCl_3$)
IR V_{max}:	3290 (N-H), 3061, 2953, 1743 (C=O), 1676 (C=O), 1604, 1570, 1510, 1456, 1336, 1305, 1253, 1213, 779 cm^{-1}

(*S*)-1-((*S*)-2-(4-(3-methyl-1,4-naphthoquinone-2-yl)butanamido)-3-phenylpropanoyl)pyrrolidine-2-carboxylic acid (**119**)

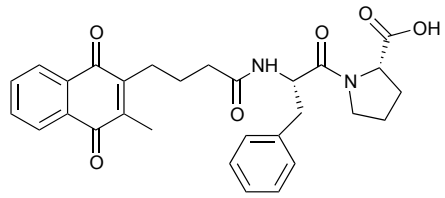

120 was prepared according to general procedure B from **70** (112 mg, 0.2752 mmol) and L-Proline *t*-butyl ester.HCl (75 mg, 0.3625 mmol) and the product purified by flash chromatography (80 % ethyl acetate/hexanes) to give the *t*-butyl ester as a yellow viscous oil in 35 % yield (53.4 mg, 0.0956 mmol). Deprotection of the *t*-butyl ester (44.1 mg, 0.0789) was performed using general procedure C. The product was purified by flash chromatography (7 % methanol/ethyl acetate) to give **120** as a yellow oil in 49 % yield (20 mg, 0.0390 mmol).

HR ESI MS:	For $C_{29}H_{30}N_2Na0_6$, predicted 525.2002, found 525.1990
$[\alpha]_D^{20}$:	-28.31 ° (*c* 0.45, $CHCl_3$)
IR V_{max}:	3293 (N-H), 3064, 2929, 1716 (C=O), 1732 (C=O), 1658, 1622, 1539, 1454, 1330, 1294, 1188, 734, 702 cm^{-1}

***N*-(2-(benzylamino)-2-oxoethyl)-2-((*S*)-3-(4-hydroxy-2,6-dimethylphenyl)-2-(4-(3-methyl-1,4-naphthoquinone-2-yl)butanamido)propanoyl)-1,2,3,4-tetrahydroisoquinoline-3-carboxamide**

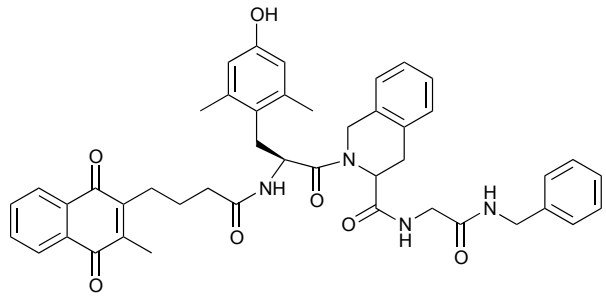

122 was prepared according to general procedure B from 4-(3-Methyl-1,4-naphthalen-2-yl)-butanoic acid (**32**) (31 mg, 01181 mmol) and DMT-Tic-Gly-Bnz.HCl (49 mg, 0.0785 mmol) and the product purified by flash chromatography (95:5:1 methanol/ethyl acetate/H_2O) to give **122** as an opaque yellow semi-solid in 27 % yield (15 mg, 0.0196 mmol).

MS *m/z* (ES+):	777 (M+Na, 45), 755 (M+, 48), 591 (100)
$[\alpha]_D^{20}$:	-26.67 ° (*c* 0.05, $CHCl_3$)
IR V_{max}:	3306 (N-H), 1653 (C=O), 1595, 1539, 1456, 1437, 1379, 1294, 1267, 1143, 1030, 734 cm^{-1}

6.2.3 Solid Phase Peptide Synthesis

SPPS procedure A: Preparation of Resin

Solid phase peptide synthesis was conducted manually in a sinter-fitted polypropylene syringe. 2-Chlorotrityl resin (100 – 200 mesh, 1.63 mmol/g resin loading) was agitated in CH_2Cl_2 for 30 mins and then drained. A solution containing fmoc-amino acid (3 eq. relative to maximum resin loading) in 0.4M DIPEA (diisopropylethylamine)/CH_2Cl_2 was added and the mixture agitated for 3 h. The resin was drained and washed with 17:2:1 CH_2Cl_2/MeOH/DIPEA (3 x 1 min), CH_2Cl_2 (2 x 1 min), DMF (2 x 1 min) CH_2Cl_2 (2 x 1 min) and DMF (2 x 1 min).

SPPS procedure B: Fmoc Deprotection

Resin was agitated with 10 % piperidine in DMF (2 x 2 mL x 3 min) then drained and washed with DMF (3 x 1 min), CH_2Cl_2 (3 x 1 min) and DMF (3 x 1 min).

SPPS procedure C: Peptide Coupling

A solution of the desired fmoc-amino acid (3 eq. relative to the maximum resin loading) and PyBOP (2.9 eq. relative to resin loading) in minimal amount of DMF was prepared. DIPEA (6 eq. relative to resin loading) was added to the solution and the mixture immediately added to the resin and

agitated for 1.5 h. The resin was drained and washed with DMF (3 x 1 min), CH_2Cl_2 (3 x 1 min) and DMF (3 x 1 min).

SPPS Proceedure D: Cleavage

After last fmoc deprotection was resin with CH_2Cl_2 (3 x 1 min) again and drained. Resin was agitated with 10 % 222,333-hexaflouro-isopropanol in CH_2Cl_2 (2 x 30 min). Cleavage solutions were combined and the solvent removed under reduced pressure to give a thin film. Diethyl ether (3 x) was added and decanted to give the desired peptide.

SPPS procedure E: Deprotection of additional protecting groups after resin cleavage

Minimal TFA (2 mL) was added to the peptides and the mixture stirred for 16 h. The reaction mixture was the solvent removed under reduced pressure to give a thin film, diethyl ether (3 x) was added and decanted to give the pure peptide as a TFA salt.

Quin-N-Arg-Tyr-Lys-Phen-OH (**123**)

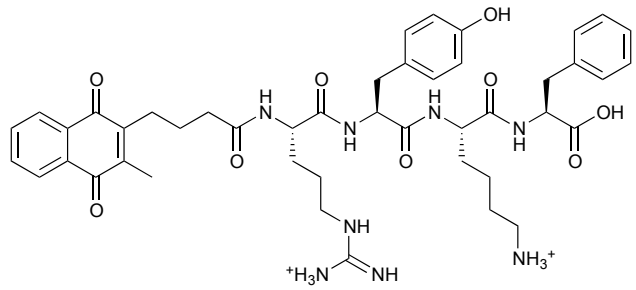

123 was prepared on a 0.086 mmol scale according to SPPS procedures A – E. The product was obtained as a TFA salt as a yellow viscous oil in 88 % yield according to the initial resin loading (82.0 mg, 0.0758 mmol). Further purification was not required.

$[\alpha]_D^{20}$: -18.00° (*c* 0.10, DMSO)

HRMS $[M^{2+}]$: For $C_{45}H_{58}N_8O_9$, predicted 427.2158, found 427.2175

Quin-N-Phen-Lys-Tyr-Arg-OH (**124**)

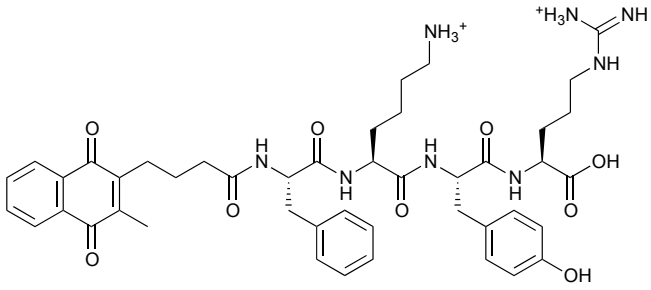

124 was prepared on a 0.086 mmol scale according to SPPS procedures A – E. The product was obtained as a TFA salt as a yellow viscous oil in quantitative yield according to the initial resin loading (90.1 mg, 0.0834 mmol). Further purification was not required.

$[\alpha]_D^{20}$: -16.93° (*c* 0.68, MeOH)

HRMS $[M^{2+}]$: For $C_{45}H_{58}N_8O_9$, predicted 427.2158, found 427.2173

Quin-Lys-Phen-Lys-Phen-OH (**125**)

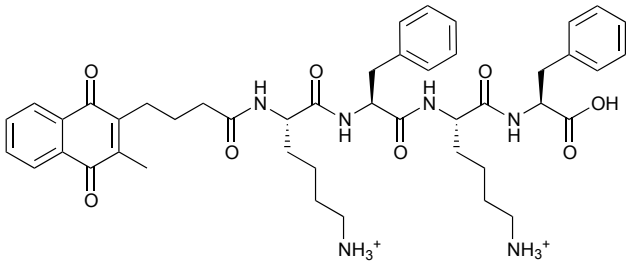

125 was prepared on a 0.17 mmol scale according to SPPS procedures A – D. The protected product was obtained as a yellow soild in 91 % yield according to the initial resin loading (155.2 mg, 1.555 mmol). Further purification was not required. Deprotection of the protected product (26.9 mg, 0.0269 mmol) using SPPS procedure E resulted in **125** as a TFA salt in quantitative yield (27.3 mg, 0.0263 mmol).

$[\alpha]_D^{20}$: -27.39° (*c* 0.46, MeOH)

HRMS $[M^{2+}]$: For $C_{55}H_{72}N_6O_{12}$, predicted 405.2153, found 405.2151

Quin-N-Lys-Phen-Phen-Lys-OH (**126**)

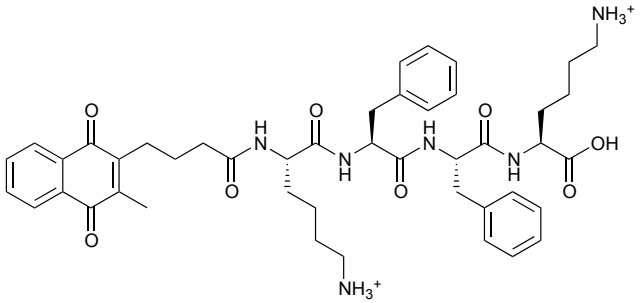

126 was prepared on a 0.086 mmol scale according to SPPS procedures A – E. The product was obtained as a TFA salt as a yellow viscous oil in 73 % yield according to the initial resin loading (65.5 mg, 0.0632 mmol). Further purification was not required.

$[\alpha]_D^{20}$: -21.46° (*c* 2.33, MeOH)

HRMS $[M^{2+}]$: For $C_{30}H_{46}N_8O_6$, predicted 405.2153, found 405.2153

Quin-N-Lys-Lys-Phen-Phen-OH (**127**)

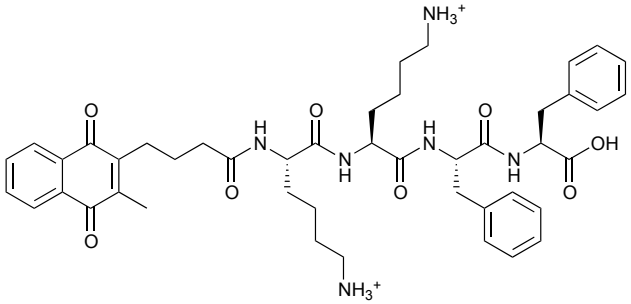

127 was prepared on a 0.086 mmol scale according to SPPS procedures A – E. The product was obtained as a TFA salt as a yellow viscous oil in 92 % yield according to the initial resin loading (82.2 mg, 0.0792 mmol). Further purification was not required.

$[\alpha]_D^{20}$: -15.24° (*c* 1.47, MeOH)

HRMS $[M^{2+}]$: For $C_{45}H_{58}N_6O_8$, predicted 405.2153, found 405.2147

Quin-N-His-Phen-His-Phen-OH (**128**)

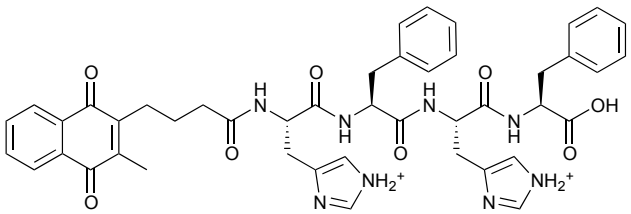

128 was prepared on a 0.086 mmol scale according to SPPS procedures A – E. The product was obtained as a TFA salt as a cream coloured soild in 86 % yield according to the initial resin loading (78.9 mg, 0.0748 mmol). Further purification was not required.

$[\alpha]_D^{20}$: -10.20° (*c* 0.49, MeOH)

HRMS $[M^{2+}]$: For $C_{45}H_{48}N_8O_8$, predicted 414.1792, found 414.1787

Quin-N-Lys-Trp-Lys-Trp-OH (**129**)

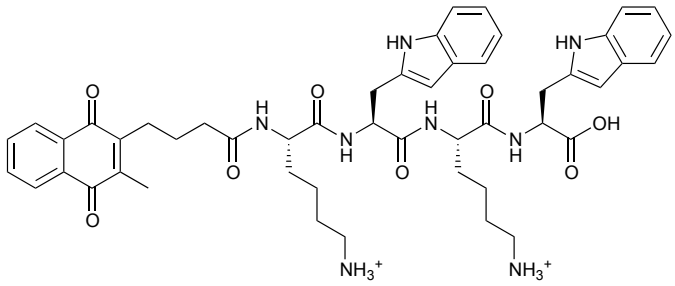

129 was prepared on a 0.086 mmol scale according to SPPS procedures A – E. The product was obtained as a TFA salt as a brown soild in 76 % yield according to the initial resin loading (71.8 mg, 0.0643 mmol). Further purification was not required.

$[\alpha]_D^{20}$: -41.71° (*c* 1.64, MeOH)

HRMS $[M^{2+}]$: For $C_{49}H_{60}N_8O_8$, predicted 444.2262, found 444.2256

6.3 Chapter 3 Experimental Details

6.3.1 Synthesis of non-methyl naphthoquinone analogues

4-(1,4-naphthoquinone-2-yl)butanoic acid (**130**) and **4,4'-(1,4-dioxo-1,4-dihydronaphthalene-2,3-diyl)dibutanoic acid** (**131**)

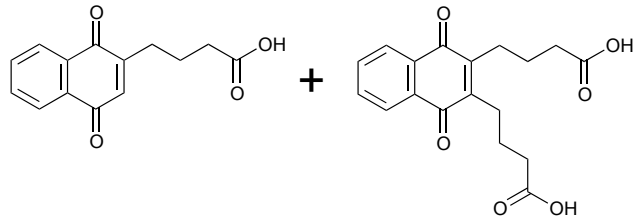

130 was prepared according to general procedure A from naphthoquinone (**4**) (1.999 g, 12.64 mmol) and glutaric acid (0.8354 mg, 6.323 mmol) and the product purified by a Reveleris ® X2 automated flash chromatography system (Eluent: gradient 0 – 80 % ethyl acetate in hexane, Column: Reveleris ® Silica 24 g, Flow rate: 18 mL/min) to give **130** as a brown solid in 42 % yield (0.655 g, 2.680 mmol) and **131** as a crystalline yellow solid in 9 % yield (185 mg, 0.5607 mmol).

4-(1,4-naphthoquinone-2-yl)butanoic acid (**130**)

Melting point:	120 – 122 °C.
^{1}H NMR δ (CD_3OD, 400 MHz):	1.90 (quin, *J* = 7.6 Hz, 2H), 2.39 (t, *J* = 7.6 Hz, 2H), 2.62 (td, *J* = 7.6, 1.1 Hz, 2H), 6.85 (t, *J* = 1.1 Hz, 1H), 7.78 – 7.80 (m, 2H), 8.02 – 8.04 (m, 1H), 8.07 – 8.10 (m, 1H)
^{13}C NMR δ (CD_3OD, 150 MHz):	24.4, 30.0, 34.2, 126.8, 127.4, 133.4, 133.7, 134.8, 134.9, 136.0, 152.4, 176.8, 186.1, 186.3
IR V_{max}:	2956 (-OH), 1699 (C=O), 1660 (C=O), 1620, 1953, 1417, 1327, 1303, 1265, 1143, 783, 661 cm^{-1}

4,4'-(1,4-dioxo-1,4-dihydronaphthalene-2,3-diyl)dibutanoic acid (**131**)

Melting point: 146 – 149 °C

^{1}H NMR δ (CD_3OD, 400 MHz): 1.80 (quin, *J* = 7.4 Hz, 4H), 2.42 (t, *J* = 7.4 Hz, 4H), 2.69 – 2.73 (m, 4H), 7.74 – 7.76 (m, 2H), 8.03 – 8.05 (m, 2H)

^{13}C NMR δ (CD_3OD, 100 MHz): 25.7, 27.2, 34.7, 127.1, 133.5, 134.6, 148.0, 176.9, 186.1

IR V_{max}: 2932 (-OH), 1697 (C=O), 1656 (C=O), 1595, 1406, 1294, 1240, 935, 721 cm^{-1}

(*S*)-*tert*-butyl-2-(4-(1,4-naphthoquinone-2-yl)butanamido)-3-phenylpropanoate (**132**)

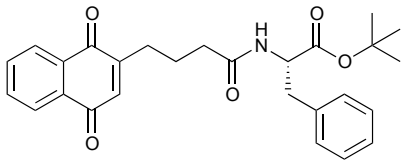

132 was prepared according to general procedure B from 4-(1,4-naphthalen-2-yl)-butanoic acid (**130**) (351 mg, 1.437 mmol) and L-phenylalanine *t*-butyl ester.HCl (496 mg, 1.925 mmol) and the product purified by flash chromatography (50 % ethyl acetate/hexanes) to give **132** as yellow viscous oil in 67 % yield (432 mg, 0.9660 mmol).

^{1}H NMR δ ($CDCl_3$, 400 MHz): 1.43 (s, 9H), 1.91 (quin, *J* = 7.5 Hz, 2H), 2.29 (td, *J* = 7.5, 2.9 Hz, 2H), 2.56 – 2.60 (m, 2H), 3.10 – 3.14 (m, 2H), 4.76 – 4.81 (m, 1H), 6.03 (d, *J* = 7.3 Hz, 1H), 7.16 -6 7.31 (m, 5H), 7.74 – 7.76 (m, 2H), 8.07 – 8.12 (m, 2H)

^{13}C NMR δ ($CDCl_3$, 100 MHz): 23.9, 28.1, 29.1, 35.8, 38.2, 53.5, 82.5, 126.2, 126.7, 127.1, 128.5 (2 x C), 129.6 (2 x C), 132.2, 132.3, 133.7, 133.8, 135.3, 136.3, 150.9, 170.9, 172.5, 185.1, 185.2

$[\alpha]_D^{20}$: +38.46° (*c* 0.39, $CHCl_3$)

IR V_{max}: 3309 (N-H), 2978, 2931, 1732 (C=O), 1662 (C=O), 1595, 1525, 1456, 1367, 1301, 1259, 1153, 700 cm^{-1}

(*S*)-2-(4-(1,4-naphthoquinone-2-yl)butanamido)-3-phenylpropanoic acid (**133**)

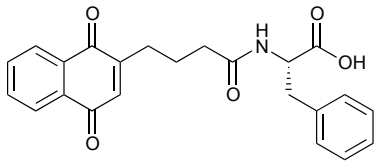

133 was prepared from the deprotection of **132** (428 mg, 0.9563 mmol), using general procedure C. The product was purified by flash chromatography (5 % methanol/ethyl acetate) to give **133** as brown solid in 92 % yield (345 mg, 0.8811 mmol) with a melting point of 110 – 112 °C.

^1H NMR δ ($CDCl_3$, 400 MHz): 1.86 (quin, *J* = 7.4 Hz, 2H), 2.40 (t, *J* = 7.3 Hz, 2H), 2.45 – 2.54 (m, 2H), 3.12 (dd, *J* = 14.0, 7.4 Hz, 1H), 3.28 (dd, *J* = 14.0, 5.2 Hz, 1H), 4.97 – 5.02 (m, 1H), 6.74 (s, 1H), 7.04 (d, *J* = 7.9 Hz, 1H), 7.17 – 7.21 (m, 3H), 7.24 – 7.28 (m, 2H), 7.71 – 7.73 (m, 2H), 7.99 – 8.06 (m, 2H)

^{13}C NMR δ ($CDCl_3$, 100 MHz): 24.0, 28.8, 35.3, 37.3, 53.5, 126.2, 126.7, 127.4, 128.8, 129.3, 131.9, 132.1, 134.0, 135.3, 135.53, 135.55, 150.7, 174.82, 174.88, 185.2, 185.6

$[\alpha]_D^{20}$: +7.87° (*c* 0.33, MeOH)

IR V_{max}: 3301 (N-H), 2929, 1708 (C=O), 1661 (C=O), 1554, 1454, 1369, 1302, 1260, 697 cm^{-1}

(*S*)-4-(1,4-naphthoquinone-2-yl)-*N*-(1-hydroxy-3-phenylpropan-2-yl) butanamide (**134**)

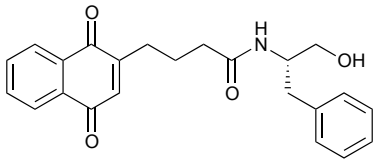

134 was prepared according to general procedure B from 4-(1,4-naphthalen-2-yl)-butanoic acid (**130**) (140 mg, 0.5728 mmol) and L-phenylalaninol (96 mg, 0.6349 mmol) and the product purified by flash chromatography (4 % methanol/ ethyl acetate) to give **134** as a dark brown semi solid in 53 % yield (115 mg, 0.3034 mmol).

^{1}H NMR δ ($CDCl_3$, 400 MHz):	1.86 (quin, *J* = 7.3 Hz, 2H), 2.25 (t, *J* = 7.3 Hz, 2H), 2.49 – 2.53 (m, 2H), 2.89 (t, *J* = 7.0 Hz, 2H), 3,04 (bs, 1H), 3.59 (dd, *J* = 11.1, 5.1 Hz, 1H), 3.70 (dd, *J* = 11.1, 3.6 Hz, 1H), 4.21 – 4.25 (m, 1H), 6.17 (d, *J* = 7.9 Hz, 1H), 6.76 (s, 1H), 7.19 – 7.29 (m, 5H), 7.71 – 7.73 (m, 2H), 8.02 – 8.07 (m, 2H)
^{13}C NMR δ ($CDCl_3$, 100 MHz):	24.9, 28.9, 35.9, 37.1, 52.8, 64.0, 126.1, 126.7, 128.6 (2 x C), 129.3 (2 x C), 132.1, 132.2, 133.8, 135.3, 137.8, 150.9, 172.7, 185.1, 185.3
$[\alpha]_D^{20}$:	-23.09° (*c* 0.97, $CHCl_3$)
IR V_{max}:	3350 (N-H), 2947, 1733 (C=O), 1645 (C=O), 1611, 1456, 1266, 1204, 1153, 1055, 735, 702 cm^{-1}

4-(1,4-naphthoquinone-2-yl)-*N*-(4-hydroxyphenethyl)butanamide (**135**)

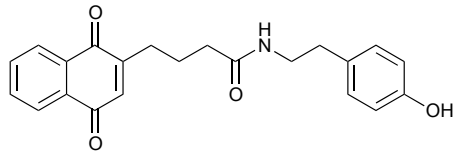

135 was prepared according to general procedure B from 4-(1,4-naphthalen-2-yl)-butanoic acid (**130**) (150 mg, 0.6149 mmol) and tyramine (89 mg, 0.6502 mmol) and the product purified by flash chromatography (80 % ethyl acetate/hexanes) to give **135** as a brown viscous oil in 33 % yield (109 mg, 0.2885 mmol).

^{1}H NMR δ ($CDCl_3$, 400 MHz): 1.85 (quin, *J* = 7.4 Hz, 2H), 2.22 (t, *J* = 7.4 Hz, 2H) 2.49 – 2.53 (m, 2H), 2.72 (t, *J* = 6.8 Hz, 2H), 3.46 – 3.50 (m, 2H), 5.89 (t, *J* = 5.27 Hz, 1H), 6.71 (s, 1H), 6.77 (d, *J* = 8.4 Hz, 2H), 6.99 (d, *J* = 8.4 Hz, 2H), 7.68 – 7.71 (m, 2H), 7.99 – 8.05 (m, 2H)

^{13}C NMR δ ($CDCl_3$, 100 MHz): 24.0, 29.0, 34.7, 35.9, 40.9, 115.7, 121.7, 126.1, 126.7, 129.9, 132.1, 132.2, 133.8, 133.9, 150.9, 155.1, 172.6, 185.1, 185.24, 185.28

IR V_{max}: 3312 (N-H), 2932, 1661 (C=O), 1594, 1539, 1455, 1302, 1265, 1042, 733, 702 cm^{-1}

***N*-(3,4-dimethoxyphenethyl)-4-(1,4-dioxo-1,4-naphthoquinone-2-yl) butanamide** (**136**)

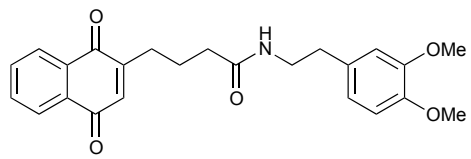

136 was prepared according to general procedure B from 4-(1,4-naphthalen-2-yl)-butanoic acid (**130**) (140 mg, 0.5748 mmol) and 3,4-

dimethoxyphenethylamine (129 mg, 0.7111 mmol) and the product purified by flash chromatography (90 % ethyl acetate/hexanes) to give **136** as brown semi solid in 36 % yield (84 mg, 0.2059 mmol).

^{1}H NMR δ ($CDCl_3$, 400 MHz): 1.90 (quin, *J* = 7.4 Hz, 2H), 2.21 (t, *J* = 7.4 Hz, 2H), 2.54 – 2.58 (m, 2H), 7.26 (t, *J* = 7.1 Hz, 2H), 3.47 – 3.52 (m, 2H), 3.83 (s, 3H), 3.85 (s, 3H), 5.63 (t, *J* = 5.5 Hz, 2H), 6.71 (s, 1H), 6.77 – 6.80 (m, 3H), 7.76 – 7.74 (m, 2H), 8.03 – 8.08 (m, 2H)

^{13}C NMR δ ($CDCl_3$, 100 MHz): 24.0, 29.1, 35.3, 35.9, 40.7, 56.00, 56.03, 111.5, 112.0, 120.7, 126.2, 126.7, 131.4, 132.2, 132.3, 133.7, 133.8, 135.2, 147.8, 149.2, 150.9, 172.0, 185.0, 185.2

IR V_{max}: 3311 (n-H), 2935, 1644 (C=O), 1593, 1516, 1328, 1302, 1263, 1236, 1157, 1141, 1028, 732 cm^{-1}

6.3.2 Synthesis of hydroxy-naphthoquinone derivatives

2-hydroxy-3-methylnaphthalene-1,4-dione (**138**)

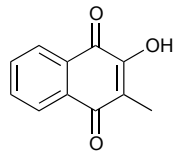

Menadione (**12**) (100 mg, 0.5825 mmol) was dissolved in methanol (1 mL) and cooled to 0 °C. A solution containing anhydrous Na_2CO_3 (26.3 mg, 0.2481 mmol) and 0.15 mL of 30% H_2O_2 in 0.5 mL H_2O was added dropwise at 0 °C. Mixture was left for 5 mins before the addition of 10 mL chilled H_2O resulting in the precipitation of 2-methyl-naphthoquinone oxide which was collected by filtration as a pale yellow solid. The solid was treated with 0.5 mL conc. H_2SO_4 and left to stand for 10 mins before the reaction mixture was diluted with 10 mL H_2O which resulted in a the precipitation of a purple solid. The product was purified by flash chromatography (25 % ethyl

acetate/hexanes) to give **138** as yellow solid in 33 % yield (36 mg, 0.1918 mmol) with a melting point of 132 – 133°C.

^{1}H NMR δ ($CDCl_3$, 400 MHz): 2.11 (s, 3H), 7.29 (s, 1H), 7.67 (t, *J* = 7.5 Hz, 1H), 7.74 (t, *J* = 7.5 Hz, 1H), 8.07 (d, *J* = 7.6 Hz, 1H), 8.12 (d, *J* = 7.6 Hz, 1H)

^{13}C NMR δ ($CDCl_3$, 100 MHz): 8.8, 120.6, 126.2, 126.8, 129.5, 133.05, 133.07, 134.9, 153.2, 181.3, 185.1

IR V_{max}: 3368 (-OH), 1651 (C=O), 1645 (C=O), 1590, 1458, 1381, 1348, 1338, 1270, 1072, 726 cm^{-1}

Ethyl 4-((1,4-dioxo-1,4-dihydronaphthalen-2-yl)oxy)butanoate (**143**)

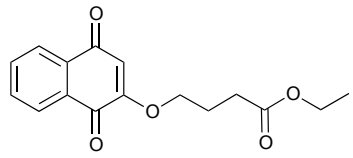

Lawsone (**139**) (516 mg, 2.963 mmol) in DMF (2 mL) was added to a solution of lithium carbonate (232 mg, 3.142 mmol) in DMF (10 mL) and stirred at room temperature for 0.25 h. A solution of ethyl bromobutyrate (0.8 mL, 1.090 g, 5.590 mmol) in DMF (2 mL) was added dropwise over a 5 min period before the reaction mixture was stirred for 1 hour. Reaction mixture was then refluxed for 3 hours before cooling and quenching with H_2O (50 mL), extracted with dichloromethane (3 x 20 mL) and washed with H_2O (3 x 20 mL). The organic extract was dried with Na_2SO_4, filtered and the product purified by flash chromatography (50 % ethyl acetate/hexanes) to give **143** as brown crystalline solid in 46 % yield (393 mg, 1.364 mmol) with a melting point of 60 – 61 °C.

^{1}H NMR δ ($CDCl_3$, 400 MHz): 1.25 (t, *J* = 7.2 Hz, 3H), 2.17 – 2.24 (m, 2H), 2.53 (t, *J* = 7.1 Hz, 2H), 4.05 (t, *J* = 6.2 Hz, 2H), 4.14 (q, *J* = 7.2 Hz, 2H), 6.14 (s, 1H), 7.66 – 7.74 (m, 2H), 8.04 – 8.06 (m, 1H), 8.08 – 8.10 (m, 1H)

^{13}C NMR δ ($CDCl_3$, 100 MHz): 14.3, 23.7, 30.4, 60.7, 68.3, 110.4, 126.2, 126.7, 131.2, 132.0, 133.4, 134.3, 159.7, 172.7, 180.0, 185.0

IR V_{max}: 2981, 2940, 1731 (C=O), 1685 (C=O), 1653 (C=O), 1608, 1577, 1330, 1244, 1209, 1181, 1043, 1022, 782, 725 cm^{-1}

4-(3-hydroxy-1,4-dioxo-1,4-dihydronaphthalen-2-yl)butanoic acid (**149**)

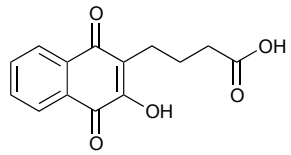

To a suspension of glutaric anhydride (6.979 g, 61.17 mmol) in H_2O (8 mL), 30 % H_2O_2 (10 mL) was added and stirred at room temperature for 1 h. The reaction mixture was cooled to 0 °C before a white precipitate was formed and the solid filtered producing digluteroylperoxide. This solid was slowly added to a hot solution (100 °C) of Lawsone (**139**) (2.844 g, 16.33 mmol) in *t*-butanol (20 mL). The reaction mixture was refluxed for 3 mins before being cooled to room temperature and quenched with H_2O (50 mL). The reaction mixture was extracted with CH_2Cl_2 (4 x 50 mL) and the organic extract was dried over $MgSO_4$, filtered and the solvent removed under reduced pressure to give the crude product **149** (4.570 g) as a yellow solid, which was unable to be purified by flash column chromatography and used in subsequent reactions as a crude mixture.

^{1}H NMR δ ($CDCl_3$, 400 MHz): 1.84 (quin, *J* = 7.5 Hz, 2H), 2.33 (t, *J* = 7.5 Hz, 2H), 2.61 – 2.65 (m, 2H), 7.69 – 7.79 (m, 2H), 8.01 – 8.08 (m, 2H)

^{13}C NMR δ ($CDCl_3$, 150 MHz): 23.4, 24.6, 34.7, 124.5, 126.8, 127.1, 131.6, 134.0, 135.4, 157.0, 177.3, 182.3, 186.4

IR V_{max}: 3352, 1705 (C-O), 1642 (C=O), 1590, 1374, 1348, 1274, 1216, 727 cm^{-1}

Note: Crude Mixture of **149** was used for synthesis of analogues **150**, **153** and **154** without purification

(*S*)-*tert*-butyl-2-(4-(3-hydroxy-1,4-dioxo-1,4-dihydronaphthalen-2-yl)butanamido)-3-phenylpropanoate (**150**)

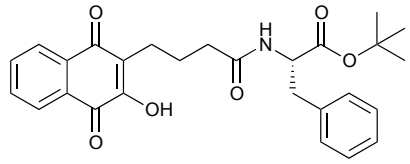

150 was prepared according to general procedure B from crude **149** (627 mg) and L-phenylalanine *t*-butyl ester.HCl (582 mg, 2.264 mmol) and the product purified by flash chromatography (45 % ethyl acetate/hexanes) to give **150** as yellow viscous oil in 9 % yield (88 mg, 0.1903 mmol).

* Yield calculated as if acid **149** was a pure compound

^{1}H NMR δ ($CDCl_3$, 400 MHz): 1.39 (s, 9H), 1.86 (quin, *J* = 7.3 Hz, 2H), 2.22 (t, *J* = 7.3 Hz, 2H), 2.63 (t, *J* = 7.3 Hz, 2H), 3.09 (d, *J* = 6.10 Hz, 2H), 4.75 – 4.80 (m, 1H), 6.23 (d, *J* = 7.7 Hz, 1H), 7.15 – 7.28 (m, 5H), 7.66 (dt, *J* = 7.5, 1.2 Hz, 1H), 7.73 (dt, *J* = 7.5, 1.2 Hz, 1H), 8.05 – 8.10 (m, 2H)

^{13}C NMR δ ($CDCl_3$, 100 MHz): 22.5, 24.1, 28.0, 35.7, 38.2, 53.6, 82.4, 123.4, 126.2, 126.8, 127.0, 128.4, 129.6, 129.8, 132.8, 133.0, 134.8, 136.3, 154.1, 170.9, 172.5, 181.3, 184.8

$[\alpha]_D^{20}$: +61.82° (*c* 0.33, $CHCl_3$)

IR V_{max}: 3314 (N-H), 2978, 2931, 1731 (C=O), 1713 (C=O), 1647 (C=O), 1594, 1457, 1368, 1274, 1217, 1155, 726 cm^{-1}

(*S*)-2-(4-(3-hydroxy-1,4-dioxo-1,4-dihydronaphthalen-2-yl)butanamido)-3-phenylpropanoic acid (**151**)

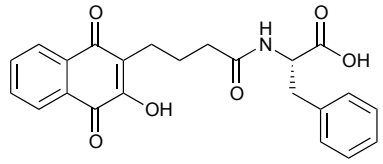

151 was prepared from the deprotection of **150** (58 mg, 0.1252 mmol), using general procedure C. The product was purified by flash chromatography (100 % ethyl acetate) to give **151** as a pale yellow solid in 74 % yield (38 mg, 0.0930 mmol) with a melting point of 110 – 112 °C.

^{1}H NMR δ (MeOD, 400 MHz): 169 – 1.76 (m, 2H), 2.20 (t, *J* = 7.78 Hz, 2H), 2.53 (t, *J* = 7.5 Hz, 2H), 2.94 (dd, *J* = 14.0, 9.1 Hz, 1H), 3.19 (dd, *J* = 14.0, 5.2 Hz, 1H), 4.65 (dd, *J* = 9.1, 5.2 Hz, 1H) 7.12 – 7.25 (m, 5H), 7.70 (dt, *J* = 7.4, 1.2 Hz, 1H), 7.75 (dt, *J* = 7.4, 1.2 Hz, 1H), 8.00 – 8.03 (m, 2H)

^{13}C NMR δ (MeOD, 100 MHz): 23.5, 25.5, 36.7, 38.4, 54.9, 124.5, 126.7, 127.1, 127.7, 129.3, 130.2, 131.6, 133.9, 134.0, 135.4, 138.4, 156.9, 174.7, 175.7, 182.2, 186.4

$[\alpha]_D^{20}$: +23.11° (*c* 0.45, MeOH)

IR V_{max}: 3328 (N-H), 2930, 1733 (C=O), 1713 (C=O), 1668 (C=O), 1645, 1593, 1539, 1369, 1274, 1217, 726, 701 cm^{-1}

4-(3-hydroxy-1,4-dioxo-1,4-dihydronaphthalen-2-yl)-*N*-(4-hydroxyphenethyl)butanamide (**153**)

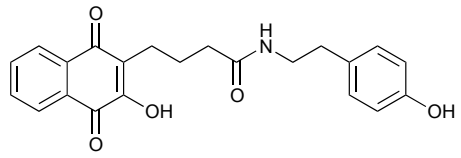

153 was prepared according to general procedure B from crude **149** (587 mg) and tyramine (292 mg, 2.129 mmol) and the product purified by flash chromatography (2 % methanol/ethyl acetate) to give **153** as yellow needles in a 4 % yield (33 mg, 0.08566 mmol) with a melting point of 122 – 123 °C.

* Yield calculated as if acid **149** was a pure compound

^{1}H NMR δ (Acetone-D6, 400 MHz): 1.83 (quin, *J* = 7.4 Hz, 2H), 2.20 (t, *J* = 7.4 Hz, 2H), 2.62 (t, *J* = 7.4 Hz, 2H), 2.68 (t, *J* = 7.4 Hz, 2H), 3.34 – 3.39 (m, 2H), 6.73 (d, *J* = 8.4 Hz, 2H), 7.03 (d, *J* = 8.4 Hz, 2H), 7.21 (bs, 1H), 7.75 – 7.84 (m, 2H), 8.02 – 8.05 (m, 2H), 8.12 (bs, 1H),

^{13}C NMR δ (Acetone-D6, 100 MHz): 22.3, 24.2, 34.6, 35.1, 40.8, 115.0, 123.2, 125.5, 125.9, 129.5, 130.1, 130.3, 132.6, 132.8, 134.2, 155.2, 155.7, 172.5, 180.9, 184.3

IR V_{max}: 3330 (N-H), 2932, 1662 (C=O), 1634 (C=O), 1593, 1516, 1368, 1273, 1217, 725 cm^{-1}

***N*-(3,4-dimethoxyphenethyl)-4-(3-hydroxy-1,4-dioxo-1,4-dihydronaphthalen-2-yl)butanamide** (**154**)

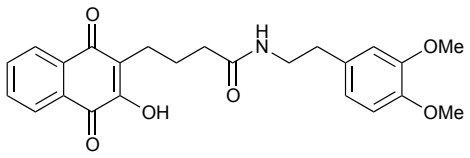

154 was prepared according to general procedure B from crude **149** (458 mg) and 3,4-dimethoxyphenethylamine (322 mg, 1.778 mmol) and the product purified by flash chromatography (100 % ethyl acetate) to give **154** as yellow solid in 5 % yield* (38 mg, 0.08879 mmol) with a melting point of 145 – 147 °C.

* Yield calculated as if acid **149** was a pure compound

^{1}H NMR δ ($CDCl_3$, 400 MHz): 1.86 (quin, *J* = 7.2 Hz, 2H), 2.18 (t, *J* = 7.2 Hz, 2H), 2.62 (t, *J* = 7.2 Hz, 2H), 2.77 (t, *J* = 7.0 Hz, 2H), 3.49 – 3.54 (m, 2H), 3.840 (s, 3H), 3.847 (s, 3H), 5.91 (t, *J* = 5.91 Hz, 1H), 6.71 – 6.74 (m, 2H), 6.78 – 6.80 (m, 1H), 7.66 (dt, *J* = 7.5, 1.2 Hz, 1H), 7.73 (dt, *J* = 7.5, 1.2 Hz, 1H), 8.05 - 8.08 (m, 2H), 8.30 (bs, 1H)

^{13}C NMR δ ($CDCl_3$, 100 MHz): 22.5, 24.3, 35.3, 35.9, 40.8, 56.00, 56.03, 111.4, 112.0, 120.8, 123.4, 126.3, 126.7, 129.8, 131.4, 132.8, 133.1, 134.8, 147.8, 149.1, 154.2, 173.1, 181.3, 185.0

IR V_{max}: 3274 (N-H), 2933, 1635 (C=O), 1592, 1516, 1349, 1262, 1235, 1157, 1140, 1026, 726 cm^{-1}

6.3.3 Synthesis of plastiquinone core and analogues

Trimethyl-*p*-benzoquinone (**5**)

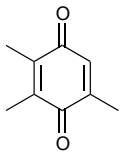

To a solution of trimethyl-*p*-hydroquinone (**157**) (518 mg, 3.405 mmol) in methanol (10 mL), iodine (47 mg, 0.1860 mmol) was added followed by 30% hydrogen peroxide (0.13 mL) and concentrated sulfuric acid (0.10 mL) and the mixture stirred at room temperature for 3 h before being diluted with diethyl ether (50 mL). The organic layer was washed with H_2O (3x 20 mL), sat. sodium thiosulfate (2x 40 mL), and brine (30 mL). The organic layer was dried over $MgSO_4$, filtered and the solvent removed under reduced pressure to afford the product **5** as a bright yellow crystalline solid in 80 % yield (411 mg, 2.738 mmol). Used without further purification.

^{1}H NMR δ ($CDCl_3$, 400 MHz): 1.91 (s, 3H), 1.93 (s, 3H), 1.95 (s, 3H), 6.46 (s, 1H)

^{13}C NMR δ ($CDCl_3$, 100 MHz): 11.9, 12.3, 15.8, 133.0, 140.6, 140.8, 1 45.2, 187.3, 187.7

Note: Spectral data consistent with that reported in the literature.[18]

4-(2,3,5-trimethyl-3,6-dioxocyclohexa-1,4-dien-1-yl)butanoic acid (**158**)

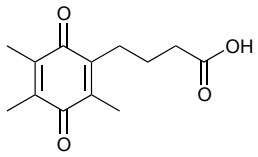

158 was prepared according to general procedure A from trimethyl-*p*-benzoquinone (**5**) (411 mg, 2.738 mmol) and glutaric acid (728 mg, 5.512 mmol) and the product purified by flash chromatography (100% dichloromethane followed by 100% ethyl acetate) to give **158** as a crystalline yellow solid in 33 % yield (216 mg, 0.9136 mmol) with a melting point of 56 – 57 °C.

^{1}H NMR δ ($CDCl_3$, 400 MHz): 1.69 (quin, *J* = 7.4 Hz, 2H), 1.95 (s, 6H), 1.98 (s, 3H), 2.36 (t, *J* = 7.4 Hz, 2H), 2.47 – 2.51 (m, 2H)

^{13}C NMR δ ($CDCl_3$, 100 MHz): 12.1, 12.35, 12.38, 23.5, 25.8, 33.7, 140.5, 140.6, 140.9, 143.1, 179.2, 187.0, 187.6

IR V_{max}: 2940, 1707 (C=O), 1642 (C=O), 1457, 1375, 1260, 1158, 717 cm^{-1}

(*S*)-*tert*-butyl-3-phenyl-2-(4-(2,4,5-trimethyl-3,6-dioxocyclohexa-1,4-dien-1-yl)butanamido)propanoate (**159**)

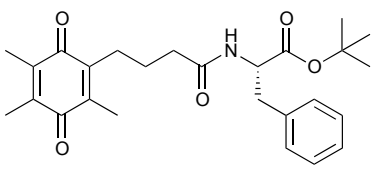

159 was prepared according to general procedure B from 4-(2,3,5-trimethyl-1,4-benzoquinone-1-yl)butanoic acid (**158**) (253 mg, 1.072 mmol) and L-phenylalanine *t*-butyl ester.HCl (284 mg, 1.105 mmol) and the product purified by flash chromatography (40 % ethyl acetate/hexane) to give **159** as yellow viscous oil in 24 % yield (111 mg, 0.2531 mmol).

^{1}H NMR δ ($CDCl_3$, 400 MHz): 1.41 (s, 9H), 1.71 (quin, *J* = 7.4 Hz, 2H), 2.01 (s, 6H), 2.02 (s, 3H), 2.22 (t, *J* = 7.4 Hz, 2H), 2.48 (t, *J* = 8.4 Hz, 2H), 3.09 – 3.11 (m, 2H), 4.77 (q, *J* = 6.7 Hz, 1H), 6.07 (d, *J* = 7.6 Hz, 1H), 7.15 – 7.29 (m, 5H)

^{13}C NMR δ ($CDCl_3$, 100 MHz): 12.2, 12.3, 12.4 24.3, 25.9, 28.0, 36.0, 38.1, 53.5, 82.3, 126.9, 128.4, 129.5, 136.3, 140.4, 140.6, 140.9, 143.4, 170.9, 171.7, 187.2, 187.7

$[\alpha]_D^{20}$: +47.24° (*c* 0.58, $CHCl_3$)

IR V_{max}: 3303 (N-H), 2978, 2933, 1738 (C=O), 1717 (C=O), 1645 (C=O), 1538, 1456, 1368, 1155, 701 cm^{-1}

(*S*)-3-phenyl-2-(4-(2,4,5-trimethyl-3,6-dioxocyclohexa-1,4-dien-1-yl)butanamido)propanoic acid (**160**)

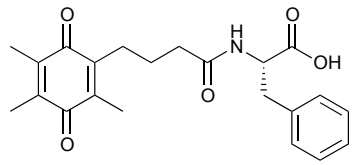

160 was prepared from the deprotection of **159** (87 mg, 0.1976 mmol), using general procedure C. The product was purified by flash chromatography (5 % methanol/ethyl acetate) to give **160** as brown solid in a quantitative yield with a melting point of 72 – 74°C.

^{1}H NMR δ ($CDCl_3$, 600 MHz): 1.54 – 1.60 (m, 2H), 1.89 (s, 3H), 1.90 (s, 3H), 1.91 (s, 3H), 2.16 (t, *J* = 7.1 Hz, 2H),

2.31 – 2.34 (m, 2H), 3.03 (dd, *J* = 14.0, 7.2 Hz, 1H), 3.18 (dd, *J* = 14.0, 5.1 Hz, 1H), 4.77 4.81 (m, 1H), 6.51 (d, *J* = 7.3 Hz, 1H), 7.08 – 7.09 (m, 2H), 7.13 – 7.20 (m, 3H)

^{13}C NMR δ ($CDCl_3$, 150 MHz): 12.2, 12.4, 12.5, 24.3, 25.7, 35.7, 37.2, 53.6, 127.4, 128.8, 129.3, 135.7, 140.5, 141.0, 141.4, 143.0, 174.2, 174.6, 187.6, 187.7

$[\alpha]_D^{20}$: +32.78° (*c* 1.88, $CHCl_3$)

IR V_{max}: 3355 (N-H), 2934, 1738 (C=O), 1717 (C=O), 1642 (C=O), 1539, 1456, 1375, 1206, 1172, 702 cm^{-1}

(*S*)-*N*-(1-hydroxy-3-phenylpropan-2-yl)-4-(2,4,5-trimethyl-3,6-dioxocyclohexa-1,4-dien-1-yl)butanamide (**161**)

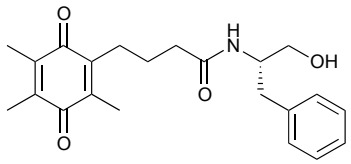

161 was prepared according to general procedure B from 4-(2,3,5-trimethyl-1,4-benzoquinone-1-yl)butanoic acid (**158**) (182 mg, 0.7692 mmol) and L-phenylalaninol (193 mg, 1.277 mmol) and the product purified by flash chromatography (2 % methanol/ethyl acetate) to give **161** as yellow viscous oil in 11 % yield (52 mg, 0.1352 mmol).

^{1}H NMR δ ($CDCl_3$, 400 MHz): 1.63 – 1.71 (m, 2H), 2.01 (s, 9H), 2.20 (t, *J* = 7.1 Hz, 2H), 2.24 (t, *J* = 7.8 Hz, 2H), 2.89 (t, *J* = 7.0 Hz, 2H), 3.59 (dd, *J* = 11.0, 5.2 Hz, 1H), 3.71 (dd, *J* = 11.0, 3.5 Hz, 1H), 4.19 – 4.27 (m, 1H), 6.14 (d, *J* = 7.8 Hz, 1H), 7.18 – 7.29 (m, 5H)

^{13}C NMR δ ($CDCl_3$, 100 MHz): 12.2, 12.41, 12.49, 24.4, 25.8, 36.2, 37.1, 52.9, 64.3, 126.6, 128.6, 129.2, 137.8, 140.4, 140.9, 141.1, 143.3, 173.0, 187.62, 187.63

$[\alpha]_D^{20}$: -26.91° (*c* 0.54, $CHCl_3$)

IR V_{max}: 3374 (N-H), 3299, 2936, 1642 (C=O), 1538, 1455, 1374, 1042, 845, 702 cm^{-1}

***N*-(4-hydroxyphenethyl)-4-(2,4,5-trimethyl-3,6-dioxocyclohexa-1,4-dien-1-yl)butanamide** (**162**)

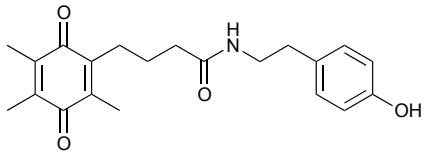

162 was prepared according to general procedure B from 4-(2,3,5-trimethyl-1,4-benzoquinone-1-yl)butanoic acid (**158**) (100 mg, 0.4240 mmol) and tyramine (66 mg, 0.4818 mmol) and the product purified by flash chromatography (90 % ethyl acetate/hexane) to give **162** as yellow viscous oil in 51 % yield (77 mg, 0.2158 mmol).

^{1}H NMR δ ($CDCl_3$, 400 MHz): 1.68 (quin, *J* = 7.4 Hz, 2H), 1.97 (s, 9H), 2.18 (t, *J* = 7.4 Hz, 2H), 2.41 – 2.45 (m, 2H), 2.72 (t, *J* = 7.0 Hz, 2H), 3.45 – 3.50 (m, 2H), 6.08 (t, *J* = 5.7 Hz, 1H), 6.75 (d, *J* = 8.3 Hz, 2H), 6.97 (d, *J* = 8.4 Hz, 2H), 7.54 (bs, 1H)

^{13}C NMR δ ($CDCl_3$, 100 MHz): 12.2, 12.42, 12.48, 24.5, 25.9, 34.7, 36.2, 41.0, 115.6, 129.7, 129.9, 140.4, 140.8, 141.1, 143.3, 155.3, 173.1, 187.5, 187.7

IR V_{max}: 3362 (N-H), 2937, 1641 (C=O), 1516, 1456, 1374, 1262, 832, 716 cm^{-1}

***N*-(3,4-dimethoxyphenethyl)-4-(2,4,5-trimethyl-3,6-dioxocyclohexa-1,4-dien-1-yl)butanamide** (**163**)

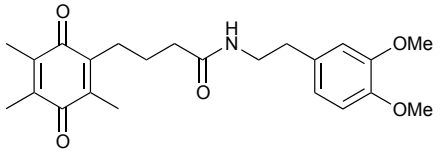

163 was prepared according to general procedure B from 4-(2,3,5-trimethyl-1,4-benzoquinone-1-yl)butanoic acid (**158**) (96 mg, 0.4053 mmol) and 3,4-dimethoxyphenethylamine (107 mg, 0.5926 mmol) and the product purified by flash chromatography (90 % ethyl acetate/hexane) to give **163** as yellow semi solid in 42 % yield (69 mg, 0.1717 mmol).

^{1}H NMR δ ($CDCl_3$, 400 MHz): 1.67 (quin, *J* = 7.7 Hz, 2H), 1.95 (s, 3H), 1.96 (s, 3H), 1.99 (s, 3H), 2.15 (t, *J* = 7.2 Hz, 2H), 2.41 – 2.45 (m, 2H), 2.73 (t, *J* = 7.0 Hz, 2H), 3.45 – 3.50 (m, 2H), 3.80 (s, 3H), 3.81 (s, 3H), 5.84 (t, *J* = 5.1 Hz, 1H), 6.68 – 6.70 (m, 2H), 6.75 (d, 8.6 Hz, 1H)

^{13}C NMR δ ($CDCl_3$, 100 MHz): 12.2, 12.3, 12.4, 24.4, 25.9, 35.5, 36.1, 40.7, 55.8, 55.9, 111.4, 111.9, 120.6, 131.4, 140.3, 140.6, 140.9, 143.3, 147.7, 149.0, 172.3, 187.3, 187.6

IR V_{max}: 3375 (N-H), 3300, 2936, 1642 (C=O), 1455, 1374, 1261, 1236, 1157, 1140, 1028, 846, 717 cm^{-1}

6.3.4 Synthesis of benzoquinone core and derivatives

2,6-dibromo-4-methylphenol (**169**)

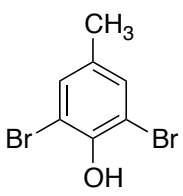

Bromine (9.5 mL, 29.63 g, 0.1854 mol) was added dropwise over 0.5 h to a solution of *p*-Cresol (**168**) (9.997 g, 0.0924 mol) in CH_2Cl_2 (30 mL) at 0 ^oC. The mixture was the stirred at room temperature for 5 h before quenching with sat. sodium metabisulfate (50 mL) and CH_2Cl_2 (50 mL). The organic layer was washed with sat. sodium metabisulfate (2 x 50 mL) and H_2O (3 x 50 mL). The organic layer was dried over $MgSO_4$, filtered and the solvent removed under reduced pressure to give the product **169** (24.86 g, 0.0935 mol) as a pale yellow coloured solid in a quantitative yield which required no further purification.

^1H NMR δ ($CDCl_3$, 400 MHz): 2.21 (s, 3H), 5.70 (s, 1H), 7.20 (s, 2H)

Spectral data consistent with data reported in the literature.[107]

3,5-dibromo-4-methoxytoluene (**170**)

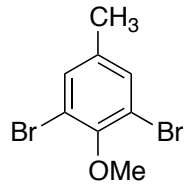

2,6-dibromo-4-methylphenol (**169**) (20.16 g, 0.0758 mol) was added to anhydrous DMF (150 mL) at room temperature under an atmosphere of N_2. To this solution, potassium carbonate (20.91 g, 0.1512 mol) and methyl iodide (5.62, 12.81 g, 0.0903 mol) was added successively and the mixture left stirring for 48 h before quenching with 100 mL H_2O. The mixture was extracted with 1:1 ethyl acetate/hexanes (3 x 100 mL) and the organic extract was washed with sat. $NaHCO_3$ (3 x 50 mL) and brine (3 x 50 mL). The organic layer was dried over $MgSO_4$, filtered and the solvent removed under reduced pressure to give the crude product which was filtered through a plug of silica (50 % ethyl acetate/ hexanes) to give the pure product **170** as a pale yellow oil in 90 % yield (19.21 g, 0.0686 mol)

^1H NMR δ ($CDCl_3$, 400 MHz): 2.24 (s, 3H), 3.83 (s, 3H), 7.27 (s, 2H)

Spectral data consistent with data reported in the literature.[154]

3,4,5-Trimethoxytoluene (**167**)

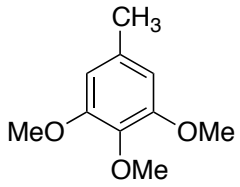

Sodium metal (15.76 g, 0.6854 mol) was added to methanol (150 mL) at room temperature, after complete formation of sodium methoxide, copper iodide (39.28 g, 0.2062 mol) was added followed by a solution of 3,5-dibromo-4-methoxytoluene (**170**) (19.21 g, 0.0686 mol) in DMF (50 mL) and the mixture heated to 110^{o}C o/n. The reaction mixture was quenched with saturated ammonium chloride (100 mL) and the mixture extracted with 1:1 ethyl acetate/hexanes (4 x 50 mL). The organic extract was washed with sat. $NaHCO_3$ (3 x 50 mL) and brine (3 x 50 mL). The organic layer was dried over $MgSO_4$, filtered and the solvent removed under reduced pressure to give the crude product which was purified by flash column chromatography (20 % ethyl acetate/hexanes) to give a mixture of 3,4,5-trimethoxytoluene (**167**) and 3,4-dimethoxytoluene (**171**) in a 3:2 ratio as a pale yellow oil in 71 % yield (8.897 g, 0.0488 mol).

^{1}H NMR δ ($CDCl_3$, 400 MHz): 2.30 (s, 3H), 3.81 (s, 3H), 3.83 (s, 3H), 6.38 (s, 3H)

^{13}C NMR δ ($CDCl_3$, 100 MHz): 21.9, 56.1, 60.9, 106.0, 133.6, 135.9, 153.1

Spectral data consistent with that reported in the literature.[155]

2,3-Dimethoxy-5-methyl-*p*-benzoquinone (**6**)

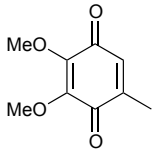

Trimethoxytoluene (**167**) (1.0548 g, 5.789 mmol) was added to 1.4 mL formic acid and 0.7 mL acetic acid. 35 % Hydrogen peroxide (2.1 mL) was added dropwise and the solution heated to 35 ^{o}C for 2 h. The reaction mixture was cooled and diluted with H_2O (15 mL) and extracted with 3 x 20 mL CH_2Cl_2.

The organic extract was washed with sat. $NaHCO_3$ (3 x 20 mL) and H_2O (3 x 20 mL). The organic layer was dried over $MgSO_4$, filtered and the solvent removed under reduced pressure to give the crude product which was purified by flash column chromatography (30 % ethyl acetate/hexanes) to give the pure product **6** as a bright yellow solid in 55 % yield (0.585 g, 3.212 mmol).

^{1}H NMR δ ($CDCl_3$, 400 MHz): 2.03 (d, *J* = 1.6 Hz, 3H), 3.99 (s, 3H), 4.01 (s, 3H), 6.42 (q, *J* = 1.6 Hz, 1H)

^{13}C NMR δ ($CDCl_3$, 100 MHz): 15.5, 61.2, 61.3, 131.3, 144.1, 144.9, 145.1, 184.2, 184.4

Spectral data consistent with that reported in the literature.[109]

4-(4,5-dimethoxy-2-methyl-3,6-dioxocyclohexa-1,4-dien-1-yl)butanoic acid (**166**)

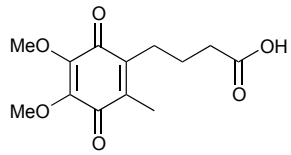

166 was prepared according to general procedure A from 2,3-dimethoxy-1,4-benzoquinone (**6**) (478 mg, 2.622 mmol) and glutaric acid (756 mg, 5.724 mmol) and the product purified by flash chromatography (30 % ethyl acetate/hexanes followed by 100% ethyl acetate) to give **166** as a yellow oil in 25 % yield (177 mg, 0.6598 mmol).

^{1}H NMR δ ($CDCl_3$, 400 MHz): 1.70 (quin, *J* = 7.7 Hz, 2H), 1.99 (s, 3H), 2.37 (t, *J* = 7.1 Hz, 2H), 2.47 – 2.51 (m, 2H), 3.94 (s, 6H)

^{13}C NMR δ ($CDCl_3$, 100 MHz): 11.9, 23.4, 25.6, 33.5, 61.21, 61.22, 139.6, 141.7, 144.41, 144.47, 178.5, 184.0, 184.5

IR V_{max}: 3340 (-OH), 2950, 1706 (C=O), 1649 (C=O), 1611, 1456, 1266, 1206, 1154, 1105, 1059, 745 cm^{-1}

(*S*)-*tert*-butyl-2-(4-(4,5-dimethoxy-2-methyl-3,6-dioxocyclohexa-1,4-dien-1-yl)butanamido)-3-phenylpropanoate (**172**)

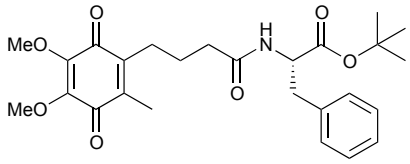

172 was prepared according to general procedure B from 4,5-dimethoxy-2-methyl-3,6-dioxocyclohexa-1,4-dien-1-yl)butanoic acid **166** (101 mg, 0.3761 mmol) and L-phenylalanine *t*-butyl ester.HCl (108 mg, 0.4190 mmol) and the product purified by flash chromatography (40 % ethyl acetate/hexane) to give **172** as yellow viscous oil in 12 % yield (21 mg, 0.0437 mmol).

^{1}H NMR δ ($CDCl_3$, 400 MHz): 1.40 (s, 9H), 1.70 (quin, *J* = 7.5 Hz, 2H), 2.00 (s, 3H), 2.21 (t, *J* = 7.5 Hz, 2H), 2.43 – 2.47 (m, 2H), 3.08 (d, *J* = 6.0 Hz, 2H), 3.98 (s, 6H), 4.72 – 4.77 (m, 1H), 5.96 (d, *J* = 7.6 Hz, 1H), 7.13 – 7.28 (m, 5H)

^{13}C NMR δ ($CDCl_3$, 100 MHz): 12.0, 24.3, 25.7, 28.0, 36.0, 38.2, 53.5, 61.2 (2 x C), 82.5, 127.0, 128.5, 129.5, 136.3, 139.6, 142.0, 144.50, 144.57, 170.9, 171.7, 184.2, 184.6

$[\alpha]_D^{20}$: +40.78° (*c* 0.25, $CHCl_3$)

IR V_{max}: 3369 (N-H), 2978, 2940, 1729 (C=O), 1652 (C=O), 1647, 1611, 1456, 1368, 1266, 1205, 1153, 1055, 701 cm^{-1}

(*S*)-2-(4-(4,5-dimethoxy-2-methyl-3,6-dioxocyclohexa-1,4-dien-1-yl)butanamido)-3-phenylpropanoic acid (**173**)

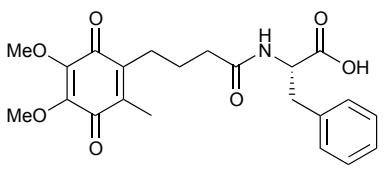

173 was prepared from the deprotection of **172** (11 mg, 0.0231 mmol), using general procedure C. The product was purified by flash chromatography (5 % methanol/ethyl acetate) to give **173** as yellow viscous oil in 84 % yield (8 mg, 0.0195 mmol).

^{1}H NMR δ (MeOD, 400 MHz):	1.59 (quin, *J* = 7.7 Hz, 2H), 1.93 (s, 3H), 2.13 – 2.25 (m, 2H), 2.28 – 2.44 (m, 2H), 2.92 (dd, *J* = 14.0, 9.4 Hz, 1H), 3.22 (dd, *J* = 14.0, 5.0 Hz, 1H), 3.952 (s, 3H), 3.955 (s, 3H), 4.67 (dd, *J* = 9.4, 5.0 Hz, 1H), 7.15 – 7.27 (m, 5H)
^{13}C NMR δ (MeOD, 150 MHz):	12.2, 25.9, 26.8, 36.6, 38.7, 55.3, 61.8, 61.9, 128.0, 129.7, 130.5, 138.9, 140.9, 143.4, 146.1, 146.2, 175.1, 175.5, 185.7, 186.2
$[\alpha]_D^{20}$:	+57.27° (*c* 0.22, $CHCl_3$)
IR V_{max}:	3350 (N-H), 2947, 1733 (C=O), 1652 (C=O), 1645 (C=O), 1611, 1456, 1266, 1204, 1153, 1055, 735, 702 cm^{-1}

(*S*)-4-(4,5-dimethoxy-2-methyl-3,6-dioxocyclohexa-1,4-dien-1-yl)-*N*-(1-hydroxy-3-phenylpropan-2-yl)butanamide (**174**)

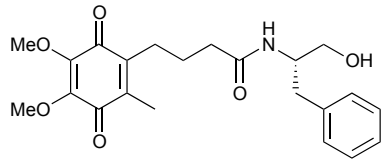

174 was prepared according to general procedure B from 4,5-dimethoxy-2-methyl-3,6-dioxocyclohexa-1,4-dien-1-yl)butanoic acid (**166**) (77 mg, 0.2818 mmol) and L-phenylalaninol (102 mg, 0.6779 mmol) and the product purified by flash chromatography (2 % methanol/ethyl acetate) to give **174** as yellow oil in 17 % yield (19 mg, 0.0483 mmol).

^{1}H NMR δ ($CDCl_3$, 400 MHz): 1.68 (quin, *J* = 7.4 Hz, 2H), 1.99 (s, 3H), 2.17 (t, *J* = 7.4 Hz, 2H), 2.39 – 2.43 (m, 2H), 2.87 (t, *J* = 6.5 Hz, 2H), 3.58 (dd, *J* = 11.0, 5.1 Hz, 1H), 3.71 (dd, *J* = 11.0, 3.5 Hz, 1H), 3.97 (s, 3H), 3.98 (s, 3H), 4.18 – 4.22 (m, 1H), 5.91 (d, *J* = 7.5 Hz, 1H), 7.18 – 7.21 (m, 3H), 7.27 – 7.29 (m, 2H)

^{13}C NMR δ ($CDCl_3$, 100 MHz): 12.0, 24.3, 25.5, 36.0, 37.1, 53.0, 61.3 (2 x C), 64.3, 126.7, 128.7, 129.3, 137.8, 139.8, 141.9, 144.4, 144.6, 172.8, 184.55, 184.56

$[\alpha]_D^{20}$: -42.76° (*c* 0.29, $CHCl_3$)

IR V_{max}: 3356 (N-H), 3293, 2942, 1645 (C=O), 1610, 1456, 1265, 1205, 1045, 702 cm^{-1}

4-(4,5-dimethoxy-2-methyl-3,6-dioxocyclohexa-1,4-dien-1-yl)-*N*-(4-hydroxyphenethyl) butanamide (**175**)

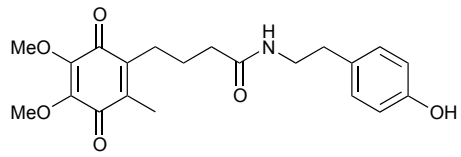

175 was prepared according to general procedure B from 4,5-dimethoxy-2-methyl-3,6-dioxocyclohexa-1,4-dien-1-yl)butanoic acid **166** (85 mg, 0.3161 mmol) and tyramine (48 mg, 0.3477 mmol) and the product purified by flash chromatography (2 % methanol/ethyl acetate) to give **175** as yellow viscous oil in 13 % yield (16 mg, 0.0413 mmol).

^{1}H NMR δ ($CDCl_3$, 400 MHz): 1.70 (quin, *J* = 7.4 Hz, 2H), 2.01 (s, 3H), 2.17 (t, *J* = 7.4 Hz, 2H), 2.43 – 2.47 (m, 2H), 2.75 (t, *J* = 7.0 Hz, 2H), 3.47 – 3.52 (m, 2H), 3.987 (s, 3H), 3.988 (s, 3H), 5.26 (bs, 1H), 5.62 (d, *J* = 4.9 Hz, 1H), 6.76 (d, *J* = 8.5 Hz, 2H), 7.04 (d, *J* = 8.5 Hz, 2H),

^{13}C NMR δ ($CDCl_3$, 150 MHz): 12.1, 24.4, 25.7, 34.7, 35.9, 41.1, 61.3 (2 x C), 115.6, 129.9, 130.4, 139.9, 141.8, 144.4, 144.6, 154.8, 172.9, 184.58, 184.59

IR V_{max}: 3348 (N-H), 3281, 2944, 1652 (C=O), 1645 (C=O), 1611, 1516, 1456, 1265, 1204, 1053, 844, 737 cm^{-1}

4-(4,5-dimethoxy-2-methyl-3,6-dioxocyclohexa-1,4-dien-1-yl)-*N*-(3,4-dimethoxyphenethyl) butanamide (**176**)

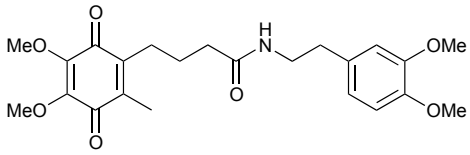

176 was prepared according to general procedure B from 4,5-dimethoxy-2-methyl-3,6-dioxocyclohexa-1,4-dien-1-yl)butanoic acid **166** (96 mg, 0.3590 mmol) and 3,4-dimethoxyphenethylamine (107 mg, 0.5926 mmol) and the product purified by flash chromatography (90 % ethyl acetate/hexane) to give **176** as yellow viscous oil in 16 % yield (25 mg, 0.0586 mmol).

^{1}H NMR δ ($CDCl_3$, 400 MHz): 1.71 (quin, *J* = 7.4 Hz, 2H), 2.02 (s, 3H), 2.17 (t, *J* = 7.4 Hz, 2H), 2.44 – 2.68 (m, 2H), 2.77 (t, *J* = 7.0 Hz, 2H), 3.49 – 3.53 (m, 2H), 3.85 (s, 3H), 3.86 (s, 3H), 3.98 (s, 6H), 5.61 (t, *J* = 5.1 Hz, 1H), 6.72 – 6.74 (m, 2H), 6.79 – 6.81 (m, 1H)

^{13}C NMR δ ($CDCl_3$, 100 MHz): 12.1, 24.4, 25.7, 35.3, 36.1, 40.8, 56.01, 56.05, 61.2, 61.3, 111.5, 112.0, 120.7, 131.4, 139.7, 141.9, 144.4, 144.5, 147.8, 149.2, 172.2, 184.4, 184.5

IR V_{max}: 3371 (N-H), 3302, 2938, 1652 (C=O), 1645 (C=O), 1645, 1516, 1455, 1263, 1237, 1156, 1028, 846 cm^{-1}

(*S*)-*tert*-butyl 3-phenyl-2-(4-phenylbutanamido)propanoate (**178**)

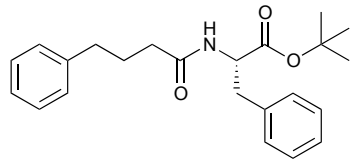

178 was prepared according to general procedure B from phenybutyric acid **177** (122 mg, 0.7442 mmol) and L-phenylalanine *t*-butyl ester.HCl (166 mg, 0.6452 mmol) to give **178** as clear oil in 81 % yield (192 mg, 0.5211 mmol) with no further purification required.

^{1}H NMR δ ($CDCl_3$, 400 MHz): 1.44 (s, 9H), 1.96 (quin, *J* = 7.5 Hz, 2H), 2.19 – 2.23 (m, 2H), 2.63 (t, *J* = 7.5 Hz, 2H), 3.06 – 3.16 (m, 2H), 4.80 – 4.85 (m, 1H), 6.13 (d, *J* = 7.8 Hz, 1H), 7.16 – 7.31 (m, 10H)

^{13}C NMR δ ($CDCl_3$, 100 MHz): 26.9, 27.9, 35.0, 35.6, 38.1, 53.3, 82.2, 125.8, 126.8, 128.3 (2 x C), 128.4, 129.4, 136.2, 141.4, 170.9, 172.1

$[\alpha]_D^{20}$: +55.74° (*c* 1.83, $CHCl_3$)

IR V_{max}: 3299 (N-H), 2978, 2931, 1735 (C=O), 1649 (C=O), 1534, 1496, 1454, 1367, 1225, 1154, 743, 699 cm^{-1}

6.3.5 Synthesis of indoloquinone core and derivatives

2-Bromohydroquinone (**194**)

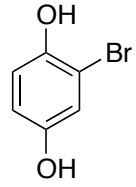

Bromine (2.85 mL, 0.0553 mol) was added to a solution of hydroquinone (**193**) (5.088 g, 0.0462 mmol) in diethyl ether (40 mL) at –13 °C and

maintained under these conditions for 2 h. The reaction quenched with H_2O (20 mL) and the organic layer washed with sat. sodium thiosulfate (4 x 20 mL) and H_2O (3 x 20 mL). The organic layer was dried over $MgSO_4$, filtered and the solvent removed under reduced pressure to give the product **194** as a light brown solid in 98% yield (8.516 g, 0.0451 mol), which was deemed pure by ^{1}H NMR and ^{13}C NMR and used without further purification.

^{1}H NMR δ ($CDCl_3$, 400 MHz): 6.70 (dd, *J* = 8.7, 2.9 Hz, 1H), 6.84 (d, *J* = 8.7 Hz, 1H), 6.99 (d, *J* = 2.9 Hz, 1H)

^{13}C NMR δ ($CDCl_3$, 100 MHz): 109.2, 115.3, 116.7, 119.0, 146.8, 150.8

Spectral data consistent with data reported in the literature.[114]

2-Bromo-1,4-dimethoxybenzene (**195**)

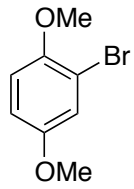

2-Bromohydroquinone (**194**) was added to NaH (60% suspension in mineral oil, 7.444 g, 0.1861 mol) in DMF (120 mL) and stirred at room temperature for 10 mins before cooling to 0 °C. Methyl Iodide (8.0 mL, 18.25 g, 0.1285 mol) was added dropwise and the mixture maintained at 0 °C for 0.5 h before warming to room temperature for 3 h. The mixture was diluted with H_2O and extracted with ethyl acetate/hexanes (1:1 v/v) and the organic extract washed with H_2O (2 x 30 mL). The organic layer was dried over $MgSO_4$, filtered and the solvent removed under reduced pressure to give the **195** as white crystals in a pale brown oil (12.24 g, 0.0564 mol). The product was taken through to the next step without purification.

^{1}H NMR δ ($CDCl_3$, 400 MHz): 3.73 (s, 3H), 3.82 (s, 3H), 6.77 – 6.83 (m, 2H), 7.11 (d, *J* = 2.5 Hz, 1H)

^{13}C NMR δ ($CDCl_3$, 100 MHz): 55.9, 56.8, 112.0, 112.9, 113.6, 119.0, 150.3, 154.0

Spectral data consistent with data reported in the literature.[156]

2,5-Dimethoxybenzaldehyde (1**83**)

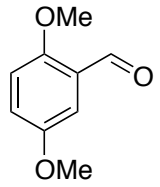

Without purification 2-Bromo-1,4-dimethoxybenzene (**195**) (11.03 g, 0.0508 mol) and butyl lithium (51 mL, 0.068 mol, 1.33 M) were combined in dry THF (60 mL) at – 78 °C under an N_2 atmosphere. DMF (17 mL) was added dropwise and the mixture warmed to room temperature and stirred for 3 h before quenching with H_2O (50 mL). The mixture was extracted with diethyl ether (3 x 50 mL) and the organic layer was washed with sat. $NaHCO_3$ (3 x 50 mL) and brine (2 x 50 mL). The organic layer was dried over $MgSO_4$, filtered and the solvent removed under reduced pressure to give the crude product, which was purified by flash chromatography (20 % ethyl acetate/hexanes) to give **183** as a pale yellow solid in 63 % yield (5.341 g, 0.0321 mol).

^{1}H NMR δ ($CDCl_3$, 400 MHz): 3.80 (s, 3H), 3.89 (s, 3H), 6.94 (d, *J* = 9.1 Hz, 1H), 7.13 (dd, *J* = 9.0, 3.3 Hz, 1H), 7.33 (d, *J* = 3.3 Hz, 1H), 10.44 (s, 1H)

^{13}C NMR δ ($CDCl_3$, 100 MHz): 55.9, 56.3, 110.5, 113.5, 123.6, 125.1, 153.7, 156.8, 189.7

Spectral data consistent with data reported in the literature.[118]

Methyl-2-azidoacetate (**184**)

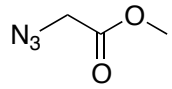

Sodium azide (10.988 g, 0.1690 mol) was added to methyl 2-bromoacetate (8.0 mL, 12.93 g, 0.0841 mol) in acetone:water (3:1, 160 mL). The solution was stirred at room temperature for 1 h before being diluted with water (100

mL), and extracted with diethyl ether (3 x 40 mL). The combined organic fractions were dried with $MgSO_4$, filtered and concentrated *in vacuo* to produce 184 as a colourless oil in 93 % yield (9.053 g, 0.0787 mol) and used without further purification.

^{1}H NMR δ ($CDCl_3$, 400 MHz): 3.80 (S, 3H), 3.88 (S, 2H)

^{13}C NMR δ ($CDCl_3$, 100 MHz): 50.4, 52.7, 168.8

2-Azido-3-(2,5-dimethoxyphenyl)-2-methyl propanoate (**185**)

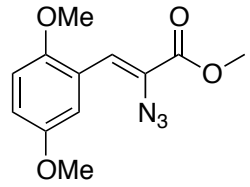

2,5-Dimethoxybenzaldehyde (**183**) (3.027 g, 18.22 mmol) was added to a solution of methyl-2-azidoacetate (**184**) (5.201 g, 45.19 mmol) in dry methanol (20 mL). The mixture was cooled to -8^{o}C and a solution of sodium methoxide (sodium metal (1.046 g, 45.37 mmol) in 20 mL of methanol) was added and stirred for 10 min before minimal THF was added until all starting material had dissolved. The mixture was stirred at –8 ^{o}C for 1.5 h and then left at 2 ^{o}C for 16 h without stirring. The yellow suspension was poured into ice-cold ammonium chloride (100 mL) and the precipitate formed was filtered and washed with ice cold H_2O (3 x 30 mL). The solid was dissolved in CH_2Cl_2, dried with $MgSO_4$, filtered filtered and the solvent removed under reduced pressure to give **185** as a yellow crystals in 59 % yield (2.836 g, 10.77 mmol) which was determined to be pure by HNMR and CNMR.

^{1}H NMR δ ($CDCl_3$, 400 MHz): 3.81 (s, 3H), 3.82 (s, 3H), 3.90 (s, 3H), 6.81 (d, *J* = 9.0 Hz, 1H), 6.87 (dd, *J* = 9.0, 3.0 Hz, 1H), 7.36 (s, 1H), 7.81 (d, *J* = 3.0 Hz, 1H)

^{13}C NMR δ ($CDCl_3$, 100 MHz): 52.9, 55.9, 56.3, 111.6, 115.9, 116.3, 119.4, 122.7, 125.3, 152.3, 153.2, 164.3

4,7-Dimethyoxy-1*H*-indole-2-methyl methanoate (**186**)

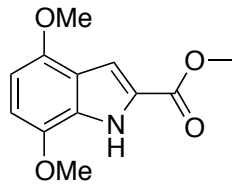

2-Azido-3-(2,5-Dimethoxyphenyl)-2-methyl propanoate (**185**) (5.923 g, 22.49 mmol) was heated in toluene (100 mL) at reflux for 5 h. The product was concentrated *in vacuo* to produce the crude yellow product which was washed with acetonitrile to produce **186** as a white powdery solid in 94% yield (4.968 g, 21.12 mmol).

^{1}H NMR δ ($CDCl_3$, 400 MHz): 3.90 (s, 3H), 3.91 (s, 3H), 3.92 (s, 3H), 6.35 (d, *J* = 8.3 Hz, 1H), 6.58 (d, *J* = 8.3 H, 1H), 7.30 (d, *J* = 2.0 Hz, 1H), 9.10 (bs, 1H)

^{13}C NMR δ ($CDCl_3$, 100 MHz): 52.0, 55.7, 55.8, 99.1, 104.4, 106.9, 120.2, 126.0, 129.2, 141.1, 148.7, 162.2

4,7-dimethoxy-1*H*-indole-2-carboxylic acid (**187**)

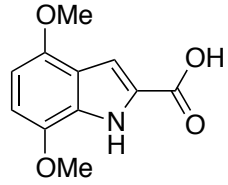

4,7-dimethyoxy-1*H*-indole-2-methyl methanoate (**186**) (832 mg, 3.560 mmol) was added to an aqueous solution of 10% sodium hydroxide (20 mL). The mixture was refluxed for 1 h and cooled in an ice-bath at 0^{o}C and neutralised with 6 M HCl. The mixture was filtered and the solid washed with H_2O and collected by dissolution in ethyl acetate. The mixture was dried with $MgSO_4$ and concentrated *in vacuo* to produce **187** as an off white solid in 60 % yield (470 mg, 2.124 mmol). Used without further purification.

^{1}H NMR δ ($CDCl_3$, 400 MHz): 3.91 (s, 3H), 3.93 (s, 3H), 6.36 (d, *J* = 8.3 Hz, 1H), 6.62 (d, *J* = 8.3 Hz, 1H), 7.44 (d, *J* = 2.3 Hz, 1H), 9.06 (bs, 1H)

^{13}C NMR δ ($CDCl_3$, 150 MHz): 55.7, 55.9, 99.2, 105.0, 108.8, 120.4, 125.1, 129.8, 141.1, 148.1, 166.1

Spectral data consistent with data reported in the literature.[121]

4,7-Dimethoxy-1*H*-indole (**182**)

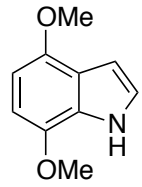

4,7-Dimethoxy-1*H*-indole-2-carboxylic acid (**187**) (470 g, 2.124 mmol) was added to quinoline (1.3 mL, 11.23 mmol) and copper (779 mg) and heated under nitrogen at 200°C for 4.5 h. The reaction mixture was quenched with sat. $KHSO_4$ (40 mL) and extracted with diethyl ether (3 x 40 mL), the organic extract was washed with sat. $KHSO_4$ (3x 40 mL) and dried over $MgSO_4$, filtered and the solvent removed under reduced pressure to give the product which was purified by flash chromatography (100 % dichloromethane) to give **182** as white cubic crystals in 61 % yield (229 mg, 1.290 mmol).

^{1}H NMR δ ($CDCl_3$, 400 MHz): 3.92 (s, 6H), 6.39 (d, *J* = 8.3 Hz, 1H), 6.51 (d, *J* = 8.3 Hz, 1H), 6.63 (t, *J* = 2.6 Hz, 1H) 7.11 (t, *J* = 2.6 Hz, 1H), 8.37 (bs, 1H)

^{13}C NMR δ ($CDCl_3$, 100 MHz): 55.7 (2 x C), 98.9, 100.4, 101.6, 120.0, 122.6, 127.7, 141.2, 147.8

Spectral data consistent with data reported in the literature.[121]

4,7-Dimethoxy-1*H*-indole-3-carbaldehyde (**188**)

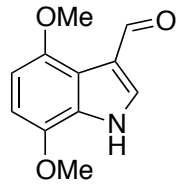

Phosphporous oxychloride (690 mg, 4.506 mmol) was added dropwise to DMF (2.5 mL) at room temperature and stirred for 0.25 h. This mixture was

diluted with DMF (5 mL) before 4,7-dimethoxyindole (**182**) (406 mg, 2.293 mmol) was added and the reaction mixture left stirring for 15h before quenching slowly with sat. $NaHCO_3$ solution (90 mL). The aqueous reaction mixture was cooled to 2 ^oC for 16 h resulting in crystallization of the product as large pale yellow crystalline needles which were filtered and washed with chilled H_2O yielding **188** as a pure solid in 70 % yield (329 mg, 1.601 mmol)

^1H NMR δ (DMSO – D6, 600 MHz): 3.87 (s, 3H), 3.88 (s, 3H), 6.62 (d, *J* = 8.4 Hz, 1H), 6.67 (d, *J* = 8.4 Hz, 1H), 7.89 (s, 1H), 10.30 (s, 1H), 12.39 (s, 1H)

^{13}C NMR δ (DMSO – D6, 150 MHz): 55.5, 55.6, 101.7, 102.9, 117.1, 118.6, 127.6, 129.0, 141.2, 147.8, 186.3

Spectral data consistent with data reported in the literature.[124]

(*E*)-Ethyl 3-(4,7-dimethoxy-1*H*-indol-3-yl)acrylate (**189**)

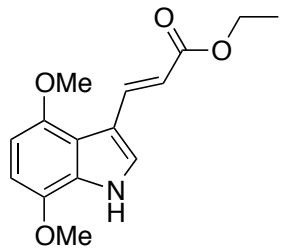

Triethyl phosphonoacetate (316 mg, 1.411 mmol) was added dropwise to a solution of sodium hydride (60 mg, 2.505 mmol) in anhydrous THF (5 mL) at 0°C before warming to room temperature for 0.25 h. The reaction mixture was then cooled to 0°C and 4,7-dimethoxyindole-3-aldehyde (**188**) (206 mg, 0.9921 mmol) was added and the reaction mixture stirred at room temperature for 16 h. The mixture was quenched with brine (30 mL) and extracted with ethyl acetate (3x 20 mL). The organic layer was dried over $MgSO_4$, filtered and the solvent removed under reduced pressure to give the product which was purified by flash chromatography (20 % ethyl acetate/hexanes) to give **189** as cream coloured needles in 27 % yield (73 mg, 0.2662 mmol).

^{1}H NMR δ ($CDCl_3$, 400 MHz): 1.33 (t, *J* = 7.2 Hz, 3H), 3.89 (s, 3H), 3.91 (s, 3H), 4.26 (q, *J* = 7.1 Hz, 2H), 6.41 (d, *J* = 16.0 Hz, 1H), 6.44 (d, *J* = 8.4 Hz, 1H), 6.53 (d, *J* = 8.4 Hz, 1H), 7.45 (d, *J* = 2.3 Hz, 1H), 8.30 (d, *J* = 16.0 Hz, 1H), 8.79 (bs, 1H)

^{13}C NMR δ ($CDCl_3$, 100 MHz): 14.5, 55.6, 55.8, 60.0, 100.6, 102.6, 114.0, 114.6, 117.4, 123.9, 128.5, 139.4, 141.0, 149.0, 168.3

Methyl 4,7-dioxo-4,7-dihydro-1*H*-indole-2-carboxylate (**196**)

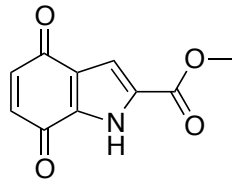

[Bis(trifluoroacetoxy)iodo]benzene (281.2 mg, 0.6539 mmol) was added to a solution of **186** (95.6 mg, 0.4064 mmol) in H_2O (2 mL) and MeOH (25µL) and stirred at r.t for 1 h. The reaction mixture was diluted with H_2O (10 mL) and extracted with CH_2Cl_2 (3 x 15 mL) and the organic extract washed with H_2O (3 x 10 mL), dried over $MgSO_4$, filtered and the solvent removed under reduced pressure. The product was purified by flash chromatography (20 % ethyl acetate/ dichloromethane) to give **196** as yellow viscous oil in 45 % yield (37.4 mg, 0.2662 mmol).

^{1}H NMR δ ($CDCl_3$, 400 MHz): 3.95 (s, 3H), 6.72 (d, *J* = 3.7 Hz, 2H), 7.23 (d, *J* = 1.7 Hz, 1H)

^{13}C NMR δ ($CDCl_3$, 150 MHz): 52.7, 112.4, 125.6, 128.2, 132.5, 136.4, 139.1, 160.6, 177.7, 182.3

IR V_{max}: 3254 (N-H), 1708 (C=O), 1658 (C=O), 1442, 1318, 1214, 840, 761 cm^{-1}

Spectral data consistent with data reported in the literature.[128]

Dimethyl-4,4',7,7'-tetraoxo-4,4',7,7'-tetrahydro-1*H*,1'*H*-[3,3'-biindole]-2,2'-dicarboxylate (**201**)

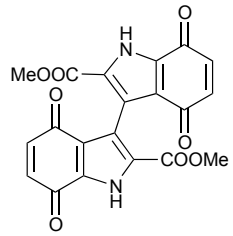

Cerric ammonium nitrate (CAN) (367 mg, 0.6610 mmol) in H_2O (1 mL) was added to a solution of Indole ester **186** (66 mg, 0.2801 mmol) in 1:1 acetonitrile/H_2O (2 mL) and stirred at room temperature for 3 h. The reaction mixture was diluted with H_2O (10 mL) and extracted with CH_2Cl_2 (3 x 20 mL) and dried over $MgSO_4$, filtered and the solvent removed under reduced pressure. The product was purified by flash chromatography (80 % ethyl acetate/ hexanes) to give **201** as yellow viscous oil in 74 % yield (42 mg, 0.1038 mmol).

^{1}H NMR δ (CD_3OD, 600 MHz): 3.71 (s, 3H), 6.57 (d, *J* = 10.3 Hz, 1H), 6.69 (d, *J* = 10.3 Hz, 1H)

^{13}C NMR δ (CD_3OD, 150 MHz): 52.3, 120.5, 124.4, 127.6, 133.4, 137.4, 139.9, 162.0, 179.1, 184.2

HRESIMS [M+Na]: For $C_{20}H_{12}N_2O_8Na$, predicted 431.0486, found 431.0487

(*S*)-*tert*-butyl-2-(4,7-dimethoxy-1*H*-indole-2-carboxamido)-3-phenylpropanoate (**206**)

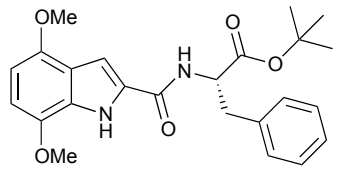

206 was prepared according to general procedure B from 4,7-dimethoxyindole-2-carboxylic acid **187** (98 mg, 0.4417 mmol) and L-phenylalanine *t*-butyl ester.HCl (131 mg, 0.5084 mmol) and the product

purified by flash chromatography (40 % ethyl acetate/hexanes) to give **206** as clear viscous oil in 50 % yield (94 mg, 0.2219 mmol).

^{1}H NMR δ ($CDCl_3$, 400 MHz):	1.43 (s, 9H), 3.19 – 3.28 (m, 2H), 3.89 (s, 6H), 4.98 – 5.03 (m, 1H), 6.35 (d, *J* = 8.2 Hz, 1H), 6.56 (d, *J* = 8.2 Hz, 1H), 6.77 (d, *J* = 7.7 Hz, 1H), 6.97 (d, *J* = 1.7 Hz, 1H), 7.19 – 7.29 (m, 5H), 9.53 (bs, 1H)
^{13}C NMR δ ($CDCl_3$, 100 MHz):	28.0, 38.3, 53.6, 55.6, 55.8, 82.6, 98.9, 100.8, 103.8, 120.1, 127.0, 128.4, 128.6, 129.2, 129.7, 136.1, 141.3, 148.3, 160.7, 170.5
$[\alpha]_D^{20}$:	+61.05° (*c* 0.66, $CHCl_3$)
IR V_{max}:	3277 (N-H), 2934, 1727 (C=O), 1643 (C=O), 1527, 1367, 1262, 1225, 1153, 1096, 740 cm^{-1}

(*S*)-*tert*-Butyl-2-(4,7-dioxo-4,7-dihydro-1*H*-indole-2-carboxamido)-3-phenylpropanoate (**207**)

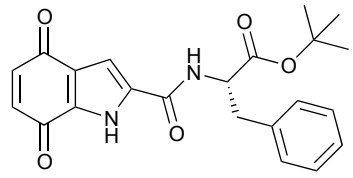

[Bis(trifluoroacetoxy)iodo]benzene (61 mg, 0.1411 mmol) was added to a solution of **206** (33 mg, 0.0773 mmol) in H_2O (1 mL) and MeOH (25µL) and stirred at r.t for 1 h. The reaction mixture was diluted with H_2O (10 mL) and extracted with CH_2Cl_2 (3 x 15 mL) and the organic extract washed with H_2O (3 x 10 mL), dried over $MgSO_4$, filtered and the solvent removed under reduced pressure. The product was purified by flash chromatography (45 % ethyl acetate/dichloromethane) to give **207** as yellow viscous oil in 25 % yield (8 mg, 0.0195 mmol).

^{1}H NMR δ ($CDCl_3$, 400 MHz): 1.44 (s, 9H), 3.25 (d, *J* = 5.6 Hz, 2H), 5.00 – 5.05 (m, 1H), 6.61 (s, 2H), 6.81 (d, *J* = 7.5 Hz, 1H), 6.93 (s, 1H), 7.17 – 7.29 (m, 5H), 10.91 (bs, 1H)

^{13}C NMR δ ($CDCl_3$, 150 MHz): 28.1, 38.1, 53.8, 83.2, 106.9, 125.7, 127.4, 128.7, 129.6, 131.1, 132.0, 135.8, 136.5, 138.7, 158.9, 170.2, 177.4, 182.6

$[\alpha]_D^{20}$: +144.76° (*c* 0.10, $CHCl_3$)

IR V_{max}: 3166 (N-H), 2977, 1717 (C=O), 1653 (C=O), 1646 (C=O), 1558, 1484, 1367, 1274, 1154, 839, 700 cm^{-1}

(*S*)-2-(4,7-Dioxo-4,7-dihydro-1*H*-indole-2-carboxamido)-3-phenylpropanoic acid (**198**)

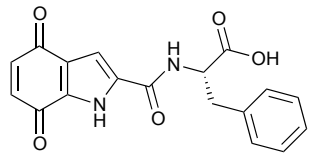

198 was prepared from the deprotection of **207** (8 mg, 0.0195 mmol), using general procedure C. The product was purified by flash chromatography (10 % methanol/ethyl acetate) to give **198** as yellow oil in 56 % yield (4 mg, 0.0109 mmol).

^{1}H NMR δ (Acetone-D6, 600 MHz): 3.14 (dd, *J* = 14.0, 9.5 Hz, 1H), 3.33, (dd, *J* = 14.0, 4.9 Hz, 1H), 4.89 – 4.92 (m, 1H), 6.68 (d, *J* = 0.5 Hz, 2H), 7.18 – 7.35 (m, 6H), 8.14 (d, *J* = 6.7 Hz, 1H), 12.0 (bs, 1H),

^{13}C NMR δ (Acetone- D6, 150 MHz): 37.9, 54.7, 108.5, 126.2, 127.5, 129.2, 130.1, 130.2, 133.0, 137.6, 138.4, 138.8, 160.0, 172.7, 178.0, 183.3

$[\alpha]_D^{20}$: -78.46° (*c* 0.13, $CHCl_3$)

IR V_{max}: 3120, 2927, 1661, 1652, 1558, 1486, 1282, 1222, 839, 701 cm^{-1}

6.4 Chapter 4 Experimental Details

6.4.1 Synthesis of quinone acids

6-hydroxy-4,4,5,7,8-pentamethylchroman-2-one (**214**)

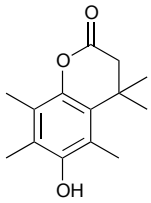

Concentrated sulfuric acid (1 mL) was added to a solution of 2,3,5-trimethylhydroquinone (1.009 g, 6.631 mmol) and 3,3-dimethylacrylic acid (0.711 g, 7.102 mmol) in toluene (20 mL) and the solution refluxed for 1h. The mixture was cooled to room temperature and quenched dropwise with sat. $NaHCO_3$. The organic layer was separated and washed with sat. $NaHCO_3$ (3x 20 mL) and H_2O (3x 20 mL). The organic layer was dried over $MgSO_4$, filtered and the solvent removed under reduced pressure and the product purified by flash chromatography (40 % ethyl acetate/hexanes) to give **214** as white crystalline solid in 38 % yield (588 mg, 2.512 mmol).

^{1}H NMR δ ($CDCl_3$, 400 MHz): 1.45 (s, 6H), 2.18 (s, 3H), 2.21 (s, 3H), 2.35 (s, 3H), 2.54 (s, 2H), 4.66 (bs, 1H)

^{13}C NMR δ ($CDCl_3$, 100 MHz): 12.4, 12.7, 14.5, 27.8, 35.6, 46.22, 119.0, 121.9, 123.5, 128.3, 143.6, 148.9, 168.9

Spectral data consistent with data reported in the literature.[135]

2,2-dimethyl-3-(2,4,5-trimethyl-3,6-dioxocyclohexa-1,4-dien-1-yl)propanoic acid (**216**)

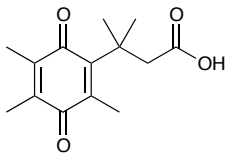

N-Bromosuccinimide (359 mg, 2.014 mmol) in acetonitrile (5 mL) was added dropwise to a solution of **214** (456.6 mg, 1.949 mmol) in 10% aqueous acetonitrile (25 mL) and the mixture left stirring at room temperature for 1 h. The mixture was extracted with ethyl acetate (3 x 20 mL) and the organic extract washed with brine (3 x 20 mL) and H_2O (3 x 20 mL). The organic layer was dried over $MgSO_4$, filtered and the solvent removed under reduced pressure and the product recrystallized from acetone/hexane to give **216** as a bright yellow crystalline solid in 98 % yield (476 mg, 1.901 mmol).

^{1}H NMR δ ($CDCl_3$, 400 MHz): 1.36 (s, 6H), 1.85 (s, 3H), 1.87 (s, 3H), 2.06 (s, 3H), 2.94 (s, 2H), 10.90 (bs, 1H)

^{13}C NMR δ ($CDCl_3$, 100 MHz): 12.0, 12.4, 14.2, 28.7, 37.9, 47.2, 138.3, 138.9, 142.9, 152.0, 178.8, 187.4, 190.8

Spectral data consistent with data reported in the literature.[135]

2-Methyl-1,4-dihydronaphthalene-1,4-diol (**217**)

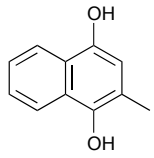

To a solution of menadione (**12**) (204 mg, 1.187 mmol) in diethyl ether (20 mL) under an atmosphere of nitrogen, 10 % w/v aqueous solution of sodium dithionite (20 mL) was added and the reaction mixture stirred vigorously for 2 h. The reaction mixture was separated and extracted with ethyl acetate (3 x 20 mL) and the organic extracts were combined and washed with brine (3x 20 mL). The organic layer was dried over $MgSO_4$, filtered and the solvent removed under reduced pressure to give the pure product **217** as a purple solid in quantitative yield (205 mg, 1.164 mmol).

^{1}H NMR δ (MeOD, 400 MHz): 2.33 (s, 3H), 6.63 (s, 1H), 7.31 – 7.34 (m, 1H), 7.39 (dt, *J* = 8.3, 1.2 Hz, 1H), 8.08 (t, *J* = 7.2 Hz, 2H)

^{13}C NMR δ (MeOD, 100 MHz): 16.5, 112.0, 120.4, 122.4, 122.9, 124.7, 125.6, 128.3, 143.1, 147.5

Spectral data consistent with data reported in the literature.[137,157]

4-ethoxy-2,2-dimethyl-4-oxobutanoic acid (**220**)

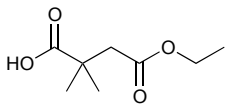

A solution of 2,2-Dimethylsuccinic anhydride (**219**) (605 mg, 4.713 mmol) in ethanol (5 mL) was heated at 50 °C for 16 h. The solvent was removed under reduced pressure to give the pure product **220** as a clear crystalline solid in 96 % yield (792 mg, 4.547 mmol).

^{1}H NMR δ ($CDCl_3$, 400 MHz): 1.16 (t, *J* = 7.2 Hz, 3H), 1.22 (s, 6H), 2.53 (s, 2H), 4.05 (q, *J* = 7.2 Hz, 2H)

^{13}C NMR δ ($CDCl_3$, 100 MHz): 14.0, 25.1, 40.4, 44.1, 60.5,171.2, 183.3

2,3-Dimethoxy-5-methyl-*p*-hydroquinone (**222**)

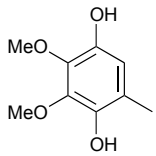

To a solution of 2,3-Dimethoxy-5-methyl-*p*-benzoquinone (**6**) (290 mg, 1.593 mmol) in diethyl ether (3 mL) was added a solution of sodium borohydride (323.9 mg, 8.562 mmol) in H_2O (6 mL). The bi-phasic mixture was stirred vigorously for 10min before diluting with H_2O (10 mL) and extracted with diethyl ether (3 x 10 mL). The organic extract was washed with H_2O (3 x 10 mL) and the organic layer was dried over $MgSO_4$, filtered and the solvent removed under reduced pressure to give the crude product which was purified by flash chromatography (30 % ethyl acetate/hexanes) to give **222** as a white solid in 54 % yield (157 g, 0.8529 mol).

^{1}H NMR δ ($CDCl_3$, 400 MHz): 2.17 (s, 3H), 3.87 (s, 3H), 3.90 (s, 3H), 5.44 (s, 1H), 5.51 (s, 1H), 6.48 (s, 1H)

^{13}C NMR δ ($CDCl_3$, 100 MHz): 15.4, 60.8, 60.9, 111.5, 119.5, 137.6, 139.2, 140.4, 141.6

Spectral data consistent with data reported in the literature.[140]

6-hydroxy-7,8-dimethoxy-4,4,5-trimethylchroman-2-one (**223**)

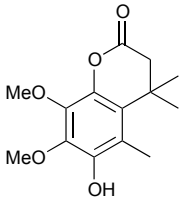

Concentrated sulfuric acid (0.5 mL) was added to a solution of 2,3,-dimethoxy-5-methylhydroquinone (**222**) (298 mg, 1.598 mmol) and 3,3-dimethylacrylic acid (243 mg, 2.431 mmol) in toluene (5 mL) and the solution refluxed for 1h. The mixture was cooled to room temperature and quenched dropwise with sat. $NaHCO_3$. The organic layer was separated and washed with sat. $NaHCO_3$ (3x 10 mL) and H_2O (3x 10 mL). The organic layer was dried over $MgSO_4$, filtered and the solvent removed under reduced pressure and the product purified by flash chromatography (40 % ethyl acetate/hexanes) followed by recrystallizationfrom 5% ethyl acetate/hexanes to give **223** as white crystalline solid in 20 % yield (83 mg, 0.3124 mmol) with a melting point of 109 – 111 °C.

^{1}H NMR δ ($CDCl_3$, 400 MHz):	1.44 (s, 6H), 2.32 (s, 3H), 2.56 (s, 2H), 3.89 (s, 3H), 3.96 (s, 3H), 5.75 (s, 1H)
^{13}C NMR δ ($CDCl_3$, 100 MHz):	13.8, 27.8, 35.9, 46.0, 61.3, 61.6, 116.4, 126.5, 138.4, 138.5, 138.7, 144.0, 167.8
IR V_{max}:	3419 (-OH), 2969, 2945, 1767 (C=O), 1489, 1418, 1357, 1238, 1113, 1083, 1028, 681 cm^{-1}

3-(4,5-Dimethoxy-2-methyl-3,6-dioxocyclohexa-1,4-dien-1-yl)-3-methylbutanoic acid (**224**)

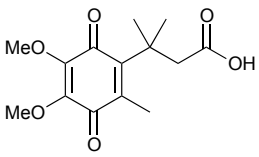

N-Bromosuccinimide (149 mg, 0.8394 mmol) in acetonitrile (2 mL) was added dropwise to a solution of **223** (141 mg, 0.5287 mmol) in 10% aqueous acetonitrile (10 mL) and the mixture immediately quenched with ethyl acetate (20 mL) and H_2O (20 mL). The mixture was separated and the aqueous extracted with ethyl acetate (2x 20 mL) and the organic extract washed with brine (3x 20 mL) and H_2O (3x 20 mL). The organic layer was dried over $MgSO_4$, filtered and the solvent removed under reduced pressure and the product recrystallized from acetone/hexane to give **224** as a bright yellow oil in 18 % yield (27 mg, 0.0956 mmol).

^{1}H NMR δ ($CDCl_3$, 400 MHz): 1.44 (s, 6H), 2.14 (s, 3H), 3.05 (s, 2H), 3.89 (s, 3H), 3.96 (s, 3H)

^{13}C NMR δ ($CDCl_3$, 100 MHz): 14.1, 29.0, 38.32, 47.31, 60.5, 60.9, 137.7, 142.5, 145.4, 149.9, 177.8, 184.5, 186.4

IR V_{max}: 3404 (-OH), 2969, 2955, 1711 (C=O), 1684 (C=O), 1596, 1457, 1309, 1233, 1197, 1112, 1026, 736 cm^{-1}

Spectral data consistent with data reported in the literature.[84]

(*S*)-*N*-(1-hydroxy-3-phenylpropan-2-yl)-3-methyl-3-(2,4,5-trimethyl-3,6-dioxocyclohexa-1,4-dien-1-yl)butanamide (**231**)

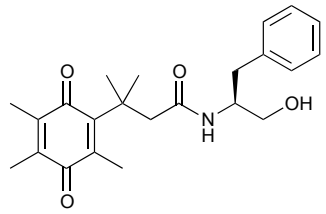

231 was prepared according to general procedure B from **216** (75 mg, 0.2993 mmol) and L-phenylalaninol (298 mg, 1.971 mmol) and the product purified by flash chromatography (70 % ethyl acetate/hexane) to give **231** as yellow oil in 35 % yield (40 mg, 0.1037 mmol).

^{1}H NMR δ ($CDCl_3$, 400 MHz): 1.32 (s, 3H), 1.38 (s, 3H), 1.94 (6H), 2.09 (s, 3H), 2.72 – 2.86 (m, 4H), 3.51 (dd, *J* =

11.0, 5.0 Hz, 1H), 3.59 (dd, *J* = 11.0, 3.6 Hz, 1H), 4.05 – 4.10 (m, 1H), 5.63 (d, *J* = 7.7 Hz, 1H), 7.14 – 7.22 (m, 3H), 7.27 – 7.29 (m, 2H)

^{13}C NMR δ ($CDCl_3$, 100 MHz): 12.2, 12.8, 14.2, 29.0, 37.0, 38.3, 49.3, 52.6, 64.4, 126.8, 128.7, 129.2, 137.6, 138.1, 138.2, 143.5, 153.1, 172.6, 187.6, 191.4

$[\alpha]_D^{20}$: +15.87° (*c* 0.31, $CHCl_3$)

IR V_{max}: 3367 (N-H), 2926, 1639 (C=O), 1538,1454, 1372, 1280, 1222, 1041, 736, 701 cm^{-1}

(*S*)-*N*-(2-hydroxy-1-phenylethyl)-3-methyl-3-(2,4,5-trimethyl-3,6-dioxocyclohexa-1,4-dien-1-yl)butanamide (**230**)

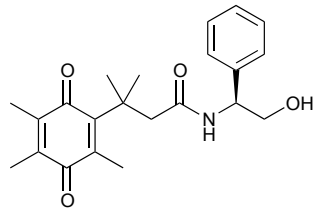

230 was prepared according to general procedure B from **216** (126 mg, 0.5030 mmol) and S-phenyl glycinol (100 mg, 0.7261 mmol) and the product purified by flash chromatography (70 % ethyl acetate/hexane) to give **230** as yellow oil in 38 % yield (70 mg, 0.1905 mmol).

^{1}H NMR δ ($CDCl_3$, 400 MHz): 1.39 (s, 3H), 1.44 (s, 3H), 1.83 (d, *J* = 1.1 Hz, 3H), 1.89 (d, *J* = 1.1 Hz, 3H), 2.08 (s, 3H), 2.60 (bs, 1H), 2.83 (d, *J* = 15.1 Hz, 1H), 2.94 (d, *J* = 15.1 Hz, 1H), 3.77 (d, *J* = 4.9 Hz, 2H), 4.90 – 4.95 (m, 1H), 6.15 (d, *J* = 7.2 Hz, 1H), 7.18 – 7.31 (m, 5H)

^{13}C NMR δ ($CDCl_3$, 100 MHz): 12.2, 12.6, 14.2, 29.3, 38.6, 49.3, 55.5, 66.4, 126.7, 127.8, 128.8, 138.2, 138.3, 139.0, 143.3, 152.9, 172.4, 187.6, 191.5

$[\alpha]_D^{20}$: +106.10° (*c* 1.64, $CHCl_3$)

IR V_{max}: 3366 (N-H), 2925, 1708 (C=O), 1641 (C=O), 1530, 1372, 1281, 1222, 1044, 701 cm^{-1}

2-(4-(1*H*-imidazol-1-yl)-2-methyl-4-oxobutan-2-yl)-3,5,6-trimethylcyclohexa-2,5-diene-1,4-dione

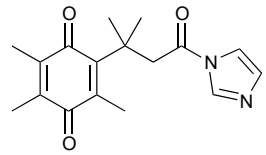

Carbonyl diimidazole (101 mg, 0.6223 mmol) was added to a solution of **216** (116 mg, 0.4647 mmol) in CH_2Cl_2 (3 mL) under an atmosphere of N_2. The mixture was stirred for 0.5 h at room temperature before being diluted with CH_2Cl_2 (20 mL). The organic layer was washed with H_2O (3 x 20 mL) and the organic layer was dried over $MgSO_4$, filtered and the solvent removed under reduced pressure to give the pure product **237** as a yellow solid in quantitative yield (135 mg, 0.4505 mmol)

^1H NMR δ ($CDCl_3$, 400 MHz): 1.49 (s, 6H), 1.84 (s, 3H), 1.94 (s, 3H), 2.17 (s, 3H), 3.57 (s, 2H), 7.03 (s, 1H), 7.39 (s, 1H), 8.11 (s, 1H)

6.4.2 Synthesis of dye fragments

4-Azido-1,8-naphthalic Anhydride (**227**)

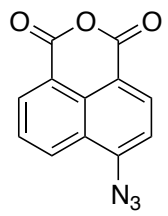

Sodium azide (253 mg, 3.892 mmol) in H_2O (0.5 mL) was added to a solution of 4-bromo-1,8-naphthalic anhydride (**226**) (798 mg, 2.8783 mmol) in DMF (5 mL) and the mixture heated to 100 °C for 0.5 h. The reaction mixture was taken of the heat and solution poured into ice – cold water (75 mL) and a

brown precipitate filtered and washed with H_2O (3 x 30 mL). The brown solid was identified to be the pure product **227** in 72 % yield (496 mg, 2.072 mmol). Used without further purification.

^{1}H NMR δ ($CDCl_3$, 400 MHz): 7.53 (d, *J* = 8.0 Hz, 1H), 7.81 (t, *J* = 8.0 Hz, 1H), 8.55 (d, *J* = 8.5 Hz, 1H), 8.61 (d, *J* = 8.0 Hz, 1H), 8.66 (d, *J* = 7.4 Hz, 1H)

4-Amino-1,8-naphthalic Anhydride (**228**)

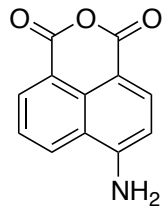

10% Pd/C was added to a solution of 4-Azido-1,8-naphthalic anhydride (**227**) (496 mg, 2.072 mmol) in anhydrous DMF (5 mL) under an atmosphere of hydrogen. The mixture was stirred at room temperature for 23 h and filtered through a bed of celite and the solution added to H_2O (100 mL). The mixture was extracted with ethyl acetate (3 x 20 mL) and CH_2Cl_2 (3 x 20 mL) and the organic layer was dried over $MgSO_4$, filtered and the solvent removed under reduced pressure to give the product **228** as a beige solid in 33 % yield (147 mg, 0.6909 mmol). Used without further purification.

^{1}H NMR δ (Acetone-D6, 400 MHz): 7.04 (d, *J* = 8.0 Hz, 1H), 7.08 (bs, 2H), 7.74 (dd, *J* = 8.2, 7.5 Hz, 1H), 8.28 (d, *J* = 8.4 Hz, 1H), 8.51 (d, *J* = 7.4 Hz, 1H), 8.68 (d, *J* = 8.3 Hz, 1H)

6-Amino-2-butyl-1*H*-benzo[*de*]isoquinoline-1,3(2*H*)-dione (**229**)

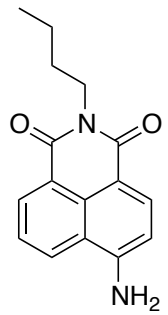

N-Butylamine (74 mL mg, 1.012 mmol) was added dropwise to a solution of 4-amino-1,8-naphthalic anhydride **228** (68 mg, 0.3194 mmol) in ethanol (5 mL) at reflux. The mixture was refluxed for 16 h and the solvent removed under reduced pressure to give the crude product, which was purified by flash chromatography (60 % ethyl acetate/hexanes) to give **229** as dark yellow solid in 82 % yield (70 mg, 0.2620 mmol).

^{1}H NMR δ (Acetone-D6, 400 MHz): 0.95 (t, *J* = 7.6 Hz, 3H), 1.40 (sextet, *J* = 7.6 Hz, 2H), 1.66 (quin, *J* = 7.6 Hz, 2H), 4.09 (t, *J* = 7.6 Hz, 2H), 6.70 (bs, 2H), 6.97 (d, *J* = 8.3 Hz, 1H), 7.66 (dd, *J* = 8.3, 7.3, Hz, 1H), 8.18 (d, *J* = 8.3 Hz, 1H), 8.49 (dd, *J* = 7.3, 1.0 Hz, 1H), 8.55 (dd, *J* = 8.3, 1.0 Hz, 1H)

^{1}H NMR δ (Acetone-D6, 150 MHz): 14.2, 21.0, 31.1, 40.1, 109.4, 110.8, 120.9, 123.8, 125.1, 129.1, 130.9, 131.7, 134.5, 152.7, 164.2, 164.9

Spectral data consistent with data reported in the literature.[134,142]

6-Azido-2-butyl-1*H*-benzo[*de*]isoquinoline-1,3(2*H*)-dione (**232**)

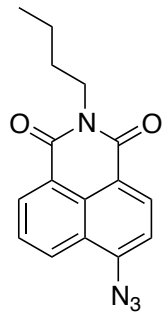

Butylamine (74 mg, 1.012 mmol) was added dropwise to a solution of 4-azido-1,8-naphthalic anhydride (**227**) (234 mg, 1.096 mmol) in ethanol (10 mL) at reflux. The mixture was refluxed for 16 h and the solvent removed under reduced pressure to give the crude product, which was purified by flash chromatography (30 % ethyl acetate/hexanes) to give **232** as dark yellow solid in 22 % yield (72 mg, 0.2436 mmol).

^{1}H NMR δ ($CDCl_3$, 400 MHz):	0.97 (t, *J* = 7.5 Hz, 3H), 1.44 (sextet, *J* = 7.5 Hz, 2H), 1.71 (quin, *J* = 7.5 Hz, 2H), 4.16 (t, *J* = 7.5 Hz, 2H), 7.45 (d, *J* = 8.0 Hz, 1H), 7.72 (dd, *J* = 8.4, 7.4 Hz, 1H), 8.41 (dd, *J* = 8.4, 1.0 Hz, 1H), 8.56 (d, *J* = 8.0 Hz, 1H), 8.61 (dd, *J* = 7.4, 1.0 Hz, 1H)
^{13}C NMR δ ($CDCl_3$, 100 MHz):	13.9, 20.5, 30.3, 40.4, 114.7, 119.1, 122.8, 124.4, 126.9, 128.8, 129.2, 131.7, 132.2, 143.4, 163.7, 164.1
IR V_{max}:	2958, 2127 ($-N_3$), 1699 (C=O), 1658 (C=O), 1581, 1386, 1354, 1288, 1234, 781 cm^{-1}

Spectral data consistent with data reported in the literature.[144]

1,8-naphthalimide-based iminophosphorane (**233**)

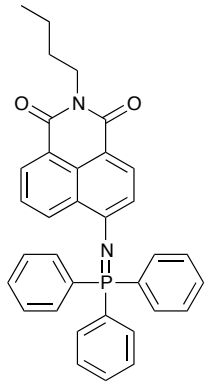

A solution of triphenylphosphine (24 mg, 0.0919 mmol) in dichloromethane (1.5 mL) was added dropwise to a solution of N-butyl-4-azido-1,8-naphthalamide **232** (21 mg, 0.0724 mmol) and 2,2-dimethyl-3-(2,4,5-trimethyl-3,6-dioxocyclohexa-1,4-dien-1-yl)propanoic acid **216** (25 mg, 0.0991 mmol) in dichloromethane (2 mL) at 0 °C under an atmosphere of nitrogen. The mixture was stirred at room temperature for 16 h and the solvent removed under reduced pressure to give the crude product, which was purified by flash chromatography (40 % ethyl acetate/hexanes) to give **233** as dark yellow oil in 67 % yield (26 mg, 0.0486 mmol).

^{1}H NMR δ ($CDCl_3$, 400 MHz): 0.94 (t, *J* = 7.4 Hz, 3H), 1.42 (sextet, *J* = 7.4 Hz, 2H), 1.67 (quin, *J* = 7.4 Hz, 2H), 4.13 (t, *J* = 7.4 Hz, 2 H), 6.44 (d, *J* = 8.3 Hz, 1H), 7.50 – 7.53 (m, 6H), 7,58 – 7.64 (m, 4H), 7.78 – 7.83 (m, 6H), 8.08 (d, *J* = 8.3 Hz, 1H), 8.56 (d, *J* = 7.3 Hz, 1H), 9.14 (d, *J* = 8.3 Hz, 1H)

Note: Spectral data consistent with data reported in the literature.[145]

6-Bromo-2-butyl-1*H*-benzo[*de*]isoquinoline-1,3(2*H*)-dione (**235**)

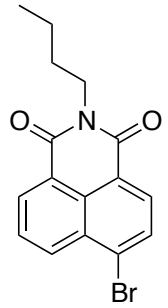

N-Butylamine (148 mg, 2.023 mmol) was added dropwise to a solution of 4-bromo-1,8-naphthalic anhydride (**226**) (303 mg, 1.095 mmol) in ethanol (10 mL) at reflux. The mixture was refluxed for 16 h and the solvent removed under reduced pressure to give the crude product, which was purified by flash chromatography (20 % ethyl acetate/hexanes) to give **235** as white crystalline solid in 78 % yield (309 mg, 0.9314 mmol).

^{1}H NMR δ ($CDCl_3$, 400 MHz): 1.00 (t, *J* = 7.5 Hz, 3H), 1.47 (sextet, *J* = 7.5 Hz, 2H), 1.70 – 1.77 (m, 2H), 4.20 (t, *J* = 7.5 Hz, 2H), 7.87 (dd, *J* = 8.5, 7.4 Hz, 1H), 8.06 (d, *J* = 7.8 Hz, 1H), 8.44 (d, *J* = 7.8 Hz, 1H), 8.59 (dd, *J* = 8.5, 1.0 Hz, 1H), 8.68 (dd, *J* = 7.4, 1.0 Hz, 1H)

^{13}C NMR δ ($CDCl_3$, 100 MHz): 13.9, 20.5, 30.2, 40.5, 122.4, 123.2, 128.1, 129.1, 130.3, 131.1, 131.2, 132.1, 133.2, 163.70, 163.72

Spectral data consistent with data reported in the literature.[146]

6-((2-aminoethyl)amino)-2-butyl-1*H*-benzo[*de*]isoquinoline-1,3(2*H*)-dione (**239**)

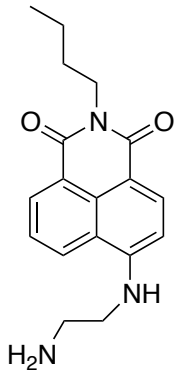

N-Butyl-4-bromo-1,8-naphthalamide **235** (124 mg, 0.3727 mmol), ethylenediamine (0.25 mL, 3.744 mmol) and $CuSO_4 \bullet 5H_2O$ (30 mg, 0.1201 mmol) were refluxed in methoxyethanol (4 mL) for 1.5 h. The mixture was poured into cold water resulting in a yellow solid forming which was filtered and purified by flash chromatography (10 % (95:5 methanol:ammonia)/ethyl acetate) to give **239** as red solid in 52 % yield (60 mg, 0.1923 mmol).

^{1}H NMR δ ($CDCl_3$, 400 MHz): 0.99 (t, *J* = 7.4 Hz, 3H), 1.46 (sextet, *J* = 7.4 Hz, 2H), 1.73 (quin, *J* = 7.4 Hz, 2H), 3.20 (t, *J* = 5.6 Hz, 2H), 3.55 (q, *J* = 5.6 Hz, 2H), 4.18 (t, *J* = 7.4 Hz, 2H), 6.16 (bs, 1H), 6.73 (d, *J* = 8.4 Hz, 1H), 7.64 (t, *J* = 7.8 Hz, 1H), 8.19 (d, *J* = 8.4 Hz, 1H), 8.48 (d, *J* = 8.4 Hz, 1H), 8.61 (d, *J* = 7.8 Hz, 1H)

^{13}C NMR δ ($CDCl_3$, 100 MHz): 13.9, 20.5, 30.4, 40.0, 40.2, 45.0, 104.3, 110.1, 120.4, 122.9, 124.6, 126.3, 129.7, 131.0, 134.4, 149.7, 164.2, 164.7

Spectral data consistent with data reported in the literature.[146]

6.4.3 Coupling of Dye to Quinone

_N_-(2-((2-butyl-1,3-dioxo-2,3-dihydro-1_H_-benzo[_de_]isoquinolin-6-yl)amino)ethyl)-3-methyl-3-(2,4,5-trimethyl-3,6-dioxocyclohexa-1,4-dien-1-yl)butanamide (**238**)

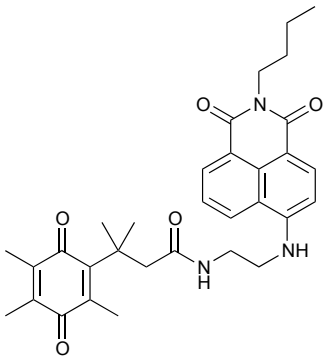

238 was prepared according to general procedure B from **216** (47 mg, 0.1870 mmol) and **239** (47 mg, 0.1522 mmol) and the product purified by flash chromatography (80 % ethyl acetate/hexane) to give **238** as yellow oil in 86 % yield (71 mg, 0.1304 mmol).

^{1}H NMR δ ($CDCl_3$, 400 MHz): 0.96 (t, *J* = 7.5 Hz, 3H), 1.39 – 1.48 (m, 8H), 166 – 1.73 (m, 5H), 1.82 (s, 3H), 2.05 (s, 3H), 2.92 (s, 2H), 3.36 (t, *J* = 5.6 Hz, 2H), 3.65 (q, *J* = 5.6 Hz, 2H), 4.15 (t, *J* = 7.5 Hz, 2H), 6.22 (t, *J* = 5.8 Hz, 1H), 6.45 (d, *J* = 8.4 Hz, 1H), 7.03 (bs, 1H), 7.39 (t, *J* = 7.5 Hz, 1H), 8.03 (d, *J* = 8.4 Hz, 1H), 8.38 (d, *J* = 8.4 Hz, 1H), 8.53 (d, *J* = 7.5 Hz, 1H)

^{13}C NMR δ ($CDCl_3$, 100 MHz): 12.1, 12.7, 14.0, 14.4, 20.5, 29.6, 30.4, 38.90, 38.98, 40.1, 46.8, 49.6, 103.4, 110.2, 120.3, 123.0, 124.8, 126.8, 128.9, 131.3, 134.5, 138.7, 139.2, 142.8, 149.8, 152.2, 164.4, 164.7, 175.5, 187.2, 191.1

IR V_{max}:	3312 (N-H), 2935, 1678 (C=O), 1629, 1582, 1398, 1362, 1274, 1243, 1126, 774 cm^{-1}
HRESIMS [M+Na]:	For $C_{32}H_{37}N_3O_5Na$, predicted 566.2631, found 566.2646

Chapter 7: References

1 R. I. Samoilova, A. R. Crofts and S. A. Dikanov, *J. Phys. Chem. A*, 2011, **115**, 11589–11593.

2 M. Erb, B. Hoffmann-Enger, H. Deppe, M. Soeberdt, R. H. Haefeli, C. Rummey, A. Feurer and N. Gueven, *PLoS ONE*, 2012, **7**, e36153–8.

3 F. D. Heitz, M. Erb, C. Anklin, D. Robay, V. Pernet and N. Gueven, *PLoS ONE*, 2012, **7**, e45182–11.

4 R. H. Haefeli, M. Erb, A. C. Gemperli, D. Robay, I. Courdier Fruh, C. Anklin, R. Dallmann and N. Gueven, *PLoS ONE*, 2011, **6**, e17963–12.

5 B. Liu, L. Gu and J. Zhang, *Recl. Trav. Chim. Pays-Bas.*, 1991, **110**, 99–103.

6 R. A. J. Smith, R. C. Hartley, H. M. Cochemé and M. P. Murphy, *Trends in Pharmacological Sciences*, 2012, **33**, 341–352.

7 A. O. Oyewole and M. A. Birch-Machin, *The FASEB Journal*, 2015, **29**, 4766–4771.

8 D. Orsucci, M. Mancuso, E. C. Ienco, A. LoGerfo and S. Siciliano, *Current Medicinal Chemistry*, 2011, **26**, 4053–4064 .

9 M. F. Beal and C. W. Shults, *BioFactors*, 2003, **18**, 153–161.

10 S. McCarthy, M. Somayajulu, M. Sikorska, H. Borowy-Borowski and S. Pandey, *Toxicol. Appl. Pharmacol.*, 2004, **201**, 21–31.

11 N. Gueven, K. Woolley and J. Smith, *Redox Biology*, 2015, **4**, 289–295.

12 Y. H. Noh, K.-Y. Kim, M. S. Shim, S.-H. Choi, S. Choi, M. H. Ellisman, R. N. Weinreb, G. A. Perkins and W.-K. Ju, *Cell Death and Disease*, 2013, **4**, e820–12.

13 H. Jin, A. Kanthasamy, A. Ghosh, V. Anantharam, B. Kalyanaraman and A. G. Kanthasamy, *Biochimica et Biophysica Acta (BBA) - Mol. Basis of Dis.*, 2014, **1842**, 1282–1294.

14 D. M. Fash, O. M. Khdour, S. J. Sahdeo, R. Goldschmidt, J. Jaruvangsanti, S. Dey, P. M. Arce, V. C. Collin, G. A. Cortopassi and S. M. Hecht, *Bioorganic Med. Chem.*, 2013, **21**, 2346–2354.

15 G. M. Buyse, N. Goemans, M. van den Hauwe and T. Meier, *Pediatr. Pulmonol.*, 2012, **48**, 912–920.

16 K. Filler, D. Lyon, J. Bennett, N. McCain, R. Elswick, N. Lukkahatai and L. N. Saligan, *BBACLI*, 2014, **1**, 12–23.

17 F. G. Blankenberg, S. L. Kinsman, B. H. Cohen, M. L. Goris, K. M. Spicer, S. L. Perlman, E. J. Krane, V. Kheifets, M. Thoolen, G. Miller and G. M. Enns, *Molecular Genetics and Metabolism*, 2012, **107**, 690–699.

18 D. Y. Duveau, P. M. Arce, R. A. Schoenfeld, N. Raghav, G. A. Cortopassi and S. M. Hecht, *Bioorganic Med. Chem.*, 2010, **18**, 6429–6441.

19 J. M. Villalba, C. Parrado, M. Santos-Gonzalez and F. J. Alcain, *Expert Opin. Investig. Drugs*, 2010, **19**, 535–554.

20 W. D. Shrader, A. Amagata, A. Barnes, G. M. Enns, A. Hinman, O. Jankowski, V. Kheifets, R. Komatsuzaki, E. Lee, P. Mollard, K. Murase, A. A. Sadun, M. Thoolen, K. Wesson and G. Miller, *Bioorganic Med. Chem. Lett.*, 2017, **21**, 3693–3698.

21 C. J. Strawser, K. A. Schadt and D. R. Lynch, *Expert Review of Neurotherapeutics*, 2014, **14**, 949–957.

22 A. A. Sadun, C. F. Chicani, F. N. Ross-Cisneros, P. Barboni, M. Thoolen, W. D. Shrader, K. Kubis, V. Carelli and G. Miller, *Archives of Neurology*, 2012, **69**, 331–338.
23 A. Pastore, S. Petrillo, G. Tozzi, R. Carrozzo, D. Martinelli, C. Dionisi-Vici, G. Di Giovamberardino, F. Ceravolo, M. B. Klein, G. Miller, G. M. Enns, E. Bertini and F. Piemonte, *Molecular Genetics and Metabolism*, 2013, **109**, 208–214.
24 G. M. Enns, S. L. Kinsman, S. L. Perlman, K. M. Spicer, J. E. Abdenur, B. H. Cohen, A. Amagata, A. Barnes, V. Kheifets, W. D. Shrader, M. Thoolen, F. Blankenberg and G. Miller, *Molecular Genetics and Metabolism*, 2012, **105**, 91–102.
25 M. P. Murphy and R. A. J. Smith, *Annu. Rev. Pharmacol. Toxicol.*, 2007, **47**, 629–656.
26 N. Gueven, M. Nadikudi, A. Daniel and J. Chhetri, *Mitochondrion*, 2016, 1–9.
27 P. Mao, M. Manczak, U. P. Shirendeb and P. H. Reddy, *BBA - Molecular Basis of Disease*, 2013, **1832**, 2322–2331.
28 D. Vlachantoni, A. N. Bramall, M. P. Murphy, R. W. Taylor, X. Shu, B. Tulloch, T. Van Veen, D. M. Turnbull, R. R. McInnes and A. F. Wright, *Human Molecular Genetics*, 2010, **20**, 322–335.
29 M. J. McManus, M. P. Murphy and J. L. Franklin, *J. Neurosci.*, 2011, **31**, 15703–15715.
30 B. J. Snow, F. L. Rolfe, M. M. Lockhart, C. M. Frampton, J. D. O'Sullivan, V. Fung, R. A. J. Smith, M. P. Murphy and K. M. Taylor, *Mov. Disord.*, 2010, **25**, 1670–1674.
31 V. P. Skulachev, V. N. Anisimov, Y. N. Antonenko, L. E. Bakeeva, B. V. Chernyak, V. P. Erichev, O. F. Filenko, N. I. Kalinina, V. I. Kapelko, N. G. Kolosova, B. P. Kopnin, G. A. Korshunova, M. R. Lichinitser, L. A. Obukhova, E. G. Pasyukova, O. I. Pisarenko, V. A. Roginsky, E. K. Ruuge, I. I. Senin, I. I. Severina, M. V. Skulachev, I. M. Spivak, V. N. Tashlitsky, V. A. Tkachuk, M. Y. Vyssokikh, L. S. Yaguzhinsky and D. B. Zorov, *BBA - Bioenergetics*, 2009, **1787**, 437–461.
32 A. M. Markovets, A. Z. Fursova and N. G. Kolosova, *PLoS ONE*, 2011, **6**, e21682–8.
33 V. N. Anisimov, L. E. Bakeeva, P. A. Egormin, O. F. Filenko, E. F. Isakova, V. N. Manskikh, V. M. Mikhelson, A. A. Panteleeva, E. G. Pasyukova, D. I. Pilipenko, T. S. Piskunova, I. G. Popovich, N. V. Roshchina, O. Y. Rybina, V. B. Saprunova, T. A. Samoylova, A. V. Semenchenko, M. V. Skulachev, I. M. Spivak, E. A. Tsybul'ko, M. L. Tyndyk, M. Y. Vyssokikh, M. N. Yurova, M. A. Zabezhinsky and V. P. Skulachev, *Biochemistry Moscow*, 2009, **73**, 1329–1342.
34 V. V. Brzheskiy, E. L. Efimova, T. N. Vorontsova, V. N. Alekseev, O. G. Gusarevich, K. N. Shaidurova, A. A. Ryabtseva, O. M. Andryukhina, T. G. Kamenskikh, E. S. Sumarokova, E. S. Miljudin, E. A. Egorov, O. I. Lebedev, A. V. Surov, A. R. Korol, I. O. Nasinnyk, P. A. Bezditko, O. P. Muzhychuk, V. A. Vygodin, E. V. Yani, A. Y. Savchenko, E. M. Karger, O. N. Fedorkin, A. N. Mironov, V. Ostapenko, N. A. Popeko, V. P. Skulachev and M. V. Skulachev, *Advances in Therapy*, 2015, **32**, 1263–1279.
35 H. H. Szeto, *Antioxidants & Redox Signaling*, 2008, **10**, 601–620.

36 J. Gruber, S. Fong, C.-B. Chen, S. Yoong, G. Pastorin, S. Schaffer, I. Cheah and B. Halliwell, *Biotechnology Advances*, 2012, 1–30.

37 H. H. Szeto, *The AASP Journal*, 2006, **8**, E277–E283.

38 K. Zhao, G.-M. Zhao, D. Wu, Y. Soong, A. V. Birk, P. W. Schiller and H. H. Szeto, *J. Biol. Chem.*, 2004, **279**, 34682–34690.

39 H. H. Szeto and P. W. Schiller, *Pharm Res*, 2011, **28**, 2669–2679.

40 N. M. Alam, W. C. Mills, A. A. Wong, R. M. Douglas, H. H. Szeto and G. T. Prusky, *Disease Models & Mechanisms*, 2015, **8**, 701–710.

41 Y.-L. Jia, S.-J. Sun, J.-H. Chen, Q. Jia, T.-T. Huo, L.-F. Chu, J.-T. Bai, Y.-J. Yu and X.-X. Y. A. J.-H. Wang, *Current Alzheimer Research*, 2016, **13**, 297–306.

42 N. Gueven and D. Faldu, *Expert Opinion on Orphan Drugs*, 2013, **1**, 331–339.

43 N. Gueven, *Biology and Medicine*, 2014, 1–6.

44 N. J. N. M. D, M. T. L. M. A and D. C. W. P. D, *American Journal of Ophthalmology*, 2014, **111**, 750–762.

45 P. Yu-Wai-Man, P. G. Griffiths and P. F. Chinnery, *Progress in Retinal and Eye Research*, 2011, **30**, 81–114.

46 V. Carelli, F. N. Ross-Cisneros and A. A. Sadun, *Progress in Retinal and Eye Research*, 2004, **23**, 53–89.

47 P. Y. W. Man, P. G. Griffiths, D. T. Brown, N. Howell, D. M. Turnbull and P. F. Chinnery, *The American Journal of Human Genetics*, 2003, **72**, 333–339.

48 P. Yu-Wai-Man, P. G. Griffiths, G. Hudson and P. F. Chinnery, *Journal of Medical Genetics*, 2008, **46**, 145–158.

49 M. A. Kirkman, P. Yu-Wai-Man, A. Korsten, M. Leonhardt, K. Dimitriadis, I. F. De Coo, T. Klopstock and P. F. Chinnery, *Brain*, 2009, **132**, 2317–2326.

50 S. B. Vafai, E. Mevers, K. W. Higgins, Y. Fomina, J. Zhang, A. Mandinova, D. Newman, S. Y. Shaw, J. Clardy and V. K. Mootha, *PLoS ONE*, 2016, **11**, e0162686–14.

51 G. M. Buyse, T. Voit, U. Schara, C. S. M. Straathof, M. G. D'Angelo, G. N. Bernert, J.-M. Cuisset, R. S. Finkel, N. Goemans, C. Rummey, M. Leinonen, O. H. Mayer, P. Spagnolo, T. Meier, C. M. McDonaldfor the DELOS Study Group, *Pediatr. Pulmonol.*, 2016, **52**, 508–515.

52 G. M. Buyse, N. Goemans, M. van den Hauwe, D. Thijs, I. J. M. de Groot, U. Schara, B. Ceulemans, T. Meier and L. Mertens, *Neuromuscular Disorders*, 2011, **21**, 396–405.

53 C. M. McDonald, T. Meier, T. Voit, U. Schara, C. S. M. Straathof, M. G. D'Angelo, G. Bernert, J.-M. Cuisset, R. S. Finkel, N. Goemans, C. Rummey, M. Leinonen, P. Spagnolo, G. M. Buyse, D. S. Group, G. Bernert, F. Knipp, G. M. Buyse, N. Goemans, M. van den Hauwe, T. Voit, V. Doppler, T. Gidaro, J. M. Cuisset, S. Coopman, U. Schara, S. Lutz, J. Kirschner, S. Borell, M. Will, M. G. D'Angelo, E. Brighina, S. Gandossini, K. Gorni, E. Falcier, L. Politano, P. D'Ambrosio, A. Taglia, J. J. G. M. Verschuuren, C. S. M. Straathof, J. J. V. Padilla, N. M. Gómez, T. Sejersen, M. Hovmöller, P. Y. Jeannet, C. Bloetzer, S. Iannaccone, D. Castro, G. Tennekoon, R. Finkel, C. Bönnemann, C. McDonald, E. Henricson, N. Joyce, S. Apkon and R. C. Richardson, *Neuromuscular Disorders*, 2016, **26**, 473–480.

54 G. M. Buyse, T. Voit, U. Schara, C. S. M. Straathof, M. G. D'Angelo, G. Bernert, J.-M. Cuisset, R. S. Finkel, N. Goemans, C. M. McDonald, C. Rummey and T. Meier, *The Lancet*, 2015, **385**, 1748–1757.

55 S. M. Fiebiger, H. Bros, T. Grobosch, A. Janssen, C. Chanvillard, F. Paul, J. Dörr, J. M. Millward and C. Infante-Duarte, *J. Neuroimmunol.*, 2013, **262**, 66–71.

56 E. Gerhardt, S. Gr ber, V. M. Szeg, N. Moisoi, L. M. Martins, T. F. Outeiro and P. Kermer, *PLoS ONE*, 2011, **6**, e28855–7.

57 T. Palecek, M. Fikrle, E. Nemecek, L. Bauerova, P. Kuchynka, W. E. Louch and I. S. A. R. Rysava, *Current Pharmaceutical Design*, **21**, 479–483.

58 C. J. Strawser, K. A. Schadt and D. R. Lynch, *Expert Review of Neurotherapeutics*, 2014, **14**, 000–000.

59 D. R. Lynch, S. L. Perlman and T. Meier, *Archives of Neurology*, 2010, **67**, 941–947.

60 V. Carelli, C. La Morgia, M. L. Valentino, G. Rizzo, M. Carbonelli, A. M. De Negri, F. Sadun, A. Carta, S. Guerriero, F. Simonelli, A. A. Sadun, D. Aggarwal, R. Liguori, P. Avoni, A. Baruzzi, M. Zeviani, P. Montagna and P. Barboni, *Brain*, 2011, **134**, e188–e188.

61 T. Klopstock, P. Yu-Wai-Man, K. Dimitriadis, J. Rouleau, S. Heck, M. Bailie, A. Atawan, S. Chattopadhyay, M. Schubert, A. Garip, M. Kernt, D. Petraki, C. Rummey, M. Leinonen, G. N. Metz, P. G. Griffiths, T. Meier and P. F. Chinnery, *Brain*, 2011, **134**, 2677–2686.

62 G. Metz, T. Klopstock, C. Gallenmuller, C. Catarino, B. von Livonius, F. Lob and T. Meier, *Acta Ophthalmologica*, 2015, **93**.

63 K. Okamoto, M. Watanabe, H. Morimoto and I. Imada, *Chemical and Pharmaceutical Bullentin*, 2004, **36**, 178–189.

64 H. Chen, A. Lum, A. Seifreid, L. R. Wilkens and L. Le Marchand, *Cancer Research*, 1999, **59**, 3045–3048.

65 M. Sarbia, M. Bitzer, D. Siegel, D. Ross, W. A. Schulz, R. B. Zotz, S. Kiel, H. Geddert, Y. Kandemir, A. Walter, R. Willers and H. E. Gabbert, *Int. J. Cancer*, 2003, **107**, 381–386.

66 B. J. Josey, E. S. Inks, X. Wen and C. J. Chou, *J. Med. Chem.*, 2013, **56**, 1007–1022.

67 K. S. Sundaram and M. Lev, *Archives of Biochemistry and Biophysics*, 1990, **277**, 109–113.

68 G. Ferland, *BioFactors*, 2012, **38**, 151–157.

69 S. Bhalerao and T. R. Clandinin, *Science*, 2012, **336**, 1241–1242.

70 M. Vos, G. Esposito, J. N. Edirisinghe, S. Vilain, D. M. Haddad, J. R. Slabbaert, S. Van Meensel, O. Schaap, B. De Strooper, R. Meganathan, V. A. Morais and P. Verstreken, *Science*, 2012, **336**, 1306–1310.

71 J. J. Rahn, J. E. Bestman, B. J. Josey, E. S. Inks, K. D. Stackley, C. E. Rogers, C. J. Chou and S. S. L. Chan, *Neuroscience*, 2014, **259**, 142–154.

72 A. A. Garcia and P. H. Reitsma, *Vitamin K*, 2008, **78 IS -**, 23–33.

73 J. Oldenburg, M. Marinova, C. Müller Reible and M. Watzka, *Vitamin K*, 2008, **78 IS -**, 35–62.

74 M. Caspers, K. J. Czogalla, K. Liphardt, J. Müller, P. Westhofen, M. Watzka and J. Oldenburg, *Thrombosis Research*, 2015, **135**, 977–983.

75 K. Woolley, 2013, Honours Thesis Title: *Synthesis of Naphthoquinones and Peptides*, University of Tasmania.

76 C. Commandeur, C. L. Chalumeau, J. Dessolin and M. Laguerre, *Eur. J. Org. Chem.*, 2007, **2007**, 3045–3052.

77 A. K. Boudalis, X. Policand, A. Sournia-Saquet, B. Donnadieu and J.-P. Tuchagues, *Protagonists in Chemistry: Piero Zanello*, 2008, **361**, 1681–1688.

78 A. V. Shtelman and J. Y. Becker, *J. Org. Chem.*, 2011, **76**, 4710–4714.

79 J. F. Yan and P. S. Fedkiw, *Journal of Applied Electrochemistry*, 1996, 175–185.

80 D. H. R. Barton, *Pure and Applied Chemistry*, 1994, **66**, 1943–1954.

81 A.-I. Tsai, Y.-L. Wu and C.-P. Chuang, *Tetrahedron*, 2001, **57**, 7829–7837.

82 J. M. Anderson and J. K. Kochi, *J. Am. Chem. Soc.*, 2001, **92**, 2450–2460.

83 J. C. Sheehan and G. P. Hess, *J. Am. Chem. Soc.*, 1955, **77**, 1067–1068.

84 L. A. Carpino, J. Xia and A. El-Faham, *J. Org. Chem.*, 2004, **69**, 54–61.

85 E. K. Woodman, J. G. K. Chaffey, P. A. Hopes, D. R. J. Hose and J. P. Gilday, *Org. Process Res. Dev.*, 2009, **13**, 106–113.

86 S. K. Verma, R. Ghorpade, A. Pratap and M. P. Kaushik, *Tetrahedron Letters*, 2012, **53**, 2373–2376.

87 C. Chen, Y.-Z. Liu, K.-S. Shia and H.-Y. Tseng, *Bioorganic & Medicinal Chemistry Letters*, 2002, **12**, 2729–2732.

88 M.-P. Brun, E. Braud, D. Angotti, O. Mondésert, M. Quaranta, M. Montes, M. Miteva, N. Gresh, B. Ducommun and C. Garbay, *Bioorganic & Medicinal Chemistry*, 2005, **13**, 4871–4879.

89 E. Braud, M.-L. Goddard, S. Kolb, M.-P. Brun, O. Mondésert, M. Quaranta, N. Gresh, B. Ducommun and C. Garbay, *Bioorganic Med. Chem.*, 2008, **16**, 9040–9049.

90 S. Bittner, S. Gorohovsky, O. P. T. Levi and J. Y. Becker, *Amino Acids*, 2002, **22**, 71–93.

91 D. X. Hu, P. Grice and S. V. Ley, *J. Org. Chem.*, 2012, **77**, 5198–5202.

92 M. I. Ahmed, J. B. Harper and L. Hunter, *Org. Biomol. Chem.*, 2014, **12**, 4598–4.

93 K. Ralhan, V. G. KrishnaKumar and S. Gupta, *RSC Advances*, 2015, **5**, 104417–104425.

94 S. Routier, L. Sauge, N. Ayerbe, G. Coudert and J.-T. Merour, *Tetrahedron Letters*, 2002, **43**, 589–591.

95 M. S. Elgawish, C. Shimomai, N. Kishikawa, K. Ohyama, M. Wada and N. Kuroda, *Chem. Res. Toxicol.*, 2013, **26**, 1409–1417.

96 J. Mauzeroll, A. J. Bard, A. Owhadian and T. J. Monks, *PNAS*, 2004, **101**, 17582–17587.

97 L. Kathawate, S. P. Gejji, S. D. Yeole, P. L. Verma, V. G. Puranik and S. Salunke-Gawali, *J. Mol. Struct.*, 2015, **1088**, 56–63.

98 N. J. Mueller, C. Stueckler, M. Hall, P. Macheroux and K. Faber, *Org. Biomol. Chem.*, 2009, **7**, 1115–5.

99 N. Kongkathip, B. Kongkathip, P. Siripong, C. Sangma, S. Luangkamin, M. Niyomdecha, S. Pattanapa, S. Piyaviriyagul and P. Kongsaeree, *Bioorganic Med. Chem.*, 2003, **11**, 3179–3191.

100 A. Y. Yakubovskaya, T. Y. Kochergina, V. A. Denisenko, D. V. Berdyshev, V. P. Glazunov and V. P. Anufriev, *Russian Chemical Bulletin*, 2006, **55**, 301–305.
101 R. R. S, S. K. H, V. Somasundaram, S. K. S, R. Nadhan, R. S. Nair and P. Srinivas, *Pharmacological Research*, 2016, **105**, 134–145.
102 B. Eldhose, M. Gunawan, M. Rahman, M. Latha and V. Notario, *Int J Oncol*, 2014, 1–9.
103 Y.-L. Hsu, C.-Y. Cho, P.-L. Kuo, Y.-T. Huang and C.-C. Lin, *Journal of Pharmacology and Experimental Therapeutics*, 2006, **318**, 484–494.
104 K. Sumalatha, M. Gowda and S. Meenakshisundaram, *J. Complement. and Integr. Med.*, 2017, **14**, 1–15.
105 N. Park, H. S. Baek and Y.-J. Chun, *PLoS ONE*, 2015, **10**, e0134760–17.
106 A. Sankaranarayanan and S. B. Chandalia, *Org. Process Res. Dev.*, 2006, **10**, 487–492.
107 D. Georgiev, B. Saes, H. Johnston, S. Boys, A. Healy and A. Hulme, *Molecules*, 2016, **21**, 88–9.
108 B. C. Soderberg and S. L. Fields, *Organic Preparations and Procedures International*, 1996, **28**, 221–225.
109 J. Wang, X. Hu and J. Yang, *Synthesis*, 2014, **46**, 2371–2375.
110 M. Alamgir, P. S. R. Mitchell, P. K. Bowyer, N. Kumar and D. S. Black, *Tetrahedron*, 2008, **64**, 7136–7142.
111 H. Xie, B. Wang, X. Shen, J. Qin, L. Jiang, C. Yu, D. Geng, T. Yuan, T. Wu, X. Cao and J. Liu, *Mol Med Report*, 2017, 1–7.
112 C. Yan, D. Kong, D. Ge, Y. Zhang, X. Zhang, C. Su and X. Cao, *Cell Physiol Biochem*, 2015, **35**, 1125–1136.
113 R. M. Phillips, H. R. Hendriks, G. J. Peterson behalf of the EORTC-Pharmacology and Molecular Mechanism Group, *Br J Pharmacol*, 2012, **168**, 11–18.
114 T. Ikawa, H. Kaneko, S. Masuda, E. Ishitsubo, H. Tokiwa and S. Akai, *Org. Biomol. Chem.*, 2015, **13**, 520–526.
115 A. F. Barrero, E. J. Alvarez-Manzaneda, R. Chahboun and C. G. Diaz, *Synlett*, 2000, 1561–1564.
116 S. Cantekin, A. Baran, R. Çalışkan and M. Balci, *Carbohydrate Research*, 2009, **344**, 426–431.
117 Z. Wu, S. R. Harutyunyan and A. J. Minnaard, *Chem. Eur. J.*, 2014, **20**, 14250–14255.
118 M. L. Kantam, R. Arundhathi, P. R. Likhar and D. Damodara, *Adv. Synth. Catal.*, 2009, **351**, 2633–2637.
119 A. G. O'Brien, F. Lévesque and P. H. Seeberger, *Chem. Commun.*, 2011, **47**, 2688–2690.
120 P. Roy, M. Boisvert and Y. Leblanc, *Org. Synth.*, 2007, **84**, 262–17.
121 R. A. Tapia, Y. Prieto, F. Pautet, N. Walchshofer, H. Fillion, B. Fenet and M.-E. Sarciron, *Bioorganic & Medicinal Chemistry*, 2003, **11**, 3407–3412.
122 N. Netz and T. Opatz, *J. Org. Chem.*, 2016, **81**, 1723–1730.
123 Y.-L. Zhang, Y.-J. Qin, D.-J. Tang, M.-R. Yang, B.-Y. Li, Y.-T. Wang, H.-Y. Cai, B.-Z. Wang and H.-L. Zhu, *ChemMedChem*, 2016, **11**, 1446–1458.
124 V. Beneteau and T. Besson, *Tetrahedron Letters*, 2001, **42**, 2673–

2676.
125 L. Legentil, J. Bastide and E. Delfourne, *Tetrahedron Letters*, 2003, **44**, 2473–2475.
126 R. A. Tapia, Y. Prieto, F. Pautet, M. Domard, M.-E. Sarciron, N. Walchshofer and H. Fillion, *Eur. J. Org. Chem.*, 2002, 4005–4010.
127 H. Tohma, H. Morioka, Y. Harayama, M. Hashizume and Y. Kita, *Tetrahedron Letters*, 2001, 6899–6902.
128 A. S. Eastabrook, C. Wang, E. K. Davison and J. Sperry, *J. Org. Chem.*, 2015, **80**, 1006–1017.
129 J. K. Howard, K. J. Rihak, A. C. Bissember and J. A. Smith, *Chem. Asian J.*, 2015, **11**, 155–167.
130 M. Grzybowski, K. Skonieczny, H. Butenschön and D. T. Gryko, *Angew. Chem. Int. Ed.*, 2013, **52**, 9900–9930.
131 T. Dohi, K. Morimoto, A. Maruyama and Y. Kita, *Org. Lett.*, 2006, **8**, 2007–2010.
132 M. C. Pierce, D. J. Javier and R. Richards-Kortum, *Int. J. Cancer*, 2008, **123**, 1979–1990.
133 B. Prasai, W. C. Silvers and R. L. McCarley, *Anal. Chem.*, 2015, **87**, 6411–6418.
134 W. C. Silvers, B. Prasai, D. H. Burk, M. L. Brown and R. L. McCarley, *J. Am. Chem. Soc.*, 2013, **135**, 309–314.
135 R. T. Borchardt and L. A. Cohen, *J. Am. Chem. Soc.*, 1972, **94**, 9175–9182.
136 R. J. Hinklin and L. L. Kiessling, *Org. Lett.*, 2002, **4**, 1131–1133.
137 S. Fujii, A. Shimizu, N. Takeda, K. Oguchi, T. Katsurai, H. Shirakawa, M. Komai and H. Kagechika, *Bioorganic & Medicinal Chemistry*, 2015, **23**, 2344–2352.
138 Y. Suhara, Y. Hirota, N. Hanada, S. Nishina, S. Eguchi, R. Sakane, K. Nakagawa, A. Wada, K. Takahashi, H. Tokiwa and T. Okano, *J. Med. Chem.*, 2015, **58**, 7088–7092.
139 Y. Suhara, N. Hanada, T. Okitsu, M. Sakai, M. Watanabe, K. Nakagawa, A. Wada, K. Takeda, K. Takahashi, H. Tokiwa and T. Okano, *J. Med. Chem.*, 2012, **55**, 1553–1558.
140 L. A. Carpino, S. A. Triolo and R. A. Berglund, *J. Org. Chem.*, 1989, **54**, 3303–3310.
141 G. Kumari and R. K. Singh, *Med Chem Res*, 2014, **24**, 171–181.
142 J. Jiang, H. Jiang, W. Liu, X. Tang, X. Zhou, W. Liu and R. Liu, *Org. Lett.*, 2011, **13**, 4922–4925.
143 J. Burés, M. Martín, F. Urpí and J. Vilarrasa, *J. Org. Chem.*, 2009, **74**, 2203–2206.
144 Z. Wu, D. Liang and X. Tang, *Anal. Chem.*, 2016, **88**, 9213–9218.
145 S. De Xu, C. H. Fang, G. X. Tian, Y. Chen, Y. H. Dou, J. F. Kou and X. H. Wu, *J. Mol. Struct.*, 2015, **1102**, 197–202.
146 Y.-T. Lu, T.-L. Chen, K.-S. Chang, C.-M. Chang, T.-Y. Wei, J.-W. Liu, C.-A. Hsiao and T.-L. Shih, *Bioorganic Med. Chem.*, 2017, **25**, 789–794.
147 J. Zhou, C. Fang, Y. Liu, Y. Zhao, N. Zhang, X. Liu, F. Wang and D. Shangguan, *Org. Biomol. Chem.*, 2015, **13**, 3931–3935.
148 M. Brownlee, *Nature*, 2001, **414**, 813–820.
149 T. Nishikawa, D. Edelstein, X. L. Du, S.-I. Yamagishi, T. Matsumura, Y.

Kaneda, M. A. Yorek, D. Beebe, P. J. Oates, H.-P. Hammes, I. GiardinoMichael, *Nature*, 1910, **404**, 787–790\.
150 B. B. Thomas, M. J. Seiler, S. R. Sadda, P. J. Coffey and R. B. Aramant, *J. Neurosci. Methods*, 2004, **138**, 7–13.
151 H. E. Gottlieb, V. Kotlyar and A. Nudelman, *J. Org. Chem.*, 1997, **62**, 7512–7515.
152 W. C. Still, M. Kahn and A. Mitra, 1978, **43**, 2923–2925.
153 D. D. D. D. Perrin, *Purification of laboratory chemicals / D. D. Perrin and W. L. F. Armarego and D. R. Perrin*, Pergamon Press, Oxford ; New York, 1980.
154 A. Kayal, A. F. Ducruet and S. C. Lee, *Inorg. Chem.*, 2000, **39**, 3696–3704.
155 R. C. Cambie, P. A. Craw, P. S. Rutledge and P. D. Woodgate, *Aus. J. Chem.*, 1988, **41**, 897–918.
156 M. M. Johnson, J. M. Naidoo, M. A. Fernandes, E. M. Mmutlane, W. A. L. van Otterlo and C. B. de Koning, *J. Org. Chem.*, 2010, **75**, 8701–8704.
157 Y. Suhara, N. Hanada, T. Okitsu, M. Sakai, M. Watanabe, K. Nakagawa, A. Wada, K. Takeda, K. Takahashi, H. Tokiwa and T. Okano, *J. Med. Chem.*, 2012, **55**, 1553–1558.

Appendix I: Redox Properties

	reduction potential	oxidation potential	Δ oxid.-reduc.
Idebenone 11	-0.71	-0.64	-0.08
Menadione 12	-0.74	-0.66	-0.08
13	-0.85	-0.77	-0.08
14	-0.85	-0.77	-0.08
16	-0.85	-0.77	-0.08
17	-0.84	-0.77	-0.07
18	-0.87	-0.78	-0.09
20	-0.81	-0.73	-0.08
21	-0.82	-0.76	-0.06
22	-0.76	-0.68	-0.08
23	-0.83	-0.73	-0.10
24	-0.84	-0.76	-0.08
25	-0.86	-0.77	-0.08
26	-0.77	-0.71	-0.07
27	-0.86	-0.77	-0.09
28	-0.83	-0.77	-0.06
29	-0.80	-0.73	-0.08
31	-0.79	-0.18	-0.61
32	-0.69	-0.10	-0.59
33	-0.81	-0.74	-0.07
34	-0.84	-0.77	-0.06
35	-0.83	-0.76	-0.07
36	-0.80	-0.73	-0.07
37	-0.81	-0.73	-0.08
38	-0.81	-0.74	-0.07
40	-0.77	-0.70	-0.07

Appendix II: Biological Experimental

Protection against mitochondrial dysfunction

Cytoprotection against mitochondrial dysfunction was measured as previously described [20]. Briefly, 5,000 cells per well were incubated with quinones (10 μM) in a 96 well plate for 2 days prior to being challenged by the mitochondrial complex I inhibitor rotenone (1 μM) for 6 hours. After post incubation with only quinones for 24h, cell viability was quantified by analysing ATP content per well using a luciferase-based reaction. Cytoprotection is displayed as a percentage of the untreated (no rotenone) control. Data represent the average of 3 independent experiments with n=6 wells within each experiment. Error bars = SD.

Acute rescue of ATP levels

Acute rescue of ATP levels in the presence of a mitochondrial inhibitor was measured as previously described [Erb et al. 2012]. Briefly, 15,000 cells per well were seeded in a 96 well plate and allowed to attach overnight. After 24h, cells were incubated with quinones (10 μM) along with the mitochondrial complex I inhibitor rotenone (10 μM) for 1 hour in glucose-free growth media before immediately measuring ATP levels using a luciferase-based reaction. Acute rescue of ATP levels is displayed as a percentage of the untreated (no rotenone) control. Data represent the average of 3 independent experiments with n=6 wells within each experiment. Error bars = SD.